PALAEOENVIRONMENTAL AND ICHNOFABRIC STUDIES OF THE CRETACEOUS BULLDOG SHALE, SOUTH AUSTRALIA

James Edward Maunder

Submitted in accordance with the requirements for the degree of Ph.D.

The University of Leeds,
Department of Earth Sciences.

March, 1996.

The candidate confirms that the work submitted is his own and that appropriate credit has been given where reference has been made to the work of others.

IMAGING SERVICES NORTH
Boston Spa, Wetherby
West Yorkshire, LS23 7BQ
www.bl.uk

CONTAINS PULLOUTS

Abstract

The Lower Cretaceous Bulldog Shale is an organic-rich argillaceous unit deposited within the intracratonic Eromanga Basin in central Australia, and now exposed around the south western margin of the basin. During the Aptian and Albian the Eromanga Basin occupied palaeolatitudes between 65° and 75°S, and regional climate at this time involved at least seasonal freezing. Core and field sections of the Bulldog Shale have been used here to define the depositional palaeoenvironments of this high latitude mudstone, and aid basin correlation.

The Bulldog Shale is a fossiliferous, glauconitic and pyritic silty mudstone, with a variable sand component, and contains carbonate concretions, cone-in-cone limestone, lonestones and glendonite nodules. Seventeen trace fossil taxa have been identified: *Anconichnus horizontalis*; *Chondrites*; *Gyrochorte comosa*; *Ophiomorpha irregulaire*; *O. nodosa*; *O. nodosa* var. *spatha*; *Palaeophycus heberti*; *P. tubularis*; *Phoebichnus*; *Planolites montanus*; *Rhizocorallium irregulare*; *Schaubcylindrichnus*; *Skolithos verticalis*; *Teichichnus rectus*; *T. zigzag*; *Terebellina*; and *Thalassinoides suevicus*. A key to aid identification of trace fossils in the marine sediments of the Eromanga Basin has been constructed.

A new scheme involving Palaeoenvironmental Fabric Types (PFTs), has been developed. It incorporates palaeoenvironmental data on percentage bioturbation; diversity, types and cross-cutting relationships of trace fossil taxa; sedimentary grain size; physical sedimentary structures and body fossils. Seven PFTs (A-G) have been defined. Depositional palaeoenvironments within the Eromanga Basin varied from relatively deep basinal conditions characterised by low bottom-water oxygen levels, which largely precluded bioturbation, and no storm influence (PFT/A), to shallower well-oxygenated conditions, where storm-derived sedimentation occured but its effects were obliterated by the ubiquitous bioturbation (PFT/E), to the shallowest conditions where storm-derived sedimentation was dominant and bioturbation was absent to scarce (PFT/G).

This scheme has been used to sub-divide the Bulldog Shale into ten sub-units (α to κ) and correlate these sub-units across a basin transect of 276km, the first time this has been accomplished on such a fine scale. Palaeobathymetric curves, developed from the PFT plots, reflect four basin-wide relative deepening and shallowing events. These are related to global eustasy, but the initial transgression that heralded Bulldog Shale deposition and the final regression that terminated it were exacerbated by epeirogenic subsidence and uplift.

Table of Contents

Chapter 1:

Introduction: overview of the Eromanga Basin and the Bulldog Shale 1

1.1 The question addressed by this thesis 5

1.1.1 Subdivision and correlation of the Bulldog Shale 5

1.1.2 Palaeoenvironmental studies of the Bulldog Shale 6

1.2 The Eromanga Basin: sedimentary and environmental history 7

1.2.1 Jurassic - Cretaceous non-marine sediments 7

Poolowanna Formation 7

Algebuckina Sandstone 8

1.2.2 Cretaceous marine sediments 9

Cadna-owie Formation 10

Mount Anna / Parabarana Sandstone Member 11

Bulldog Shale 14

Definition and age 14

Environment of deposition 14

Eustatic sea-level movements 16

Palaeontology 16

Oodnadatta Formation 17

Coorikiana Sandstone 17

Oodnadatta Formation 18

Toolebuc Formation / Wooldridge Limestone Member 18

Allaru Mudstone 19

Mackunda Formation / Mount Alexander Sandstone Member 20

1.2.3 Cretaceous non-marine sediments 20

Winton Formation 20

Mount Howie Sandstone 20

1.2.4 Overlying sediments 20

Chapter 2:

Field and core analyses of the Bulldog Shale 21

2.1 Introduction and localities 21

2.1.1 Core and field sections analysed in this study 29

Core preparation for study 31

2.2 The Bulldog Shale in core and field section 31

2.2.1 Finniss 2 core 33

Thickness 33

Completeness 33

Dating and palaeoenvironmental interpretation 33
Sedimentary description 33
2.2.2 Alford 1 core 36
Thickness 36
Completeness 36
Dating and palaeoenvironmental interpretation 36
Sedimentary description 36
2.2.3 CBH 2 core 37
Thickness 37
Completeness 38
Dating and palaeoenvironmental interpretation 38
Sedimentary description 38
2.2.4 Mount Yerila field section 41
Thickness 41
Completeness 41
Dating 41
Sedimentary description 41
2.2.5 SPH 1 core 42
Thickness 42
Completeness 42
Dating and palaeoenvironmental interpretation 43
Sedimentary description 43
2.3 Basal boundary of the Bulldog Shale 45
2.3.1 Bulldog Shale directly overlying basement 45
2.3.2 Bulldog Shale overlying Cadna-owie Formation and the Parabarana Sandstone Member 49
Bulldog Shale overlying Cadna-owie Formation 49
Bulldog Shale overlying Parabarana Sandstone 50
2.4 Upper boundary of the Bulldog Shale 54
2.5 Carbonate concretions 57
2.5.1 Occurrence 57
2.5.2 Preserved fabric 57
2.5.3 Incorporated material 60
2.6 Lonestones 60
2.7 Mineralogy of the Bulldog Shale 63
2.7.1 Iron minerals 63
Pyrite 63
Marcasite 64
Jarowsite 64

2.7.2 Manganese minerals 65
2.7.3 Gypsum 65
2.8 Glendonite nodules 65
2.9 Macropalaeontology 66
2.10 Trace fossils 68

Chapter 3:
Ichnology of the Bulldog Shale 69
3.1 Introduction 69
3.1.1 Intergradation and morphological similarities between trace fossil taxa 70
3.1.2 The ethological classification of the Bulldog Shale trace fossils 71
3.2 Systematic ichnology of the trace fossils in the Bulldog Shale 73
Ichnogenus ANCONICHNUS 73
Anconichnus horizontalis 73
Ichnogenus CHONDRITES 77
Ichnogenus GYROCHORTE 79
Gyrochorte comosa 80
Ichnogenus OPHIOMORPHA 83
Ophiomorpha irregulaire 83
Ophiomorpha nodosa 84
Ophiomorpha nodosa var. *spatha* 88
Ichnogenus PALAEOPHYCUS 90
Palaeophycus heberti 90
Palaeophycus tubularis 92
Ichnogenus PHOEBICHNUS 94
Ichnogenus PLANOLITES 95
Planolites montanus 96
Ichnogenus RHIZOCORALLIUM 97
Rhizocorallium irregulare 97
Ichnogenus SCHAUBCYLINDRICHNUS 100
Ichnogenus SKOLITHOS 102
Skolithos verticalis 103
Ichnogenus TEICHICHNUS 106
Teichichnus rectus 106
Teichichnus zigzag 109
Ichnogenus TEREBELLINA 111
Ichnogenus THALASSINOIDES 113
Thalassinoides suevicus 113

3.3 A key to the Bulldog Shale trace fossils 115

Chapter 4:

Palaeoenvironmental Fabric Type analysis 118

4.1 Bioturbation and ichnofabrics: an overview 118

4.1.1 Trace fossil tiering 118

4.1.2 Ichnofabric defined 119

4.1.3 Controlling factors on ichnofabric 120

Substrate character 120

Sediment accumulation rate 121

Bottom-water oxygenation levels 122

Trace fossil tiering / oxygen-related biofacies model 122

The behavioural model 124

4.1.4 Index measurements of bioturbation and ichnofabric 126

Droser and Bottjer's ichnofabric index 126

Taylor and Goldring's ichnofabric analysis model 128

4.1.5 Problems with these schemes, and a solution 129

4.2 Palaeoenvironmental fabric type methodology 131

4.3 Palaeoenvironmental fabric types of the Bulldog Shale 132

4.3.1 Palaeoenvironmental fabric type A 135

General characteristics 135

Example: Finniss 2, 84.60-84.45m 135

Example: CBH 2, 366.80-366.70m 136

4.3.2 Palaeoenvironmental fabric type B 138

General characteristics 138

Example: CBH 2, 363.50-363.40m 138

Example: SPH 1, 413.40-413.30m 139

4.3.3 Palaeoenvironmental fabric type C 141

General characteristics 141

Example: CBH 2, 356.70-356.60m 141

Example: SPH 1, 404.50-404.40m 143

4.3.4 Palaeoenvironmental fabric type D 143

General characteristics 143

Example: Alford 1, 53.20-53.10m 145

Example: SPH 1, 385.70-385.60m 145

Example: SPH 1, 350.00-349.90m 148

4.3.5 Palaeoenvironmental fabric type E 148

General characteristics 148

Example: Finniss 2, 53.43-53.28m 151

Example: Finniss 2, 37.20-37.00m 153
Example: Finniss 2, 30.25-30.08m 153
Example: Finniss 2, 29.25-29.15m 156
Example: Finniss 2, 29.15-29.00m 156
Example: Finniss 2, 29.00-28.82m 159
Example: Finniss 2, 28.82-28.71m 159
Example: Finniss 2, 28.66-28.48m 162
Example: Alford 1, 60.40-60.30m 162
4.3.6 Palaeoenvironmental fabric type F 162
General characteristics 162
Example: Alford 1, 57.90-57.80m 165
Example: CBH 2, 342.40-342.30m 166
Example: SPH 1, 291.80-291.70m 167
Example: SPH 1, 290.40-290.30m 168
4.3.7 Palaeoenvironmental fabric type G 170
General characteristics 170
Example: Alford 1, 40.45-40.35m 170
Example: CBH 2, 350.80-350.70m 172
Example: CBH2, 339.15-339.05m 173
Example: SPH 1, 304.70-304.60m 173
4.4 Palaeoenvironmental implications and trends from the Bulldog Shale palaeoenvironmental fabric types 173
4.4.1 Tiering changes in an idealised PFT/A - G transition 173
Transition: PFT/A - PFT/E 173
Transition: PFT/E - PFT/G 176
4.4.2 The control on tiering changes: palaeoenvironmental trends and variation 177
Palaeoenvironmental fabric type A 178
Palaeoenvironmental fabric type E 178
Palaeoenvironmental fabric type G 178
Water depth, the primary control on PFT 179
Palaeobathymetric implications 181
4.4.3 Discrepancies and variation in tiering profiles 181
Mutual cross-cutting relationships and sediment character 181
Sudden shifts in palaeoenvironmental fabric type 182
4.5 Internal independent tests 183

Chapter 5:

Palaeoenvironmental fabric types: application to logged sections and further analyses 184

5.1 Palaeoenvironmental fabric types in logged sections 184

5.2 Further analysis of the palaeoenvironmental fabric types 184

5.2.1 Macropalaeontology of the PFTs 190

Allochthonous material 190

Autochthonous material 190

5.2.2 Thin section analyses of the Bulldog Shale 192

Clay minerals 192

Quartz grains 192

Glauconite grains 193

Organic material 196

Minerals opaque in cross section 198

Shelly fossil fragments 200

5.2.3 Clay mineralogy 201

Methodology 201

Sample analysis 201

Results and analysis 202

Other studies and palaeoenvironmental implications 204

5.2.4 Organic carbon geochemistry 204

Methodology 204

Sample preparation 204

Results 205

Palaeoenvironmental implications and previous work 205

Chapter 6:

Correlation across the Eromanga Basin using the PFT scheme: a new approach 208

6.1 Sub-units of the Bulldog Shale 208

6.1.1 Sub-units of the Bulldog Shale in individual sections 209

CBH 2 209

SPH 1 212

Finniss 2 213

Alford 1 216

Mount Yerila section 217

6.1.2 Bulldog Shale sub-units: use as a tool 218

6.2 Bulldog Shale section correlation 219

6.2.1 The value of geophysical logs 219

6.2.2 Variation between sections 222
6.3 Other cores containing Bulldog Shale 223
6.3.1 Toodla 1 224
Thickness 224
Completeness 224
Sub-unit description 224
6.3.2 Skeleton 2 226
Thickness 226
Completeness 226
Sub-unit description 226
6.3.3 Correlation with the other five sections 228
6.4 Paleoenvironmental interpretation 230
6.4.1 Comparison of the Bulldog Shale palaeobathymetric curve with other studies and relative sea level curves 234
Paleoenvironmental interpretations from palynomorph studies 234
Comparison with Morgan's relative sea level curve 236

Chapter 7:
Discussion 241
7.1 Introduction 241
7.2 The Bulldog Shale: a black shale 241
7.2.1 Black shale deposition: processes and implications 242
7.2.2 Black shale deposition within epeiric seas 243
Shallow waters and seasonal anoxia 244
7.2.3 Transgressive black shales 245
7.2.4 Anoxic oceanic events 245
7.3 Bulldog Shale climatic indicators 248
7.3.1 Lonestones 248
7.3.2 Glendonites 250
7.3.3 Other analyses 251
Palaeontology 251
Oxygen isotopes 252
Computer modelling 253
7.3.4 Seasonally freezing climates and the Bulldog Shale 253
7.4 Bulldog Shale palaeobathymetry 254
7.4.1 The roles of eustasy, sediment supply, epeirogeny and local tectonics 254
7.4.2 Comparison with other Australian basins 256

7.4.3 Palaeobathymetry of the Eromanga Basin and global considerations 257
Comparison with published sea level curves 257
7.5 Comparison of the Eromanga Basin to other high latitude Cretaceous basins 260
7.5.1 James Ross Basin 260
7.5.2 Svalbard Basin 262
7.5.3 Sverdrup Basin 264

Chapter 8:
Conclusion 266
8.1 Suggestions for further work 269

Reference list 271

Appendix 1:
Structure of the south-west Eromanga Basin Mesozoic fill 292

Appendix 2:
Palaeoenvironmental Fabric Types of field localities 294

Appendix 3:
X-ray diffraction for clay mineral analysis: sample preparation methodology 296

Appendix 4:
Organic carbon geochemistry: sample preparation and analysis 297

List of Figures

1.01 Geological setting of the Eromanga Basin. Redrawn from Veevers (1984).. 2
1.02 A: Stratigraphic and palynological terminology of the south-western Eromanga Basin. Modified from Krieg *et al.* (1991) and Morgan (1980). B: Stratigraphic units and terminology of the Eromanga and Surat Basins. From Moore (1986a)..... 3
1.03 Reconstruction of the position of the southern continents in the Aptian. Redrawn from Veevers (1984)..... 4
1.04 Australian shorelines during the Aptian. Redrawn from Frakes *et al.* (1987)..... 10
1.05 Palaeogeographic interpretation of the south-western part of the Eromanga Basin during latest Barremian - earliest Aptian. Modified from Cowley and Martin (1991)..... 13
1.06 Outcropping Bulldog Shale in the South Australian part of the Eromanga Basin..... 15

2.01 South-western margin of the Eromanga Basin in South Australia with field and core localities..... 22
2.02 Peake and Denison Range field sites..... 23
2.03 Lake Eyre South field and core sites..... 24
2.04 Northern Flinders Ranges field and core sites..... 25
2.05 Petermorra Creek field sites..... 26
2.06 Yerila Creek field sites..... 27
2.07 Moolawatana field sites..... 28
2.08 Key to symbols utilised in Bulldog Shale logs..... 30
2.09 Palynostratigraphy of the Bulldog Shale. Redrawn from Krieg *et al.* (1991)..... 30
2.10 Laterally persistent interbedded clay and silt horizons..... 32
2.11 Summary log of the Finniss 2 Bulldog Shale succession..... 35
2.12 Summary log of the Alford 1 Bulldog Shale succession..... 37
2.13 Summary log of the CBH 2 Bulldog Shale succession..... 40
2.14 Summary log of the Mt. Yerila Bulldog Shale succession..... 42
2.15 Summary log of the SPH 1 Bulldog Shale succession..... 44
2.16 Basement highs at Melon Springs..... 46
2.17 Bulldog Shale pediment onlapping Peake and Denison Ranges..... 46
2.18 Boulder beach..... 48
2.19 Summary log of the boulder beach section..... 49

2.20 Summary log of the Cadna-owie - Bulldog Shale boundary at Bulldog Creek 50
2.21 Summary log of Petermorra Creek sections 52
2.22 Moolawatana shearing shed section 53
2.23 Bulldog Shale overlain by Coorikiana Sandstone and Oodnadatta Formation at Mount Yerila 55
2.24 Large scale, low angle foresets in basal Coorikiana Sandstone 56
2.25 Cone-in-cone limestone and carbonate concretions 58
2.26 Preserved sedimentary fabric in carbonate concretions 59
2.27 Incorporated material in carbonate concretions 61
2.28 Lonestones 62
2.29 Marcasite and associated jarowsite 64
2.30 Glendonite nodules 67

3.01 Ethological categorisation of Bulldog Shale trace fossils 72
3.02 *Anconichnus horizontalis* 74
3.03 *Chondrites* 78
3.04 *Gyrochorte comosa* 81
3.05 *Ophiomorpha irregulaire* 85
3.06 *Ophiomorpha nodosa* 86
3.07 *Ophiomorpha nodosa* var. *spatha* 89
3.08 *Palaeophycus heberti* 91
3.09 *Palaeophycus tubularis* 93
3.10 *Phoebichnus* 95
3.11 *Planolites montanus* 97
3.12 *Rhizocorallium irregulare* 98
3.13 *Schaubcylindrichnus* 101
3.14 *Skolithos verticalis* 104
3.15 *Teichichnus rectus* 108
3.16 *Teichichnus zigzag* 110
3.17 *Terebellina* 112
3.18 *Thalassinoides suevicus* 114

4.01 Tiering of infauna as recognised from the study of trace fossils. From Droser and Bottjer (1993) 119
4.02 Changes in burrow size, bioturbation depth and tiering structure associated with a declining oxygen gradient. Redrawn from Savrda and Bottjer (1987b) 123

4.03 Model for oxygen-controlled ichnofabric composition based on dominant trace maker feeding behaviour. From Ekdale and Mason (1988)..... 125
4.04 Criteria used to define palaeoenvironmental types in the Bulldog Shale..... 132
4.05 Palaeoenvironmental fabric type A, schematic trace fossil tiering diagram.. 135
4.06 Finniss 2, 84.60-84.45m..... 136
4.07 CBH 2, 366.80-366.70m..... 137
4.08 Palaeoenvironmental fabric type B, schematic trace fossil tiering diagram.. 138
4.09 CBH 2, 363.50-363.40m..... 139
4.10 SPH 1, 413.40-413.30m..... 140
4.11 Palaeoenvironmental fabric type C, schematic trace fossil tiering diagram.. 141
4.12 CBH 2, 356.70-356.60m..... 142
4.13 SPH 1, 404.50-404.40m..... 144
4.14 Palaeoenvironmental fabric type D, schematic trace fossil tiering diagram.. 145
4.15 Alford 1, 53.20-53.10m..... 146
4.16 SPH 1, 385.70-385.60m..... 147
4.17 SPH 1, 350.00-349.90m..... 149
4.18 Palaeoenvironmental fabric type E, schematic trace fossil tiering diagram.. 151
4.19 Finniss 2, 53.43-53.28m..... 152
4.20 Finniss 2, 37.20-37.00m..... 154
4.21 Finniss 2, 30.25-30.08m..... 155
4.22 Finniss 2, 29.25-29.15m..... 157
4.23 Finniss 2, 29.15-29.00m..... 158
4.24 Finniss 2, 29.00-28.82m..... 160
4.25 Finniss 2, 28.82-28.71m..... 161
4.26 Finniss 2, 28.66-28.48m..... 163
4.27 Alford 1, 60.40-60.30m..... 164
4.28 Palaeoenvironmental fabric type F, schematic trace fossil tiering diagram.. 165
4.29 Alford 1, 57.90-57.80m..... 166
4.30 CBH 2, 342.40-342.30m..... 167
4.31 SPH 1, 291.80-291.70m..... 168
4.32 SPH 1, 290.40-290.30m..... 169
4.33 Palaeoenvironmental fabric type G, schematic trace fossil tiering diagram.. 170
4.34 Alford 1, 40.45-40.35m..... 171
4.35 CBH 2, 350.80-350.70m..... 172
4.36 CBH 2, 339.15-339.05m..... 174
4.37 SPH 1, 304.70-304.60m..... 175
4.38 Trends in palaeoenvironmental fabric type defining and controlling factors 177
4.39 Starfish skeleton from PFT/G material..... 179

5.01 Finniss 2 Bulldog Shale log with PFT plot 185
5.02 Alford 1 Bulldog Shale log with PFT plot 186
5.03 CBH 2 Bulldog Shale log with PFT plot 187
5.04 Mt. Yerila Bulldog Shale log with PFT plot 188
5.05 SPH 1 Bulldog Shale log with PFT plot 189
5.06 Bivalve material 191
5.07 Bulldog Shale quartz grains in thin section 194
5.08 Bulldog Shale glauconite grains in thin section 195
5.09 Organic matter in thin section 197
5.10 Opaque minerals associated with trace fossil burrows in thin section 199
5.11 Bulldog Shale scaphopod and foraminifera in thin section 200
5.12 Bulldog Shale clay mineral diffraction line plots 203
5.13 A: Graph of total organic carbon for PFTs A, B, D, E and F.
B: Graph of $\delta^{13}C$ for PFTs A, B, D, E and F 206
5.14 A: Graph of mean total organic carbon values for all PFTs.
B: Graph of mean $\delta^{13}C$ for all PFTs 207

6.01 Summary log of the CBH 2 Bulldog Shale succession with the sub-units delineated 210
6.02 Summary log of the SPH 1 Bulldog Shale succession with the sub-units delineated 214
6.03 Summary log of the Finniss 2 Bulldog Shale succession with the sub-units delineated 215
6.04 Summary log of the Alford 1 Bulldog Shale succession with the sub-units delineated 216
6.05 Summary log of the Mt. Yerila Bulldog Shale succession with the sub-units delineated 218
6.06 South western margin of the Eromanga Basin in South Australia with location of logged core and field sections included in sub-unit correlation.. 220
6.07 Correlation diagram for the Bulldog Shale sub-units from the five analysed sections 221
6.08 Summary log of the Toodla 1 Bulldog Shale succession 225
6.09 Summary log of the Skeleton 2 Bulldog Shale succession 227
6.10 Expanded correlation diagram for the Bulldog Shale sub-units 229
6.11 Vertical PFT and sub-unit successions for the Finniss 2, Alford 1, CBH 2, Mt. Yerila and SPH 1 Bulldog Shale sections with inferred palaeobathymetric curves 231
6.12 Palaeobathymetric curve for the CBH 2 Bulldog Shale succession 232

6.13 Comparison of the CBH 2 Bulldog Shale palaeobathymetric curve with that of Morgan (1980) 237

7.01 Model for the deposition of transgressive black shales in an epicontinental basin setting. Redrawn from Wignall (1991) 246
7.02 Comparison of the Bulldog Shale palaeobathymetric curve with other palaeodepth and eustatic curves for the Aptian - Middle Albian 258
7.03 Locality map of James Ross Island and the Larsen Basin. From Pirrie and Marshall (1991) 260
7.04 Locality map of the Svalbard Basin. From Aga *et al.* (1986) 262
7.05 Locality map for the Christopher and Isachsen Formations within the Sverdrup Basin. Redrawn from Embry (1985) 265

List of Tables

4.1 Bioturbation Index. From Taylor and Goldring (1993)..... 128
4.2 Palaeoenvironmental fabric types of the Bulldog Shale..... 134
4.3 Characteristics of Aigner and Reineck's (1982) storm-derived facies..... 180

6.1 Summary table of the Bulldog Shale sub-units and their characteristics..... 209
6.2 Characteristics of the sub-units from the CBH 2 Bulldog Shale succession. 211
6.3 Characteristics of the sub-units from the SPH 1 Bulldog Shale succession.. 212
6.4 Characteristics of the sub-units from the Finniss 2 Bulldog Shale succession..... 213
6.5 Characteristics of the sub-units from the Alford 1 Bulldog Shale succession..... 217
6.6 Characteristics of the sub-units from the Mt. Yerila Bulldog Shale succession..... 217
6.7 Distance from palaeoshoreline for the sections analysed in this study..... 222
6.8 Summary table of palaeoenvironmental interpretations of Bulldog Shale sub-unit material from palynomorph studies..... 234

Acknowledgements

My appreciation goes first to Dr. Jane Francis who, for three and a half years, has provided unceasing enthusiasm, good advice and all-round excellent supervision. To Dr. Paul Wignall also for his ideas and contributions.

At Mines and Energy, South Australia (MESA), my third supervisor Dr. Neville Alley provided everything, and more, that I asked for, good advice, friendship and an over-supply of the finest South Australian red wine. Dr. Graham Krieg also provided information of use and was always there to talk to. Thanks to Dr. Malcolm Sheard for his interest and whom, with Neville, introduced me to the delights of Australian field work and who has everything you could ever need in the bush.

Back, for the moment, to Leeds. My project could not have been completed without the help of the following: Dr. Simon Bottrell and Dave Hatfield for my organic carbon analyses and for the fun and enjoyment in the lab; Alan Gray for my clay mineral analyses and for his enthusiasm, interest and tales; Keith Reid and Keith Cowling for finding a way of producing thin sections from the Bulldog Shale; and Neil Woodhouse for good times in the Seddy lab and for all the ink.

For "critical" comments and advice at conferences my thanks goes to Dr. John Pollard and Dr. Andrew Taylor, who both helped in the identification of Bulldog Shale trace fossils, and to Dr. Roland Goldring.

Once more to MESA, my gratitude also goes to: Lyn Broadbridge (we never did go crab fishing!), Tina Nezic, Marigold White (I'm glad Air Nissan wasn't more of a disaster!), Andy "cornflakes" Rowett, Rick Aldam, John Moreton and Pru Freeman for all their friendly help and advice, and to everyone else who helped while I was in Adelaide. Thanks also to Bron and Tim. From the core library I thank Brian Logan for his good humour and enthusiasm and Michael Pate for cutting more Bulldog Shale than he'd care to remember.

At the University of Adelaide my gratitude goes to Prof. Larry Frakes and to Dr. David McKirdy for questions answered.

Thank you also to my friend Fran Parker (and of course Nick and Sammy), shall we do lunch at Skillogalee sometime?

To all at Kathleen Lumley College and to all the wonderful friends I made there, thank you for those fantastic days.

Back at Leeds, life would have been much poorer without the friendship of my flatmates over the years, in particular the current crew: Cap'n Pete Kelly, Ewan D'Laws and Mountain Leader Andy Barker, and also - from the past - Hetty Lamb. In the Department of Earth Sciences there are far too many people to name individually, but they include Jo "double grapevine" Wilkin, Karen "spacker" Braithwaite, Klaus "Winghingen" Strohle, Richard "golden boy" Twitchett, Fariborz Masoudi, Behzad "burbling Bezzie" Mehrabi, Jim "factual" Graham and Peta Hayes.

Fond thankyous also to Jo's partner in aerobic crime Barbara Lonsdale.

Finally, many, many thankyous to my wonderful Mother and Father, and to my brother - I'm proud that they're my family.

Lastly, to Mary, for all the wonder of the past, and for all that will be.

The Eromanga Basin from the slopes of Parabarana Hill.

From this viewpoint, on an Aptian day. A broad expanse of blue-green inland ocean, chopped by cool spring breezes, stretches away to the east and north. Around the basin margin are the hills of the northernmost Flinders Ranges, clad in forests of ferns, conifers and cycadophytes. Low clouds, occasionally parting to reveal a chink of blue, scud overhead, periodically dulling the sea surface with icy rain. Upon this inland sea ride blocks of ice released from wintry rivers and shores. Within the ice, black stones and boulders plucked from the river beds and shorelines during winters icy grasp, are released with the springtime melting and fall to the muddy sea floor.

Chapter 1

Introduction: overview of the Eromanga Basin and the Bulldog Shale

The Eromanga Basin extends over one million square kilometres of central Australia (Fig.1.01), and contains sediments of Early Jurassic (Toarcian) to Late Cretaceous (Turonian) age (Krieg *et al.*, 1991) (Fig. 1.02). It forms part of a larger complex of intracratonic basins which together comprise the hydrogeological Great Artesian Basin (Morgan, 1980). Component basins of the Great Artesian Basin complex are the Carpentaria, Eromanga, Surat and Clarence-Moreton Basins (Fig.1.01), though only the first three contain extensive Cretaceous sediments. Marine Cretaceous sediments are also known to underlie the Tertiary Murray Basin (Fig.1.01) and are considered to have been lithologically continuous with sediments of the southern Eromanga Basin (Morgan, 1980). The Eromanga Basin is directly connected to the Carpentaria and Surat Basins across shallow basement ridges, namely the Euroka Arch and the Nebine Ridge respectively (Fig.1.01). The Euroka Arch was generated during the Late Jurassic and remained static during the Cretaceous, while the Nebine Ridge "rose spasmodically" during the Cretaceous (Exon and Senior, 1976). For a review regarding the structural geology of the Eromanga Basin and its Mesozoic fill, see Appendix 1.

As indicated in Fig.1.03, during the Aptian and Albian, Australia was much further south than it is today, and occupied palaeolatitudes between 80°S (south-eastern seaboard) and 50°S (western seaboard) (Veevers, 1984). The Eromanga Basin itself occupied palaeolatitudes between 75°S and 65°S.

It was within the Eromanga Basin, during the Aptian and Albian of the Early Cretaceous (Fig.1.02), that the organic-rich and argillaceous Bulldog Shale was deposited. The deposition of the Bulldog Shale, and other associated units, was the result of marine transgression from the open ocean to the north, through the Carpentaria Basin.

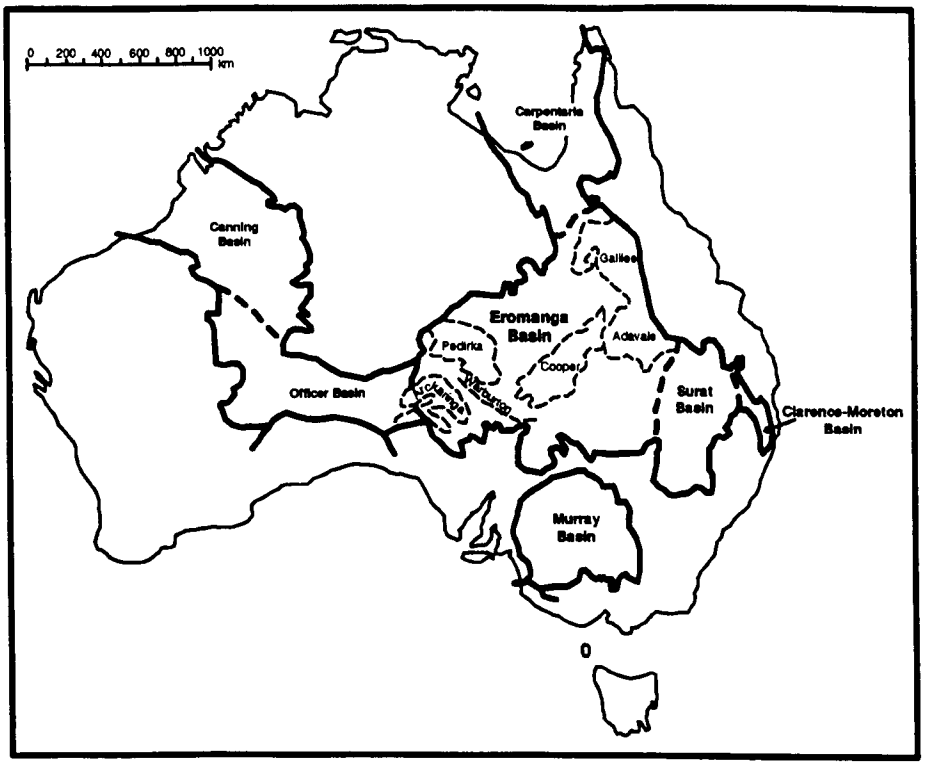

Fig.1.01 Geological setting of the Eromanga Basin and interlinked Carpentaria, Surat and Clarence-Moreton Basins; position of Murray Officer and Canning Basins included for completeness, boundaries marked with solid lines. The location of the older Warburton, Adavale, Arckaringa, Pedirka, Cooper and Galilee Basins is also included. Redrawn from Veevers (1984).

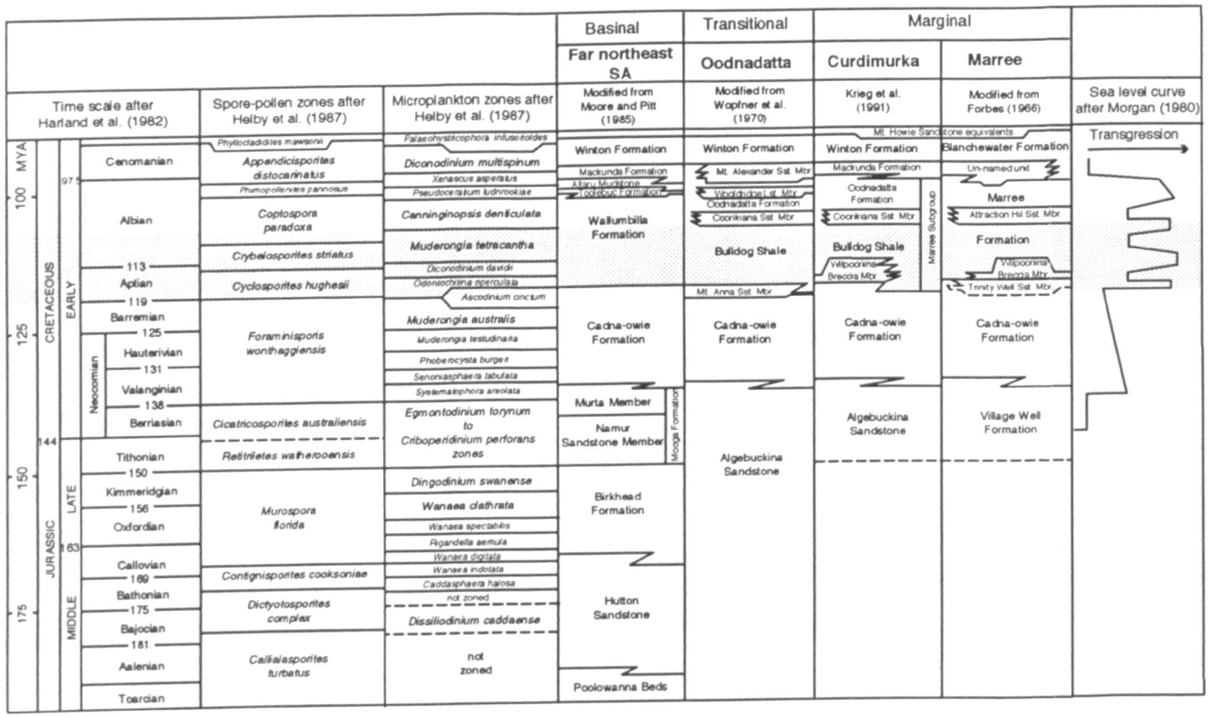

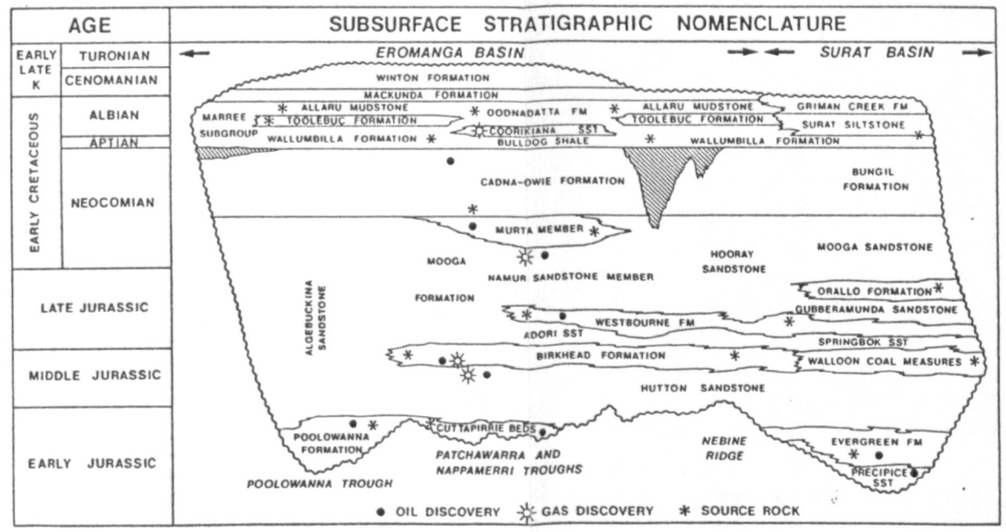

Fig.1.02 A) Stratigraphic and palynological terminology of the south-western Eromanga Basin. Modified from Krieg *et al.* (1991). Sea level curve for the Eromanga Basin redrawn from Morgan (1980).
B) Stratigraphic units and terminology of the Eromanga and Surat Basins, in a transect from west to east. From Moore (1986a)

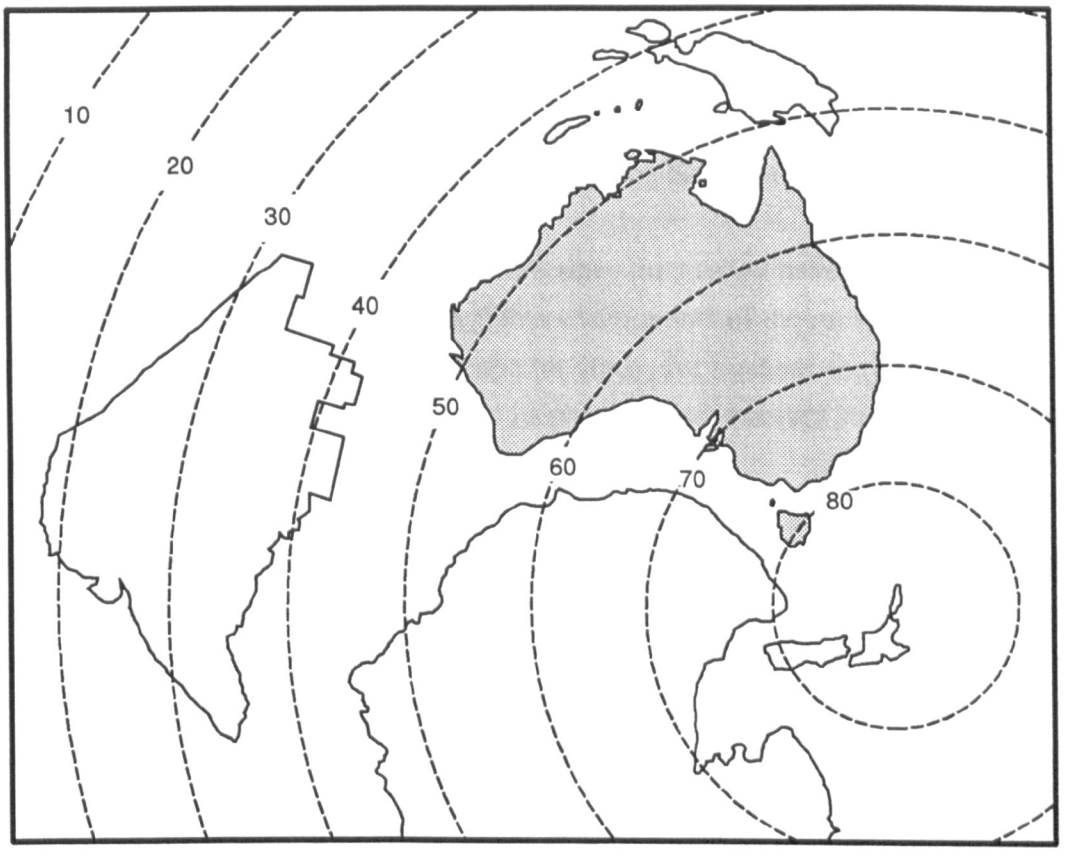

Fig.1.03 Reconstruction of the position of the southern continents in the Aptian. Redrawn from Veevers (1984).

1.1 The question addressed by this thesis

The primary focus of this thesis are the trace fossils of the Bulldog Shale. These are utilised to: (1) provide a new means for subdivision and correlation within the Bulldog Shale and; (2) study the local and regional depositional environments prevailing within the Eromanga Basin during deposition of the Bulldog Shale and associated units.

Trace fossils have been concentrated on here since they as yet have gone unstudied, and are highly variable and well preserved. Other components of the rock fabric are also analysed here, though they offer less scope for study, for instance the Bulldog Shale typically lacks a diverse macrofauna, and its physical sedimentary structures are largely unremarkable.

While the Bulldog Shale is the principle unit under study here, other underlying and overlying units are also mentioned. In addition, the principles developed and applied here can also be utilised on other marine-origin units of the Eromanga Basin fill. Therefore, the bulk of this chapter (§1.2) deals with a brief description of the stratigraphy and sedimentology of the Eromanga Basin. Chapter 2 narrows the focus with analysis of the Bulldog Shale in surface and subsurface sections, while Chapter 3 deals exclusively with the Bulldog Shale trace fossils. Subsequent chapters are concerned with the application of the characteristics detailed in Chapters 2 and 3.

1.1.1 Subdivision and correlation of the Bulldog Shale

Accurate identification and correlation of individual stratigraphic units, and their internal variations, of the Eromanga Basin is important since the region is considered to be the most prospective onshore area in Australia for hydrocarbon exploration (Moore, 1986a). Hydrocarbon discoveries have been made at several stratigraphic horizons within the Eromanga Basin (Fig.1.02b). The Bulldog Shale itself is important in this respect, for in part it is the likely source of gas reservoired in the overlying Coorikiana Sandstone (McKirdy *et al.*, 1986).

Of particular importance for future field analyses and mapping projects, the subdivision and correlation scheme developed here for the Bulldog Shale from subsurface material, has the benefit of also being capable of application to field sections. The stratigraphic position of such sections can therefore now be identified, providing sufficiently unweathered material can be obtained for fabric analysis as described herein and dating.

Previously, lithological and dating studies provided only a broad mechanism for stratigraphical position identification.

1.1.2 Palaeoenvironmental studies of the Bulldog Shale

Until the early 1980s, the climate of the Early Cretaceous was widely regarded to have been "warm and equable", a term defined by Sloan and Barron (1990) to mean two things: (1) a substantially reduced annual cycle of temperature and; (2) a lack of extremes, particularly the lack of seasonally sub-zero temperatures at the poles.

However, in more recent years, a considerable revolution has occurred in the consensus of opinion regarding Cretaceous climates. This new view, based on palaeontological, sedimentological and isotopic evidence, and backed up by computer modelling studies, considers that the Earth could not have been ice-free during the Cretaceous, and that regions at high palaeolatitude experienced at least seasonal freezing in continental interiors and on high mountains.

The Bulldog Shale, therefore, appears to have been deposited in marine conditions within an epicontinental basin at high palaeolatitudes under a cold, seasonally freezing regional climate. The nature of such sediments and the environments prevailing during their deposition is poorly known, both in terms of ancient and modern deposits. This is a result, at least in part, of the inaccessibility of most Cretaceous high latitude black shales, and a lack of modern environmental analogues.

It is therefore a purpose of this thesis to study the local and regional depositional sedimentary environments prevailing within the Eromanga Basin during deposition of the Bulldog Shale and associated units. This will provide an example of a high latitude black shale depositional environment, against which future studies and other rock suites can be compared. Indeed, some comparisons with published details of other high latitude black shales are made in Chapter 7.

1.2 The Eromanga Basin: sedimentary and environmental history

The sediments of the Eromanga Basin may be broadly subdivided into three major units based on their environment of deposition: Jurassic non-marine sediments (Poolowanna Formation and Algebuckina Sandstone), Cretaceous marine sediments (Cadna-owie Formation, Mount Anna Sandstone Member, Bulldog Shale, Coorikiana Sandstone and Oodnadatta Formation, all of which largely correlate to the Marree Subgroup (Fig.1.02), and the Toolebuc Formation, Allaru Mudstone and Mackunda Formation) and Cretaceous non-marine sediments (Winton Formation and Mount Howie Sandstone). Stratigraphic nomenclature used here will follow that of Krieg *et al.* (1991) (Fig.1.02) for the south-western Eromanga Basin. Sediments of the Eromanga Basin are defined both on their facies and age, as determined chiefly from palynological studies. Palynology is the main tool in discriminating between sedimentary deposits of the Eromanga Basin, particularly those of the Early Cretaceous which are often of similar lithology, and which weathering renders visually indistinguishable. Alley (1993) described how some palynological zonal boundaries coincide with rock boundaries, this phenomenon being associated with either regional or basinal environmental changes.

Jurassic and Cretaceous sedimentation in the Eromanga Basin took place after a period of erosion during much of the latest Triassic and earliest Jurassic which affected most of the land surface. Wopfner *et al.* (1970, p.406) considered that the sediments of the Eromanga Basin were deposited on a "senile, low-relief, tectonically stable landscape". The thickest pile of sediment within the Eromanga Basin accumulated in the Cooper Basin area (Fig.1.01), particularly in the central Nappamerri and Patchawarra Troughs (Fig.1.02), from which Moore and Pitt (1984) reported in excess of 1600m of Cretaceous sediments.

The following section describes the main units of the Eromanga Basin, their stratigraphic relationships, sedimentology, and some previous palaeoenvironmental interpretation.

1.2.1 Jurassic-Cretaceous non-marine sediments

Poolowanna Formation

The Poolowanna Formation comprises the oldest and lowermost beds of the Eromanga Basin, laid down unconformably over the sediments of the Triassic Simpson Desert Basin in the Poolowanna Trough depocentre (Moore, 1986b) (Fig.1.02). The

Poolowanna Formation dates from Sinemurian to middle Bajocian (Early to Middle Jurassic), and comprise up to 200m of fluvial, floodplain and swampy deposits (Moore, 1986a; 1986b). In most areas the Poolowanna Formation is conformably overlain by the Algebuckina Sandstone. However, in more basin-marginal areas the Poolowanna Formation laterally grades into the fluviatile sediments of the basal part of the Algebuckina Sandstone, and thus there was some synchroneity in deposition of the two units.

Algebuckina Sandstone

The Algebuckina Sandstone and its laterally equivalent units, which include the Hutton Sandstone, Birkhead Formation and Mooga Formation of more basinal areas (Fig.1.02), date from middle Bajocian (basal regions may date from middle Sinemurian, being in part a lateral equivalent of the Poolowanna Formation) to early Valanginian (middle Neocomian) (Moore, 1986b) (Fig.1.02). During the middle Early Jurassic, sedimentation expanded from the Poolowanna Trough and the Surat Basin depocentres, and eventually in the late Early Jurassic the Eromanga, Surat and Carpentaria Basins were linked by the growth of an extensive, bedload-dominated, sandy fluviatile system which spread over the region. The sediment forming this system was derived from the Gawler Craton to the south-west and from the Amadeus Basin to the west and north-west, with the Algebuckina Sandstone comprising the coarsest and mineralogically least mature deposits when compared to more distil equivalents (Wopfner *et al.*, 1970; Moore, 1986a, 1986b). In the Poolowanna Trough the Algebuckina Sandstone lies conformably over the Poolowanna Formation, but elsewhere it rests unconformably on older Palaeozoic sediments and Precambrian basement (Fig.1.05).Throughout its distribution the Algebuckina Sandstone is overlain both gradationally/conformably and disconformably by the Cadna-owie Formation (Wopfner *et al.*, 1970; Moore and Pitt, 1985; Moore, 1986b; Krieg *et al.*, 1991) (Fig.1.05), though the Algebuckina Sandstone may be absent over basement highs (Fig.1.05) and is laterally impersistent in the south-western Eromanga Basin. In regions where the Cadna-owie Formation is absent, Bulldog Shale disconformably overlies the Algebuckina Sandstone (Cowley and Martin 1991) (Fig.1.05). The Algebuckina Sandstone has highly variable thickness, with a maximum of approximately 40m.

The Algebuckina Sandstone consists of two units, both of fine-grained sandstone to pebble conglomerate with considerable vertical and lateral variation, but with the lower part being kaolinitic and poorly sorted and the upper being clean and well sorted. Fossil content of the Algebuckina Sandstone is restricted to land plant material (Wopfner *et*

al., 1970), without any marine fauna (Moore, 1986b). The lower unit represents deposition under low gradient, fluviatile conditions; in addition, the presence of case-hardened pebbles and dreikanters led Wopfner *et al.* (1970) to infer an arid to semi-arid palaeoclimate during deposition. Krieg *et al.* (1991) disagreed with this palaeoenvironmental interpretation and suggested that the fluctuating discharge, of which this unit is representative, may be due to a pronounced snow melt season. Such a palaeoenvironmental interpretation is supported by palynofloral analyses which indicate a vegetation typical of areas dominated by high precipitation and cool temperate to temperate conditions. The change from the lower to the upper sandstone may signify a transition to a consistently higher energy environment, resulting from an increase in slope gradient due to a slight drop of the basin margin, and the onset of a moister subtropical climatic regime (Wopfner *et al.*, 1970). In addition, this upper unit was deposited by rivers of stronger, more uniform flow than those which deposited the lower part; the result of a change to a wetter climate with more uniform precipitation, according to Krieg *et al.* (1991).

1.2.2 Cretaceous marine sediments

The Cretaceous sediments of the Eromanga Basin record a series of major marine transgressions and regressions. Frakes *et al.* (1987) related the development of interior seaways and basins marginal to the Australian continent primarily to eustacy, though also to local balance between sedimentation, subsidence and tectonics. During the Valanginian-Hauterivian a shallow extension of the sea entered the Eromanga Basin from the north, via the Carpentaria Basin; this broadened and lengthened to reach its maximum extent during the Aptian, at which time the Eromanga Sea was linked to the open ocean to the north by the Carpentaria Basin, to the east by the Surat and Clarence-Moreton Basins, and also possibly to the west via poorly defined connections with the Canning and Officer Basins (Figs.1.01, 1.04). By the Cenomanian the sea had fully regressed from the Eromanga Basin, although it remained in the northernmost reaches of the Carpentaria Basin. These transgressions and regressions were summarised by Morgan (1980) (Fig.1.02).

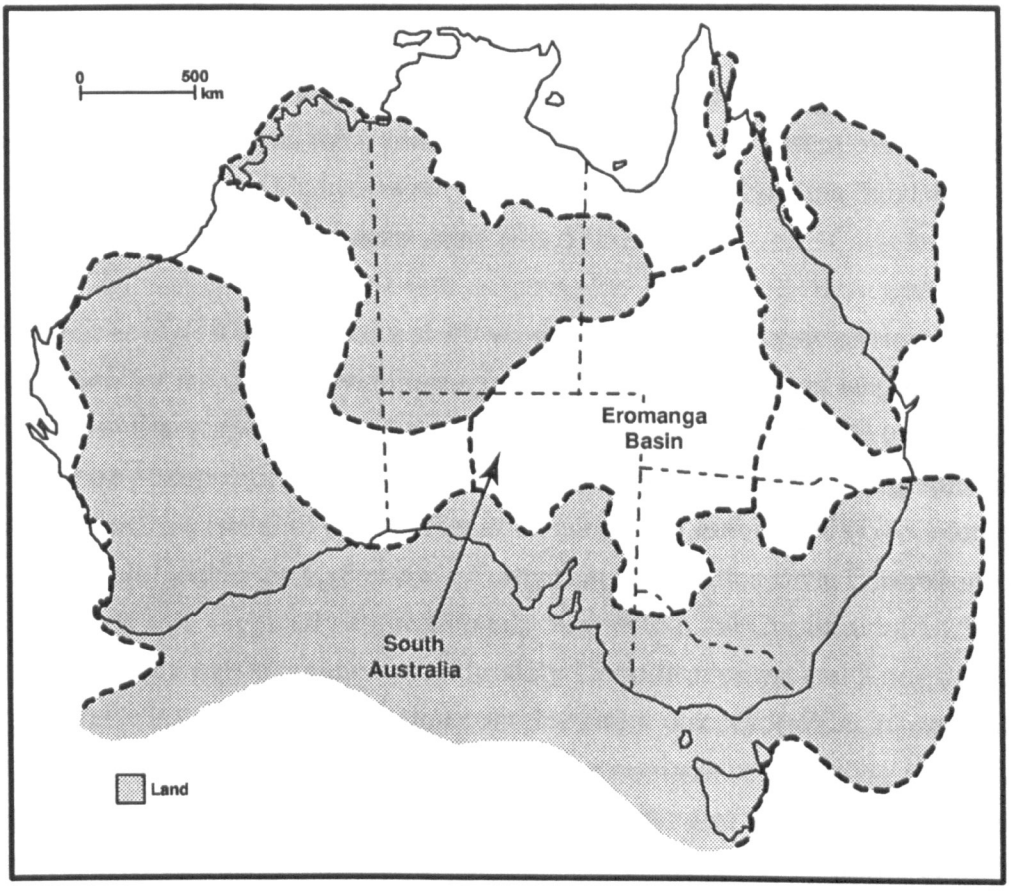

Fig.1.04 Australian shorelines during the Early Cretaceous (Aptian) marine transgression, and development of the Eromanga Sea. Redrawn from Frakes *et al.* (1987).

Cadna-owie Formation

The Cadna-owie Formation dates from the early to middle Valanginian to the latest Barremian or earliest Aptian, and is also known as the Pelican Well Formation or the Transition Beds (Krieg *et al.*, 1991) (Fig.1.02). An age of early Aptian for part of the Cadna-owie Formation makes it partly coeval to Bulldog Shale material deposited in more basinal settings (Alley, 1988) (Fig.1.05). The Cadna-owie Formation represents the onset of the Early Cretaceous marine transgression, and comprises a sequence of sandstone, siltstone and shale (Wopfner *et al.*, 1970; Morgan, 1980; Moore and Pitt, 1985; Krieg *et al.*, 1991), with a maximum thickness of 92m. This transgression is marked in some areas by an undulating erosional disconformity or angular unconformity at the Cadna-owie Formation's base where it overlies the Algebuckina Sandstone. However, in most areas the Cadna-owie Formation conformably overlies the Algebuckina Sandstone, and is conformably overlain by the finer Bulldog Shale,

although observations of reflection seismic data reveal apparent erosional channels up to 100m deep incised into the Cadna-owie Formation (Moore and Pitt, 1985). These may indicate local unconformities with the overlying Bulldog Shale. Like the Algebuckina Sandstone, the Cadna-owie Formation can be absent over basement highs, and in some locations Cadna-owie Formation onlaps Algebuckina Sandstone and rests directly on basement Adelaidean strata (Fig.1.05).

Wopfner *et al.* (1970) inferred a shallow-water, marginal marine environment of deposition for the Cadna-owie Formation; they also noted abrupt lateral and vertical changes in lithology which they related to rapid deposition and mild tectonic instability at the time of deposition, coupled with deposition in different yet geographically close marginal marine (paralic) environments. In addition, Lemon (1988) recorded estuarine tidal deposits within the Cadna-owie Formation. The Cadna-owie Formation is surprisingly thin (typically approximately 50m within the Curdimurka 1:250 000 map area) for a rock unit spanning approximately 15 million years, and Krieg *et al.* (1991) suggested it is probable that the unit contains major disconformities representing non-deposition, and/or erosion, as a result of marine regressions within the overall transgressive event. In addition, the upward coarsening of the Cadna-owie Formation may represent a shift from non-marine (probably lacustrine) deposition in the basal part of the formation to paralic deposition in the overlying sandier beds (Moore and Pitt, 1985). This interpretation is based on palaeontological data which indicate a marine influence in the middle and upper regions of the Cadna-owie Formation only, and not in the basal part. However, some Cadna-owie Formation sections, particularly the type section, exhibit a total lack of marine influence, and this may be indicative of the incompleteness of these sections and the unit as a whole.

Characteristic of the upper Cadna-owie Formation is the occurrence of large exotic boulders (Krieg *et al.*, 1991). Such boulders are more common in the Bulldog Shale.

Mount Anna/Parabarana Sandstone Member

The Mount Anna Sandstone Member, and its lateral equivalents the Parabarana Sandstone, the Wyandra Sandstone Member and the Trinity Well Sandstone Member, is latest Barremian to earliest Aptian in age (Krieg *et al.*, 1991) (Fig.1.02). The Mount Anna Sandstone Member is limited to the south-western region of the Eromanga Basin, and in many areas it conformably overlies the Cadna-owie Formation (Wopfner *et al.*, 1970). This unit, approximately 10m thick, is characterised by an abundance of pebbles and cobbles of red porphyritic rhyolite derived from the Gawler Range Porphyry, now

exposed in the Gawler Ranges, and by large-scale, graded cross bedding. The Mount Anna Sandstone Member represents fan deposits according to Wopfner *et al.* (1970), terminating in deltas or estuaries, protruding into the transgressing sea at the foot of a fault scarp, produced as a result of the major tectonic uplift of the Gawler Ranges which occurred at this time (Fig.1.05). However, Cowley and Martin (1991) considered it probable that the restricted distribution of the Mount Anna Sandstone Member in the Kingoonya 1:250 000 map area could be a result of its deposition in a braided river system incised into, and reworking, the Cadna-owie Formation and Algebuckina Sandstone (Fig.1.05). This confined braided river system opened out northwards into braid-plain and deltaic environments in the Billa Kalina 1:250 000 map area where the unit is thicker and more widespread.

Also of importance in the southern Eromanga Basin of South Australia is the Parabarana Sandstone Member, which crops out in the area covered by the Marree 1:250 000 map sheet (Forbes, 1986). The Parabarana Sandstone is a quartzitic and calcareous sandstone approximately 20m thick containing both marine megafossils and plant fossils, representing deposition in shallow marine, possibly littoral, conditions (Ludbrook, 1966). Such palaeoenvironmental determinations are supported by palynomorph analyses by Alley (pers. comm. 1995) which have also indicated that the Parabarana Sandstone was deposited in marginal marine conditions. In addition, Alley (pers comm. 1995) determined an age of Hauterivian (upper Neocomian) for Parabarana Sandstone cropping out in Petermorra Creek (§2.2.2), a similar age as that obtained for typical Cadna-owie Formation material obtained from sections in the Moolawatana area (§2.2.2) and elsewhere in the Eromanga Basin (Alley 1988). Thus, deposition of the Cadna-owie Formation and its Parabarana Sandstone Member, and by inference its lateral equivalents, were in part synchronous, and undoubtedly related to the proximity to the uplifting Gawler Block and its outflowing streams. Indeed Alley (1988) noted that deposition of the Cadna-owie Formation in the south-western Eromanga Basin was contemporaneous with that of the Parabarana Sandstone/Mount Anna Sandstone equivalent Wyandra Sandstone Member in deeper parts of the basin.

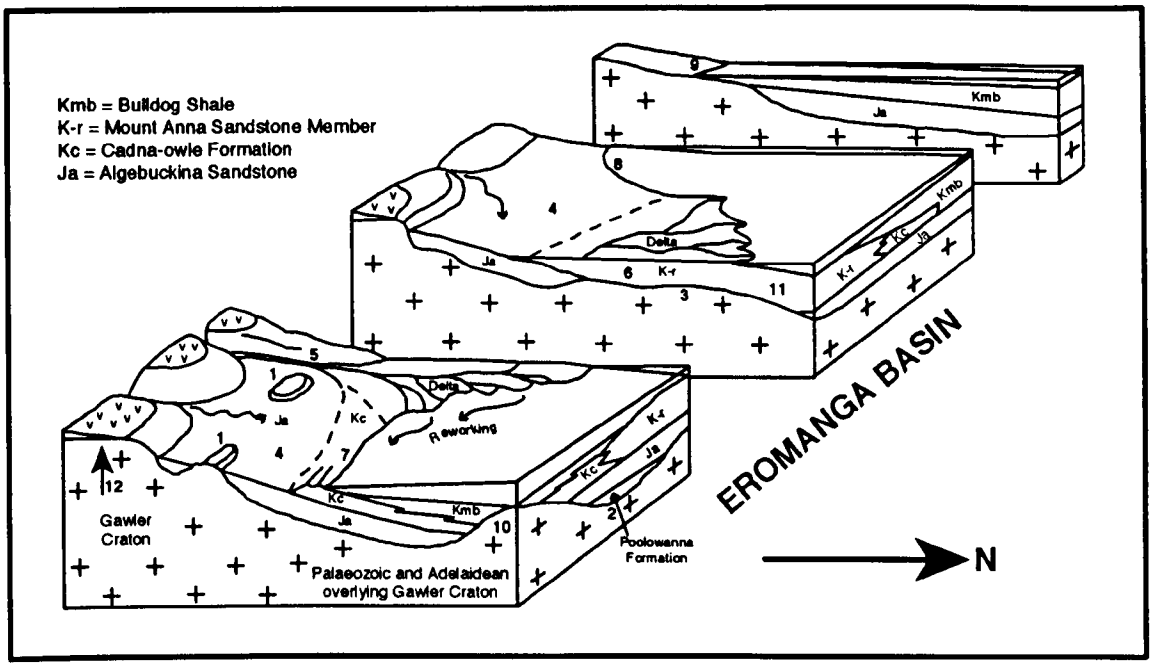

Fig.1.05 Palaeogeographic interpretation of the south-western part of the Eromanga Basin during latest Barremian - earliest Aptian, with possible synchronous deposition of the Cadna-owie Formation, Mount Anna Sandstone Member and the Bulldog Shale, demonstrating facies relationships and environments. 1 = Algebuckina Sandstone deposited around basement highs. 2 = Algebuckina Sandstone overlying Poolowanna Formation in basement troughs. 3 = Algebuckina Sandstone missing from basement high. 4 = Possible kaolinisation and silicification of exposed Algebuckina Sandstone. 5 = Mount Anna Sandstone Member confined to incised channels. 6 = Mount Anna Sandstone Member deposition opened out onto braid plain and delta, Algebuckina Sandstone is absent and deposition is directly onto basement. 7 = Fluvio-deltaic Mount Anna Sandstone Member reworked by shoreline processes into the marginal marine Cadna-owie Formation. 8 and 9 = sediment-starved shorelines, Cadna-owie Formation not developed, instead Bulldog Shale transgresses onto Algebuckina Sandstone or onlaps directly onto basement. 10 = prominent basement highs transgressed only by Bulldog Shale. 11 = Porphyry pebbles in the Mount Anna Sandstone Member derived from Gawler Ranges to south in headwaters of rivers such as 4. 12 = Uplift of the Gawler Ranges region providing detritus for Mount Anna Sandstone Member. Not to scale and vertically exaggerated.
Redrawn and modified from Cowley and Martin (1991).

Bulldog Shale

Definition and age

The Bulldog Shale dates from the earliest Aptian to middle Albian (Fig.1.02) (Krieg *et al.*, 1991). This unit was originally described by Freytag (1966) who defined a type section 8km south of Bulldog Creek, a tributary of the Neales River, on the eastern side of the Peake and Denison Ranges (Fig.1.06), though the unit is also widely exposed around the south-west margin of the Eromanga Basin in South Australia (Fig.1.06). The Bulldog Shale is a typically dark grey, shaly, fossiliferous mudstone, in part carbonaceous, glauconitic, pyritic, with variable amounts of silt and sand grade material, and containing layers rich in concretionary bluish-grey limestone nodules. These limestone concretions are mainly spherical, but some do have an ellipsoid shape, are frequently fossiliferous, contain rare coquinoid layers, and are commonly associated with cone-in-cone limestone material (Freytag, 1966; Ambrose and Flint, 1981). Fossil wood fragments, typically calcified, but often replaced with pyrite, are also a common component of Bulldog Shale material, particularly in the lower part of the unit (Freytag 1966). The Bulldog Shale was laid down during the continuation of the basin-wide marine transgression (McKirdy *et al.*, 1986). The lower third of the unit is particularly dark and shaly, and possibly a lateral facies equivalent of the Doncaster Member of the basal Wallumbilla Formation (Moore and Pitt, 1985). The Bulldog Shale is also particularly rich in lonestones (large exotic pebbles, cobbles and boulders) emplaced within typical Bulldog Shale material. In addition, glendonite nodules, stellate aggregations of calcite, have also been reported (Frakes and Francis, 1988; Sheard, 1990).

Environment of deposition

The Bulldog Shale thickens basinwards, and reaches a maximum known thickness of 340m in the Nappamerri Trough of the Southern Cooper Basin region (Fig.1.01), and it is lithologically indistinguishable from the laterally adjacent, more basinal, Wallumbilla Formation. The principal depocentres of the Bulldog Shale and Wallumbilla Formation were located in the Patchawarra, Nappamerri and Windorah Troughs (Moore and Pitt, 1985). The Bulldog Shale overlies the Cadna-owie Formation and the Mount Anna Sandstone Member/Parabarana Sandstone Member (Fig.1.05), a boundary considered by Moore and Pitt (1985) to be conformable. However, Alley (pers. comm. 1995), through palynomorph analyses, has determined a significant hiatus between the Parabarana Sandstone and the Bulldog Shale which is not evident in field or core sections. The Bulldog Shale also directly overlies the Algebuckina Sandstone in areas

where the Cadna-owie Formation was not deposited (Fig.1.05), and in places onlaps directly onto Precambrian basement (Fig.1.05). Indeed, surfaces which were apparently polished by waves of the Eromanga Sea are evident at localities where the boundary between the siliciclastic marine Mesozoic deposits and the Precambrian basement is exposed (Sheard and Flint, 1992). Furthermore, Rogers and Freeman (in prep) describe apparent high energy boulder beach facies directly overlain by Bulldog Shale material. Also important at some localities is the Wilpoorinna Breccia Member, a thin (approximately 0.5m thick) pebbly unit at the base of the Bulldog Shale, which is laterally very discontinuous and may represent a basal transgressive conglomerate (Forbes, 1966; Krieg *et al.*, 1991).

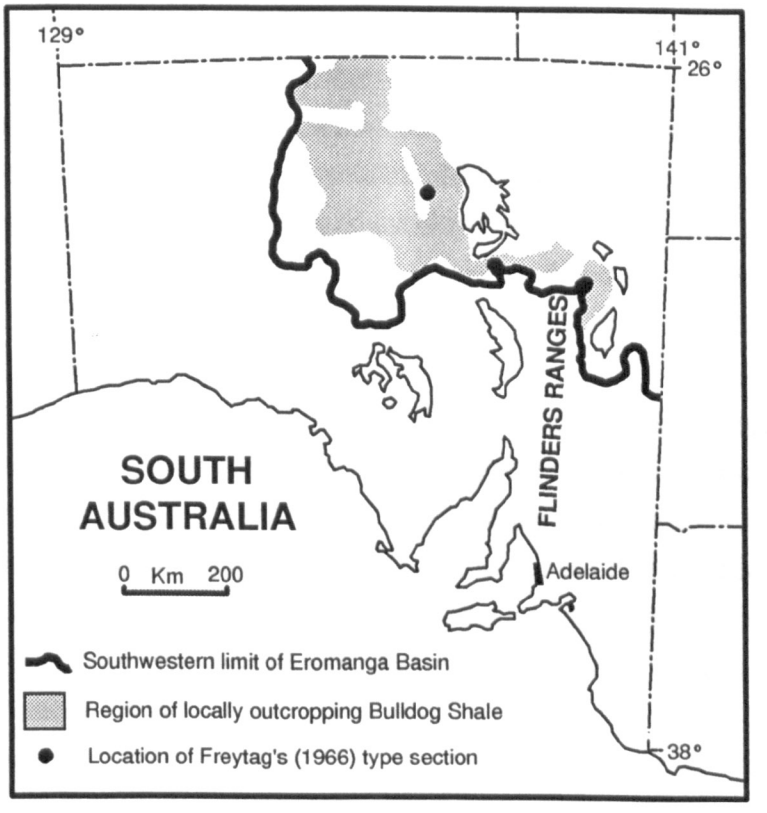

Fig.1.06 Cropping out Bulldog Shale in the South Australian part of the Eromanga Basin.

Over most of the south-western Eromanga Basin the Bulldog Shale is conformably overlain by the Coorikiana Sandstone Member of the Oodnadatta Formation, though around the north-east Flinders Ranges the Coorikiana sandstone is absent and the Bulldog Shale passes imperceptibly up into the lithologically similar Oodnadatta Formation (Moore and Pitt, 1985; Forbes, 1986).

The Bulldog Shale was deposited in marine conditions, probably below wave base, as the Early Cretaceous marine transgression reached its maximum extent (McKirdy *et al.*, 1986; Alley in Rogers *et al.*, 1989). The lower parts of the unit were deposited under transgressive conditions. The upper part of the unit was deposited in more restricted marine to paralic conditions. Marine regression terminated deposition of the Bulldog Shale and led to the deposition of the overlying Coorikiana Sandstone (Moore and Pitt, 1985; Morgan, 1980). Such observations are further backed up by trace fossil and sedimentary evidence, in which glauconite and pyrite associations from the trace fossil burrows represent alternating oxic and anoxic conditions at the time of deposition (McKirdy *et al.*, 1986). It is likely that the Eromanga Sea would have been subject to major storm events, but this only resulted in limited aeration of the bottom waters, particularly during deposition of the lower third of the Bulldog Shale, in which the common occurrence of pyrite and carbonised wood fragments, along with low diversity microplankton assemblages, indicate anaerobic conditions at the sediment-water interface (Krieg *et al.*, 1991). However, abundant bioturbation within parts of the Bulldog Shale is indicative of intermittently well oxygenated bottom waters.

Eustatic sea level movements

At least two marine regressions and transgressions occurred during deposition of the Bulldog Shale, between the major transgression that heralded the start of Bulldog Shale deposition, and the regression its cessation and the subsequent deposition of the Coorikiana Sandstone (Morgan, 1980). During deposition of the Bulldog Shale equivalent Wallumbilla Formation, sea depths of less than 50m prevailed according to Haig and Lynch (1993), and thus similar or shallower depths can be tentatively suggested for the Bulldog Shale.

Palaeontology

The Bulldog Shale contains shell beds and large bivalves of the genus *Maccoyella* Etheridge, jr., 1892. Other fossil material includes gastropods, belemnites, foraminifera, echinoderms, fish and marine reptiles (Krieg *et al.*, 1991).

Bioturbation is common in the Bulldog Shale, though it has not yet been studied in detail.

Plant fossils from the south-western Eromanga Basin, dated as being from the same time period as Bulldog Shale deposition, indicate forests bordering the basin, in which

conifers, podocarps, ferns and herbaceous plants were all important components of the flora (Krieg *et al.*, 1991).

Oodnadatta Formation

The Oodnadatta Formation overlies the Bulldog Shale. Throughout much of South Australia the Coorikiana Sandstone forms the basal part of the Oodnadatta Formation (Fig.1.02).

Coorikiana Sandstone

The Coorikiana Sandstone Member conformably overlies the Bulldog Shale across a gradual contact, with a sharp, though conformable, upper boundary with the overlying Oodnadatta Formation (Krieg *et al.*, 1991). Palynomorph studies indicate a middle Albian age for the Coorikiana Sandstone (Rogers *et al.*, 1989) (Fig.1.02).

The Coorikiana Sandstone is a highly variable unit comprising, in most locations, a coarsening upwards sequence of moderately sorted very fine to medium-grained feldspathic, glauconitic, micaceous and carbonaceous sandstone and sandy siltstone, with occasional minor interbeds of muddy, silty, coarse sandy and gritty material. Pebbles, typically of Precambrian basement quartzite, are also a major component of this unit, and conglomeratic layers of imbricated concretionary pebbles are present (Krieg *et al.*, 1991). Fossil wood fragments with associated *Teredolites* borings are also present. Sedimentary structures include medium-scale cross-bedding (tabular, low-angle and festoon), ripple marks, ripple cross-lamination, erosive scour and subsequent fill structures, parallel lamination, clay intraclasts and as yet undescribed biogenic structures.

The Coorikiana Sandstone Member ranges in thickness between 8m and 15m (Krieg *et al.*, 1991). Based on a survey of outcrop and subsurface data it is evident that the Coorikiana Sandstone extends for over 1000km as a thin sheet around the south-western Eromanga Basin. Where the Coorikiana Sandstone is absent the Bulldog Shale passes imperceptibly up into the lithologically similar Oodnadatta Formation (Forbes 1986), and in all areas the shales of the Marree Subgroup occur conformably above and below the Coorikiana Sandstone (Moore and Pitt, 1985; Moore *et al.*, 1986). The lithological uniformity of the Coorikiana Sandstone over such a large area, its coarsening-upwards nature, its lateral continuity and the general shape of the sand body, indicates that it was a regressive marine shoreface deposit, laid down in response to a eustatic fall in sea level. Furthermore, the lithology and sedimentary structures of

the Coorikiana Sandstone represent deposition within high-energy intertidal environmental conditions, with conglomerate layers being the remnants of gravel bars and beaches, and possibly tidal channel deposits (Krieg *et al.*, 1991). The regression marked by the Coorikiana Sandstone would have initiated stream rejuvenation with subsequent influx of terrigenous clastics into the Eromanga Basin. Sea level fall would have exposed older rock units, notably the Bulldog Shale, to the effects of subaerial and submarine erosion in marginal basin areas, and it is likely that much of the coarse clastic material, particularly the concretionary clasts within the Coorikiana Sandstone, has been reworked from the Bulldog Shale.

Oodnadatta Formation

The Oodnadatta Formation dates from middle to late Albian (Moore and Pitt, 1985; Krieg *et al.*, 1991) (Fig.1.02), and conformably overlies the Coorikiana Sandstone Member, or grades imperceptibly into the underlying and lithologically similar Bulldog Shale (Forbes 1986) in the south-western Eromanga Basin. Further north and east in more basinal areas where the Coorikiana Sandstone Member is absent, the lateral equivalent to the Oodnadatta Formation is the upper part of the Wallumbilla Formation, and indeed the Wallumbilla Formation in its entirety may be taken to be the lateral equivalent of the Marree subgroup as defined in the south-western Eromanga Basin (Fig.1.02). The Oodnadatta Formation is generally overlain conformably by the Mackunda Formation, though occasionally the Toolebuc Formation overlaps with the Coorikiana Sandstone and forms the upper conformable boundary of the Oodnadatta Formation.

The Oodnadatta Formation reaches maximum thickness of about 300m on the flanks of the Nappamerri Trough thinning gradually to the south, and was deposited under low energy marine conditions (Moore and Pitt, 1985). Deposition of the Oodnadatta Formation commenced in response to a major transgression which reinstated the marine conditions within the south-western Eromanga Basin that characterised deposition of the upper Bulldog Shale (Morgan, 1980). Major marine regression in the late Albian was responsible for the cessation of Oodnadatta Formation deposition.

Toolebuc Formation / Wooldridge Limestone Member

Within the lower Oodnadatta Formation is the Wooldridge Limestone Member. This unit is laterally equivalent to the Ursino beds in the south-eastern Eromanga Basin, and the important source rock of the more basinal Toolebuc Formation which conformably overlies the Wallumbilla Formation in the central, northern and eastern Eromanga

Basin (Fig. 1.02) (Ozimic, 1986). The Wooldridge Limestone Member comprises a thin unit of calcareous siltstone with concretionary limestone interbeds, and has an average thickness of 14m. The Toolebuc Formation is very different form the Wooldridge Limestone Member, and it comprises various proportions of calcareous oil shale and coquinite, and can be divided into two distinct laterally equivalent facies (Ozimic, 1986; 1988).

These three time equivalent units were deposited in the Eromanga Basin at a time when conditions were not laterally continuous throughout it. The Toolebuc Formation was deposited in relatively deep basinal and shallower transitional settings within low and fluctuating bottom-water oxygenation levels. Meanwhile, in the south-eastern Eromanga Basin, the Ursino beds were deposited within low energy marine deltaic environments, and in the south-western Eromanga Basin the Wooldridge Limestone Member was deposited under fluctuating non-marine and marine influences with increased fluvial input.

Analyses of foraminiferal faunas have indicated that the deposition of the Toolebuc Formation and equivalents was preceded by a major transgressive pulse which produced peak sea levels within the Eromanga Basin of 50-100m. The increase in sea levels varied from up to 100m in marginal Australian basins to only 10-20m in the south-east Eromanga Basin (Haig and Lynch, 1993). The observation that the transgressive pulse is most evident in the northern marginal basins and diminishes within the epeiric basins towards the south indicates that the northern basins were the main connecting seaway between the shallow Eromanga Sea and the open ocean.

Allaru Mudstone

Conformably overlying the Toolebuc Formation, and laterally equivalent to the middle and upper parts of the "lithologically indistinguishable" Oodnadatta Formation which lie above the Wooldridge Limestone Member (Moore and Pitt, 1985) in the south-western region of the Eromanga Basin, is the Allaru Mudstone. This Albian unit exceeds 300m thickness in places, and represents deposition within shallow, low-energy marine conditions. Both the Allaru Mudstone and the Oodnadatta Formation are overlain conformably by the Mackunda Formation, and in places by its basal Mount Alexander Sandstone Member (Fig.1.02). The Allaru Mudstone and its lateral equivalents represent gradual diachronous regression from the Eromanga Basin (Morgan, 1980) (Fig.1.02).

Mackunda Formation / Mount Alexander Sandstone Member

The Mackunda Formation and the at least partly equivalent Mount Alexander Sandstone Member (Moore and Pitt, 1985) lie conformably over the Allaru Mudstone and the Oodnadatta Formation throughout much of the Eromanga Basin. These units date from the latest Albian to the earliest Cenomanian (Krieg *et al.*, 1991) (Fig.1.02). The Mackunda Formation represents deposition in marginal marine to paralic conditions along a low-energy shoreface deposited in response to a basin-wide regression (Fig.1.02).

The Mackunda Formation and Mount Alexander Sandstone Member are equivalent to the lower part of Forbes' (1966) Blanchewater Formation, which comprises both the Mackunda Formation/Mount Alexander Sandstone Member and the overlying Winton Formation.

1.2.3 Cretaceous non-marine sediments

Winton Formation

The Winton Formation, laterally equivalent to the upper part of Forbes' (1966) Blanchewater Formation, dates from the early to latest Cenomanian (Moore and Pitt, 1985; Krieg *et al.*, 1991) (Fig.1.02). The unit comprises thinly interbedded calcareous sandstones and carbonaceous shales and coals, which represent deposition within non-marine, low-energy fluvial, lacustrine and paludal environments. Deposition of the Winton Formation eventually extended over the entire Eromanga Basin and marked wholesale marine regression (Morgan, 1980) (Fig.1.02).

Mount Howie Sandstone

The Mount Howie Sandstone and its equivalents unconformably overlie Winton Formation in some limited areas and comprise up to 20m of fine to very coarse grained sand. These sediments were deposited as a result of uplift at the end of the Cenomanian and associated change in the depositional regime from that of the Winton Formation to one of localised high-energy channels which eroded into it (Krieg *et al.*, 1991).

1.2.4 Overlying sediments

The Jurassic and Cretaceous sediments of the Eromanga Basin are overlain by a relatively thin veneer of fluviatile, lacustrine and aeolian sediments assigned principally to the mid Tertiary to modern day Lake Eyre Basin (Moore, 1986a).

Chapter 2

Field and core analyses of the Bulldog Shale

2.1 Introduction and localities

Bulldog Shale crops out over large areas of central and northern South Australia (Fig.1.06). Where the unit crops out, the Bulldog Shale is characteristically deeply weathered, and consequently easily eroded; this makes for low-lying flat topography where the only reasonable exposures for study are sections cropping out in the banks of ephemeral outback creeks, or heavily weathered sections in the slopes of mesas and buttes - the remnants of a once higher land surface. Creek sections are rarely in excess of 5m thickness, while sections in hill slopes reach up to about 25m thick, though their deep weathering typically prohibits detailed study. As described in §1.2.2, the Bulldog Shale can reach considerable thicknesses, often in excess of 200m, and on a large scale appears lithologically rather homogeneous; assessing the stratigraphic position of a particular field site and correlation of field sites is thus extremely difficult. The locations of field sites visited in this study are illustrated in Figs.2.01-2.07.

Due to the difficulties of working on field sections, the principle source of data has been obtained from cored material, which provides near complete, relatively unweathered, vertical sections. The location of analysed core holes is illustrated in Figs.2.01-2.07, in which localities of other published cores included in correlations in Chapter 6 are also illustrated. From the above statements it is evident that the study of cored material has implicit advantages over field material. However, field sites also possess their own inherent importance for this study, in that they allow analysis of lateral variation in the deposit.

The trace fossils of the Bulldog Shale are the primary focus of this study. However, these are not dealt with in detail here, for this chapter is intended as a broad introduction to the nature of the Bulldog Shale and its component parts. The ichnotaxonomy of the Bulldog Shale is dealt with in detail in Chapter 3. Furthermore, a model utilising the Bulldog Shale trace fossils in palaeoenvironmental determination is presented in Chapter 4, and is applied to the cored sections described here in that same chapter. The classification of Bulldog Shale field sites, described here, within this scheme, along with details of their trace fossil taxonomy, is given in Appendix 2.

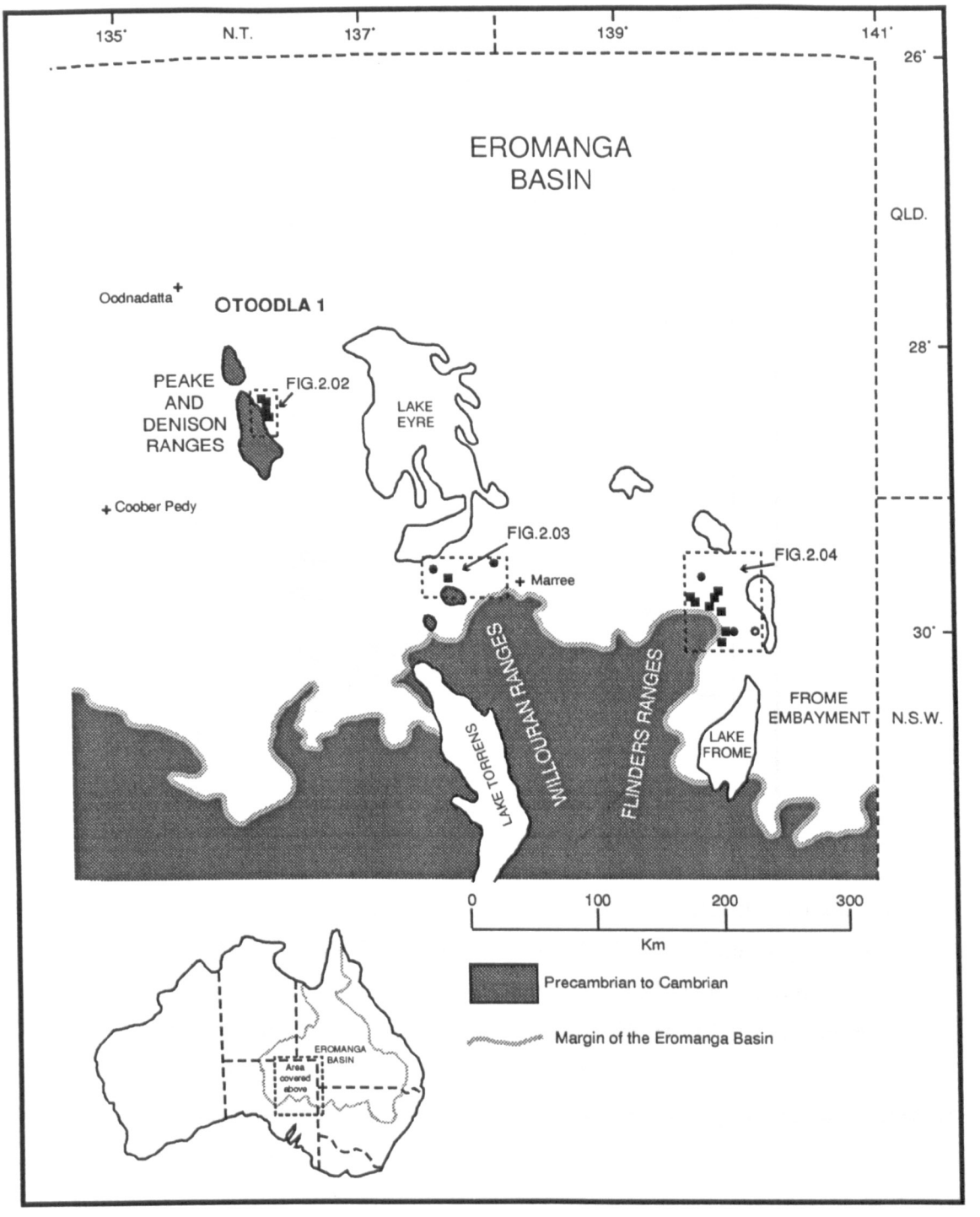

Fig.2.01 South western margin of the Eromanga Basin in South Australia, illustrating regions of outcropping Bulldog Shale, and positions of analysed core hole localities (solid circles), non-analysed core hole localities included for correlative purposes only (open circles) (Toodla 1 (Latitude 27°43'47"S; Longitude 135°50'55"E) is labelled, and field localities (solid squares). Dashed boxes refer to areas illustrated in other figures.

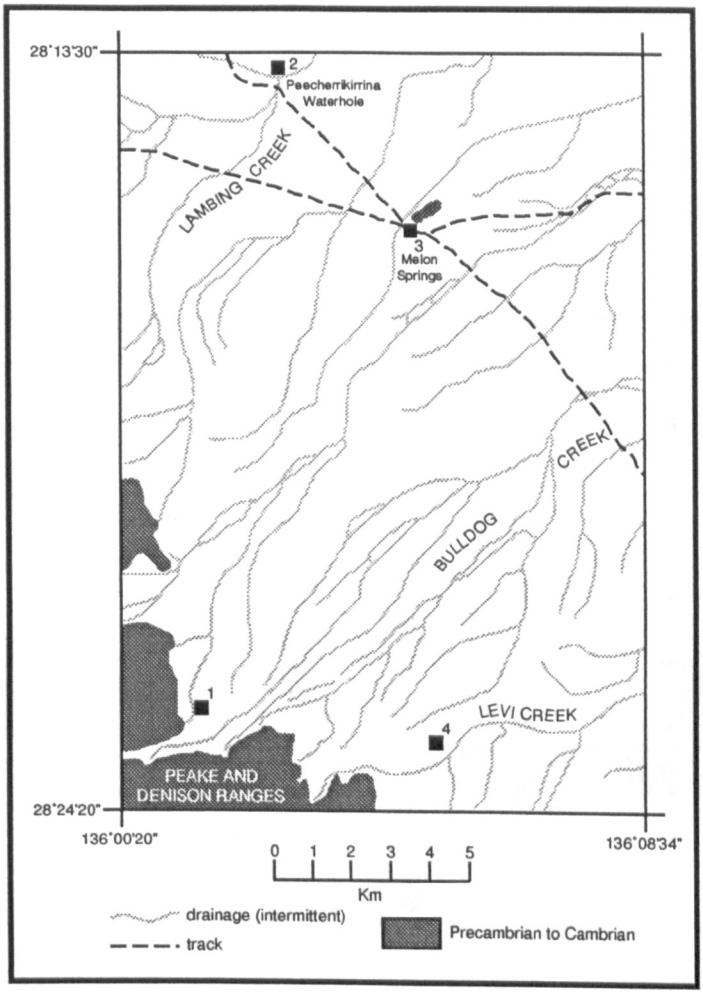

Fig.2.02 Peake and Denison Range field and core sites. 1= Bulldog Creek site (Latitude 28°22'55"S; Longitude 136°01'14"E); 2= Lambing Creek (Peecherrikirrina Waterhole) (Latitude 28°13'51"S; Longitude 136°02'33"E); 3= Melon Springs (Latitude 28°16'00"S; Longitude 136°04'34"E); 4= Levi Creek (Latitude 28°23'14"S; Longitude 136°05'00"E). Redrawn from Umbum 1:87 000 topographic and 1:100 000 geological map sheets.

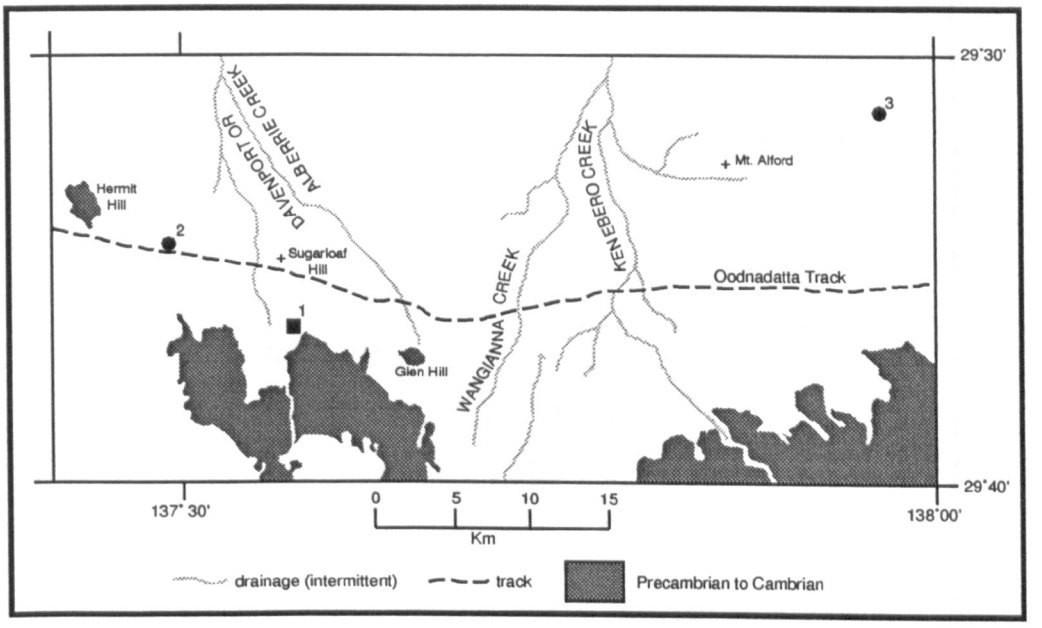

Fig.2.03 Lake Eyre South field and core sites. 1= Davenport Springs site (Latitude 29°39'52"S; Longitude 137°34'31"E); 2= Finniss 2 core hole (Latitude 29°36'52"S; Longitude 137°29'04"E); 3= Alford 1 core hole (Latitude 29°32'11"S; Longitude 137°57'27"E). Redrawn from Curdimurka 1:250 000 geological map sheet.

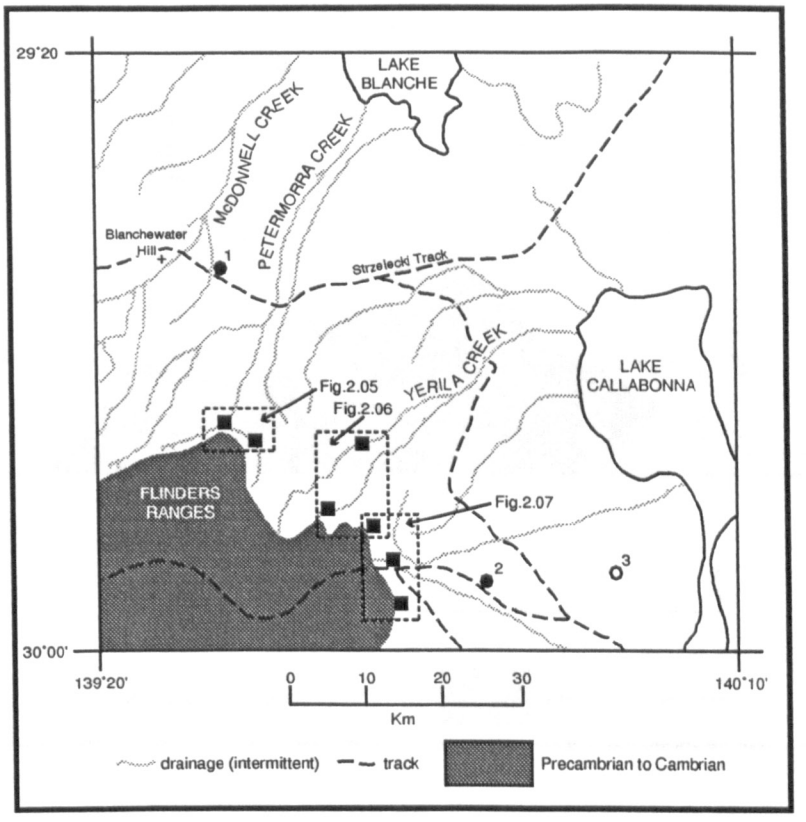

Fig.2.04 Northern Flinders Ranges field and core sites. 1= CBH 2 core hole locality (Latitude 29°34'50"S; Longitude 139°30'00"E); 2= SPH 1 core hole locality (Latitude 29°51'53"E; Longitude 139°51'43"E); 3= Skeleton 2 core hole locality, not analysed - included for correlative purposes only (Latitude 29°54'30"S; Longitude 140°00'54"E). Dashed boxes represent areas figured in greater detail.

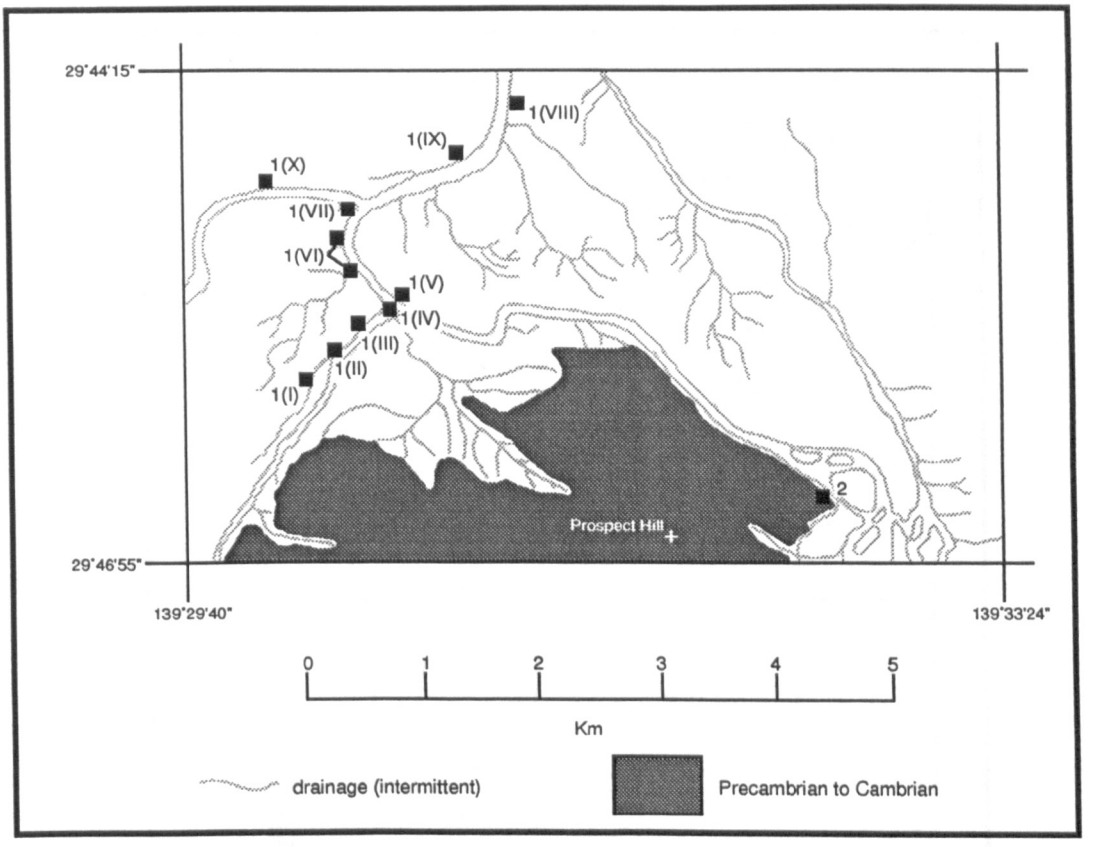

Fig.2.05 Petermorra Creek field and core sites. 1I-X= Petermorra Creek sites (Latitude 29°45'00"S; Longitude 139°30'34"E); 2= Petermorra Springs site (Latitude 29°46'19"S; Longitude 139°32'56"E). Redrawn from Moolawatana 1:50 000 topographic and 1:50 000 geological map sheet, and air photograph: survey 3453 photograph 007.

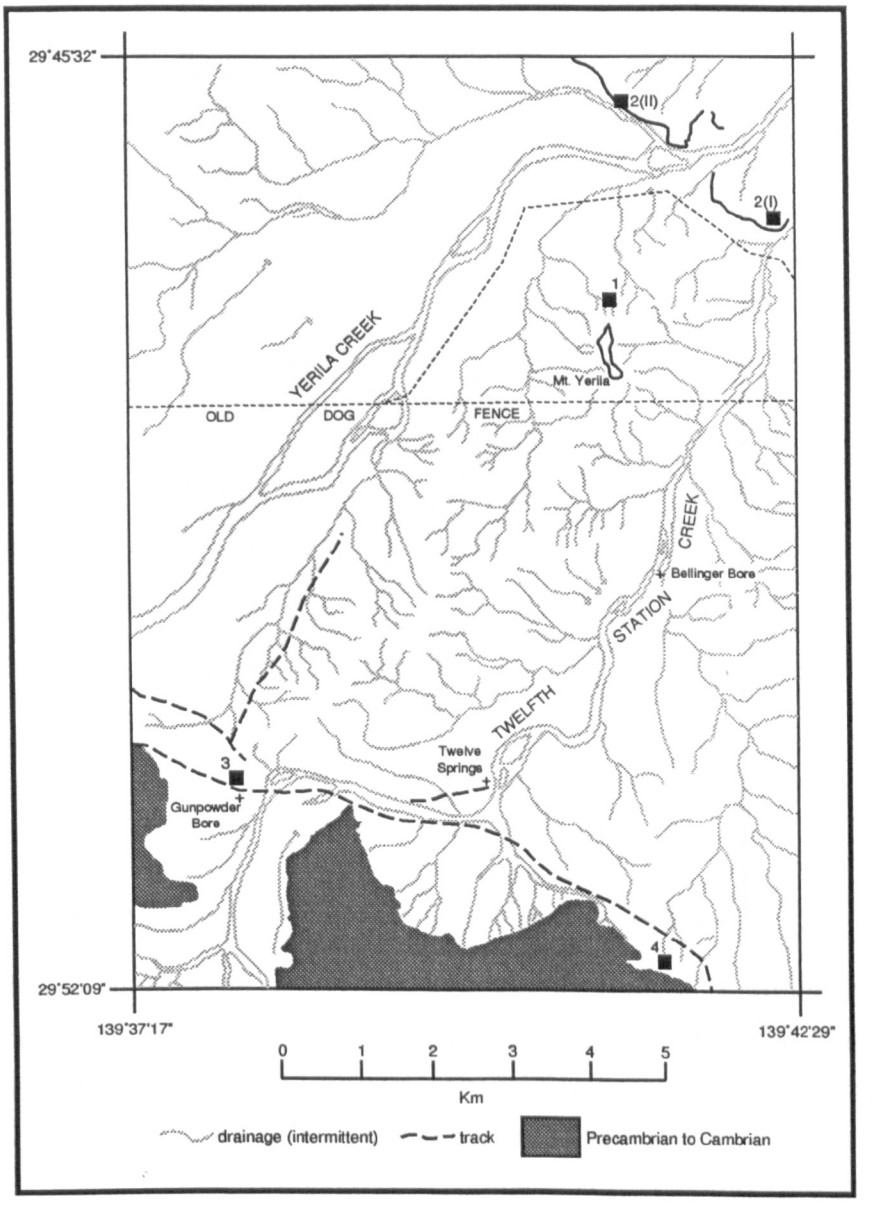

Fig.2.06 Yerila Creek field sites. 1= Mount Yerila logged section (29°47'18"S; Longitude 139°40'56"E); 2I-II= Yerila Creek localities (Latitude 29°45'00"S; Longitude 139°40'34"); 3= Gunpowder Bore (Latitude 29°50'46"S; Longitude 139°37'53"E); 4= boulder bed site (Latitude 29°51'58"S; Longitude 139°41'18"E). Redrawn from Moolawatana 1:50 000 topographic 1:50 000 geological map sheets, and air photographs: survey 3453 photograph 003; survey 3456 photograph 176.

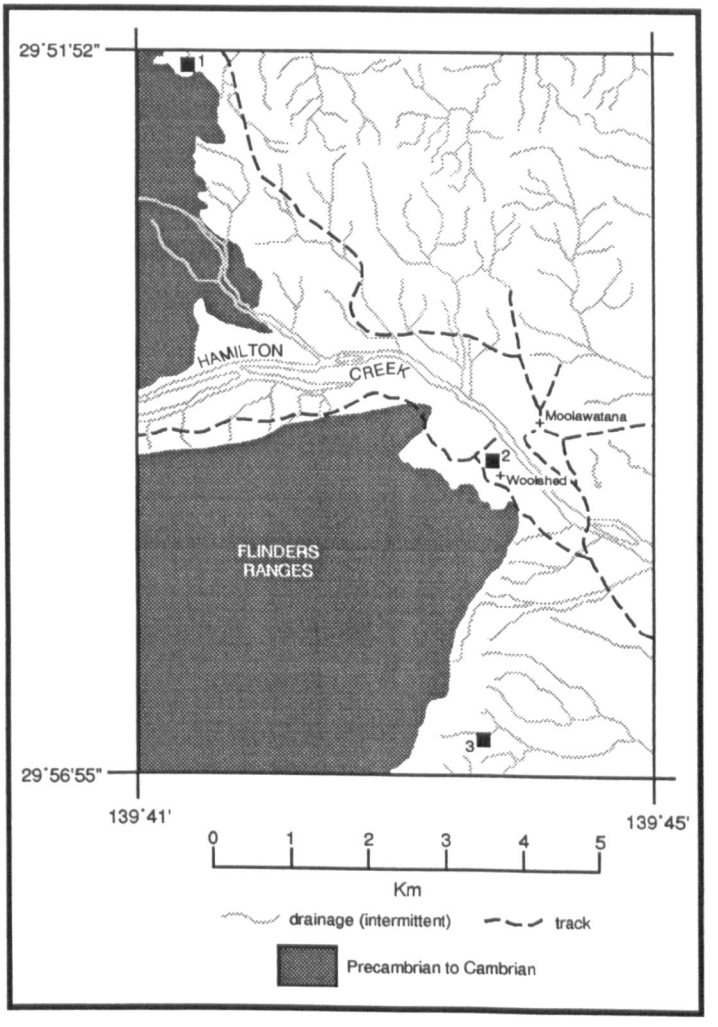

Fig.2.07 Moolawatana field and core sites. 1= boulder bed site (Latitude 29°51'58"S; Longitude 139°41'18"E); 2= Moolawatana shearing shed site (Latitude 29°54'42"S; Longitude 139°43'41"E); 3= Parabarana Hill site (Latitude 29°56'39"S; 139°43'37"E). Redrawn from Moolawatana 1:50 000 topographic and 1:50 000 geological map sheets, and air photographs: survey 3456 photograph 176 ; survey 3457 photograph 104.

Such is the importance of trace fossils in the Bulldog Shale that they cannot go unmentioned in any account of the rock. Therefore, in this chapter, a simple approach is taken, and trace fossils, or more accurately bioturbation, is divided into three groups. Bioturbation is the term which refers to the mixing of sediments by organisms (Richter, 1952), and which leads to the obliteration of the original sedimentary structures and the creation of new structures which may be preserved as trace fossils (Bromley, 1990). In this chapter, bioturbation levels are divided into: low, referring to intensities of 0-30% of the rock fabric, and taxonomic diversity from 0-4 ichnotaxa; moderate, referring to intensities of 30-90%, and diversity from 4-7 ichnotaxa; and high, referring to intensities of 90-100%, and diversity from 7-12 ichnotaxa.

2.1.1 Core and field sections analysed in this study

Summary logs and details of each of the four cores analysed in this study (Finniss 2, Alford 1, CBH 2 and SPH 1) are presented here along with those for the extensive Mount Yerila field section (§2.2). Only one field section is included here, since it is a rare example of a vertically extensive exposure. All cores are stored in the Mines and Energy South Australia core library in Adelaide. Other cores are available, and more were initially planned for study, however it was found most useful to study a few cores in detail rather than many vaguely.

Location of the cores and field section are given in Fig.2.01 (all cores and section), Fig.2.03 (Finniss 2 and Alford 1), Fig.2.04 (Mount Yerila, CBH 2 and SPH 1) and Fig.2.06 (Mount Yerila).

A key to the symbols utilised in the summary logs here, in the logs of Chapter 5 and in the logs and basin correlation diagrams of Chapter 6 are given in Fig.2.08.

Palynostratigraphic dates are applied to the core and field sections (as described in §1.2) where available. The palynostratigraphy zonation followed here is that defined by Helby *et al.* (1987), and is that most commonly utilised in the dating of Eromanga Basin Mesozoic sediments (Fig.2.09).

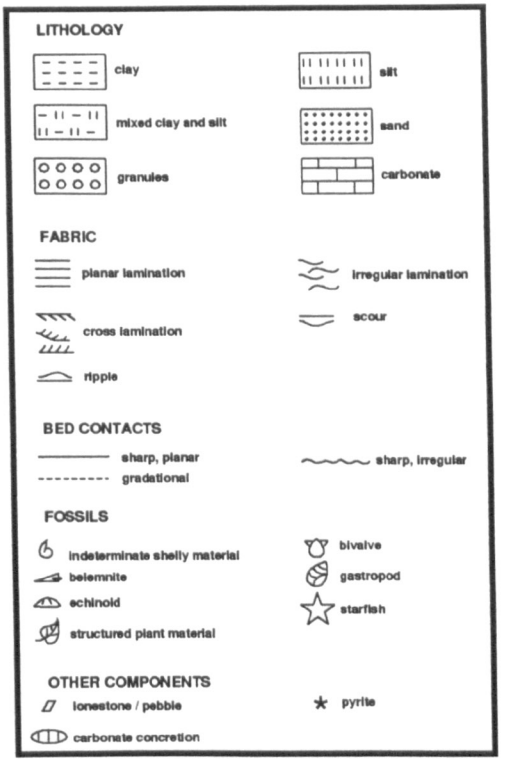

Fig.2.08 Key to the symbols utilised in all Bulldog Shale logs presented here and in Chapters 5 and 6.

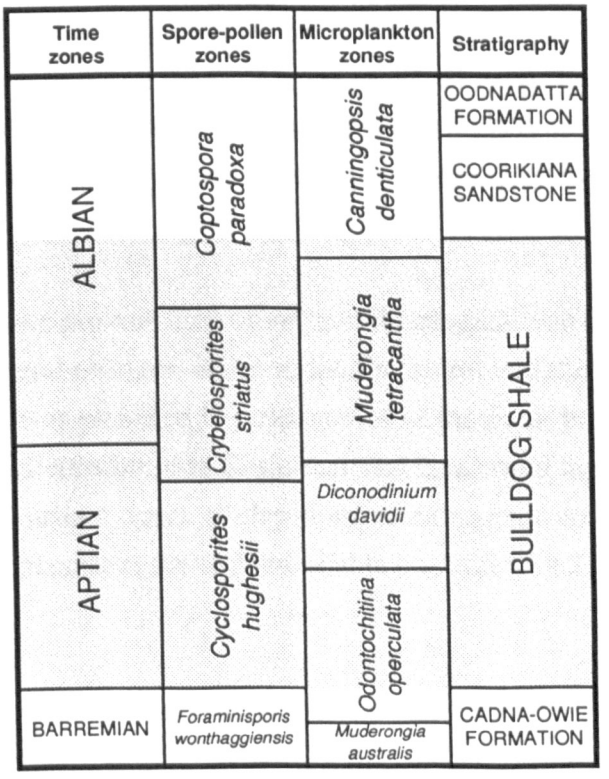

Fig.2.09 The palynostratigraphy of the Bulldog Shale as proposed by Helby *et al.* (1987). Redrawn from Krieg *et al.* (1991).

Core preparation for study

Flat, fresh and clean surfaces of core were required for the logging of the cored sections, and associated palaeoenvironmental analyses (§Chapter 4). To achieve such faces the cored rock was cut in half utilising a water-reticulated diamond saw. Unfortunately, the highly friable nature of the Bulldog Shale and its large content of "swelling clays" resulted in near total disintegration when the water reticulation was in use, even when cut down to minimum levels. Dry cutting on the other hand produced excellent results, however the high levels of dust produced with this technique required the saw operator to wear protective clothing and a face mask. An industrial vacuum cleaner was placed near the saw blade to reduce dust. In analysing the cut core faces, water was applied to wash off dust and to enhance differences between clay-rich parts of the rock and silt-rich regions, which resulted in only minor fragmentation when used sparingly. Quarter core samples were taken for later geochemical and microscope analyses, and for future reference. Core photography was conducted using a tripod mounted camera with natural Australian daylight as the sole source of illumination.

2.2 The Bulldog Shale in core and field section

Logs of the core and field sections are presented and described here in order from west to east. Brief sedimentary descriptions are given and serve as lithological summaries of the unit. Elsewhere, descriptions of lithology and variation are provided in Figs.2.19, 2.20 and 2.21 from this chapter. Lithological characterisation and variation, and illustration of physical sedimentary structures, are also provided in the Palaeoenvironmental Fabric Type methodology (§ Chapter 4).

While cored sections provide data of vertical lithological variation, they allow little appreciation of lateral changes. More scope for lateral variation of the Bulldog Shale and associated units is provided in field studies of the basal boundary (§2.3) and upper boundary (§2.4). Middle Bulldog Shale material (see cored material for lithological detail) comprises various scales of clay-dominated and silt-dominated interbeds typically laterally persistent throughout visible outcrop (Fig.2.10).

Fig. 2.10 Laterally persistent interbedded clay-dominated and silt-dominated horizons from site IX, Petermorra Creek (Fig.2.05 for locality).

Elsewhere, variation can occur over a scale of less than 10m, probably in response to sampling at various points on large bedforms; for example in the Mt. Yerila section (Fig.2.06 for locality; Fig.2.13 for summary log), lateral impersistence of silt and sand-dominated bodies is noted.

Other components of the Bulldog Shale, namely: carbonate concretions, lonestones, various minerals and glendonite nodules, also exhibit varying lateral distributions, and are dealt with later in this chapter.

Also of fundamental importance is the composition of the Bulldog Shale in thin section microscopy studies. Descriptions of component parts of Bulldog Shale material in thin section material are given in Chapter 5, where they are interpreted in relation to the method of palaeoenvironmental classification and determination outlined in Chapter 4.

2.2.1 Finniss 2 core

Location: Latitude 29°36'52"S; Longitude 137°29'04"E (Core report by Rogers *et al.*, 1989).

Thickness

Total depth reached in Finniss 2 is 106.57m from a ground elevation of +23.15m, and solely comprises a 101.00m thick Bulldog Shale succession unconformably overlying Precambrian Adelaidean metasediments at 104.00m (Fig.2.11).

Completeness

The Finniss 2 Bulldog Shale succession comprises a nearly complete fully cored sequence of the lower part of the unit.

Dating and palaeoenvironmental interpretation

Palynostratigraphic studies indicate that all the Bulldog Shale from Finniss 2 is from the basal part of the section (Rogers *et al.*, 1989), comprising sediments from the *Cyclosporites hughesii* spore-pollen zone and the *Odontochitina operculata* dinoflagellate zone (Fig.2.09). Rogers *et al.* (1989) noted that the palynostratigraphy indicates that sediments between 104-68m depth were deposited in open marine conditions, while sediments from 68m and above, to the top of the Finniss 2 Bulldog Shale succession, represent shallower and more restricted, possibly even paralic, conditions.

Sedimentary description

The summary log of the Finniss 2 Bulldog Shale succession is given in Fig.2.11.

In Finniss 2, the Bulldog Shale rests unconformably on Adelaidean metasediments, the upper 4cm of which exhibit weathering, a result of subaerial exposure prior to Bulldog Shale deposition. The metasediments from this locality were bypassed by sedimentation prior to deposition of the Bulldog Shale, for they form the 'basement' high of Hermit

Hill. The lowermost 25m of the Bulldog Shale in Finniss 2 comprises a series of fining upwards and coarsening upwards layers of variable clay and silt content, erosively based, often with a lag of reworked lonestones of various lithologies (§2.6). Indeed, lonestones are common within the Finniss 2 core particularly towards the base, both as lags to fining upwards cycles and as isolated units within otherwise fine grained material. The concentration of lonestones in the basal 10m of the section provided the reasoning for Rogers *et al.* (1989) designation of that region to the Wilpoorinna Breccia Member (§1.2.2). That designation is not held here, for although lonestones are common in this region they are emplaced within typical Bulldog Shale material and do not reach concentrations high enough to match other sections of the Wilpoorinna Breccia Member. Bioturbation levels and diversity within the basal 25m are highly variable, though they exhibit a gradual transition from high, in some regions total, bioturbation at the base, to very low levels by 80m. Physical sedimentary structures in this region comprise planar and irregular laminae, interbedded with thin (less than 5mm thick) silty and sandy interbeds, which bear scoured bases, planar lamination and rippled lamination, and which decline in thickness and frequency up-core. Laminae are typically 0.5-1.0mm thick.

From 80-51m, the rock comprises clay-dominated material, with a silt component from 0-40%. Physical sedimentary structures comprise planar and irregular lamination, and very occasional rippled lamination. Bioturbation is typically low intensity.

The region 51-27m consists of a gradual coarsening upwards succession from clay-dominated material to siltstone, with a corresponding increase in silty interbeds, rippled lamination, and cross-lamination. Bioturbation also increases, and much of the region between 39-27m is totally bioturbated.

The uppermost part of the Finniss 2 core, from 27-3m consists of clay-dominated silty claystone, bearing planar and irregular laminations and occasional cross-lamination. Bioturbation is at generally low levels.

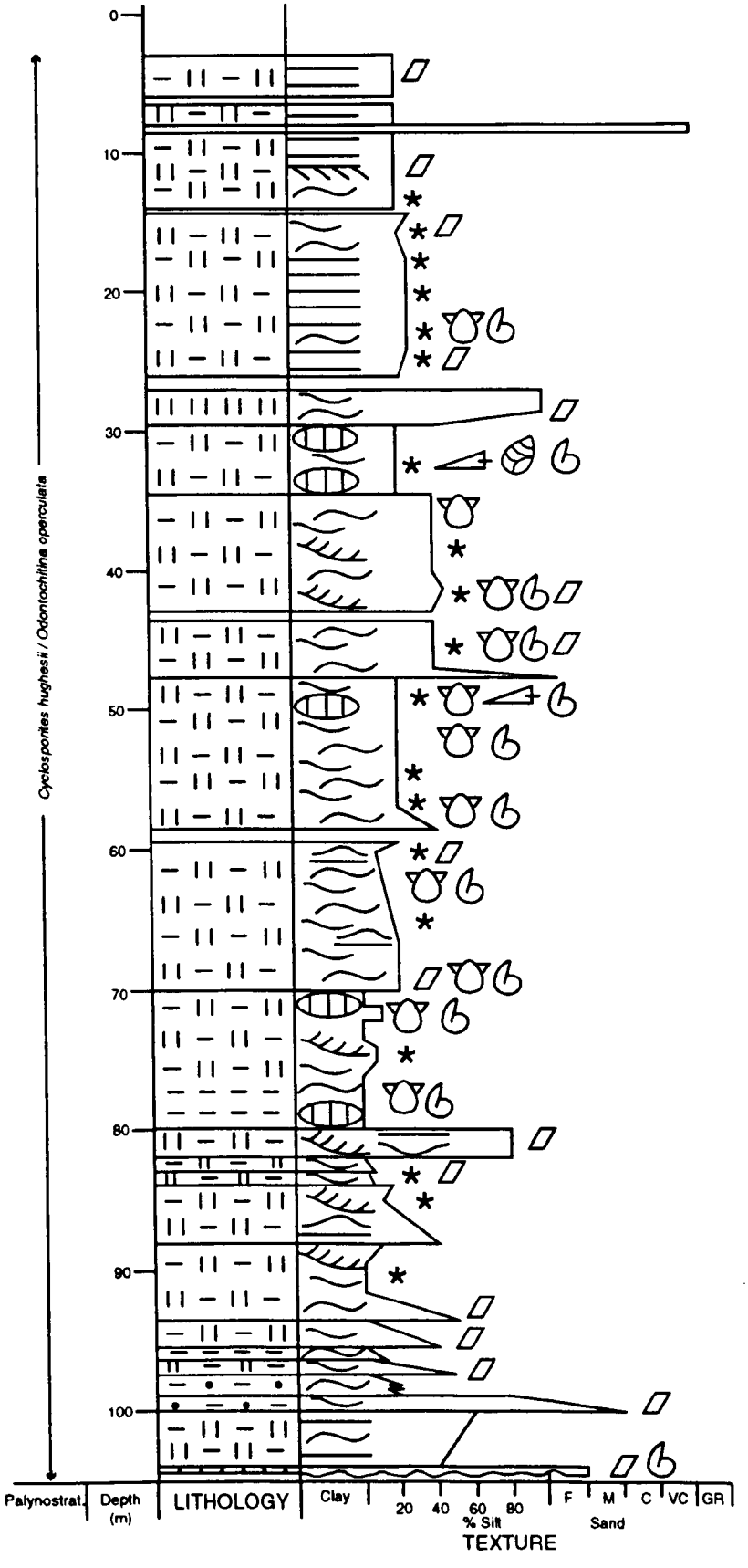

Fig.2.11 Summary log of the Finniss 2 Bulldog Shale succession. For key to symbols see Fig.2.08.

2.2.2 Alford 1 core

Location: Latitude 29°32'11"S; Longitude 137°57'27"E (Core report by Rogers *et al.*, 1989).

Thickness

Total depth reached in Alford 1 is 70.00m from a ground elevation of +65.10m. Of this succession, the Bulldog Shale comprises the basal 28.40m, and is overlain by Coorikiana Sandstone at 41.60m depth.

Completeness

The Alford 1 Bulldog Shale succession comprises a complete, fully cored sequence of the upper Bulldog Shale.

Dating and palaeoenvironmental interpretation

Bulldog Shale sediments here represent only the uppermost part of the section in this area, corresponding to the *Coptospora paradoxa* spore-pollen zone (Rogers *et al.*, 1989) (Fig.2.09), and thus it is likely that significant parts of the Bulldog Shale section are missing between the top of the cored section in Finniss 2 and the base of the cored section in Alford 1. Studies of microplankton diversity indicate that these Bulldog Shale sediments were deposited in shallow water to paralic conditions, with possibly slightly deeper water indicated in the basal part of the section (Rogers *et al.*,1989).

Sedimentary description

The summary log of the Alford 1 Bulldog Shale succession is given in Fig.2.12.

The Bulldog Shale in Alford 1 comprises a coarsening upwards succession, from silty claystone (silt content approximately 45%) at the base of the core (70m), to near pure siltstone at the top of the unit. Silty interbeds are common, and increase in thickness and frequency up-core. Bioturbation is generally moderate to high from 70-50m, where it typically obscures the physical sedimentary structures. Where present these comprise planar and irregular silty lamination, cross and rippled lamination. Above this, from 50m to the top of the succession, bioturbation is low to moderate, and silty and sandy cross and planar laminations dominate.

At 41.60m the Bulldog Shale is overlain by the Coorikiana Sandstone, across a boundary which experienced at least minor erosion between deposition of the two units.

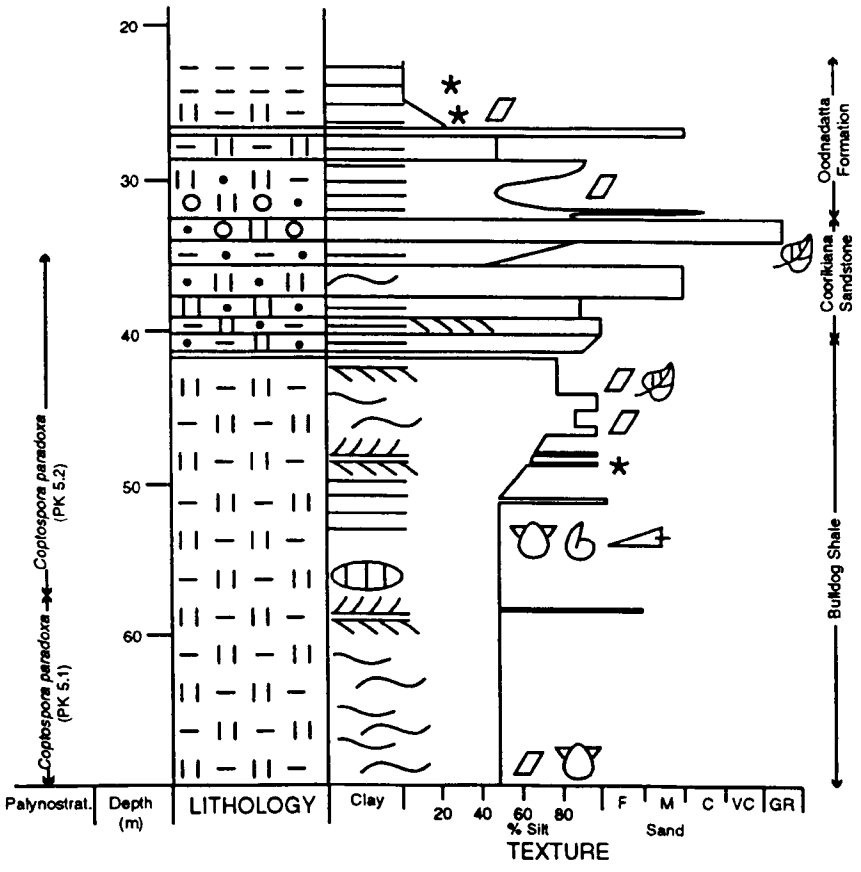

Fig.2.12 Summary log of the Alford 1 Bulldog Shale succession. For key to symbols see Fig.2.08.

2.2.3 CBH 2 core

Location: Latitude 29°34'50"S; Longitude 139°30'E (Preiss and Harris, 1982).

Thickness

Total depth reached in CBH 2 is 750.00m from a ground elevation of approximately +50.00m. The Mesozoic sequence unconformably overlies a sedimentary sequence of possible Cambrian age at approximately 605.50m (Preiss and Harris, 1982). The Bulldog Shale sequence from CBH 2 overlies Cadna-owie Formation at 509.60m, and is overlain by Coorikiana Sandstone at 314.50m. In total, the CBH 2 Bulldog Shale comprises a section 195.10m in thickness.

Completeness

The CBH 2 Bulldog Shale succession comprises a near complete fully cored sequence of the entire unit.

Dating and environmental interpretation

Palynostratigraphic studies are summarised in the summary log (Fig.2.13). It is evident that the lowermost Bulldog Shale (below 461.00m) in CBH 2 represents the *Odontochitina operculata* dinoflagellate zone (Harris, 1982), while one sample from 343.70m represents the *Crybelosporites striatus* spore-pollen zone and the *Muderongia tetracantha* dinoflagellate zone (Alley pers. comm. 1995), and samples from the uppermost Bulldog Shale at 337.70m and 314.40m represent the *Coptospora paradoxa* spore-pollen zone (Alley pers. comm. 1995) (Fig.2.09). Alley (pers. comm. 1995) also noted that the samples from 343.70m and 337.70m were indicative of open marine conditions, while the sample from 314.40m was indicative of very marginal marine conditions.

Sedimentary description

The summary log of the CBH 2 Bulldog Shale succession is given in Fig.2.13.

In CBH 2 the Bulldog Shale rests on Cadna-owie Formation, and the boundary is marked by a cone-in-cone limestone layer from 510.10-509.60m depth, probably correlative with the "C" horizon. The "C" horizon forms a basin-wide concretionary layer which is thought to occur just below or at the Cadna-owie / Bulldog Shale boundary (Alley and Sheard pers. comm. 1993). Beneath this layer typical Cadna-owie Formation material is evident, composed of poorly sorted clay, silt and fine to coarse-grained sandy sediments, with large amounts of plant material, bioturbation variable and is in some places total. Basal Bulldog Shale material overlies the "C" horizon, and is composed of several fining-upwards cycles superimposed over a general fining-upwards trend from 509.60-507.00m. These sediments are generally poorly sorted silts, sands and muds, physical sedimentary structures are not well preserved, partly due to generally near complete bioturbation.

Overlying this basal assemblage, between 507.00m and 495.00m, is a succession of near pure claystone with silt content increasing from negligible to approximately 10% by 495.00m. Physical sedimentary structures comprise planar lamination and rare cross lamination. Laminae approximately 0.5mm thick. Bioturbation is virtually absent.

The depth interval 495.00m to 491.50m comprises a coarsening upwards succession from clay dominated silty claystone to near pure siltstone. This is overlain, across an erosive boundary, by near pure siltstone up to 483m depth. Bioturbation is low in this region, and silty physical sedimentary structures form much of the rock fabric.

Overlying this region is a thick clay-dominated succession from 483.00m to 355.00m, characterised by planar lamination and low to moderate bioturbation. Some fluctuations do occur, notably between 462.50m and 421.50m, where silt content is higher (only rarely over 40%), and bioturbation reaches moderate levels.

Above 355.00m the sediments coarsen upwards to become near pure siltstone by 350.00m. Bioturbation also increases, though above 353.50m silty physical sedimentary structures dominate. Between 353.50m and the boundary between Bulldog Shale and Coorikiana Sandstone at 326.50m, near pure siltstone dominates, characterised by well preserved physical sedimentary structures, namely planar silty lamination, cross lamination and hummocky cross-stratification. Interbedded with these sediments are slightly muddier horizons in which bioturbation is total.

It is likely that the top Bulldog Shale experienced some erosion prior to deposition of the Coorikiana Sandstone.

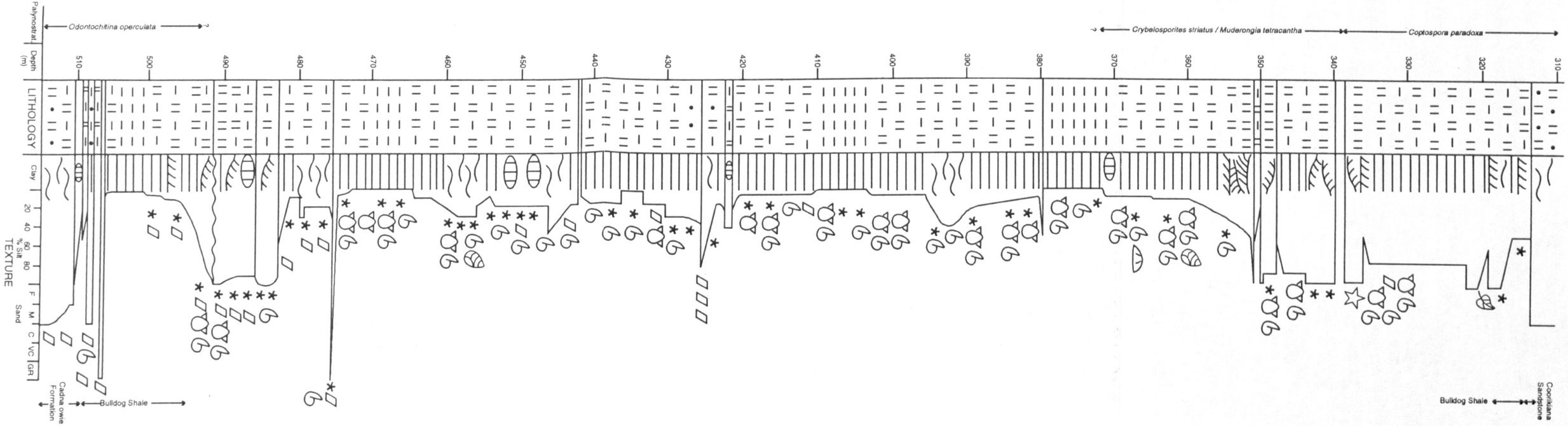

Fig.2.13 Summary log of the CBH 2 Bulldog Shale succession. For key to symbols see Fig.2.08.

2.2.4 Mount Yerila field section

Location: Latitude 29°47'18"S; Longitude 139°40'56"E.

Thickness

The Mount Yerila section comprises upper Bulldog Shale material of 26m thickness, overlain by the Coorikiana Sandstone.

Completeness

The Mount Yerila section provides a complete succession of the upper Bulldog Shale, though considerable time must be spent removing weathered layers. The section is exposed in creek banks and the northern slopes of Mount Yerila.

Dating

Palynostratigraphic studies have defined this section as representing the *Crybelosporites striatus* spore-pollen zone (Fig.2.09) (Alley pers. comm. 1994).

Sedimentary description

The summary log of the Mount Yerila section is presented in Fig.2.14.

The Bulldog Shale succession at Mt. Yerila comprises similar material to the upper Bulldog Shale described from Alford 1 and CBH 2. The succession is composed of dm to m scale interbeds of near pure silt/sand horizons, dominated by physical sedimentary structures, and more clay rich layers of cm scale interbedded silts and clays. In these latter beds, the silty layers are typically planar laminated and slightly bioturbated, while the more clay-rich layers are moderately to highly bioturbated, with only poorly preserved sedimentary structures.

The boundary surface between the Bulldog Shale and the Coorikiana Sandstone bears evidence of erosion prior to Coorikiana Sandstone deposition (§2.4).

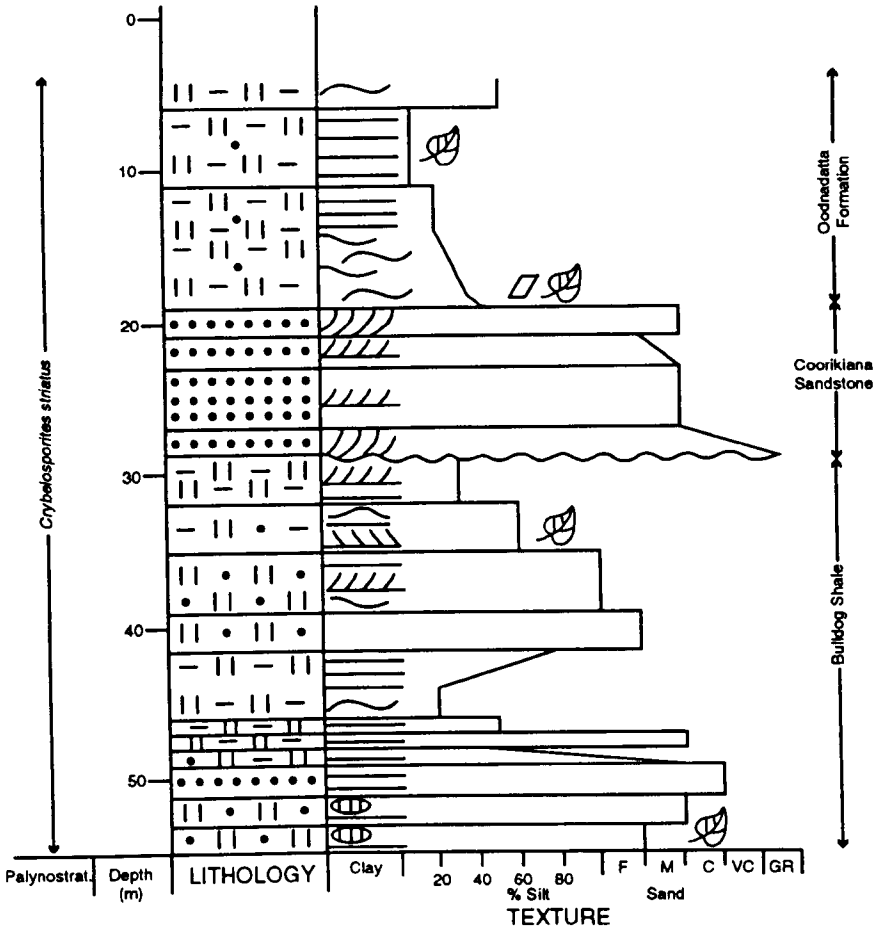

Fig.2.14 Summary log of the Mount Yerila Bulldog Shale succession. For key to symbols see Fig.2.08.

2.2.5 SPH 1 core

Location: Latitude 29°51'53"S; Longitude 139°51'43"E within the Frome embayment of the Eromanga Basin (Fig.2.01; 2.04).

Thickness

Total depth reached in SPH 1 is 627.00m from a ground elevation of +53.00m, and is completely cored from depth 276.00m to the base. Bulldog Shale directly overlies basement rocks at 414.00m, and a Bulldog Shale succession of 138.00m thickness has been recovered.

Completeness

The SPH 1 Bulldog Shale succession comprises a nearly complete fully cored succession of almost the entire sequence. Only the very uppermost parts of the unit, and its contact with the Coorikiana Sandstone are missing (Fig.2.15).

Dating and palaeoenvironmental interpretation

Palynostratigraphic studies indicate that the Bulldog Shale from sample depths 413.95m and 381.30m date from the *Cyclosporites hughesii* spore-pollen zone and the *Odontochitina operculata* dinoflagellate zone, while the Bulldog Shale sediments from sample depths 278.50m and 274.30m date from the *Crybelosporites striatus* spore-pollen zone (Fig.2.09; 2.15) (Alley pers. comm. 1994). It should be noted that these samples, while giving dates for the basal and uppermost Bulldog Shale, do not constrain the position of the *Cyclosporites hughesii / Crybelosporites striatus* zonal boundary. Alley (pers. comm. 1994) also noted that the sample from 413.45m represents deposition in open marine conditions, while that from 381.30m is indicative of deposition in shallow marine conditions, and those from 278.50m and 274.30m are indicative of deposition in very shallow marine conditions.

Sedimentary description

The summary log of the SPH 1 section is presented in Fig.2.15.

Bulldog Shale material in the core SPH 1 overlies 'basement' metasediments, on a weathered surface at 414.00m. In this core the base of the Bulldog Shale comprises a poorly preserved lag of coarse-grained, predominantly quartz, sand with granule and pebble-sized angular and sub-spherical clasts. This basal layer grades up into typical grey and waxy, slightly silty claystone within 10cm. None of the fining and coarsening upwards cycles present in Finniss 2 and CBH 2 exist in the SPH 1 section.

The bulk of SPH 1 is dominated by near pure claystone, from 413.90m to 315.00m. Within this region, planar and irregular lamination dominates (individual laminae 0.5-1.0mm thick), and bioturbation is typically at low, or more occasionally moderate, levels. Regions of notable exception are 385.00-377.50m and 352.50-343.50m, where silt contents are slightly higher (up to 30%), sedimentary structures comprise thin (approximately 5mm thick) silty interbeds and irregular lamination, and bioturbation is at moderate levels. More aberrant is a thin sand-rich layer between 337.00m and 336.00m.

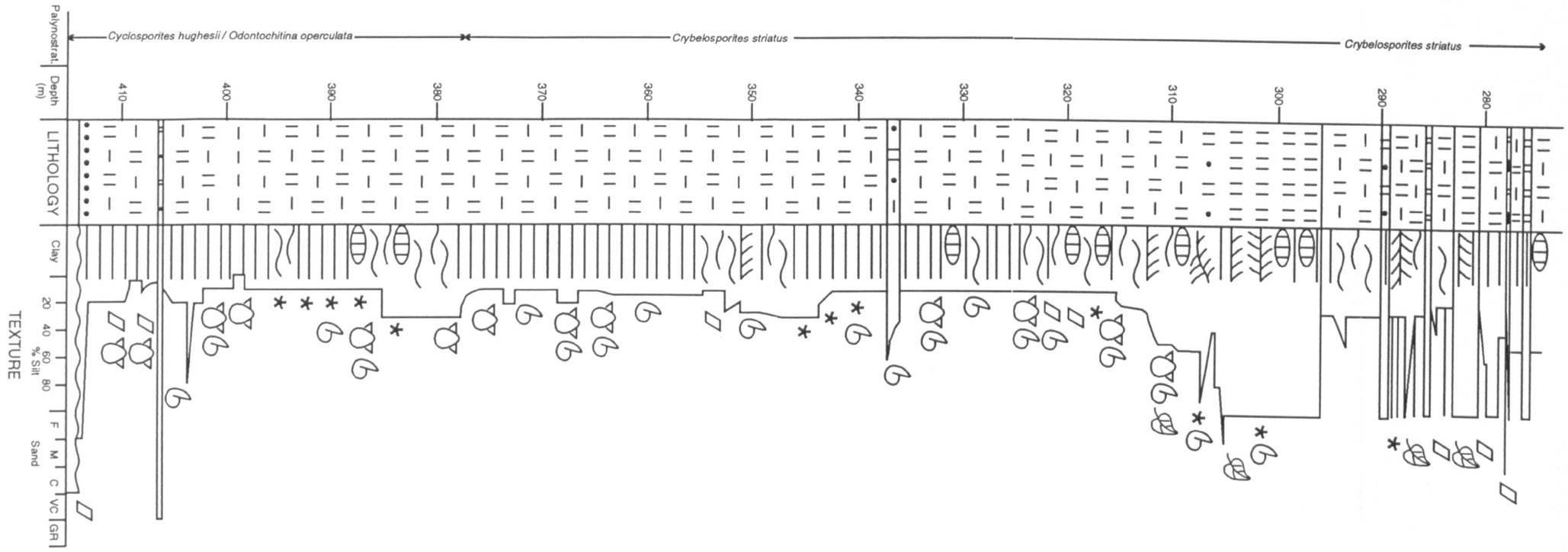

Fig.2.15 Summary log of the SPH 1 Bulldog Shale succession. For key to symbols see Fig.2.08.

Between 315.00m and 307.50m the core rapidly coarsens upwards to reach approximately equal amounts of clay and silt material. Bioturbation is dominant in this region, and the rock fabric is nearly totally bioturbated. Thus, physical sedimentary structures are almost completely obliterated, though where present they comprise irregular lamination and cross lamination.

Above 307.50m up to the top of the core at 276.00m, the rock is dominated by silt and sand dominated horizons bearing well preserved physical sedimentary structures, namely planar silty lamination, cross lamination and hummocky cross stratification. Interbedded with these horizons are more clay-rich units of cm-scale interbedded clay-dominated and silt-dominated horizons, both bearing variable amounts of physical and biogenic sedimentary structures.

2.3 Basal boundary of the Bulldog Shale

In the south-western Eromanga Basin, the basal Bulldog Shale unconformably overlies Precambrian and Cambrian basement rocks, and conformably to disconformably overlies upper Cadna-owie Formation or Parabarana Sandstone (Fig.1.05).

2.3.1 Bulldog Shale directly overlying basement

Bulldog Shale typically directly overlies topographic high basement rocks, where earlier Mesozoic sedimentary deposits were either simply not deposited or suffered erosion prior to Bulldog Shale deposition. Good examples of such basement highs occur at Melon Springs, 5km south west of Peecherrikirrina Waterhole in Lambing Creek (Fig.2.02, 2.16), and where the Bulldog Shale directly onlaps the Peake and Denison Ranges (Fig.2.02, 2.17), though this contact is, at least in part, faulted (Alley, pers. comm. 1993). It is likely that these basement highs were, at least at times, islands within the Eromanga Sea at the time of Bulldog Shale deposition.

Elsewhere, the boundary between basement rocks and Bulldog Shale exhibits additional features. At Petermorra Springs (Fig.2.05), the basement material has been imparted with a smooth polished glass-like surface which is rapidly weathered upon exposure. Sheard and Flint (1992) interpreted this, and similar features elsewhere, to represent polishing by wave action, while Rogers and Freeman (in prep) go further and state that the polished surfaces most likely represent wave-cut rock platforms formed during the transgression of the sea during the time of Bulldog Shale deposition.

Fig.2.16 Basement highs rising out of the flat Bulldog Shale landscape at Melon Springs.

Fig.2.17 Bulldog Shale pediment onlapping basement highs of the Peake and Denison Ranges - maximum height 239m, photograph taken from 30m elevation (approx.).

Sheard and Flint (1992) also noted the occurrence of basal boulder facies and coquina layers from the Peake and Denison region, also interpreted as shore facies.

A boulder-dominated basal Bulldog Shale unit resting directly on basement, and interpreted by Alley and Sheard (pers. comm. 1993) as resulting from high energy beach processes, is also exposed in a tributary of Twelfth Station Creek, 3.4km south east of Twelve Springs (Fig.2.06, 2.07). This deposit is 2-3m thick, directly overlies basement material and is itself overlain by basal Bulldog Shale. The boulder beach dips approximately northwards towards the basin centre, and comprises well rounded boulders of medium to high sphericity with the interstices infilled with a carbonate-cemented matrix composed of coarse sandstone, cone-in-cone limestone and occasional shelly material (Fig.2.18). Individual boulders are mostly locally derived basement metasediments and granites, with some Gawler Range volcanics and occasional Devonian sandstone lithology; individual boulders exhibit a high degree of polishing and some imbrication, and are often associated with shell hash material (Fig.2.18). In addition, many boulders are overlain by up to 30cm of cone-in-cone carbonate.

The Bulldog Shale directly overlies the boulder beach, and in places partially infills the interstices, and presumably was deposited as the sea transgressed and the shoreline migrated further south, away from the basin centre. Typical basal Bulldog Shale fabric associations are observed here, comprising near pure silt horizons up to 10mm thick interbedded with clay-dominated horizons (Fig.2.19). Physical sedimentary structures comprise planar lamination, with some low angle cross-lamination in the silty interbeds. Bioturbation is at variable levels. The sudden deposition of these relatively deep water clay-dominated sediments (§4.4.2), observed here and elsewhere (see basal Bulldog Shale from SPH 1 core (Fig.2.15)), and the lack of shallower-water sediments representing deposition through the lower shoreface and transition zone indicates sediment starvation, at least during the initial transgression.

Cored Bulldog Shale successions resting unconformably on basement material have also been recovered and, of the cores analysed in this study, both Finniss 2 (§2.2.1) and SPH 1 (§2.2.5) exhibit this arrangement.

A

B

Fig.2.18 A: General view of boulder beach; M. Sheard for scale. B: Close up view of individual boulders, which include grey local metasediments and red granite porphyry; yellow scale = 50cm.

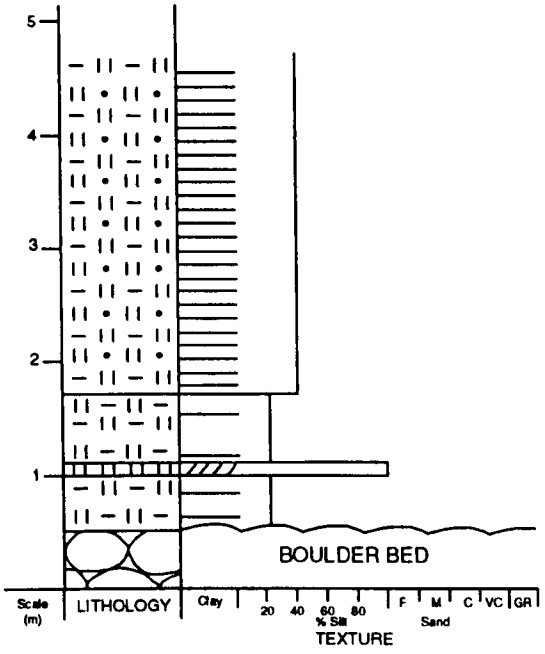

Fig.2.19 Summary log of boulder beach section. For key to symbols see Fig.2.08.

2.3.2 Bulldog Shale overlying Cadna-owie Formation and the Parabarana Sandstone Member

Away from isolated basement highs the Bulldog Shale is generally underlain by the Cadna-owie Formation. The boundary between the two units is considered to be in places conformable and in others disconformable (§1.2.2). Two types of boundary are considered here: those where the Bulldog Shale rests directly over typical Cadna-owie Formation, generally in those exposures more distal to the basin margin; and those where the Bulldog Shale rests on the Parabarana Sandstone Member of the upper Cadna-owie Formation, typically in those exposures more proximal to the basin margin (§1.2.2).

Bulldog Shale overlying Cadna-owie Formation

The boundary between upper Cadna-owie Formation and the Bulldog Shale is well exposed at Bulldog Creek and Levi Creek to the east of the Peake and Denison Ranges (Fig.2.01, 2.02). At the Bulldog Creek site, the uppermost Cadna-owie Formation comprises poorly sorted sandy material overlying a carbonate concretionary and cone-in-cone limestone bearing horizon (Fig.2.20) which may be correlative with the "C" horizon. The overlying Bulldog Shale comprises interbedded planar laminated clay dominated and silt-sand dominated units, bioturbation levels variable from absent to moderate. This material gradually fines upwards into planar laminated thick slightly

silty claystone units of absent to low bioturbation. At the same locality, Bulldog Shale material has been deposited within a channel cut into Cadna-owie Formation, and thus the Cadna-owie / Bulldog Shale boundary may be considered disconformable, representing a hiatal surface with localised erosion.

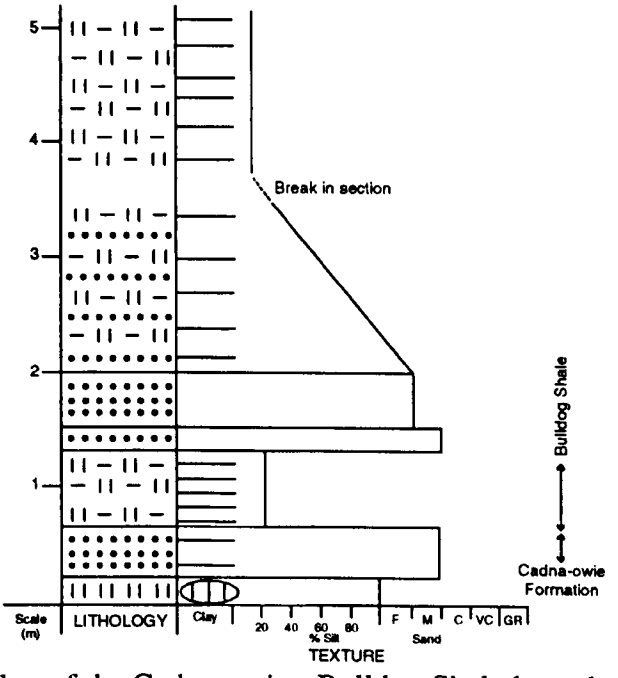

Fig.2.20 Summary log of the Cadna-owie - Bulldog Shale boundary at Bulldog Creek. For key to symbols see Fig.2.08.

At Levi Creek (Fig.2.01, 2.02), Cadna-owie Formation is uplifted such that it directly overlies basement material along the flanks of the Peake and Denison Range. Due to this structural uplift, the Cadna-owie Formation of Levi Creek dips at up to 40° east, and thus its contact with the Bulldog Shale is exposed downstream in the creek banks, beyond which the beds rapidly flatten out to become near horizontal. At this locality a carbonate horizon (possibly the "C" horizon) marks the actual boundary between Cadna-owie Formation and the Bulldog Shale, and the basal Bulldog Shale once again comprises interbedded clay-dominated and silt-sand dominated interbeds grading upwards into planar laminated thick silty claystones of low bioturbation.

In the core CBH 2 Bulldog Shale also directly overlies Cadna-owie Formation (§2.2.3).

Bulldog Shale overlying Parabarana Sandstone

The boundary between the Parabarana Sandstone and the Bulldog Shale has been inspected at three sites: Petermorra Creek - Chimney Springs; Gunpowder Bore; and Moolawatana shearing shed.

The banks of Petermorra Creek (Fig.2.01; 2.05) provide a useful section through parts of the upper Cadna-owie Formation and its boundary with the Parabarana Sandstone, and the boundary between this unit and the Bulldog Shale. However, parts of the section are missing, owing to poor creek bank exposure. In addition, in creek bank sections where boundaries are not present, stratigraphic determination is complicated by the existence of broad low amplitude folding in the Mesozoic sediments which leads to a high degree of section repetition downstream.

At Petermorra Creek site I (Fig.2.05), the boundary between Cadna-owie Formation and Parabarana Sandstone is exposed. Cadna-owie Formation just below the boundary comprises well laminated silty and sandy claystone with a high carbonate content and abundant plant material; the boundary itself appears partly erosional (Fig.2.21), with the basal Parabarana Sandstone consisting of a cobbley and bouldery lag with associated high angle cross-lamination.

Further downstream (250m) at site II (Fig.2.05), the boundary of the Parabarana Sandstone with the Bulldog Shale is exposed in highly weathered creek banks. This boundary is transitional, and the differences between the two units are subtle, with the uppermost Parabarana Sandstone containing Bulldog Shale-like silty claystone horizons. However, the Parabarana Sandstone is siltier and richer in plant material than the Bulldog Shale, particularly evident in exposures at site III, and contains sand-rich interbeds (Fig.2.21) in sand and silt dominated material bearing relatively high energy sedimentary structures (silty planar lamination, cross lamination and hummocky cross stratification), a product of its deposition in presumably very marginal marine conditions. The basal Bulldog Shale is finer grained, planar laminated, though it does comprise interbedded silt-dominated and clay-dominated horizons, contains less plant material, and was clearly deposited in considerably deeper waters (Fig.2.21). Bioturbation is generally low.

Further downstream (250m) at the confluence of two Petermorra Creek tributaries at site IV (Fig.2.05), as a result of folding, the Parabarana Sandstone - Bulldog Shale boundary is again present, though not exposed, the actual boundary occurring beneath the creek bed. However in the eastern bank of the creek typical upper Parabarana Sandstone is exposed, while in the western creek bank basal Bulldog Shale material is evident, with typical interbedded clay and silt-dominated horizons, fragmented bivalve material, occasional fossilised wood, and large carbonate concretions (§2.5) (Fig.2.21). Bioturbation is variable, from low to high.

Slightly higher into the section at site V (Fig.2.05) the Bulldog Shale has fined to a slightly silty claystone, with occasional bivalve material, and lonestones with associated gravel lenses (§2.6) (Fig.2.21). Bioturbation is at low levels.

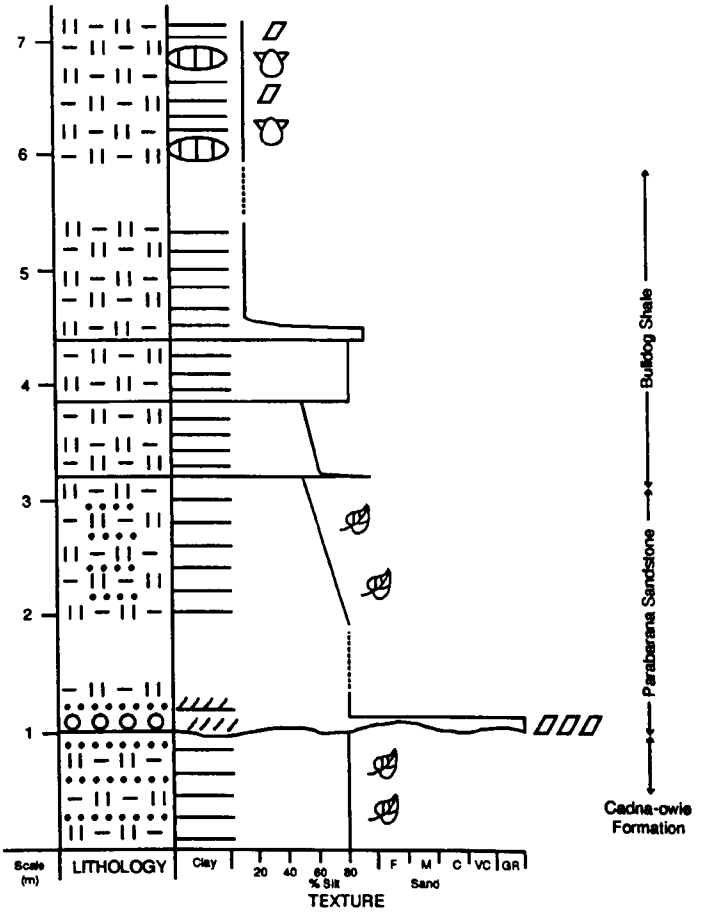

Fig.2.21 Summary log of Petermorra Creek sections, illustrating: boundaries between the Cadna-owie Formation and the Parabarana Sandstone, and the Parabarana Sandstone and the Bulldog Shale; and various sections of Bulldog Shale material. Dashed regions illustrate uncertainty regarding exact stratigraphic relationship. For key to symbols see Fig.2.08.

At Gunpowder Bore (Fig.2.06) only the uppermost 40cm of Parabarana Sandstone are exposed, overlain by a thin layer of Bulldog Shale. At this location the upper Parabarana Sandstone is cemented, probably being part of the "C" horizon, and comprises poorly sorted medium-grained sandstone commonly with polycrystalline quartz and lithic granules, pebbles and occasional boulders. In places the rock is micaceous and has interbedded shalier regions composed of poorly sorted clay, silt, sand and granule-grade material. Occasional trace fossils are present, though the rock is

dominated by planar and cross lamination. The overlying Bulldog Shale is extremely weathered and comprises typical silty basal Bulldog Shale material.

The Moolawatana shearing shed site (Fig.2.07) consists of the north facing bank of Hamilton Creek, in which up to 8m of Parabarana Sandstone are exposed, overlain by a probable "C" horizon (cone-in-cone limestone) and subsequently by a very thin remnant basal Bulldog Shale layer. The Parabarana Sandstone here consists of interbedded and interfingering muddy overbank deposits and gravely channel lags, which rapidly fines upwards into a more homogeneous clay and silt-rich medium to coarse grained sandstone (Fig.2.22). Some of the uppermost layers resemble basal Bulldog Shale material, and lingulid brachiopods have been recovered from these beds (Alley pers. comm. 1993). This site is thus a record of the marine transgression which initiated the change in environment from fluvial to marine, and thus the change from Cadna-owie Formation / Parabarana Sandstone non-marine deposition to upper Cadna-owie / Parabarana Sandstone marine deposition, and the subsequent deposition of the Bulldog Shale.

Fig.2.22 Moolawatana shearing shed section. Note change in lithology (at approximately head height) from interbedded and interfingering muds and gravels to more homogeneous clay, silt and sand-rich deposits N.F. Alley, M.J. Sheard and A.I. Rowett for scale.

2.4 Upper boundary of the Bulldog Shale

Over much of the area where Bulldog Shale crops out in creek banks and hill slopes the rock is unconformably overlain by a thin layer of Quaternary and Recent deposits. Elsewhere, in outcrop and in the subsurface, the Bulldog Shale is overlain conformably to disconformably by the Coorikiana Sandstone Member and subsequently the Oodnadatta Formation (§1.2.2), or unconformably by the Palaeocene and Eocene Eyre Formation.

The upper boundary of the Bulldog Shale with the Coorikiana Sandstone Member is well exposed in creek bank sections cut into the northern slopes of Mount Yerila (Fig.2.06). Here the interbedded silt and sand-dominated, and clay-dominated horizons of the upper Bulldog Shale (§2.1.1), are overlain by the Coorikiana Sandstone over a slightly erosive boundary surface which bears broad amplitude ripples (Fig.2.23).

The base of the Coorikiana Sandstone is marked by a gravely lag containing quartz and lithic clasts up to 3.0cm across, well rounded and of medium to high sphericity, overlain by poorly sorted, fine to very coarse-grade sandstone, comprising quartz, feldspar, mica and occasional lithic fragments. This sandstone also contains large-scale, low angle cross-bedding (Fig.2.24), the foresets of which often fine upwards and are topped with clay drapes, features indicative of episodic waxing and waning flows, possibly under tidal conditions as advocated by Krieg *et al.* (1991) (§1.2.2). Elsewhere, gravel lags are common, as are clay rip-up clasts and balls. In addition, the basal lag of the Coorikiana Sandstone also contains well rounded boulders, some with diameters of more than 95cm, presumably emplaced under very high flow conditions as a result of stream rejuvenation

At the Mount Yerila site the Coorikiana Sandstone is between 8 and 10m thick, and is overlain by the Oodnadatta Formation. The basal Oodnadatta at Mt. Yerila is virtually indistinguishable from basal Bulldog Shale, consisting of a series of clay-dominated fining and coarsening upwards layers, with associated bivalve material (Fig.2.14 for summary log). Bioturbation is variable from low to high, and in some places the rock is completely bioturbated.

A

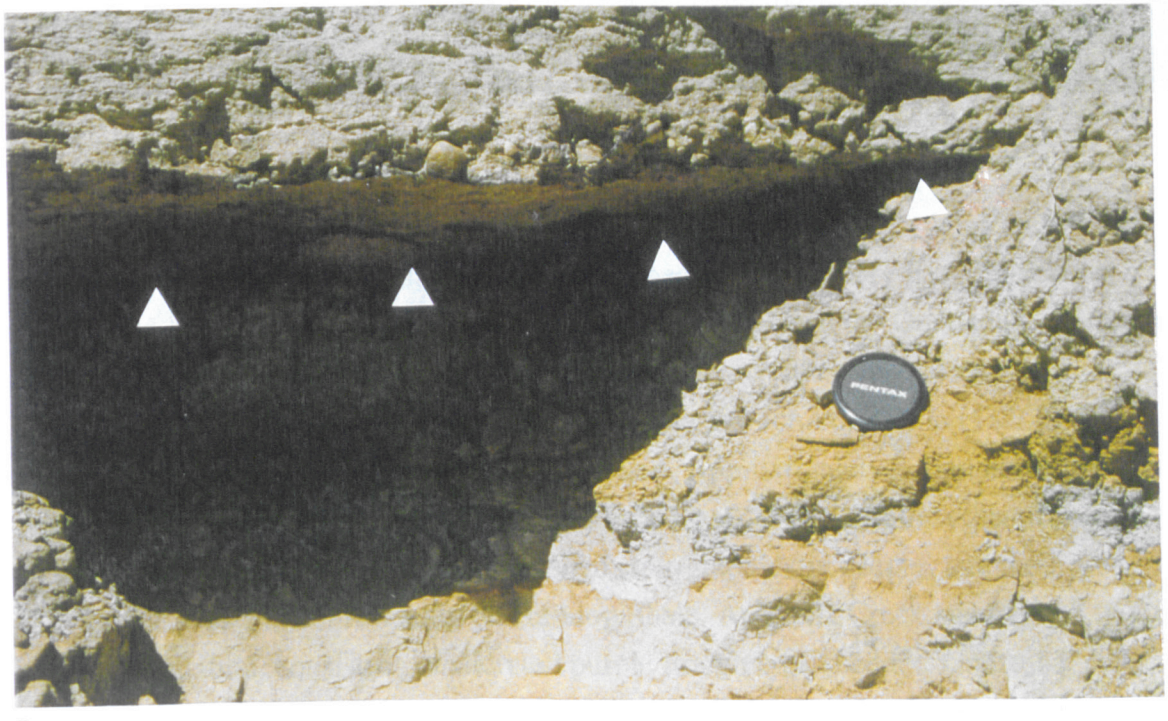

B

Fig.2.23 A: Bulldog Shale overlain by Coorikiana Sandstone and Oodnadatta Formation, northern slopes of Mt. Yerila. Contact between Bulldog Shale and Coorikiana Sandstone marked by large arrows; contact between Coorikiana Sandstone and Oodnadatta Formation marked by small arrows. B: Close up of the contact (marked by arrows) between the Bulldog Shale and the Coorikiana Sandstone.

Fig.2.24 Large scale, low angle foresets in basal Coorikiana Sandstone.

The Oodnadatta Formation on Mt. Yerila is only about 15m thick (Alley and Sheard pers. comm. 1994), and is unconformably capped by the Tertiary Eyre Formation, which in this area has been silcreted. The boundary between the Oodnadatta Formation and the Eyre Formation represents considerable erosion after deposition of the Oodnadatta Formation, Mackunda Formation and Winton Formation (§1.2.2), and before deposition of the fluvial Eyre Formation. Approximately 2.5km north from the Mt. Yerila section, in the north banks of Yerila Creek (Fig.2.06) the erosion surface on which the Eyre Formation rests has eroded stratigraphically deeper, and the Eyre Formation rests unconformably on Bulldog Shale. At Yerila Creek site I (Fig.2.06), the Eyre Formation, consisting of silcreted purple trough cross-bedded sandstone, rests directly on typically low to moderately bioturbated and clay-dominated middle Bulldog Shale. Yerila Creek site II (Fig.2.06), a further 2.5km north-west, exhibits a different arrangement, with Eyre Formation overlying a 20m thick intensely weathered, kaolinised Bulldog Shale layer, which in turn overlies more typical clay dominated and low to moderately bioturbated Bulldog Shale. This kaolinised layer may be interpreted as representing a period of humid weathering after erosion of the overlying layers and before deposition of the Tertiary Eyre Formation.

In the cored material studied here, Bulldog Shale is overlain by typical Coorikiana Sandstone, above an at least slightly erosive boundary surface, in both Alford 1 (§2.2.2; Fig.2.12) and CBH 2 (§ 2.2.3; Fig.2.13).

2.5 Carbonate concretions

2.5.1 Occurrence

Carbonate concretions and cone-in-cone limestones occur at irregular intervals throughout the Bulldog Shale. In addition, carbonate concretions occur in all Bulldog Shale lithologies and palaeoenvironmental fabric types, and typically take on the grain-size of the host sediment. Carbonate concretions and cone-in-cone structures often occur together, with cone-in-cone limestone either both above and below the solid concretion and in effect completely surrounding it, or just above (Fig.2.25C) or below the concretion. In addition, both solid carbonate concretions and cone-in-cone limestone structures can occur in isolation.

From field observations it is evident that carbonate concretions occur both as isolated units and as part of laterally persistent beds. For example, cone-in-cone limestone bodies form a laterally persistent feature at Davenport Springs (Fig.2.03), where a 40cm thick cone-in-cone limestone unit forms a discontinuous bed of 30-40m long limestone units separated by 5-10m gaps of undisturbed Bulldog Shale material (Fig.2.25A). Elsewhere, for example at Petermorra Creek site IX (Fig.2.05), solid carbonate concretions form stratigraphically controlled, laterally persistent features (Fig.2.25B). In addition, carbonate concretions and cone-in-cone limestone units also occur in isolation and not part of any larger laterally persistent body (Fig.2.25C).

2.5.2 Preserved fabric

Cone-in-cone limestone material preserves no original fabric as it is an expansion rather than a replacement feature. Also, in the majority of cases, carbonate concretions are internally structureless. However, this is not always so, and sedimentary and biogenic fabrics are occasionally well preserved (Fig.2.26).

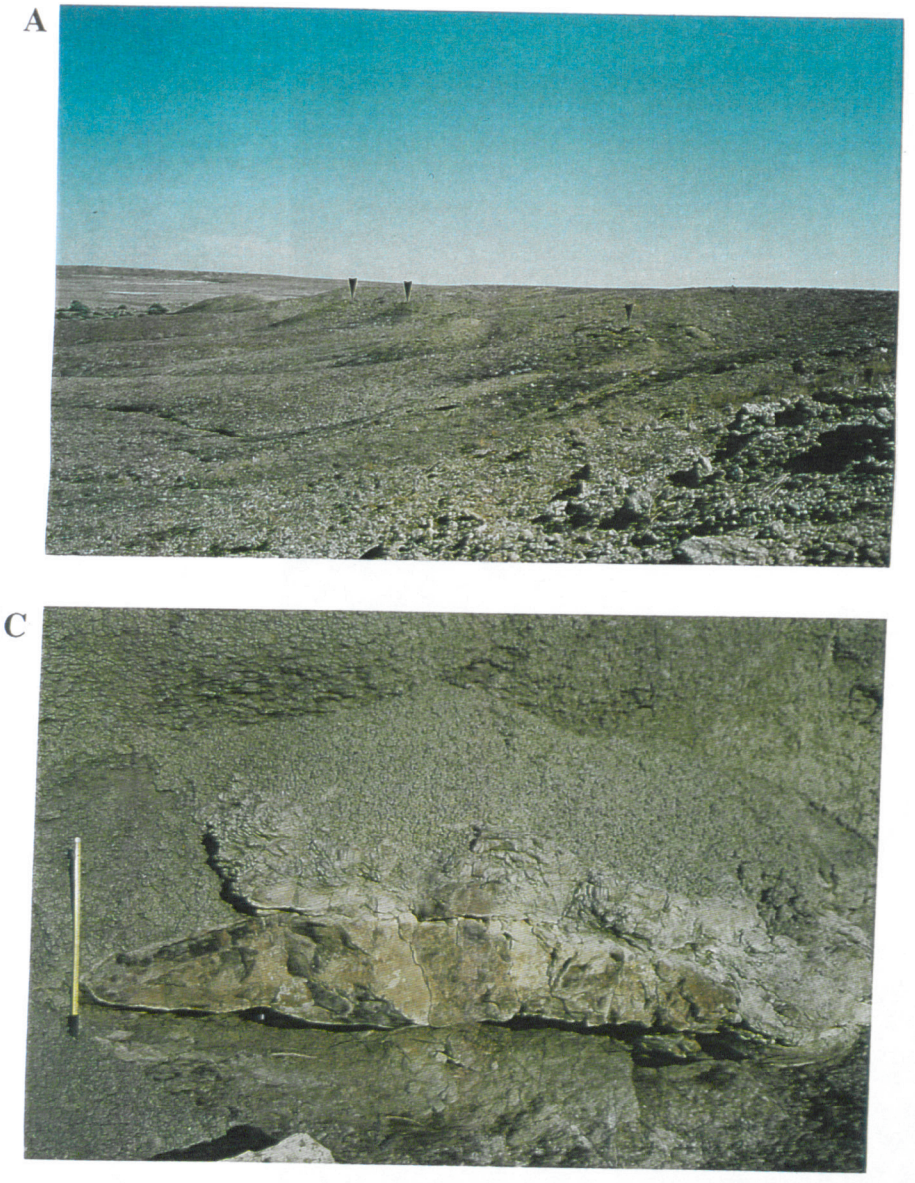

Fig.2.25 A: Laterally persistent, discontinuous cone-in-cone limestone bed (marked by arrows) outcropping across a hillside at Davenport Springs. B: Laterally persistent, discontinuous carbonate concretion-rich bed (marked by arrows) at Petermorra Creek site IX. C: Isolated lens-shaped carbonate concretion and overlying cone-in-cone structure at Petermorra Creek site VIII.

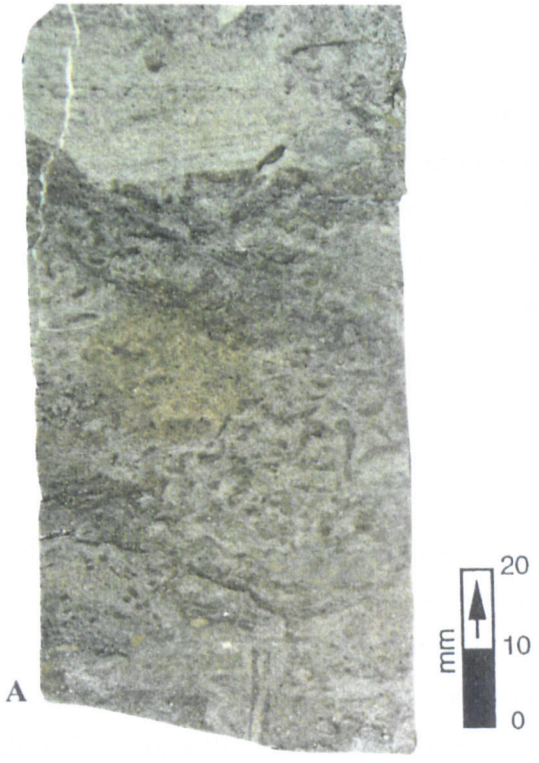

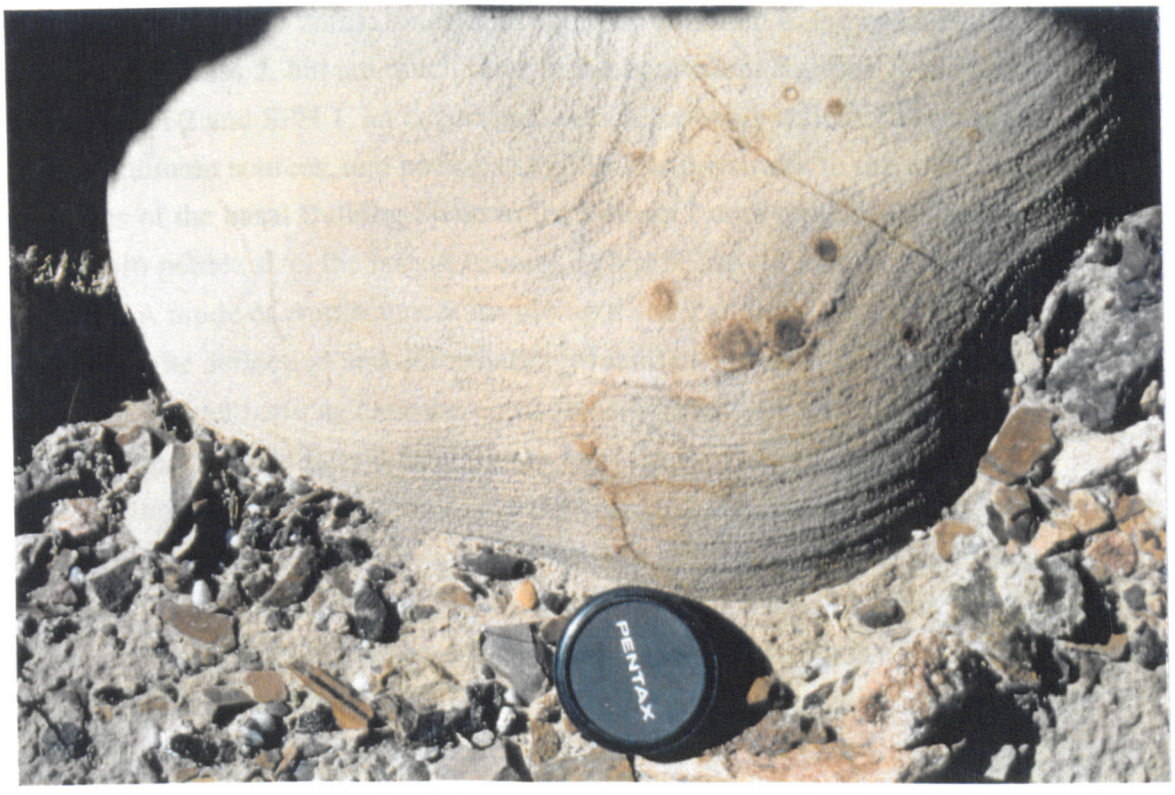

B

Fig.2.26 A: Well bioturbated horizon within carbonate concretion from CBH 2, 485.95-485.80m. B: Sandy, planar and cross-laminated sediments preserved in a carbonate concretion from the upper Bulldog Shale at Mount Yerila.

2.5.3 Incorporated material

More occasionally, various components of typically non-carbonate regions of the Bulldog Shale are found within, and may have initiated the growth of, a carbonate concretion. Such matter includes bivalve and other indeterminate shelly material, fossilised wood and glendonite nodules (Fig.2.27). In addition, where a carbonate concretion has fractured, septarian nodules are commonly formed, with the cavities infilled with large carbonate crystals (Fig.2.27).

2.6 Lonestones

Lonestones are exotic clasts of variable size from granules to boulders emplaced within a finer matrix. Within cored material, lonestones comprise vary coarse sand to pebble-sized material. In addition, lonestones occur throughout the Bulldog Shale, though they are common and in excess of granule size typically only in the basal third of the unit (§2.2 summary logs). Lonestone lithology is typically sandstone or quartzite. There is some variation between cores: lonestones are very common in the basal Bulldog Shale recovered in Finniss 2, but are much rarer in the equivalent Bulldog Shale recovered in the cores CBH 2 and SPH 1, an occurrence which probably reflects separate and different sediment sources, and perhaps slightly less proximity to the palaeoshoreline. Lonestones of the basal Bulldog Shale in the Finniss 2 core typically comprise material of granule to pebble size, the largest recorded clast being 40mm across in longest dimension. A mode of emplacement involving a vertical drop into the sediment is indicated by the deflection and deformation of laminae beneath the lonestones, and by the draping of later laminae over the clasts. Nowhere is there any evidence for lonestone deposition by lateral flow. In the lower part of the succession some lonestones have also been reworked into the base of fining upwards layers, a result of storm derived erosion and deposition in relatively shallow water depths during the initial marine transgression (§4.4.2; 6.4). Many Bulldog Shale lonestones are highly rounded and were probably sourced from fluvial and/or shoreline environments prior to transportation and subsequent deposition in the Bulldog Shale. Surface textures are smooth. Lonestones from the upper Bulldog Shale, evident in the cores Alford 1, CBH 2 and SPH 1, are typically only of coarse sand to granule grade, though where visible, laminae are still deflected beneath the clast.

In the field, lonestones are much more spectacular, and are commonly of boulder size (Fig.2.28), some in excess of 1.0m across, though these large clasts are only evident

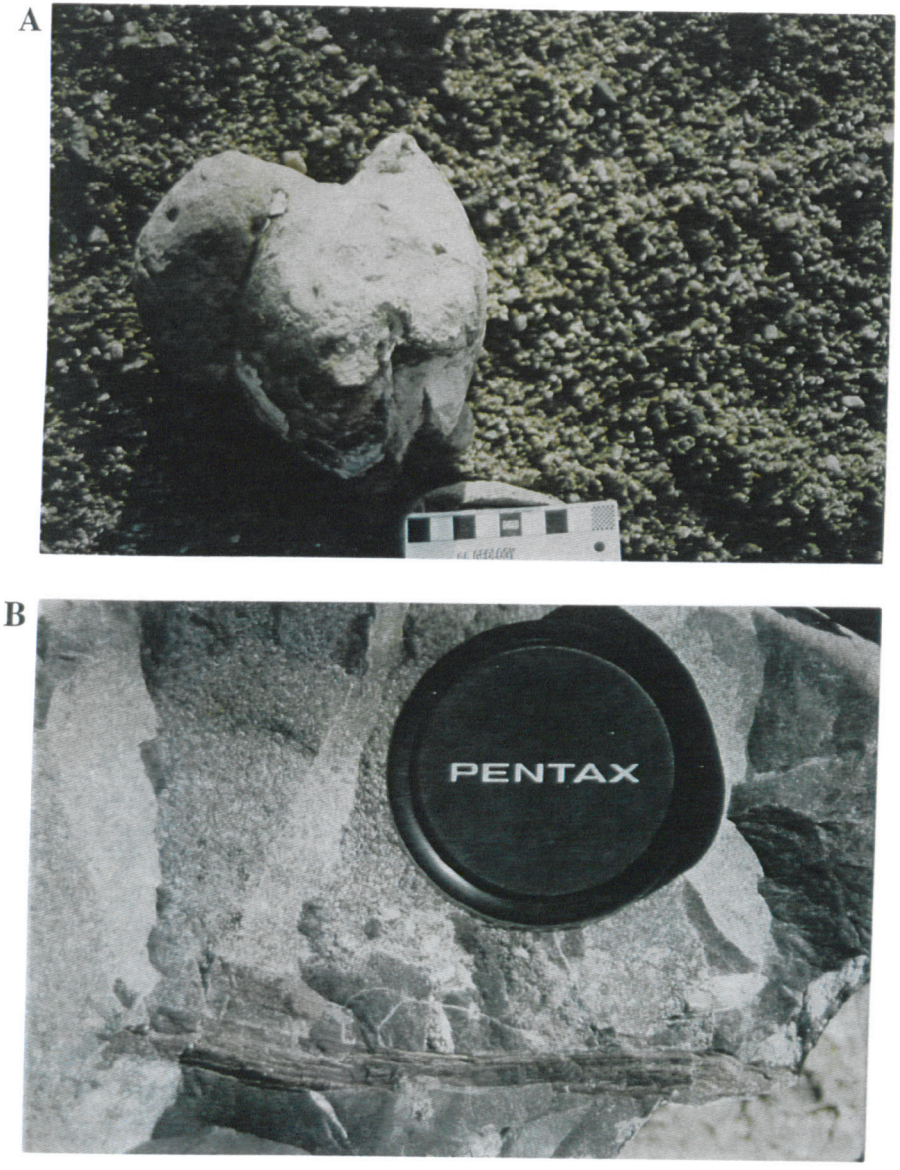

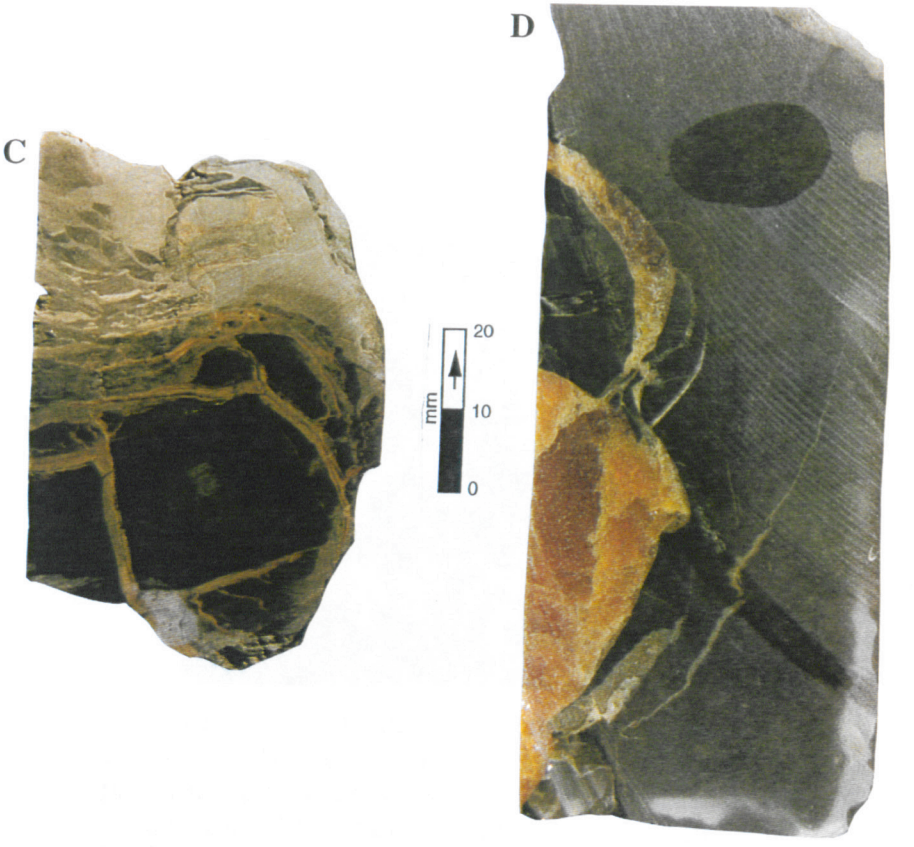

Fig.2.27 A: *Maccoyella* sp. bivalve forming and partly within a carbonate concretion; from Petermorra Creek site VIII. B: Fossilised wood within a carbonate concretion from Petermorra Creek site X. C: Large pyrite crystal within a carbonate concretion from the core SPH 1, 384.50-384.40m. D: Septarian nodule from the core SPH 1, 318.90-318.80m.

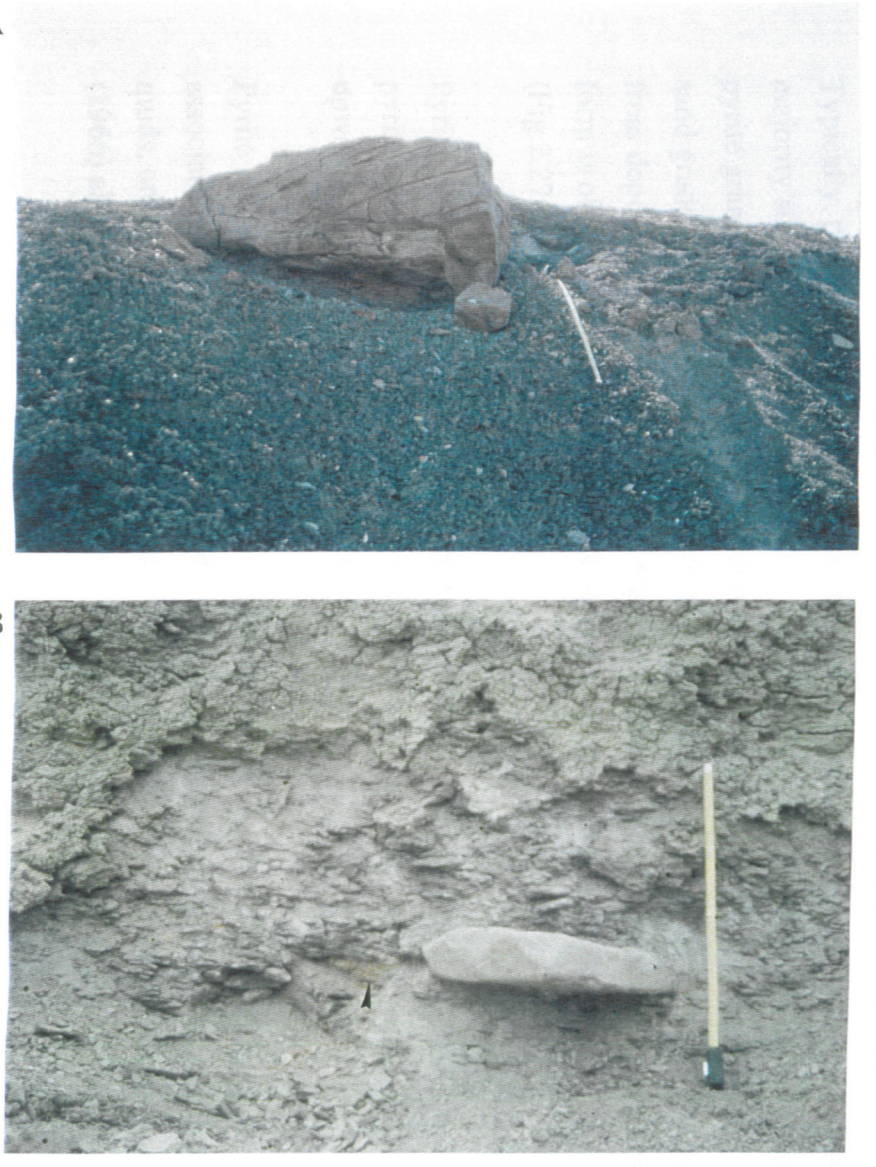

Fig.2.28 A: Large rounded sandstone lonestone in clay-dominated Bulldog Shale at Davenport Springs, palynologically dated as being from the base of the succession (Alley pers. comm.), rule = 1.0m. B: Rounded, flat quartzite lonestone in basal Bulldog Shale material at Petermorra Creek site V, partly within and overlying a laterally discontinuous gravel lens of diamictite-like material (arrowed); gravel lens is deflected beneath boulder, rule = 50cm. C: Well rounded quartzite boulder within basal Bulldog Shale material at Petermorra Creek site VI, overlying and depressing a laterally extensive diamictite-like layer (arrowed), rule = 25cm.

within basal Bulldog Shale material. At Petermorra Creek site VI (Fig.2.05) lonestones occur associated with very poorly sorted sandy and gravely diamictite-like layers (Fig.2.28B-C).

2.7 Mineralogy of the Bulldog Shale

2.7.1 Iron minerals

Most common among the Bulldog Shale minerals are the iron minerals, including pyrite, marcasite, and their weathering product jarowsite.

Pyrite

From core studies it is evident that pyrite is common throughout the Bulldog Shale, though in the field it is rarely encountered owing to the highly weathered nature of the majority of outcrops. In core however, pyrite is nearly ubiquitous, its presence recorded from all sedimentary fabrics, though it is apparently more common within poorly bioturbated clay-dominated material than in well bioturbated and/or siltier sediments (§2.2 summary logs).

In the Bulldog Shale, pyrite takes both the typical cubic form and also a granular form, as observed both in thin section studies (§5.2.2) and in hand specimen analysis. Typically, pyrite granules and crystals attain maximum diameter of 4.0mm, with the majority substantially below this and in the size range of 1.0-3.0mm; in addition, many pyrite granules take the form of framboids, barely visible specks of coarse silt and fine sand grade. Very occasional larger crystals are also present, one from the CBH 2 core from depth interval 490.00-489.90m reaches 25mm in longest dimension, and a similar form is observed within a carbonate concretion in the core SPH 1, depth 384.50m (Fig.2.27C).

Pyrite is often associated with mud and silt-infilled trace fossils (Fig.5.10), and all pyrite commonly bears an iron-stain halo resulting from internal weathering by upwardly travelling groundwater flow.

Pyrite is often found associated with glauconite in the Bulldog Shale (§5.2.2), an association taken by Deer *et al.* (1966) to indicate formation within sediments, typically muds, on the sea floor in shallow waters and under reducing conditions. Deer *et al.* (1966) also noted that the production of the spherical particles of pyrite within

sediments may be attributed to the action of micro-organisms, presumably those utilising sulphate reduction mechanisms as indicated by Berner (1981).

Marcasite

Marcasite is a dimorph of pyrite, and forms radiating fibrous masses (Deer *et al.* 1966). Marcasite is much rarer than the more typical pyrite in Bulldog Shale material, and in the present study has been recorded only from sites VI and X at Petermorra Creek (Fig.2.05). At both sites the marcasite takes the form of small nodules, typically less than 10cm across. At site X, however the marcasite nodules form a laterally persistent band (M. Sheard traced the band over more than 1km until available exposure disappeared) up to 10cm thick, the central marcasite surrounded by haloes of secondary yellow jarowsite (Fig.2.29). Palynological analyses indicate that the Bulldog Shale at this exposure is from the basal part of the succession (Alley pers. comm. 1994). In addition, the rock is largely clay-dominated, planar laminated with low intensity and diversity bioturbation (§5.2.2).

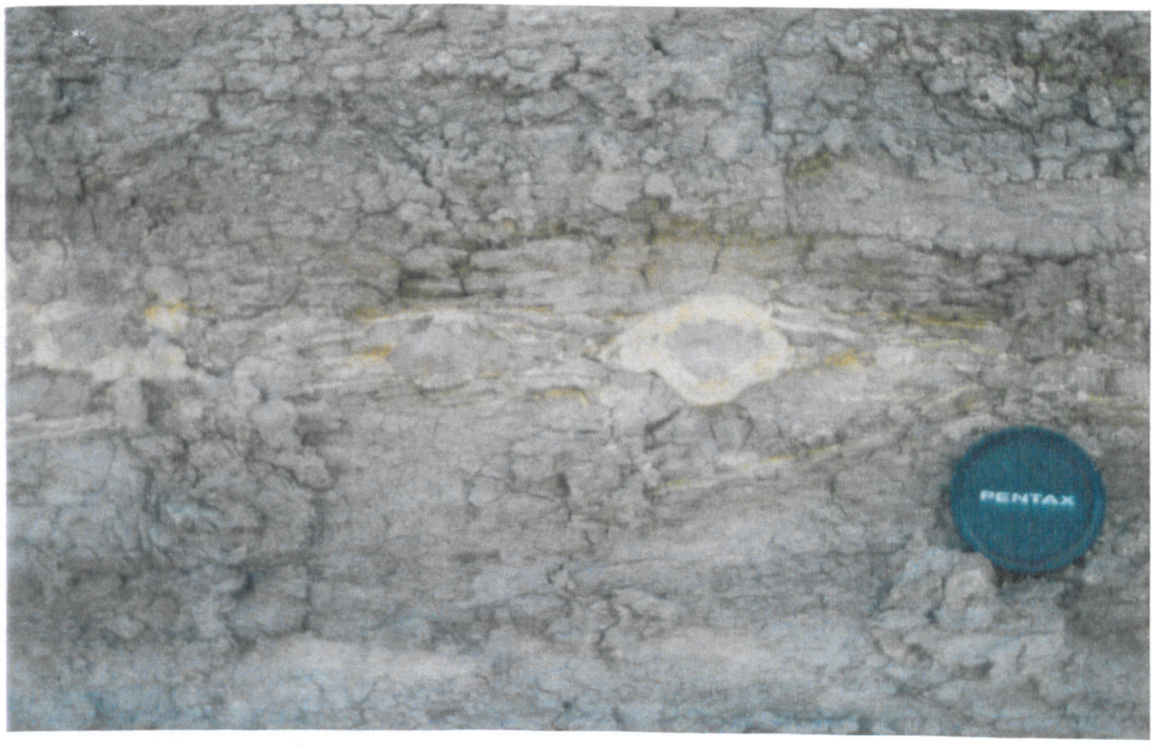

Fig.2.29 Marcasite and associated jarowsite at Petermorra Creek site X.

Jarowsite

Jarowsite is very common in field exposures, and reflects the weathering of pyrite and marcasite within the Bulldog Shale. Jarowsite commonly picks out burrow fills, and this can be related to the occurrence of pyrite observed in cored burrows.

2.7.2 Manganese minerals

Very occasionally, blue-black manganese staining is evident, and represents the mineral pyrolusite (MnO_2), a relatively common secondary mineral formed in paludal or shallow marine sediments. In the present study this mineral has been observed only from basal Bulldog Shale material at the Peecherrikirrina Waterhole and Levi Creek localities (Fig.2.02).

2.7.3 Gypsum

Gypsum is a very common secondary component of the Bulldog Shale, and is formed as a result of the upward migration of saline artesian groundwaters through the rock along faults and as diffuse discharge, and the subsequent evaporation of this flow at the surface. Gypsum is typically formed within 15m of the current land surface, both along fractures and bedding planes, and in the upper 2-5m can lead to the almost complete destruction of the rock fabric.

The groundwater movement which occurs through the Bulldog Shale is the result of the overpressurised nature of the underlying artesian waters and the imperfect nature of the Bulldog Shale as an aquitard (Aldam pers. comm. 1994). This groundwater movement has led to considerable internal weathering of the Bulldog Shale, as evident above in the degradation of pyrite crystals and pyrite-bearing burrow fills to partly ferrugenous material. Aldam (pers. comm. 1994) noted that the affect of this internal weathering has been to severely alter the geochemical signature of the Bulldog Shale, particularly with regard to iron and sulphur. However, McKirdy (pers. comm. 1994) noted that organic matter and associated carbon isotopic ratios have probably largely escaped alteration. Thus, total organic carbon and ∂C^{13} analyses have been performed (§5.2.4), whereas sulphur isotopic studies, and analyses of degree of pyritization, which in unweathered rock may prove very useful in palaeoenvironmental interpretation, have not.

2.8 Glendonite nodules

Few glendonite-bearing sites are known from the Bulldog Shale, and those glendonites considered here originate from the Petermorra Creek site described by Sheard (1990), here designated Petermorra Creek site VII (Fig.2.05). It should be noted also, that a few small (less than 4cm across) glendonites are also evident in the Parabarana Sandstone at Petermorra Creek site III.

At the site described by Sheard (1990), glendonites are ubiquitous within Bulldog Shale determined, through palynological analyses, to be from the lower part of the unit (Alley pers. comm. 1994), and comprising planar and irregular laminated clay-dominated material with some thin (less than 5mm thick) silty interbeds. Bioturbation is of variable, low to high levels. The individual stellate glendonite nodules are of variable size, from 25mm to over 100mm in maximum dimension (Fig.2.30) though with relatively consistent stellate morphology. The latter forms clearly represent lengthy periods of growth, and are thus probably indicative of very slow sedimentation rates or periods of hiatus in sedimentation. Glendonites occur both within typical Bulldog Shale material (Fig.2.30A), in which their growth evidently deflected and deformed the laminations around them, and within carbonate concretions (Fig.2.30B), which indicates that glendonite growth occurred prior to carbonate concretion development, at shallow depths within the sediment. Within the glendonite-bearing outcrop, bivalve material is also evident, including *Maccoyella* valves (Fig.2.30C). Fossilised wood is also present at this outcrop.

2.9 Macropalaeontology

The fossils of the Bulldog Shale fall into two important categories: those that are allochthonous and those that are autochthonous. These two groups provide distinct lines of mutually exclusive information, and thus while one group may be considered more useful than the other, neither should be ignored.

For a detailed review of the macro- and micro-palaeontology of the Bulldog Shale and associated Mesozoic units, the reader is directed to Ludbrook (1966).

The macropalaeontology, as observed in cored material and in the field, is discussed in Chapter 5, with reference to the palaeoenvironmentally mediated fabrics devised in Chapter 4.

Fig.2.30 A: Stellate glendonite nodule within weathered Bulldog Shale. B: Cross-section of a glendonite within carbonate concretion. C: Glendonite and *Maccoyella* sp. bivalve in weathered Bulldog Shale.

2.10 Trace Fossils

Perhaps the most useful features of the Bulldog Shale for palaeoenvironmental analysis are its abundant and diverse trace fossils. These have never before been described in detail, and are thus described and classified here in Chapter 3. The use of these trace fossils as a tool for palaeoenvironmental interpretation, and the delineation of several palaeoenvironmental rock fabrics, is explained and defined in Chapter 4. These palaeoenvironmental fabrics are further discussed in Chapter 5, with relation to thin section, macropalaeontological analysis, and geochemical studies. In Chapter 6, the ultimate use of the palaeoenvironmental fabrics, namely the delineation of Bulldog Shale sub-units and their use in section correlation, and the construction of palaeobathymetric curves, is described and presented.

Chapter 3

Ichnology of the Bulldog Shale

3.1 Introduction

As mentioned previously (§1.1), trace fossils provide the primary focus of this study. This is due to their abundance, diversity and assemblage variation in the Bulldog Shale which, in terms of lithology and macropalaeontology, is remarkably homogeneous. The trace fossils were principally studied from freshly cut core faces, prepared as described in §2.1.1, though fresh, relatively unweathered field samples have also proved useful. Taxonomic identification was made with recourse to Häntzschel (1975), Taylor (1987), Chamberlain (1978), and from Taylor and Goldring (pers. comm. 1993). This chapter is concerned with the identification and description of the trace fossil taxa of the Bulldog Shale

Trace fossils are defined and identified on the basis of several morphological characters or ichnotaxobases. These were summarised by Bromley (1990) as being:

1) General form. Basic shape and orientation. Bromley (1990) did not consider size to be an important factor, but it does play a part in defining several ichnotaxa.

2) Burrow boundary. Bromley (1990) noted that the definition and identification of several ichnotaxa is based on the structure of the wall, and defined seven main categories of wall structure:
(i) No structure;
(ii) Dust film, the production of very thin linings by the trapping of fine grained material in burrows lined with mucus for strengthening;
(iii) Constructional walling of carbon-rich material or more typically of sediment grains applied to the burrow walls as building and strengthening measures;
(iv) Zoned fill, where an apparent wall lining is in fact the outermost part of a zoned fill;
(v) Wall compaction, in which the sediment immediately external to the burrow wall exhibits disturbance from the burrowing activity;
(vi) Diagenetic haloes, resulting from diagenesis in the region of the trace, initiated by oxidation, mucus impregnation and/or compaction of the substrate;
(vii) Wall ornament.

3) Branching. Bromley (1990) considered that, where present, branching of burrows can take four forms:
(i) False branching, produced by accidental intersection and incomplete preservation;
(ii) Secondary successive branching, produced from an unbranched backfilled burrow where the trace maker follows along the earlier fill and then deviates from it, this type of branching is that exhibited by mobile deposit feeders;
(iii) Primary successive branching, a cumulative structure produced from an initially unbranched burrow by successive probing movements as is the case with *Chondrites*;
(iv) Simultaneous branching, a network of open and branched passages, common in domichnia structures.

4) Burrow fill and structure. Bromley (1990) considered that the important features of the burrow fill are twofold:
(i) Fill nature, does it resemble the host sediment or is it different from it;
(ii) Fill genesis, is it passive - gravitationally entering the burrow after habitation and thus having no taxonomic importance, or is it active - emplaced by the burrower and thus bearing significant taxonomic importance?

Utilising these ichnotaxobases the trace fossils of the Bulldog Shale have been defined, most to ichnospecies level, though a few could only be assigned to ichnogeneric level. Those assigned to ichnogenus only were done so as a result of either the incomplete sampling of large trace fossil structures by coring (as is the case with *Phoebichnus* and *Schaubcylindrichnus*), or to the current uncertainty regarding ichnospecies of those ichnogenera considered to be form taxa (as is the case with *Chondrites*).

3.1.1 Intergradation and morphological similarities between trace fossil taxa

Variation within defined trace fossil taxa is very large, more than is the case with any body fossil. The reason for this is primarily to do with what is being categorised. With body fossils, genetically defined morphology is used as the basis for definition, and variation due to environmental input (ecophenotypic variation) is generally small. In trace fossils, the picture is not so clear. While it may be argued that it is again morphology that is used to define the fossil, that morphology is imparted by the behaviour of the trace maker in response to a complicated array of environmental conditions. Even though the behavioural responses of the trace maker are genetically programmed, these responses are not specific to any one trace making taxon, and are strongly mediated by extremely variable environmental factors. Thus, distinctions

between trace fossil taxa are blurred and traces which are intergradational between trace fossil taxa are common.

3.1.2 The ethological classification of the Bulldog Shale trace fossils

The classification of trace fossils into behavioural or ethological groups is a logical result of the acceptance that trace fossils represent the behaviour of the trace maker. Seilacher (1953; 1964) devised the standard ethological classification of trace fossils, defining five main ethological groups, later revised by Bromley (1990):
(i) Repichnia or crawling traces; tracks representing directed locomotion by the trace maker;
(ii) Pascichnia or grazing traces; winding, meandering or spiralled traces representing the efficient exploitation of an area for food by the trace maker;
(iii) Fodinichnia or feeding traces; traces produced by deposit feeders, and representing the combined function of feeding and dwelling;
(iv) Domichnia or dwelling traces; traces representing the permanent to semi-permanent shelters produced by vagile or hemisessile predators, scavengers or suspension feeders;
(v) Cubichnia or resting traces; traces produced by vagile animals residing within the sediment for a period of time before leaving, usually by the route of entry.

These categories were amended by Ekdale (1985), who expanded the scheme to include eight such groups, though he considered them to be subsets of four more fundamental aspects of behaviour, namely dwelling, feeding, locomotion and resting. Ekdale's (1985) additional three groups were, as revised by Bromley (1990):
(vi) Agrichnia or traps and gardening traces, also termed graphoglyptids; traces resulting from highly patterned burrow systems with possible functions as traps for migrating meiofauna or gardening systems for microbe culture;
(vii) Praedichnia or predation traces; traces resulting from obvious predation activity, though these typically occur only on hard biological substrates;
(viii) Fugichnia or escape traces; traces produced by the rapid movement of endobenthic animals in response to sudden sediment aggradation or degradation.
Bromley (1990) also added a ninth category:
(ix) Equilibrichnia or equilibrium traces; representing the gradual shift in burrow position in response to slowly aggrading and degrading sea floors.

There is natural overlap between these ethological categories. Such overlap is particularly evident in the case of equilibrichnia and fugichnia, which must also fulfil another of the ethological groups according to the fundamental behaviour of the trace maker, whether dwelling, feeding, travelling or resting.

As is evident in the following discussion on systematic ichnology, the trace fossils of the Bulldog Shale can largely be assigned to fodinichnia or domichnia, while some also represent equilibrichnia (Fig.3.01).

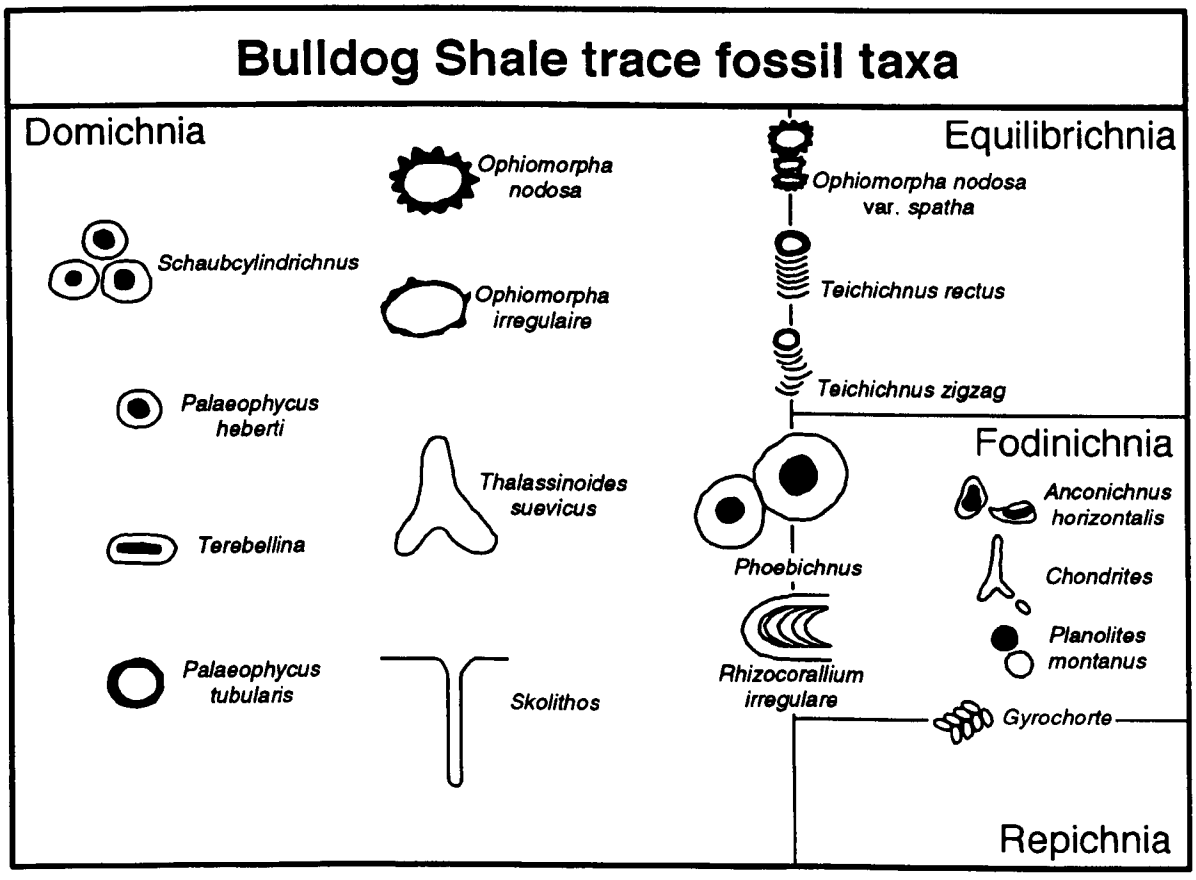

Fig.3.01 Ethological categorisation of Bulldog Shale trace fossils.

3.2 Systematic ichnology of the trace fossils in the Bulldog Shale

Ichnogenus ANCONICHNUS Kern, 1978

Diagnosis. Small, U-shaped to complex burrow, regular or irregular in form. Limbs of U-shaped tube descend from paired entrances and extend, typically but not uniquely with one above the other and parallel or nearly parallel to stratification, to connect by one or more U-shaped bends, often but not uniquely oriented in a vertical plane.

Anconichnus horizontalis Kern, 1978

1978 *Anconichnus horizontalis* Kern, p.190, figs. 4, 5.

1988 *Helminthopsis* Heer; Bjerstedt, p.515, fig. 10.10.

1990 *Helminthopsis horizontalis* Bromley, p.232, figs.11.20, 12.1, 12.3, 12.4, 12.7-12.11, 12.15.

1991 *Anconichnus horizontalis* Kern; Ekdale and Lewis, p.265, fig.2.

1991 *Anconichnus horizontalis* Kern; Goldring, Pollard and Taylor, pp.250-263, figs.1-13.

1994 *Phycosiphon incertum* Fisher-Ooster (1858); Wetzel and Bromley, pp.1396-1402, figs.1-6.

Horizon/locality. Present throughout Bulldog Shale material, both from core and field. Particularly well defined in cored material from the following depth intervals: Finniss 2, 22.22-28.05m; Alford 1, 58.70-58.60m; CBH 2, 356.70-326.40m (parts); SPH 1, 285.85m

Diagnosis. As for ichnogenus. Characterised by regularity of burrow form within any assemblage (Kern, 1978).

Description. Preserved as endichnia, oblique and normal cross-sections and longitudinal sections in core and field material. Each *Anconichnus horizontalis* trace comprises a dark and muddy faecal core surrounded by a diffuse pale silty halo, giving a characteristic frog spawn appearance (Fig.3.02). This appearance is particularly prevalent in assemblage, as individual *Anconichnus horizontalis* traces are always closely spaced (Fig.3.02). The close spacing of traces often results in the loss of definition of individual silty haloes, and only the dark faecal cores remain evident, a feature which is particularly evident in pale silty sediment where the silty haloes are very indistinct (Fig.3.02). In any case, the silty haloes are irregular, and where present may enclose the faecal core entirely or partially, reaching a maximum thickness

comparable to the diameter of the faecal core. Faecal core diameters range from 0.25mm to 1.5mm, both within and between burrows, though the faecal cores of individual traces within any assemblage tend to be on average approximately similar in size (Fig.3.02). Burrow branching is not present.

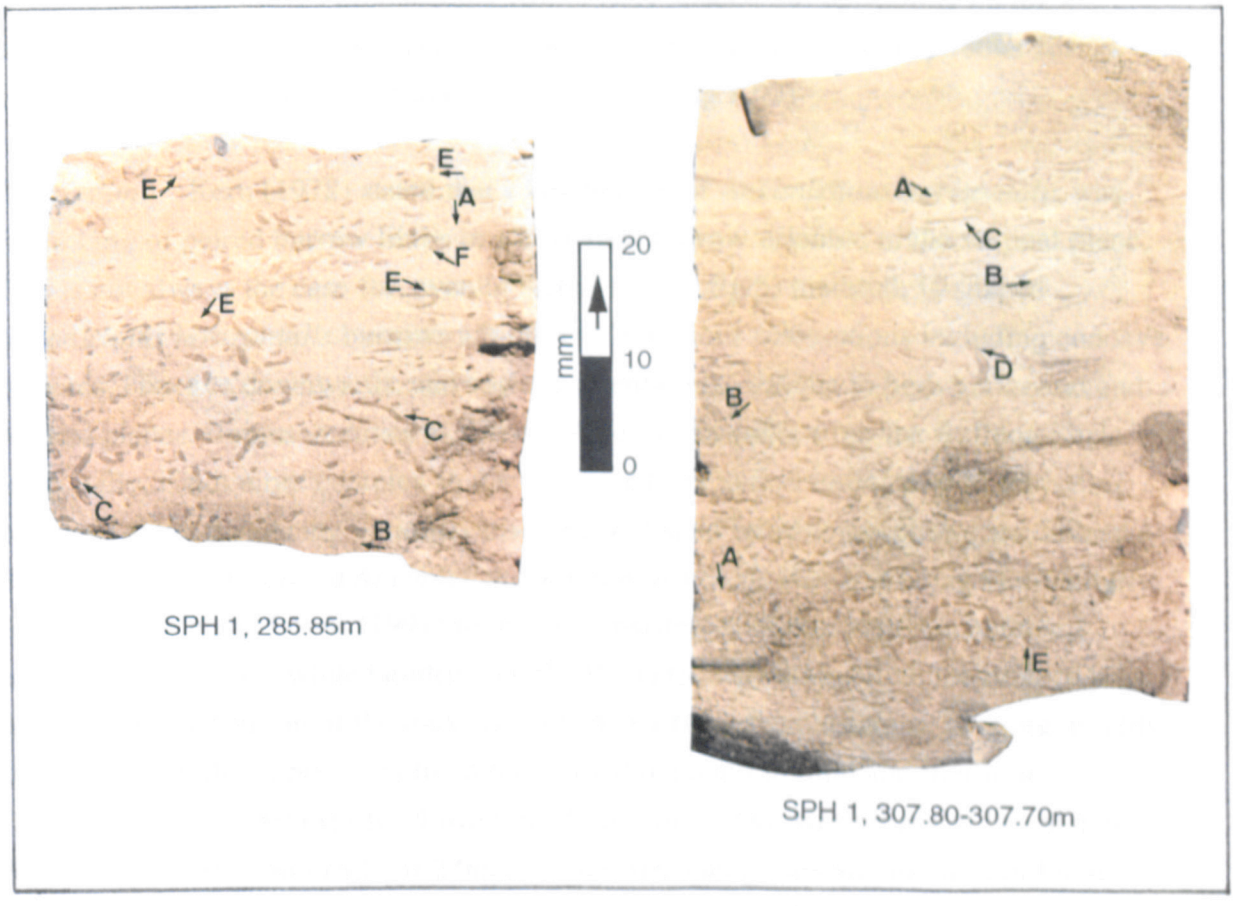

Fig.3.02 *Anconichnus horizontalis* dominated assemblages on cut core faces. Large *Anconichnus horizontalis* traces exhibiting characteristically close spacing, intergradation of neighbouring silty haloes, and the typical frog spawn appearance.

Variable orientation of burrows, as exhibited in different cross-sectional shapes: A = typical normal cylindrical cross-sections; B = irregular oblique cross-sections; C = longitudinal sections, note discontinuity of faecal core in some specimens; D = hook-shaped oblique sections; E = variously oriented U-shaped burrows; F = variously oriented S-shaped burrows.

Orientation of *Anconichnus horizontalis* traces is extremely variable (Fig.3.02) and this is expressed in the vertical plane of core and field material in the form of: regular cylindrical cross-sections; irregular oblique cylindrical to sub-cylindrical cross-sections; horizontal, oblique, and vertical longitudinal sections including sections in which some discontinuity of the faecal core is evident; hook-shaped sections; U-shaped burrows with the limbs oriented variably in the vertical and horizontal planes producing side-facing, oblique-facing, up and down facing U-burrows; vertically and horizontally oriented S-shaped curves produced by two closely spaced but oppositely facing U-turns; and intergradations between these section-types including near-circular forms, possibly sections through a spiralled burrow form (Fig.3.02).

Discussion. Kern (1978) stated that a key feature of *Anconichnus horizontalis* was the linking of paired burrow limbs in a U-shaped burrow oriented in the vertical plane. This is not always the case for, even in Kern's (1978; fig.5) material, U-shaped *Anconichnus horizontalis* burrows are present in various orientations including concave upwards, concave downwards, and various orientations oblique to both horizontal and vertical planes. Representatives of *Anconichnus horizontalis* from the Bulldog Shale are equally, if not more complex in their burrow form and orientation, with opposing double U-tubes producing variously oriented S-shaped burrow morphologies. Indeed, Bromley (1990) described *Anconichnus horizontalis* equivalents as being vermicularly tangled. Ekdale and Lewis (1991) found no consistent orientation of *Anconichnus horizontalis* U-tubes, while Goldring *et al.* (1991) (p.250) dropped all mention of U-tubes in their definition of the trace as being a "narrow, discontinuous, twisting, muddy faecal string within a poorly defined burrow fill depleted in mud and inertinite." Goldring *et al.*'s (1991) study allowed the definition of two size ranges of faecal core diameter (0.25-0.75mm and 1.0-2.0mm). Such size categories are not discernible in Bulldog Shale material in which burrows of all sizes through a minimum to maximum range are discernible.

Of some uncertainty is the nature of the silty halo surrounding the faecal core. In Bulldog Shale material it is distinctive by its irregularity, a feature also noted by Ekdale and Lewis (1991) and Goldring *et al.* (1991). Ekdale and Lewis (1991) considered the silty haloes to be the result of oxidation of organic substances in the sediment immediately adjacent to the burrows. Such an interpretation appears unlikely for, as evident in the present study, and as noted by Goldring *et al.* (1991) the faecal core is only occasionally in the centre of the pale halo, and is often very eccentric to it. Furthermore, although Ekdale and Lewis (1991) inferred low levels of interstitial

oxygen in their environmental analysis of *Anconichnus horizontalis*, and (Bromley, 1990) (fig.11.6) placed the trace in a deep tier, possibly below the redox discontinuity, not all occurrences of the trace can be so interpreted. Goldring *et al.* (1991) interpreted their *Anconichnus horizontalis* material to have occupied a mid to shallow tier above the redox discontinuity and absent from sites of low oxygenation. Indeed, in the present study, while a deep tier is inferred for *Anconichnus horizontalis* (§4.3), and in many cases the trace appears to be tolerant of low oxygen conditions, this is not always the case for it is also extremely common in sediments deposited under well-oxygenated conditions and the trace is probably more indicative of opportunism under conditions which precluded the existence of other trace makers and/or trace making behaviours. Byers (1982) suggested that the formation of a faecal core and a silty halo was due to grain segregation by the deposit-feeding trace-maker, whereby the animal exercised size-selection by ingesting clay and organic detritus and rejecting coarser particles. This infers that the entire burrow (core and halo) represents the width of the trace-maker, and Goldring *et al.* (1991) suggested that *Anconichnus horizontalis* could be produced by a polychaete employing both defecation of ingested mud (producing the faecal core) and parapodial sorting of the sediment (producing the silty halo).

Anconichnus horizontalis traces are probably much more common in siliciclastic rocks than the limited literature on these traces suggests. Goldring *et al.* (1991) produced an extensive comparison with similar, and in some cases identical, traces in various siliciclastic sequences, and concluded that *Anconichnus horizontalis* traces (under a variety of ichnogeneric names) are extremely common in those siliciclastic rocks deposited under certain depositional environments, namely those commonly associated with the lower shoreface to upper offshore zones. Furthermore, Wetzel and Bromley (1994) reviewed *Anconichnus* material and concluded that it was identical to that used to define the trace fossil *Phycosiphon incertum* Fisher-Ooster (1858). Wetzel and Bromley (1994) therefore stated that *Anconichnus horizontalis* is a junior synonym of *Phycosiphon incertum*.

Ichnogenus CHONDRITES von Sternberg, 1833

For detailed synonymy of the ichnogenus *Chondrites*, see Osgood (1970) and Häntzschel (1975).

Horizon/locality. Occasionally present in Bulldog Shale material. Particularly well defined in cored material from the following depth intervals: CBH 2, 430.00-429.90m, 342.40-342.30m, 323.40-323.30m

Diagnosis. Tunnel systems comprising a small number of near-vertical master shafts open to the surface. These ramify laterally at depth often forming a pinnate branching structure. Individual branches may or may not cross-over and interpenetrate. Burrow system frequently becomes horizontal distally. Tunnel diameter constant within one burrow system, varies between systems from 0.5mm to 5.0mm.

Description. Preserved as endichnia, vertically and obliquely sectioned in core and field material. Burrow diameters are constant within individual systems, though between systems burrow diameters vary between 0.5 and 1.0mm. Burrows are always infilled with structureless silt. Burrow walls are sharp and unlined and un-ornamented (Fig.3.03). Entire colonies have not been defined, rather sections of apparent colonies are evident. The classic *Chondrites* branching pattern of pinnate downwards Y-branching from a central near-vertical master shaft is evident in several sections (Fig.3.03). Individual branches do not interpenetrate or cross-cut (Fig.3.03)

Discussion. *Chondrites* material from the Bulldog Shale is defined to ichnogenus only. This is the result of two important considerations. Firstly, *Chondrites* is not common within the Bulldog Shale and that material which does exist is, in the most part, fragmentary. Secondly, the ichnogenus *Chondrites* is itself considered to be in some disarray and in drastic need of redefinition, as Osgood (1970) (p.330) stated: "*Chondrites* contains such a wide range of morphological variations that at present it is a form genus of the widest possible sense." Osgood (1970) went on to suggest that however desirable, a complete restudy would be an arduous and time consuming undertaking as the ichnogenus *Chondrites* contains more "ichnospecies" than virtually any other, and such a study would probably lead to the establishment of several new ichnogenera.

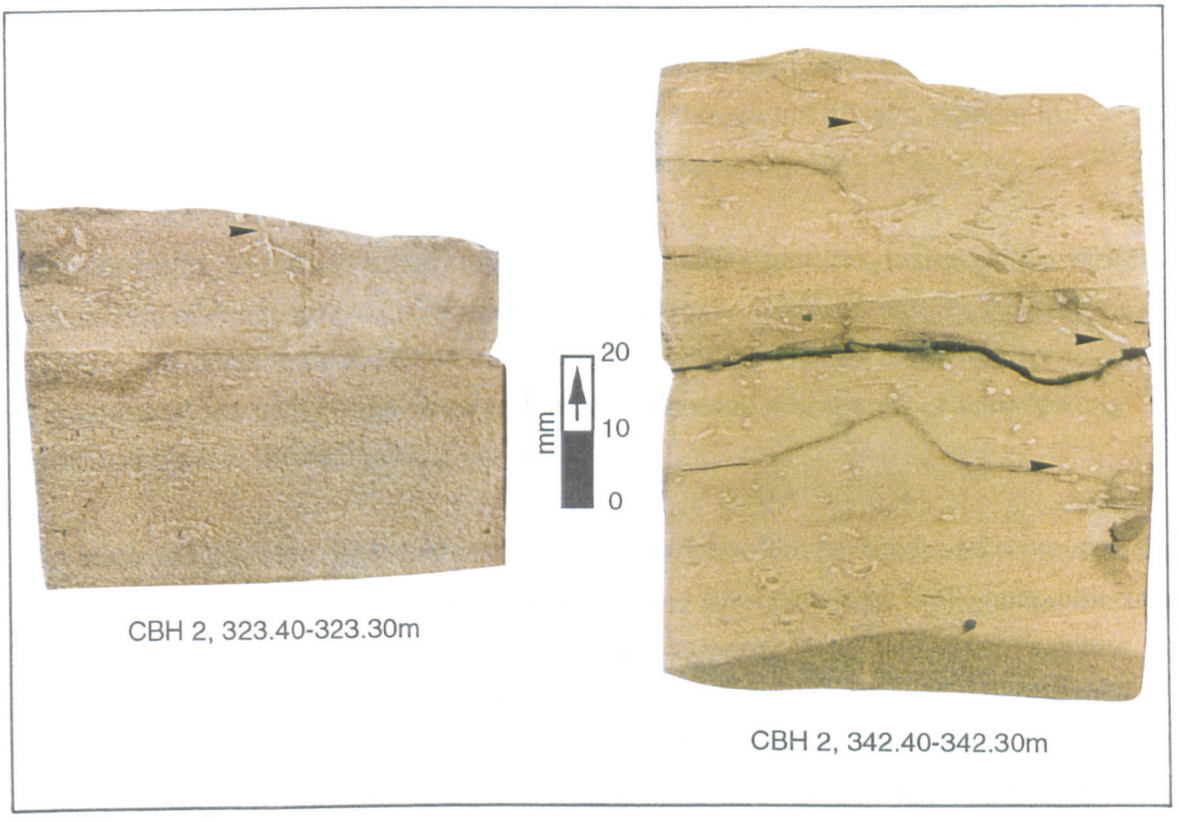

Fig.3.03 *Chondrites*, marked by arrows, in vertically sectioned core material. Note downwards Y branching form central vertical shafts.

Chondrites are considered to be fodinichnia, the feeding structures of sediment-eating animals (Richter, 1927; Seilacher, 1955; Simpson, 1956; Osgood, 1970; Häntzschel, 1975; Bradley, 1981; Bromley and Ekdale, 1984; Vossler and Pemberton, 1988a), not the domichnia of suspension feeders postulated by Tauber (1949), a theory clearly dismissed by Simpson (1956). Simpson (1956) considered that *Chondrites* structures were produced by organisms, possibly sipunculid worms, working from a fixed centre on the surface of the sediment and producing the tunnels by means of an extensible proboscis which lined them with mucus or some other organic material to prevent burrow collapse during proboscis withdrawal. Simpson's (1956) theory is partly based on the phenomenon of phobotaxis first described by Richter (1927), whereby where one branch of a *Chondrites* system encounters another it is always the more proximal branch that stops short, apparently sensing the pre-existing burrow by some chemical means and then deliberately avoiding it. This feature led Simpson (1956) to conclude that, in *Chondrites* systems, burrowing commenced distally and proceeded towards the origin of the burrow at the surface, producing a pattern of tunnelling that efficiently exploited the sediment without unnecessary crossings. Osgood (1970) produced a

comprehensive review of the ethological interpretation of *Chondrites* traces, and he concluded that Simpson's (1956) theory, despite the lack of modern analogues, is the most fitting model for *Chondrites* production. Indeed, Simpson's (1956) theory is backed up by the phobotaxis which is frequently, though not always, evident in Osgood's (1970) own material from the Cincinnati area.

Bradley (1981) described tiered composite trace fossil structures, comprising a vertical succession of *Radionereites*, *Chondrites* and *Phycodes*. These structures Bradley (1981) considered to be the result of repeated burrowing feeding behaviour by Anthoptiloid sea pens, which involved the insertion and withdrawal of their feeding mechanisms into the sediment.

Bromley and Ekdale (1984) indicated that *Chondrites* often occupies and represents the deepest tier in a trace fossil assemblage, exploiting food resources in the anaerobic zone beneath the redox discontinuity. In black shale sequences, deposited under very low oxygen levels *Chondrites* is frequently the only trace fossil in otherwise barren rock. These occurrences in supposedly strongly dysaerobic to anaerobic conditions can easily be explained if the organism was located on the sediment surface and was merely probing the sediment, rather than being wholly located within it. The exploitation of deeply buried organic matter beneath the redox discontinuity was also described by Vossler and Pemberton (1988a), who linked high abundances of *Chondrites* to repeated feeding from storm deposited organic rich sediment layers beneath the redox discontinuity, a food source unavailable to other organisms and behaviours. Since the organism sits on the sediment surface in relatively oxygen-rich waters it is able to burrow, using some form of extendible proboscis, into dysaerobic to anaerobic sediments to find food sources.

Ichnogenus GYROCHORTE Heer, 1865

Diagnosis. Plaited ridges with biserially arranged, obliquely aligned pads of sediment, preserved in positive epirelief. In hyporelief the trace is preserved as two smooth biserial grooves separated by a median ridge. Strongly winding, the trace may intersect itself or other traces (Häntzschel 1975).

Gyrochorte comosa Heer, 1865

1895 *Gyrochorte comosa* Heer, p.142.

1879 *Gyrochorda* Schimper; Schimper and Schenk, p.51.

1886 *?Equihenia* Meunier, p.567.

1962 *Gyrochorte comosa* Heer; Häntzschel, p.W196, fig.122-1.

1970 *Gyrochorte comosa* Heer; Hallam, pp.190-195, figs.1, 2, pl.1.

1975 *Gyrochorte comosa* Heer; Häntzschel, p. W65, fig.40-1.

Horizon/locality. Discovered and described only from field locality 4km NNE of Parabarana Hill (Fig.6.07), samples '93.67, '93.68.

Diagnosis. As for ichnogenus.

Description. Preserved as positive epirelief, corresponding negative hyporelief structures not evident in Bulldog Shale material. Sediment of burrow matches that of host rock. Specimens 4-5mm in width, dimensions constant within individual burrows. The individual pads of sediment, from which the burrow is constructed, are of length 1.5mm-2.0mm, and width 0.75mm-1.0mm, dimensions variable between burrows, and also within individual burrows in response to burrow curvature. Angle of pads to median groove variable within and between burrows from 50° to 70°. Burrows commonly curved, generally in short sections (up to 2.0cm long), separated by straight burrow sections up to 7.0cm in length (Fig.3.04).

Discussion. While the basic morphology of *Gyrochorte* is well understood, the method of its formation is the subject of some debate. Hallam (1970, p.192) reviewed the means by which *Gyrochorte* could have been produced and arrived at the conclusion that "*Gyrochorte* could only have been produced by the movement through the sediment of some organism such as a gastropod, crustacean or worm". However, in examining the evidence Hallam (1970) noted that none of these three most likely candidates conclusively fitted the bill. He did discern however that the direction of movement indicated by *Gyrochorte* was in the direction of the acute intersection of the transverse pads, which represent sediment moved and packaged by the travelling organism.

Fig.3.04 *Gyrochorte*, marked with arrows, on bedding plane surfaces from Parabarana Hill locality (Fig.2.07). Coin for scale is 24mm in diameter.

Heinberg (1973) disagreed, and on the basis of internal structure analysis suggested that *Gyrochorte* was produced by the movement of a cylindrical worm-like organism obliquely through the sediment. This conclusion was the result of analyses of *Gyrochorte* material preserved, not in the typical epirelief, but in full endichnial relief within very micaceous sandstones.

The high mica content of the burrowing medium allowed Heinberg (1973) to analyse the mechanics of *Gyrochorte* production through the study of the orientation of the mica grains. Heinberg (1973) noted that *Gyrochorte* is classically defined as an epichnial feature comprising two plaited ridges separated by a median groove, with a corresponding hypichnial feature of two grooves and a median ridge; all these features were present in his material, along with the preserved connection between the epichnial and hypichnial features. This connection was picked out by mica grain orientation, representing the repetition of the double ridge epichnial structure down through the sediment producing a spreite-like structure up to 160mm from top to bottom, the hypichnion perfectly matching the curve of the epichnion.

Heinberg (1973) also defined three of what he termed discontinuity planes, sharply defined vertical cleavage zones marking the two lateral and the single median boundaries of the burrows. Of particular importance to Heinberg's (1973) theory is the existence of an undulation located on the lateral discontinuity planes oriented at 40-45° from the bedding plane; he also noted that mica grains in the epichnion were dipping at 20-40° from the bedding plane in the same direction as the undulations. These features of the trace, when combined with two and three dimensional modelling, led Heinberg (1973) to conclude that *Gyrochorte* were produced by a cylindrically shaped organism oriented obliquely at about 40° to the horizontal plane, progressing through the sediment in a direction opposite to dip. The production of the epichnial ridge is also dealt with by Heinberg's (1973) model, which explains its formation through the transport of the individual sediment pads in a plane at right angles to the axis of the trace making animal, that is from a lower to a higher level in the sediment.

Heinberg's (1973) study also resolved the mechanics of burrowing in *Gyrochorte*; the presence of the three discontinuity planes and the vertical extension of the trace indicate that the trace maker actively dug through the sediment, as passive ploughing would only produce a median discontinuity plane, with a gradual transition from disturbed into undisturbed sediment at the lateral margins of the burrow.

While explaining the production of *Gyrochorte* in a thorough and convincing manner, Heinberg's (1973) theory has one potentially serious problem in that the energy expenditure for an animal burrowing along its entire length is very high, much higher for instance than in an animal oriented and burrowing horizontally through the sediment. Heinberg (1973) admitted this problem, and explained that the oblique orientation of the trace maker may have been an adaptation for the better exploitation of

the sediment for food, indeed he went on to suggest that the body of the trace maker may have had a primary function of selecting food over its entire length and passing this material to the mouth.

Gyrochorte from the Bulldog Shale are only partially preserved, only the epichnial component of the trace is evident, neither the hypichnial nor the endichnial components can be discerned. While this may raise doubts on the validity of comparisons with other more complete material, it should be noted that the epichnial component of the trace forms the key feature for identification, and that the epichnia of Bulldog Shale *Gyrochorte* perfectly match the epichnial components of this other material. The lack of hypichnial and endichnial components obviously precludes the assignment of Bulldog Shale *Gyrochorte* to either of the two mechanisms of emplacement discussed, be it horizontal or oblique tunnelling, and as such agreement must be made with Häntzschel (1975) (p.W65) who noted that the trace was "doubtless made by tunnelling through sediment, producer unknown". As such *Gyrochorte* may prove to be either repichnia, fodinichnia, or possibly a mixture of both.

Ichnogenus OPHIOMORPHA Lundgren, 1891

Diagnosis. Simple to complex three-dimensional burrow systems with vertical and horizontal components distinctly lined with agglutinated pelletoidal sediment. Burrow lining more or less smooth interiorly; densely to sparsely mammalated or nodose exteriorly. Individual pellets or pelletal masses may be discoid, ovoid, mastoid, bilobate, or irregular in shape. Characteristics of the lining may vary within a single specimen (Frey *et al.*, 1978).

Ophiomorpha irregulaire Frey, Howard and Pryor, 1978

For detailed synonymy of the ichnospecies *Ophiomorpha irregulaire*, see Frey *et al.* (1978).

Horizon/locality. Occasionally present in cored and field material. Particularly well defined in cored material from the following depth intervals: Finniss 2, 55.88-55.72m, 36.91-36.71m, 28.22-28.05m; CBH 2, 344.70-344.60m

Diagnosis. Burrow walls mainly consisting of sparse, irregularly distributed, ovoid to mastoid single pellets or pelletal masses (Frey *et al.*, 1978).

Description. Preserved as endichnia, oblique and normal cross-sections in cored material. Sections through vertical elements are extremely rare, and *Ophiomorpha irregulaire* burrows in Bulldog Shale material represent burrow networks dominated by horizontal elements. Burrows are cylindrical to subcylindrical and are usually viewed in oblique section. Burrow diameters are variable, from 5.0mm to 10.0mm. Wall linings are typically thin (<0.5mm) and highly irregular with occasional, generally solitary, pellets. Some *Ophiomorpha irregulaire* burrows are almost *Thalassinoides*-like, the only difference being the presence of a very thin dark wall. Branching is not evident. Burrow fill is structureless and is typically of similar lithology, or slightly siltier than, the host rock. In some cases the burrow fill has been extensively re-bioturbated by *Anconichnus horizontalis*, although in such cases the *Ophiomorpha irregulaire* wall lining is usually not affected (Fig.3.05).

Discussion. See discussion for *Ophiomorpha nodosa.*

Ophiomorpha nodosa Lundgren, 1891

For detailed synonymy list of the ichnospecies *Ophiomorpha nodosa*, see Frey *et al.* (1978).

Horizon/locality. Ubiquitous in Bulldog Shale material. Particularly well defined in cored material from the following depth intervals: Finniss 2, 36.91-36.71m, 30.00-29.80m, 29.25-29.15m, 28.66-28.48m, 28.22-28.05m; Alford 1, 56.80-56.70m, 42.90-42.80m; CBH 2, 511.10-511.00m; SPH 1, 308.70-308.60m

Diagnosis. *Ophiomorpha* with burrow walls predominantly consisting of dense, regularly distributed single discoid, ovoid, elliptical, or irregular polygonal pellets (Kennedy and MacDougal, 1969; Frey *et al.*, 1978).

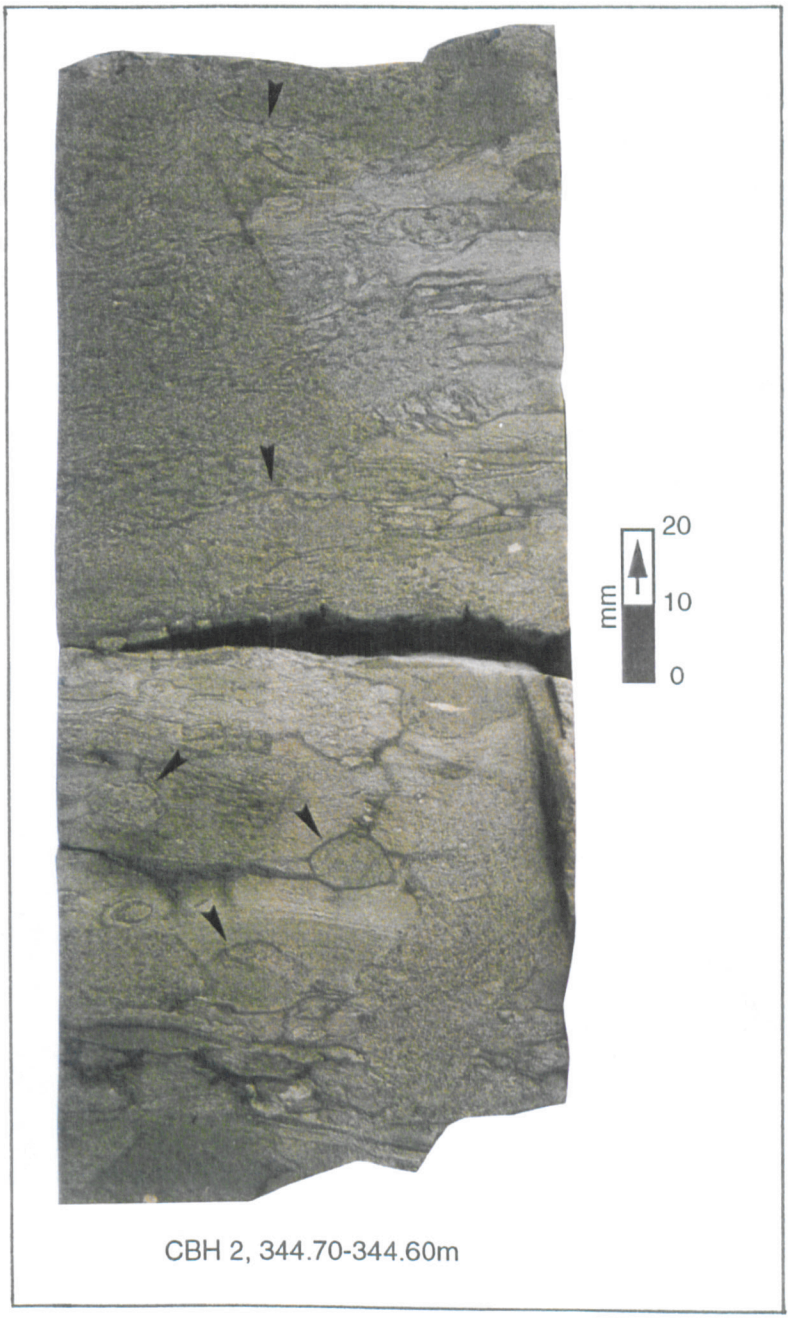

Fig.3.05 Horizontally oriented *Ophiomorpha irregulaire*, marked by arrows, in vertically sectioned core material.

Description. Preserved as endichnia, oblique and normal cross-sections and longitudinal sections in core and field material. *Ophiomorpha nodosa* from the Bulldog Shale represent burrow systems dominated by horizontal and shallowly inclined elements, though vertical and steeply inclined elements are not uncommon. Branching not encountered. Diameter is very variable, ranging between 2.5mm and 20.0mm, though most burrows exist in the range of 4.0mm to 10.0mm (Fig.3.06).

Wall linings are sharply defined and pelleted, thickness is between 0.5 and 1.0mm, though in exceptional cases wall linings can reach 2.0mm thickness. In some cases thick wall linings are restricted to the upper surface of the burrow, and may be absent or considerably thinner along the tunnel's base. In occasional, more extreme forms, the burrow wall lining may also be lost from the burrow sides (Fig.3.06). Wall linings are dark and muddy, without the substantial sand fraction reported by (Frey *et al.*, 1978).

Burrow infill is typically structureless and of similar or slightly siltier lithology to the host rock. Occasionally, *Ophiomorpha nodosa* burrow infills have been extensively re-bioturbated by *Anconichnus horizontalis* burrows, though in these cases the walls of the *Ophiomorpha nodosa* burrows are generally unaffected (Fig.3.06).

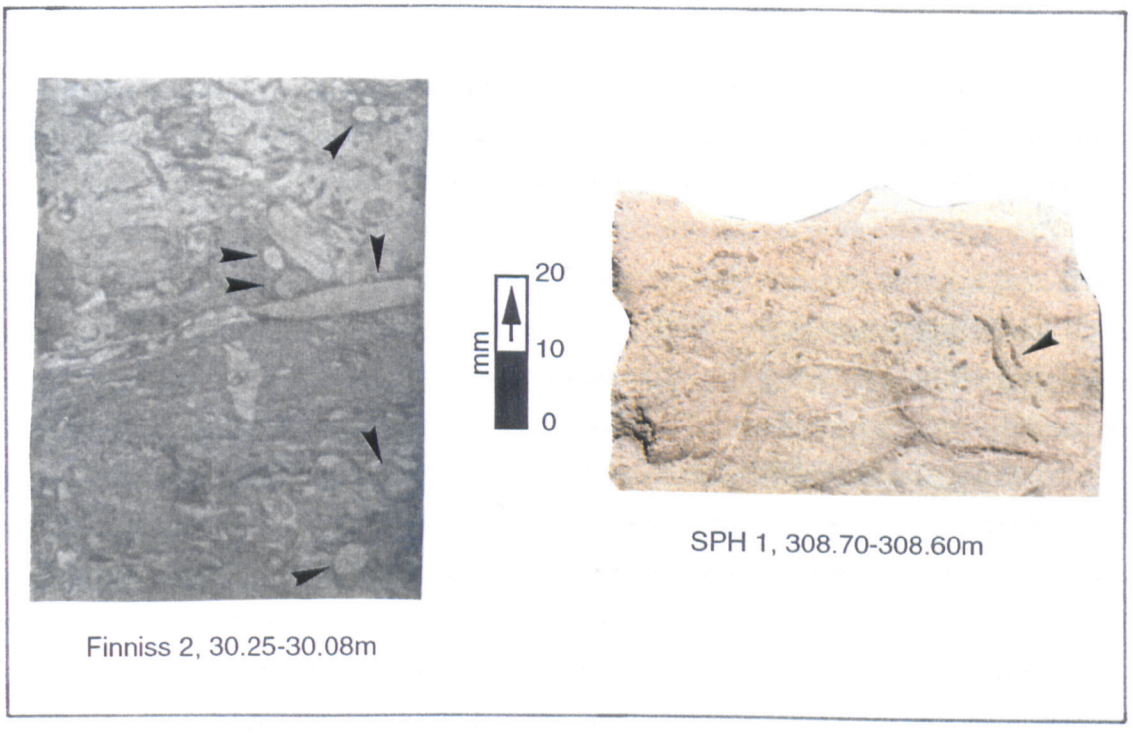

Fig.3.06 *Ophiomorpha nodosa*, marked by arrows, in vertically sectioned core material.

Discussion. Frey *et al.* (1978) summarised and refined the taxonomy of the ichnogenus *Ophiomorpha*, while reviewing the trace's morphology and environmental significance. Frey *et al.* (1978) considered that the primary taxonomic feature of *Ophiomorpha* which identifies it as an ichnogenus is the presence of the distinct nodulose burrow lining, the nature of which they used to subdivide the ichnogenus into three ichnospecies. Not all workers have agreed, for example Fürsich (1973) noted that

the wall lining which apparently defines *Ophiomorpha* is in fact intergradational with geometrically similar burrow types which possess no wall lining, namely *Thalassinoides* and the poorly defined ichnogenus *Spongeliomorpha*. Fürsich (1973) subsequently suggested that *Ophiomorpha* along with *Thalassinoides* should be considered junior synonyms of *Spongeliomorpha*, and the presence or absence of pelleted wall linings retained as an ichnospecific feature. However, subsequent workers on *Ophiomorpha* have not upheld Fürsich's (1973) suggestion. Bromley and Frey (1974) stated that variations, such as those in the wall lining of *Ophiomorpha* and its intergradation with other taxa, are to be expected in trace fossil taxa, and are the result of variations in environment within the sedimentary column. Indeed, Bromley and Frey (1974) went on to advise the abandonment of the ichnogenus *Spongeliomorpha* owing to its poorly defined status, and the retention of the ichnogenera *Ophiomorpha* and *Thalassinoides*, a distinction based on the presence or absence of a wall lining.

The pelleted wall lining of *Ophiomorpha* burrows perform two possible functions, namely they provide structural reinforcement and also a place to dispose of sediment dug out during burrow excavation and/or feeding activities (Frey *et al.*, 1978). It is likely that structural reinforcement is the primary function, for it can be related to substrate stability, and where substrates are firm and stable the wall lining is lost. For instance, Bromley and Frey (1974) and Frey *et al.* (1978) noted that in horizontal components burrows commonly possess a thicker roof lining than that of the burrow sides and floor, and in some cases the floor lining is lost altogether, a feature related to the need for a stronger retaining wall above the excavation than below it; while in vertical to steeply inclined tunnels a gradation is sometimes evident from a thick-walled *Ophiomorpha nodosa* type burrow to a thinner walled *Ophiomorpha irregulaire* type burrow at depth, such a transition is related to variations in substrate coherence and thus the need for burrow strengthening, with incohesive or loose host sediment in the upper part of the sedimentary column becoming increasingly coherent and compact with depth. In addition, several studies have observed that nodular lined *Ophiomorpha* burrows are often restricted to sandy/silty horizons, and parts of the same burrow system extending into muddier horizons lose the structural reinforcing lining and become *Thalassinoides* (Kern and Warme, 1974; Frey *et al.*, 1978).

Modern analogues of *Ophiomorpha* burrows are well known, and have been largely attributed to the activity of decapod crustaceans. Weimer and Hoyt (1964) documented the first such analogue, the dwelling structure of the thalassinidean shrimp *Callianassa major* Say, which is highly abundant in beach sands and the sublittoral sands seaward

of them off the Georgia coast in the U.S.A. Such occurrences led to the use of *Ophiomorpha* burrows as indicators for these very shallow marine environments (Kennedy and MacDougal, 1969). However, Frey *et al.* (1978) noted that, while the burrows of *Callianassa major* are common in beach and near-shore sublittoral sands, they are by no means limited to these regions and occur offshore wherever salinities and current energy are moderately high, and the substrate consists mainly of sand. In addition, Frey *et al.* (1978) stated that *Callianassa major* is by no means the only modern producer of *Ophiomorpha*-type burrows; other *Callianassa* species and other genera of thalassinidean shrimp have been documented to produce similar burrows in a variety of substrate types and water depths. Frey *et al.* (1978) concluded that it is the energy levels in the depositional environment that exert influence both on the ranges of the trace making animals, and the kinds of burrowing and feeding adaptations employed by them. Pollard *et al.* (1993) inferred shoreface, offshore tidal shelf and estuarine palaeoenvironments for three *Ophiomorpha nodosa*-rich trace fossil associations. Frey *et al.* (1978) noted that vertical and steeply inclined shafts predominate in higher energy environments, and horizontal to gently inclined components predominate in lower energy environments, and that how, in a Cretaceous shore profile, vertical *Ophiomorpha* burrows extend downward for 3-5m in the sublittoral zone to join a gallery of interconnecting horizontal burrows which become progressively closer to the sediment-water interface offshore. Such features of modern and ancient *Ophiomorpha* burrows are of importance to the analysis of Bulldog Shale palaeoenvironments, where the predominant burrow orientation is horizontal to gently inclined and the supposed depth of burrowing is considerably less than 2m.

Ophiomorpha nodosa var. *spatha* Hester and Pryor, 1972

1972 *Ophiomorpha nodosa* var. *spatha* Hester and Pryor, pp.677-687, figs.2, 4-5, 7-8, 10.

1975 c.f. *Teichichnus* Seilacher; Häntzschel, p.W85.

1978 c.f. *Teichichnus* Seilacher; Frey, Howard and Pryor, p.207, fig.6B.

Horizon/locality. Rare, only one defined occurrence from the Bulldog Shale, in cored material from the following depth interval: Finniss 2, 37.20-37.00m

Diagnosis. Vertically stacked array of horizontal to inclined *Ophiomorpha nodosa* burrows (Hester and Pryor, 1972).

Description. Preserved as endichnia. Stacked array of small horizontal to slightly inclined *Ophiomorpha nodosa* burrows. Burrow orientation varies slightly giving the composite stack a domed appearance. Individual burrow diameters vary between 2.0mm and 5.0mm, and these low values may represent vertical compression of the burrow fill. Burrow fills are typically structureless with no re-bioturbation. Burrow wall linings vary between 0.25mm and 1.5mm, and the linings of vertically adjacent burrows coalesce in places giving the composite trace the appearance of a stretched out *Teichichnus* (Fig.3.07).

The composite stacked trace is obliquely longitudinally sectioned on a cut core surface, and extends vertically over 6.5cm, comprising up to 27 individual *Ophiomorpha nodosa* burrows (Fig.3.07).

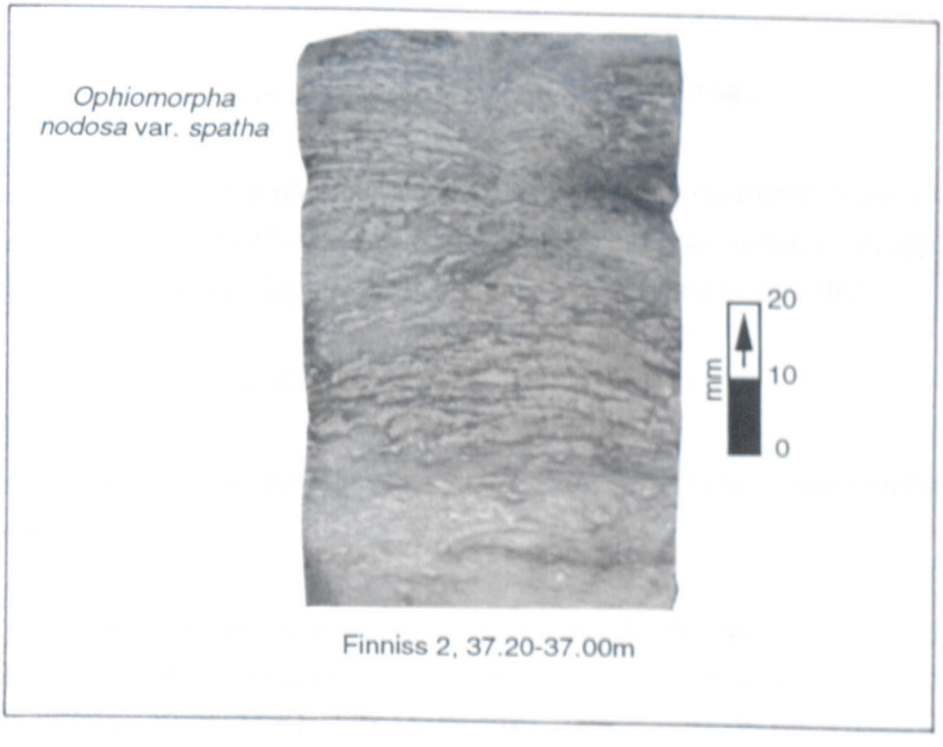

Fig.3.07 *Ophiomorpha nodosa* var. *spatha* in vertically sectioned core material.

Discussion. Hester and Pryor (1972) were the first to describe vertically stacked, blade-shaped burrow composites of *Ophiomorpha nodosa*, which they gave the informal name *spatha*, and compared to *Teichichnus*. The burrows Hester and Pryor (1972) described included branching and cross-cutting forms, not observed from Bulldog Shale material, all including the basic vertically stacked form. This upward migration of *Ophiomorpha nodosa* burrows Hester and Pryor (1972) attributed to

abandonment of the previous burrow "because it had become a putrefying habit" (p.615). Frey *et al.* (1978) also reported vertically stacked *Teichichnus*-like *Ophiomorpha nodosa* burrows, and while they acknowledged Hester and Pryor's (1972) account for the formation of stacked *Ophiomorpha nodosa* burrows, they also suggested that the older parts of the stacked array may represent receptacles for wastes and sediments not pumped out of the burrow, or the need to maintain equilibrium with a slowly aggrading substrate. In Bulldog Shale material, the similarity of the burrow infill in *Ophiomorpha nodosa* var. *spatha* with that of the host substrate indicates that the latter suggestion is most likely.

While, like *Ophiomorpha irregulaire* and *Ophiomorpha nodosa* these burrows represent domichnia, they are also representative of the equilibrichnia of (Bromley, 1990).

Ichnogenus PALAEOPHYCUS Hall, 1847

Diagnosis. Branched or unbranched, wall smooth or ornamented, lined, essentially cylindrical, predominantly horizontal burrows of variable diameter; infill typically structureless, of same lithology as host rock (Pemberton and Frey, 1982).

Palaeophycus heberti (Saporta, 1872)

For detailed synonymy of the ichnospecies *Palaeophycus heberti*, see Pemberton and Frey (1982).

Horizon/locality. Common component of Bulldog Shale trace fossil assemblages. Particularly well defined in cored material from the following depth intervals: Finniss 2, 45.00-44.79m, 38.00-37.82m, 28.82-28.71m; Alford 1, 48.80-48.70m; CBH 2, 445.30-445.20m, 352.60-352.50m, 342.90-342.80m, 329.60-329.50m; SPH 1, 385.70-385.60m, 350.00-349.90m, 293.00-292.90m

Diagnosis. *Palaeophycus* which comprise smooth and thickly lined, unornamented cylindrical burrows (Pemberton and Frey, 1982).

Description. Preserved as endichnia, obliquely and normally cross-sectioned and longitudinally sectioned horizontal burrows in core and field material. Diameter of

burrows constant within individual traces, though between traces it varies from 2.0mm to 7.0mm, with the majority in the range from 3.0mm to 6.0mm. The thick wall linings (generally over 1.0mm) typically comprise pale silty material, and often have a thickness equivalent to or greater than the diameter of the dark muddier fill. The fill is structureless and usually of the same or slightly darker material as the host rock. Occasionally, an *Ophiomorpha nodosa*-style lining wholly or partially surrounds the trace (Fig.3.08), and probably represents an extra layer of burrow wall lining, added for further burrow strengthening.

Burrow branching and ornamentation not evident.

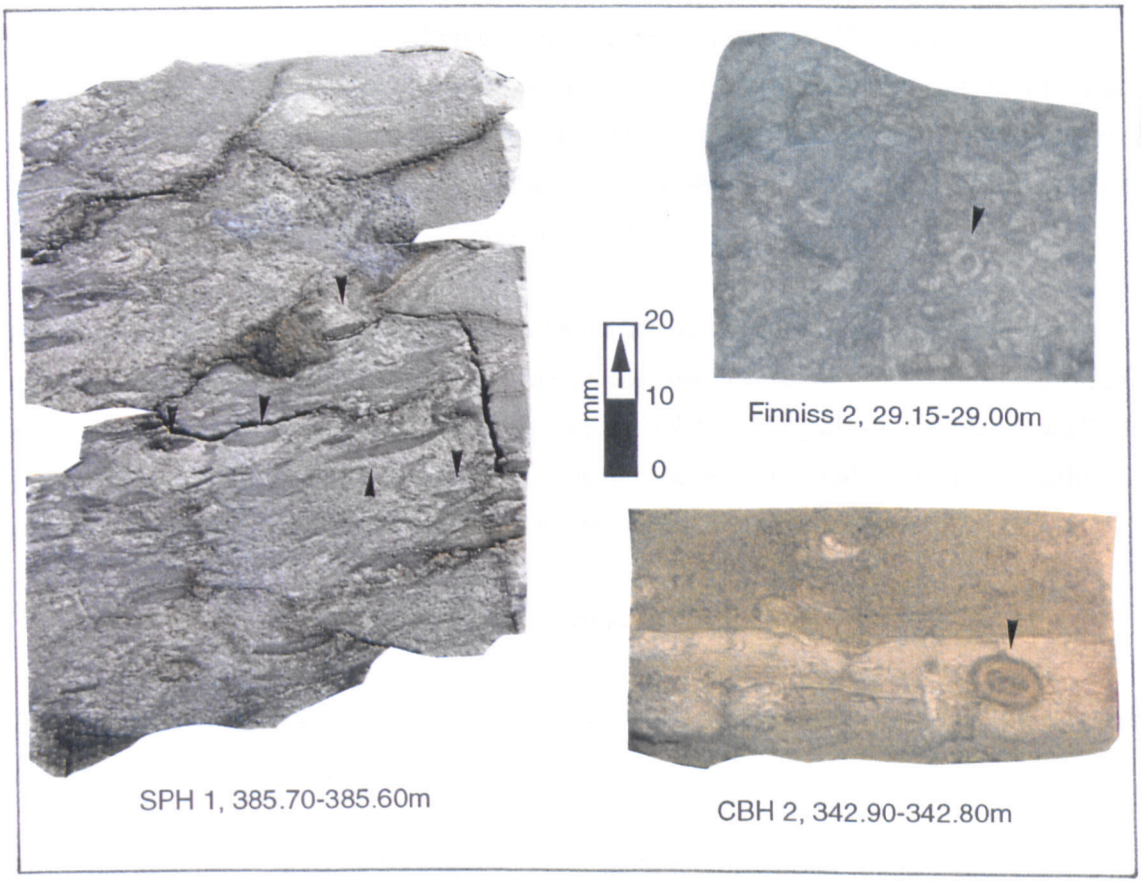

Fig.3.08 *Palaeophycus heberti*, marked by arrows, in vertically sectioned core material.

Discussion. The distinction between the trace fossil taxa *Palaeophycus* and *Planolites* has long proved problematic. In his work on Cincinnatian ichnology Osgood (1970) reviewed the evidence and suggested that the key taxonomic character providing for the division of the two taxa was the nature of the burrow fill: the fill of

Palaeophycus differs little from the host sediment, while the fill of *Planolites* exhibits strong differences. Pemberton and Frey (1982), in a thorough review of the two taxa agreed, basing the division of the two taxa on the basis of the nature of the burrow fill, and on the presence or absence of wall lining material: *Palaeophycus*, along with a burrow fill similar to that of the host sediment, possesses various wall lining structures, while *Planolites*, along with burrow fills different from those of the host rock, has no wall linings. Fillion (1989) sounded a note of caution, however, when he stated that taphonomic and diagenetic effects can complicate the identification of *Palaeophycus* and *Planolites*, and he produced figures as an aid to identification of these ichnogenera in various diagenetic and taphonomic scenarios. In their review Pemberton and Frey (1982) discounted Alpert's (1975) claim that *Planolites* and *Palaeophycus* can be distinguished by the presence or absence of branching, the former being unbranched and the latter bearing branches. Pemberton and Frey (1982) (p.870) noted that both *Planolites* and *Palaeophycus* can be branched, though irregularly and rarely, and that Alpert's (1975) scheme "failed to account for the fundamental physical and ethological differences between the two ichnogenera", and that the analysis of burrow linings and sediment fills provided a more realistic approach.

Ethologically, *Palaeophycus heberti* represent the domichnia of suspension feeders, detritus feeders or predators, the wall lining indicating occupation and stabilisation of a semi-permanent to permanent burrow (Bromley, 1990). The particularly thick wall of *Palaeophycus heberti* Bromley (1990) assigned to constructional walling, whereby sediment grains are applied to the burrow wall as building material.

Palaeophycus tubularis Hall, 1847

For detailed synonymy list of the ichnospecies *Palaeophycus tubularis*, see Pemberton and Frey (1982).

Horizon/locality. Relatively common component of Bulldog Shale trace fossil assemblages. Particularly well defined in cored material from the following depth intervals: Finniss 2, 54.10-54.00m, 28.66-28.48m; Alford 1, 57.10-57.00m; CBH 2, 507.70m, 354.50-354.40m; SPH 1, 404.50-404.40m

Diagnosis. Smooth, unornamented *Palaeophycus* burrows of variable diameter, thinly but clearly lined (Pemberton and Frey, 1982).

Description. Preserved as endichnia, obliquely and normally cross-sectioned and longitudinally sectioned horizontal burrows in core and field material. Burrow diameter is constant in individual burrows, but between burrows it varies between 2.5mm and 7.0mm, though the majority of tunnels fall in the 4.0mm-5.0mm size range. Wall lining is sharp and thin, typically darker and muddier than the burrow fill which strongly resembles the host rock lithology. Wall thickness is generally about 0.5mm, though it may be as much as 1.0mm in some specimens. There is no evidence for wall thickness variation around the burrow (Fig.3.09).

Burrow branching and ornamentation not evident.

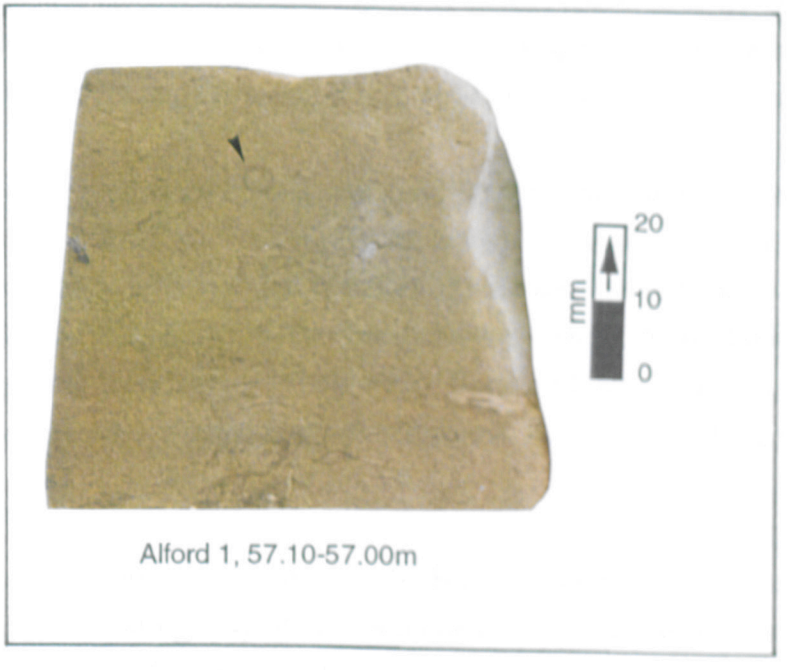

Fig.3.09 *Palaeophycus tubularis*, marked by arrows, in vertically sectioned core material.

Discussion. See discussion for *Palaeophycus heberti*.

Bromley (1990) attributed the thin, characteristically muddy wall of *Palaeophycus tubularis*, not to constructional origin as in *Palaeophycus heberti*, but to the passive trapping of fine grained material in a mucus lining originally created to stabilise the burrow walls.

Ichnogenus PHOEBICHNUS Bromley and Asgaard, 1972

1972 *Phoebichnus* Bromley and Asgaard, p.23-30, figs.10-14.

1975 *Phoebichnus* Bromley and Asgaard; Häntzschel, p.W93, fig.58.

1990 *Phoebichnus* Bromley and Asgaard; Bromley, pp.149-150, 229, 241, figs.9.5-9.6, 12.6.

Horizon/locality. Rare component of Bulldog Shale trace fossil assemblages. Particularly well defined in cored material from the following depth intervals: Finniss 2, 31.44-31.24m, 29.15-28.82m, 28.66-28.48m

Diagnosis. Central vertical shaft of unknown depth and approximately 6-8cm diameter with numerous long, straight burrows radiating essentially horizontally from it. The radial tunnels consist of an actively filled lumen approximately 1cm diameter, and a discretely annulated wall 5mm thick. The wall imparts an annulation both to the surface of the lumen fill and the surrounding sediment (Bromley and Asgaard, 1972).

Description. Preserved as endichnia, recorded from cored material only in cross-section form. Only a small part of the original burrow system is evident, comprising between 2 and 3 clustered horizontal burrows of between 7.0 and 16.0mm diameter. Dark muddy fill and frequently diffuse thick silty wall lining. Wall thickness typically equivalent or greater than burrow fill diameter. Inner and outer margins of wall lining smooth, unornamented. Fill apparently structureless. Burrow branching not evident (Fig.3.10).

Discussion. *Phoebichnus* material from the Bulldog Shale is very incomplete, with all the specimens consisting only of between one and three cross-sectioned radial burrows in cored material. Without information regarding the entire three dimensional burrow form an attempt at identification to ichnospecies level cannot be made.

Bromley and Asgaard (1972) utilised mica orientation within the linings and fills of the horizontal radiating components of the fossil to infer a mode of creation. Bromley and Asgaard's (1972) studies indicated that the trace-maker lived in the central shaft, and from this shaft radial tunnels were constructed and infilled by the trace-maker, presumably for the exploitation of the sediment for food. Such excursions from the central shaft implicitly contained two phases; on the outward phase mica orientations indicated that the wall lining was constructed, while during the return phase the burrow was actively backfilled. It is uncertain whether the radiating feeding tunnels were the

result of movement of the entire trace maker, or whether some form of proboscis was utilised. Bromley and Asgaard (1972) designated the entire trace to be a fodinichnion, while Häntzschel (1975) considered that only the radiating arms could be considered as fodinichnia, and that the central shaft was in fact a domichnion.

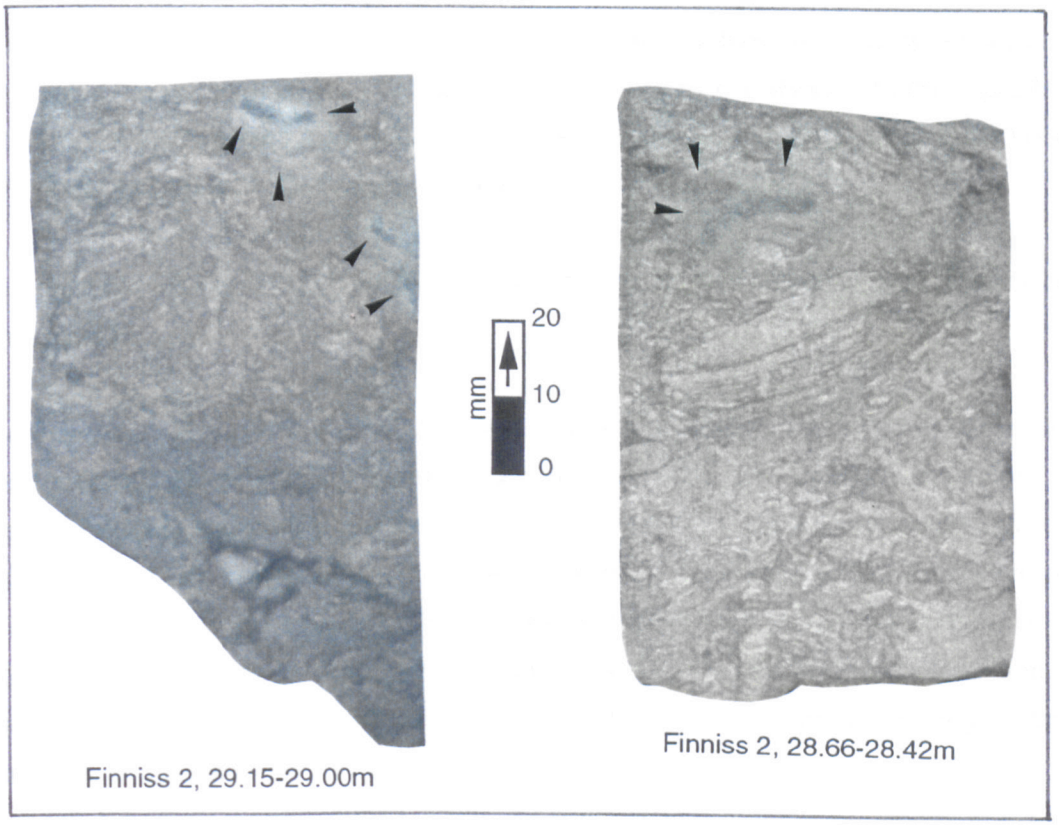

Fig.3.10 Horizontal components of *Phoebichnus*, marked by arrows, in vertically sectioned core material.

Ichnogenus PLANOLITES Nicholson, 1873

Diagnosis. Unlined, rarely branched, straight to tortuous, smooth to irregularly walled or annulated burrows, circular or elliptical in cross-section, of variable dimensions and configurations; structureless infill which differs in lithology from host rock (Pemberton and Frey, 1982).

Planolites montanus Richter, 1937

For detailed synonymy list of the ichnospecies *Planolites montanus*, see Pemberton and Frey (1982).

Horizon/locality. Near ubiquitous component of Bulldog Shale trace fossil assemblages. Particularly well defined in cored material from the following depth intervals (*Planolites* with pale and silty infills except where stated): Finniss 2, 29.00-28.71m, 28.22-28.05m; Alford 1, 60.10-60.00m; CBH 2, 495.90m; SPH 1, 400.00-399.90m, 387.90-387.70m (dark, muddy infill), 385.70-385.60m

Diagnosis. Relatively small *Planolites* burrows, curved to contorted (Pemberton and Frey, 1982).

Description. Preserved as endichnia, oblique and normal cross-sections in core and field material. Horizontal, cylindrical burrows of individually constant diameter, though between burrows diameter varies from 1.5 to 6.0mm, however most fall in the 2.0 to 3.5mm size range. Most *Planolites montanus* are infilled with pale silty material, though occasionally the fill is of darker mud-rich sediment; in any case the burrow fill always contrasts with the surrounding host sediment. Burrow walls are sharp and unlined and unornamented. In plan view *Planolites montanus* exhibit gently curved burrows. Branching is not evident (Fig.3.11).

Discussion. Pemberton and Frey (1982) distinguished *Planolites* from the morphologically similar *Palaeophycus* on the basis of the former being infilled with material different from that of the host rock and lacking any wall lining structure; for more complete discussion on this point, see discussion for *Palaeophycus heberti.*

Planolites are interpreted to represent the actively backfilled burrow of a vagile deposit feeder (Pemberton and Frey, 1982; Bromley, 1990). Furthermore, Bromley (1990) (p.179) considered that *Planolites* could be ethologically classified as a pascichnion, as "the accent is on mobility", though the lack of tightly spaced forms in Bulldog Shale material indicates that ethological designation as fodinichnia is more appropriate.

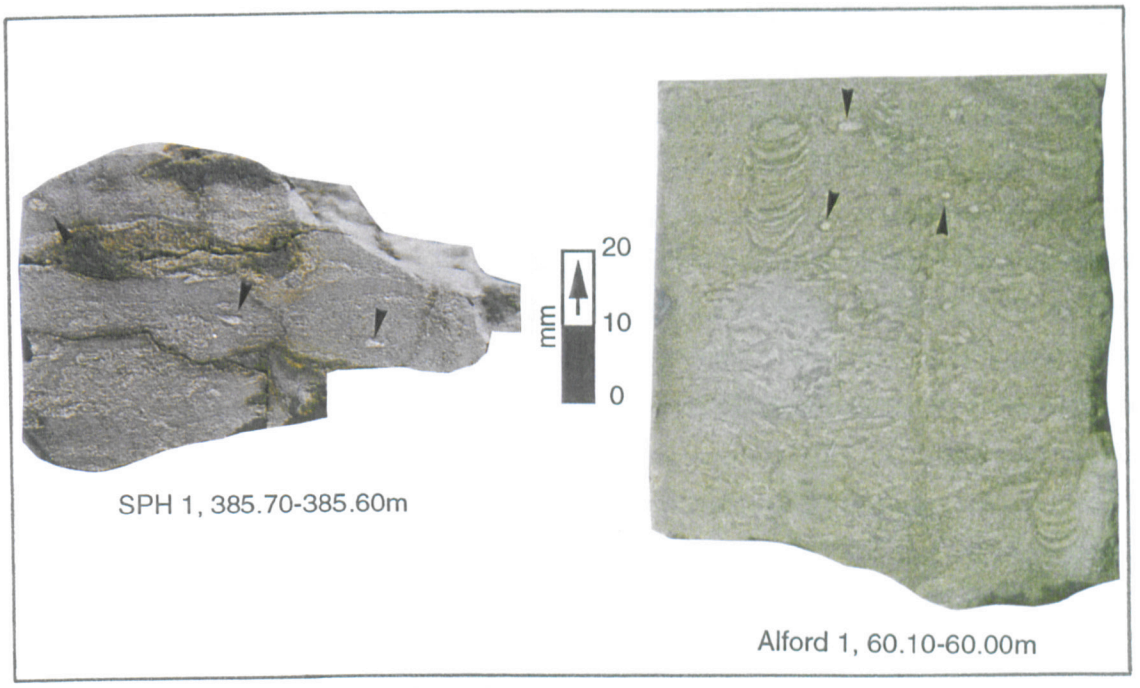

Fig.3.11 *Planolites montanus*, marked by arrows, in vertically sectioned core material.

Ichnogenus RHIZOCORALLIUM Zenker, 1836

Diagnosis. U-shaped spreiten burrows, parallel or oblique to bedding; limbs approximately parallel and distinct; ratio of tube diameter to diameter of spreite usually >1:5 (Fürsich, 1974).

Rhizocorallium irregulare Mayer, 1954

1954 *Rhizocorallium irregulare* Mayer, p.82, pls.2-3.

1974 *Rhizocorallium irregulare* Mayer; Fürsich, p.24, figs.1-2.

1994 *Rhizocorallium irregulare* Mayer; Buckman, p.135-136, fig.1.

Horizon/locality. Occasional component of Bulldog Shale trace fossil assemblages. Particularly well defined in cored material from the following depth intervals: Finniss 2, 36.91-36.71m, 28.82-28.71m, 28.66-28.48m; CBH 2, 433.50-433.40m, 330.20-330.10m

Diagnosis. Long, sinuous, bifurcating or planispiral *Rhizocorallium* burrows; predominantly horizontal (Fürsich, 1974).

Description. Preserved as endichnia in cored material. Vertically sectioned material typically intersecting the spreite only, more rarely one limb of the U-tube. Spreite oriented in the vertical plane, never bounded by wall structures, at extremities grades into host sediment, between 4.5 and 12mm thick. Burrow of *Rhizocorallium irregulare* of same diameter as spreite thickness, U-tube structure oriented with the two limbs in horizontal plane. Burrow fill typically the same as the host sediment; sharp and smooth wall lining of dark muddy material, between 0.5 and 1.0mm thick. Spreite consists of alternating pale and dark elements representing previous burrow fills and linings. Pale silty elements characteristically thicker (up to 3.0mm thick at centre) than the dark and muddy elements (approximately 0.5mm thick at centre) and this reflects the difference in original thicknesses of fill and lining. Both spreite element types gradually taper towards each lateral margin (Fig.3.12).

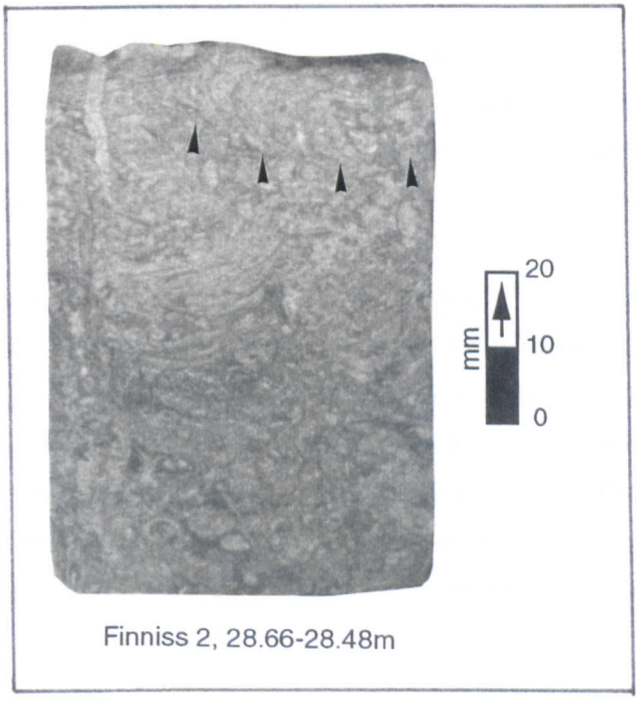

Fig.3.12 *Rhizocorallium irregulare*, marked by arrows, in vertically sectioned core material.

Discussion. Despite the incomplete nature of the Bulldog Shale *Rhizocorallium* material, owing to only partial recovery of specimens in core, it can safely be ascribed to the ichnospecies *Rhizocorallium irregulare* based on the taxonomic features outlined by Fürsich (1974), namely those of burrow length and orientation. The predominantly horizontal and slightly sinuous and irregular nature of Bulldog Shale *Rhizocorallium* is sufficient to assign it to *Rhizocorallium irregulare* and to distinguish it from the short

and oblique *Rhizocorallium jenense* and the three dimensionally coiled *Rhizocorallium uliarense*.

Fürsich (1974) considered that the three species of *Rhizocorallium* represented two separate methods of feeding; the short and oblique structures of *Rhizocorallium jenense* he inferred to be the domichnion of a suspension feeder, while the longer burrows of *Rhizocorallium irregulare* and *Rhizocorallium uliarense* he ascribed to be the fodinichnia of deposit feeders, arguing that the length and complexity of these burrows precluded the maintenance of the constant circulation of water required for suspension feeding behaviour, while conferring little extra benefit in terms of defence to the organism. This interpretation differs from that of Sellwood (1970), who considered that the burrows of *Rhizocorallium* could not provide sufficient food for deposit feeding behaviour. However, Fürsich (1974) noted that his suggestions regarding the trace making behaviour of *Rhizocorallium* were supported by palaeoenvironmental studies, in that the short and oblique burrows of *Rhizocorallium jenense* tend to be associated with those depositional environments which favour suspension feeding behaviour, while the long, sinuous and branching burrows of *Rhizocorallium irregulare* are more characteristic of muddy sediments, the ideal substrates for deposit feeders.

Veevers (1962) reviewed the occurrence of *Rhizocorallium* from Australian siliciclastic sediments and noted that almost all originated from Lower Cretaceous rocks. In consideration of this fact Veevers (1962) tentatively considered *Rhizocorallium* in Australia to be an index for the Lower Cretaceous. Such a correlation is misguided, however, for the occurrence of *Rhizocorallium* records a certain behavioural response by trace-makers to the prevalence of certain environmental conditions, albeit conditions that were evidently common in Australia during the Lower Cretaceous and rare at other times.

In trace fossil assemblages like those of the Bulldog Shale, in which traces of both *Rhizocorallium irregulare* and *Teichichnus* occur, care in identification is required, since in certain orientations they can be confused, a fact noted by Sellwood (1970) and Buckman (1994).

Ichnogenus SCHAUBCYLINDRICHNUS Frey and Howard, 1981

1910 Clustered *Terebellina* Ulrich.

1976a Clustered *Terebellina* Ulrich; Chamberlain, fig.1.

1976b Clustered *Terebellina* Ulrich; Chamberlain, fig.1.

1978 Clustered *Terebellina* Ulrich; Chamberlain, p.154, figs.61-62, 108-110, 131.

1981 *Schaubcylindrichnus* Frey and Howard, p.801-803, figs.1b, 3.

1985 *Schaubcylindrichnus* Frey and Howard; Curren, p.268, pl.4, figs. C-D; pl.5, figs. B-C.

1990 Clustered *Terebellina* Ulrich; Bromley, fig.12.12b.

1991 *Schaubcylindrichnus* Frey and Howard; Frey and Pemberton, pp.595-602, figs. 1, 4-5, 7-8, 10.

Horizon/locality. Occasional component of Bulldog Shale trace fossil assemblages. Particularly well defined in cored material from the following depth intervals: Finniss 2, 45.00-44.79m; CBH 2, 446.80-446.70m, 445.80-445.70m, 445.20-445.10m

Diagnosis. Distinct, isolated groups or bundles of congruent, lined tubes that ordinarily do not branch or interconnect. Preserved as endichnia (Frey and Howard, 1981).

Description. Preserved as endichnia, oblique and normal cross-sections of clustered horizontal burrows in cored material, resembling closely grouped burrows of *Palaeophycus heberti*, and in some cases, *Terebellina*. Between 3 and 12 burrows are clustered together, though in general the higher the number of individual burrows, the looser the cluster. Individual burrows comprise a dark and muddy fill, and a pale silty wall, both of which are sharply defined and exhibit no ornamentation. Fills are structureless, typically cylindrical but occasionally vertically compressed into rectangular or oval forms; wall linings are smooth both internally and externally, however the wall linings of individual burrows in a cluster can interconnect and exact boundaries between burrows can be difficult to define. Burrow diameters are constant for any one burrow, but burrows within a cluster may have a variety of diameters from 2.0 to 4.0mm. Wall lining thickness is equal to, or slightly greater than the diameter of the burrow fill. All the burrows in a cluster tend to have similar orientation. No branching of individual burrows is evident (Fig.3.13).

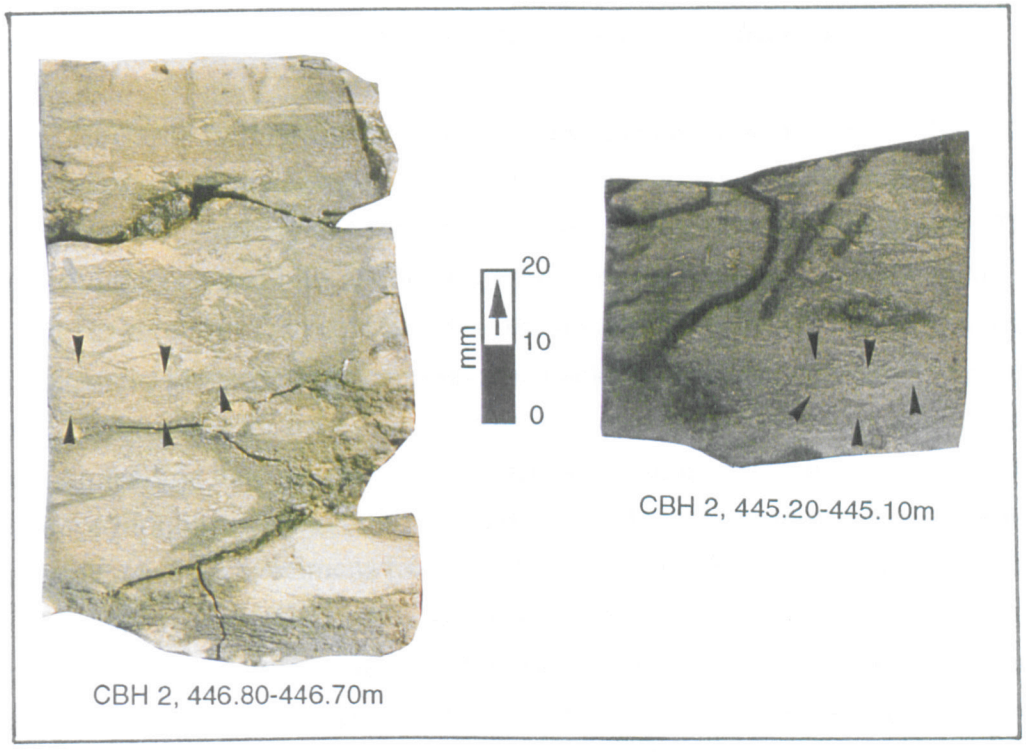

Fig.3.13 *Schaubcylindrichnus*, marked by arrows, in vertically sectioned core material.

Discussion. *Schaubcylindrichnus* from the Bulldog Shale are not defined to ichnospecies owing to incomplete recovery of specimens in cored material; the full geometry of the material is not known. Sections of horizontal components only have been observed, whereas the type species *Schaubcylindrichnus coronus*, as defined by Frey and Howard (1981) is partly identified on the curving nature of its tubes, being near vertical at the sediment-water interface and horizontal only near the distal ends.

Problems can arise with accurate identification of *Schaubcylindrichnus* in assemblages rich in *Palaeophycus heberti* and *Terebellina*, both very similar traces to *Schaubcylindrichnus*, but comprising single-tube burrows only. Indeed, Frey and Howard (1981) considered that single *Schaubcylindrichnus*, perhaps representing initial colonisation, must also occur, though they are probably mis-identified as *Palaeophycus heberti*. However, Frey and Pemberton (1991) recorded significant size differences between specimens of *Schaubcylindrichnus*, *Palaeophycus heberti* and *Terebellina* from the same trace fossil assemblage, and noted that single-tube varieties of *Schaubcylindrichnus* are rare, probably because individual tubes were possibly emplaced rapidly and in pairs. Problems of identification may occur with other

typically clustered burrow forms, namely *Phoebichnus*, though this burrow type is characteristically larger and more diffuse than *Schaubcylindrichnus*.

Frey and Howard (1981) considered that the discrete clusters of burrows that form the composite trace of *Schaubcylindrichnus*, and the congruency of those burrows, indicates a close genetic relationship between the components in each cluster. This feature, and the fact that bifurcation and interconnection probably do not occur, led Frey and Howard (1981) to conclude that the trace-makers of *Schaubcylindrichnus* were obligatory gregarious tracemakers; the thick and smooth wall linings producing a structural reinforcing for the dwelling structures of animals that either employed a suspension feeding mechanism or one of deposit feeding, using the lower aperture of the tube for foraging. Curran (1985) supported the latter hypothesis, and described *Schaubcylindrichnus* specimens from a Late Cretaceous assemblage, in which the distal ends of *Schaubcylindrichnus* tubes merge with unlined radiating burrows infilled with clean and well-sorted quartz sand. Such structures were commonly found to penetrate horizons rich in organic matter, and thus he interpreted them as representing deposit feeding by the trace maker of *Schaubcylindrichnus*. In this scenario the typical *Schaubcylindrichnus* tubes as described by Frey and Howard (1981) represent domichnia, while the associated burrows described by Curran (1985) represent fodinichnia. Such fodinichnial burrows are not present in recovered Bulldog Shale material. Frey and Pemberton (1991) suggested that variation in tube diameter and wall thickness between individual tubes in a group indicates that they were made by different animals rather than by a single trace maker, further supporting the notion that the producers of *Schaubcylindrichnus* were gregarious (coeval) trace makers. Frey and Pemberton (1991) also related the occurrence of *Schaubcylindrichnus* burrows to palaeoenvironment; they recorded their apparent affinity with the nearshore transition zone setting of mixed *Skolithos* and *Cruziana* ichnofacies.

Ichnogenus SKOLITHOS Haldeman, 1840

Diagnosis. Single, vertical, unbranched burrows, cylindrical or subcylindrical (very occasionally prismatic where the burrows are in contact), lined or unlined. Burrows perfectly straight to curved and can be inclined to the vertical. Diameter 1-15mm, may vary slightly along length of burrow, length from a few centimetres up to a metre. Burrow wall distinct to indistinct, smooth to rough, may be annulated. Sediment infill generally structureless, may exhibit a passive meniscate nature (Alpert, 1974).

Skolithos verticalis (Hall, 1843)

For detailed synonymy list of the ichnospecies *Skolithos verticalis*, see Alpert (1974).

Horizon/locality. Common component of Bulldog Shale trace fossil assemblages. Particularly well defined in cored material from the following depth intervals: Finniss 2, 38.00-37.82m (var. B), 36.91-36.71m (var. C), 34.39-34.28m (var. D), 29.15-29.00m (var. F), 29.00-28.82m (var. D); Alford 1, 48.90-48.80m (var. F); CBH 2, 485.95-485.80m (var. C), 349.80-349.70m (var. F); SPH 1, 314.30-314.20m (var. B)

Diagnosis. Burrows cylindrical to prismatic (where in contact), straight to curved, vertical to inclined. Diameter 1-4mm, length 2-15cm. Burrow wall smooth, rarely annulated (Alpert, 1974).

Description. Preserved as endichnia, longitudinally sectioned in cored material. Cylindrical in cross-section. Typically straight and vertical, but occasional curved and/or inclined forms do exist. Diameter constant in individual tubes, but varies between burrows from 1.0mm to 10.0mm, though most exhibit a diameter of between 2.0mm and 5.0mm. Overall burrow length cannot be ascertained in any specimen. Branching does not occur. Four variants of *Skolithos verticalis* are defined, as described and delineated by Taylor (1987).

Type B is distinguished by the existence of a thin, dark and muddy wall lining (equal to or less than 0.5mm) and a structureless pale silty infill. Internal and external wall lining boundaries are sharply defined and smooth, ornamentation is not present (Fig.3.14).

Type C is distinguished by the existence of a thick, dark and muddy lining (>0.5mm, often approximately 1.0mm thick) and a structureless pale silty infill. Internal and external wall lining boundaries are sharply defined and smooth, ornamentation is not present (Fig.3.14).

Type D is distinguished by the existence of a pale and silty lining (between 0.5mm and 1.0mm thick) and a structureless dark and muddy infill. Internal and external wall lining boundaries are sharply defined and smooth, ornamentation is not present (Fig.3.14).

Type F is distinguished by the lack of any wall lining combined with a structureless pale and silty infill. Burrow walls are sharp and well defined, ornamentation is absent (Fig.3.14).

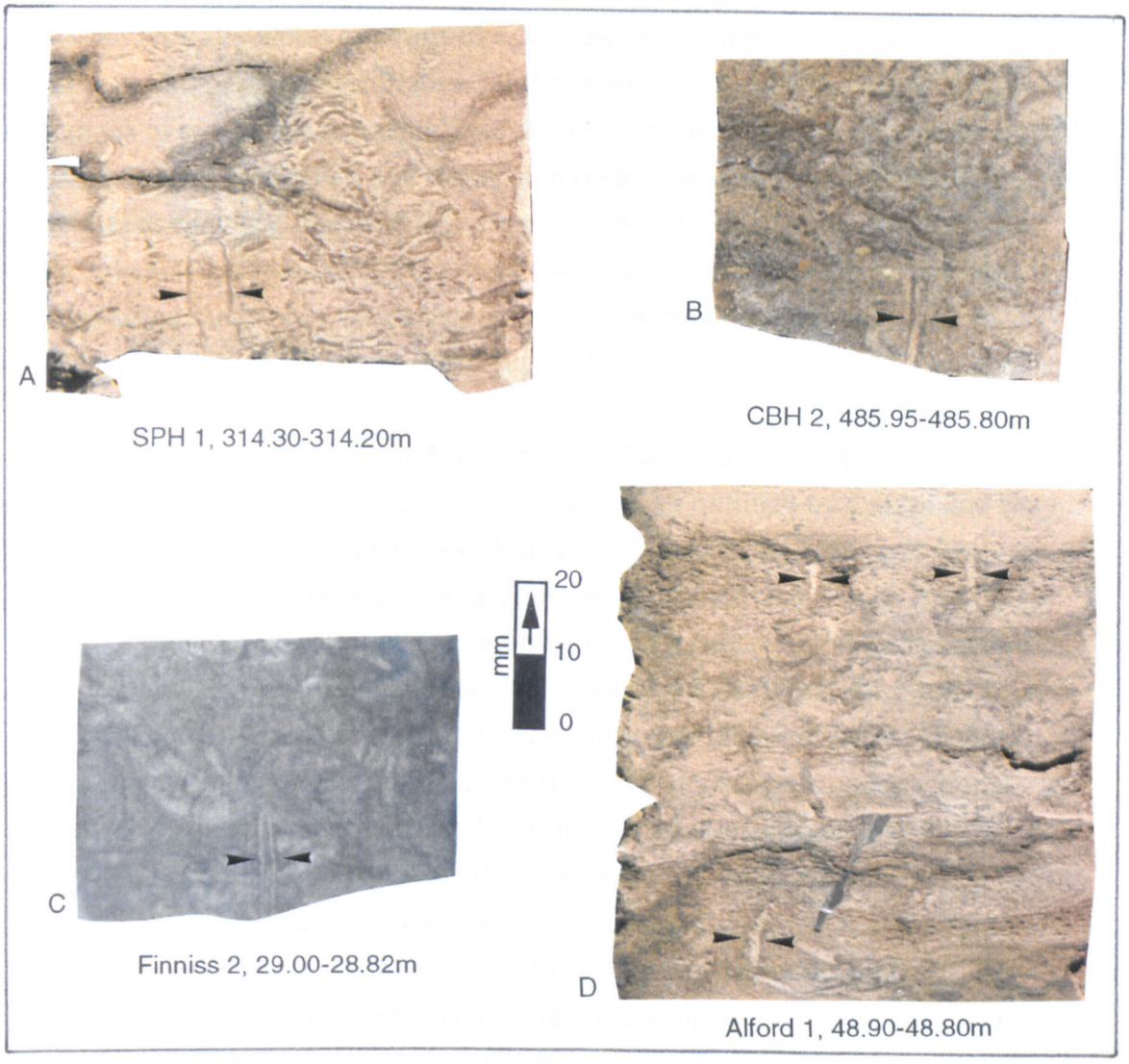

Fig.3.14 *Skolithos verticalis*, marked by arrows, in vertically sectioned core material.
(A) *Skolithos verticalis* var. B.
(B) *Skolithos verticalis* var. C.
(C) *Skolithos verticalis* var. D.
(D) *Skolithos verticalis* var. F.

Discussion. Alpert (1974) produced a review of the systematics of the ichnogenus *Skolithos*, in so doing he reduced 35 nominal ichnospecies to just 5, largely based on burrow size, orientation, and the regularity and consistency of size and orientation.

According to Alpert's (1974) scheme, all of the Bulldog Shale material fits the criteria of *Skolithos verticalis*, despite variations in burrow lining and fill. Such variations within this ichnospecies are acceptable however, for they merely represent environmentally mediated variations to a generalised trace-making behaviour process. As reviewed by Curran and Frey (1977) modern animals which produce *Skolithos*-like burrows are typically worm or worm-like, and use the burrows as domichnia, all producing mucus or chitin-lined tubes. Furthermore, statistical analyses of *Skolithos* distributions in two separate assemblages showed random distribution, a pattern typically exhibited by modern day suspension feeders, and which led Pemberton and Frey (1984) to conclude that *Skolithos* were probably the domichnia of suspension feeding animals. In addition, Vossler and Pemberton (1988b) described *Skolithos* from storm deposited sandstones which they inferred as representing the activities of opportunistic colonists following storm depopulation.

Variations in the wall lining of the Bulldog Shale *Skolithos verticalis* burrows is not a record of variation in the basic trace-making behaviour outlined by Curran and Frey (1977) and Pemberton and Frey (1984), but reflects the varying structural reinforcing required to construct and maintain such a burrow in different substrates. Both thick muddy wall linings and wall linings composed of silt-grade material reflect active constructional wall lining production within an inherently unstable substrate. Thin muddy walls however represent a thin layer of very fine material trapped in the burrow's mucus lining, produced in a more stable substrate where constructional walling is not required. Indeed, on the basis of the evidence presented by Curran and Frey (1977), it would seem likely that those burrows with no preserved muddy or silty lining, which make up the bulk of the Bulldog Shale *Skolithos* material, did have a mucus lining during the active habitation of the burrow. Variations in the filling material of *Skolithos* burrows reflects passive infill with varying sediments, and does not represent any behaviour of the trace maker.

Ichnogenus TEICHICHNUS Seilacher, 1955

Diagnosis. Long, wall-shaped septate structures consisting of a pile of gutter-shaped laminae (Fillion and Pickerill 1990).

Teichichnus rectus Seilacher, 1955

1955 *Teichichnus rectus* Seilacher, pp.122-123.

1962 *Teichichnus rectus* Seilacher; Häntzschel, p.W218, fig.136-7a-b.

1965 *Teichichnus rectus* Seilacher; Häntzschel, p.91-92.

1970 *Teichichnus* sp. Seilacher; Chisholm, pp.32-35, 38-47 (parts), fig.6, pl.VIII, figs1-2, 4-5.

1975 *Teichichnus rectus* Seilacher; Häntzschel, p.W114, fig.71-4a-d.

1985 *Teichichnus rectus* Seilacher; Frey and Bromley, pp.812-813, figs.7B, 16A-C, 18C, 33.

1990 *Teichichnus rectus* Seilacher; Fillion and Pickerill, p.61, pl.16, figs.13, 17.

Horizon/locality. Very common component of Bulldog Shale trace fossil assemblages. Particularly well defined in cored material from the following depth intervals: Finniss 2, 36.91-36.71m, 30.00-29.80m, 29.00-28.00m; Alford 1, 64.30-64.20m, 60.80-60.70m, 60.40-59.20m; CBH 2, 352.90-352.70m, 345.00-344.90m, 330.00-329.90m, 316.00-315.90m; SPH 1, 290.40-290.30m

Diagnosis. Long, straight, unbranched *Teichichnus*, planar to slightly irregular, exclusively retrusive spreite oriented at various angles to bedding (Frey and Bromley, 1985; Fillion and Pickerill, 1990).

Description. Preserved as endichnia, oblique and normal cross-sections and longitudinal sections in core and field material. Individual spreite stacks extend vertically in excess of 11cm, though most are typically 5cm or less in vertical extent (Fig.3.15). Spreite stacks are made up of alternating dark and muddy and pale and silty elements which are in all cases concave upwards and represent the upward migration of the *Teichichnus rectus*-forming burrow. The silty spreite elements are typically thicker than the muddy elements, but with increasing depth from the latest formed burrow they become increasingly compressed, and both dark and pale elements attain similar thicknesses comparable to that of the latest formed burrow wall. Spreite element thickness is constant for each element, and the spreite stack is bounded by dark muddy walls. Stacks are generally vertical and straight, though oblique forms and forms exhibiting changes in direction are not uncommon. Where obliquity of the stack occurs,

deepest concavity of each spreite element is not at the centre of that element, but is closer to the uppermost side of the stack (Fig.3.15).

Burrows responsible for the formation of the *Teichichnus rectus* stacks are of diameter 3.0 to 9.0mm, infilled with structureless pale, silty material similar to that of host sediments, and lined with a dark, muddy, smooth to frequently pelleted lining. The wall lining is variable in thickness between specimens (from less than 0.5mm to 1.0mm), but is relatively constant within individual traces. The presence of a pelleted lining to *Teichichnus*-forming burrows leads to comparison with *Ophiomorpha* burrows. Branching is not exhibited (Fig.3.15).

Discussion. *Teichichnus* burrows are largely considered to represent the deposit feeding strategies of various organisms, Häntzschel (1975) (p.W114) for instance considered the trace to be "fodinichnia, producer unknown". In their description of *Teichichnus zigzag* from chalk sediments, Frey and Bromley (1985) described a meniscate backfill structure in the last formed burrow, and subsequently inferred a deposit feeding mode of life for the trace maker, combining vertical and horizontal movement and feeding.

Creation via a deposit feeding behaviour type cannot be inferred for Bulldog Shale *Teichichnus rectus* and *Teichichnus zigzag* specimens, all of which have a constructed muddy wall lining, some pelleted and others smooth, around the last formed burrow. Such features in a burrow indicate a domichnial rather than fodinichnial role. The maintenance of *Teichichnus* as a permanent or semi-permanent burrow is further confirmed by the nature of the infilling material which bears the characteristics of passively filling the burrow after habitation. Unfortunately, complete *Teichichnus* specimens have not been recovered, however its characteristically horizontal to slightly inclined orientation indicate a relatively shallow position in the sediment column, the bulk of the burrow being horizontal with shallowly inclined sections rising to the sediment-water interface. Such a shallow location within the sediment column is also indicated by cross-cutting relationships with other trace fossil taxa (§4.3.5). Considering the incomplete nature of the material, the possibility exists that *Teichichnus* from the Bulldog Shale may have taken the form of shallow U-tubes, though this is pure speculation. The spreite stacks that form much of the composite *Teichichnus* structure represent the maintenance of a constant position within the sediment column by the trace maker. In all analysed specimens the spreite is retrusive

and the trace maker was responding to sediment aggradation, but the possibility must exist that the presence of protrusive forms is also possible.

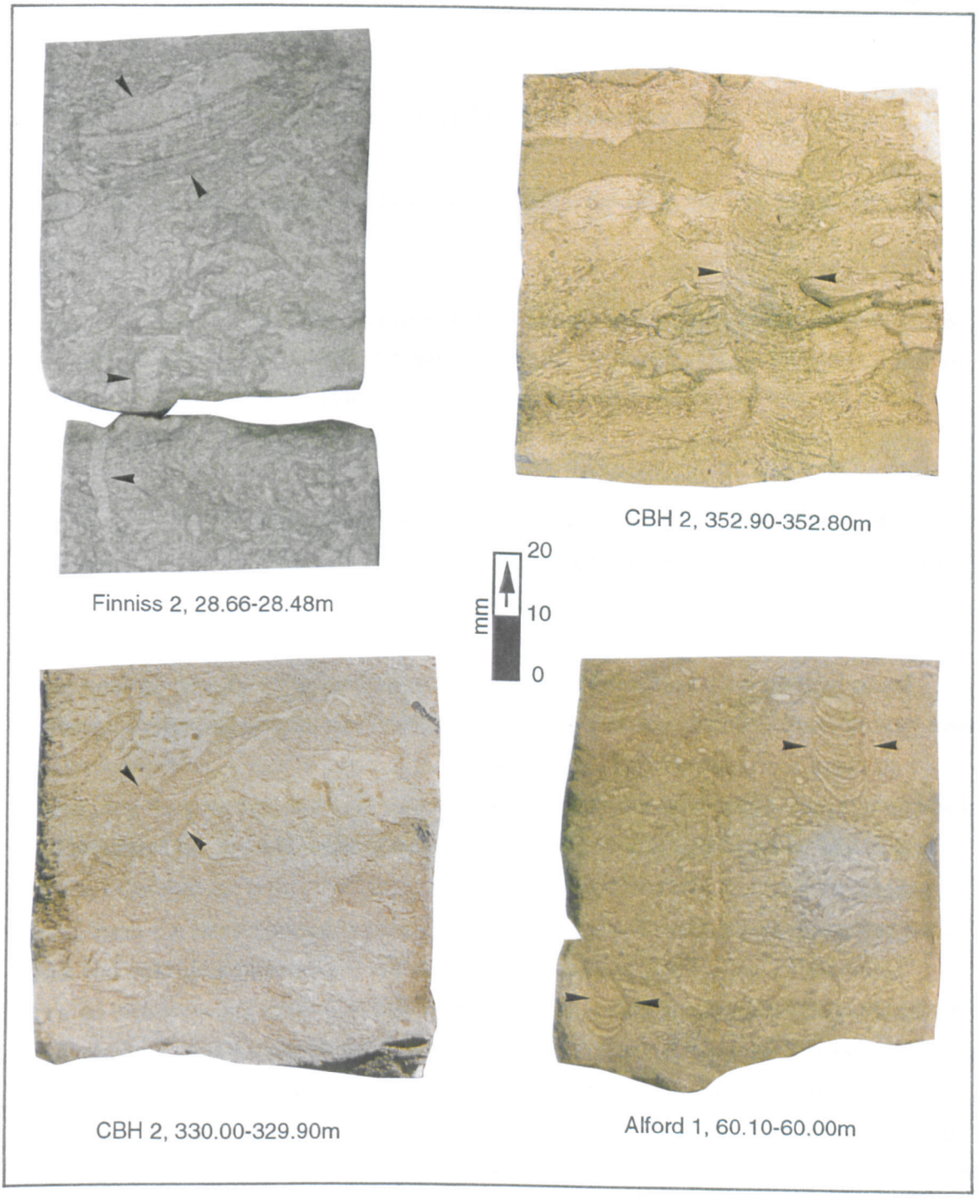

Fig.3.15 *Teichichnus rectus*, marked by arrows, in vertically sectioned core material.

The dissimilarity of the inferred mode of life for *Teichichnus*-forming trace makers in the Bulldog Shale to that inferred for very similar traces from other sediments is entirely to be expected. This is an example that not only can very different trace makers produce similar traces, but so can different modes of life, provided there is similarity in the behaviour that determines the trace's basic characteristics. While these traces may be considered to be domichnia, they also fulfil the criteria for equilibrichnia defined by Bromley (1990).

Teichichnus zigzag Frey and Bromley, 1985

1985 *Teichichnus zigzag* Frey and Bromley, pp.813-815, figs.6B, 8, 9B, 15A, 17A-C, 18A, 25B, 32, 33.

Horizon/locality. Occasional component of Bulldog Shale trace fossil assemblages. Particularly well defined in cored material from the following depth intervals: Finniss 2, 29.80-29.60m, 29.25-29.15m, 28.66-28.48m; Alford 1, 60.40-60.30m, 48.50-48.40m; CBH 2, 345.20-345.10m

Diagnosis. *Teichichnus* in which cross-sectional views of the spreite exhibit a definite zigzag pattern; overall width of the zigzagged spreite exceeds the diameter of the component burrow fills forming the spreite (Frey and Bromley, 1985).

Description. Preserved as endichnia, oblique and normal cross sections in cored material. Individual spreite stacks extend vertically downwards up to 9cm, though most are typically 5cm or less in vertical extent (Fig.3.16). Spreite stacks are made up of alternating dark muddy and light silty elements which are in all cases concave upwards and represent the upward migration of the *Teichichnus*-forming burrow. The silty spreite elements are typically thicker than the muddy elements, but with increasing depth from the latest formed burrow they become increasingly compressed, and both dark and pale elements attain similar thicknesses comparable to that of the latest formed burrow wall (approximately 1.0mm). Spreite element thickness is constant for each element, and the spreite stack is bounded by dark muddy walls. Stacks exhibit some degree of horizontal movement, and regular changes in the direction of that movement, producing a zigzag outline in cross-section. Thus, the *Teichichnus zigzag* stack is formed from a series of inclined sections of alternate direction, even though the main movement inferred from the retrusive spreite is vertically upwards. The deepest concavity of each spreite element is not at the centre of that element, unless the element

is in a rare vertically oriented part of the stack, but is closer to the uppermost side of the stack (Fig.3.16).

Fig.3.16 *Teichichnus zigzag*, marked by arrows, in vertically sectioned core material.

Burrows responsible for the formation of the *Teichichnus zigzag* stacks are of diameter 3.0 to 5.0mm, infilled with structureless pale, silty material similar to that of host sediments, and lined with a dark, muddy, smooth to frequently pelleted lining. The wall lining is variable in thickness between specimens (from less than 0.5mm to 1.0mm),

but is relatively constant within individual traces. The common occurrence of a pelleted lining to *Teichichnus*-forming burrows leads to comparison with *Ophiomorpha*. Branching is not exhibited (Fig.3.16).

Discussion. See discussion for *Teichichnus rectus*.

Ichnogenus TEREBELLINA Ulrich, 1910

1910 *Terebellina* Ulrich

1988 *Terebellina* Ulrich; Vossler and Pemberton, fig.6c.

1990 *Terebellina* Ulrich; Bromley, p.23, fig.12.3, 12.7-12.8, 12.14 (c.f. *Palaeophycus heberti*).

1992 *Terebellina* Ulrich; Pemberton, Van Wagoner and Wach, p.371, figs.10, 13B, 15D-E.

Horizon/locality. Very occasional component of Bulldog Shale trace fossil assemblages. Particularly well defined in cored material from the following depth intervals: Finniss 2, 53.43-53.23m, 30.25-30.08m; CBH 2, 511.60-511.50m, 399.20-399.10m

Diagnosis. Sub-cylindrical, horizontal to inclined, gently to strongly curved burrows with typically elliptical cross-sections. Highly variable diameter, and the tubes taper distally. Very distinct lining; infill similar in composition to host rock (Pemberton *et al.*, 1992).

Description. Preserved as endichnia, oblique and normal cross-sectioned examples in cored material. Small vertically compressed horizontal traces, diameter 1.5mm to 3.0mm in horizontal plane. Traces comprise a distinct pale and silty wall lining and a structureless infill of similar lithology to the host rock. Wall lining thickness varies between 0.5mm and 1.0mm according to trace diameter (the larger the trace the thicker the lining). Wall lining boundaries are sharply defined, smooth and unornamented both internally and externally. Branching is not evident (Fig.3.17).

Discussion. The validity of *Terebellina* as a trace fossil is a matter of some debate. The characteristic feature that allows recognition of the trace in cored material is its vertically compressed nature, which Bromley (1990) attributed to crushing of the trace after only partial infilling. However, had the trace been completely infilled and not subsequently crushed it would express all the characteristics of *Palaeophycus heberti*.

Chamberlain (1978) noted that *Terebellina* are frequently clustered, curving distally from the sediment-water interface to assume a horizontal orientation. Such characteristics indicate that *Schaubcylindrichnus* traces can also suffer from the partial infilling and crushing inferred for *Palaeophycus heberti*. In addition, Ulrich's (1910) original description of *Terebellina* stated that the tubes were short, horizontal to oblique, tapering and closed distally, further evidence for an affinity with *Schaubcylindrichnus*. *Terebellina* therefore represents *Palaeophycus heberti* and *Schaubcylindrichnus* tubes which were only partly infilled, and which suffered subsequent crushing.

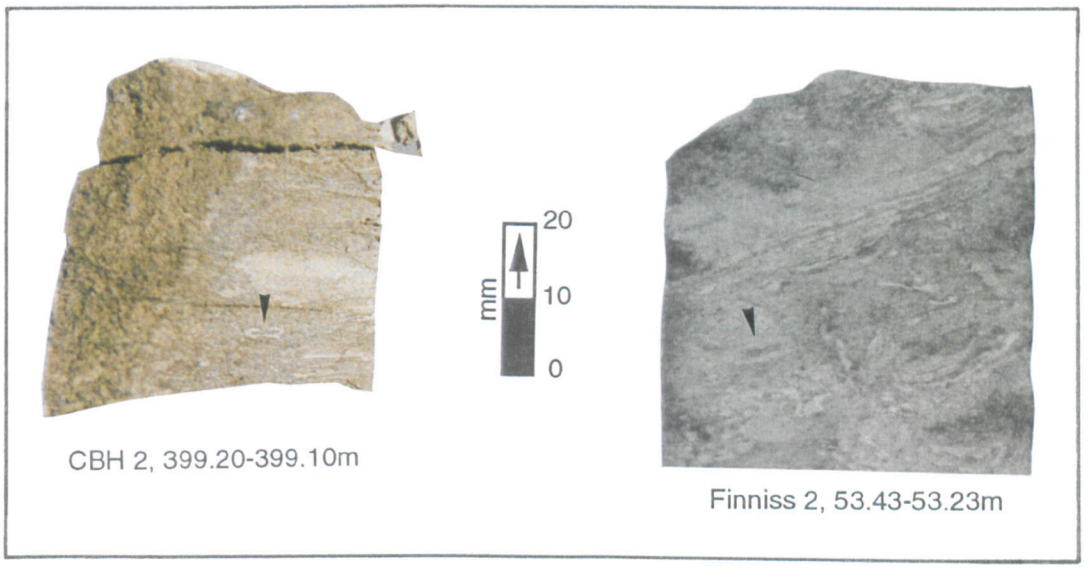

Fig.3.17 *Terebellina*, marked by arrows, in vertically sectioned core material.

These characteristics, despite producing a trace fossil of striking appearance, are determined by environmental parameters. For example, Bromley (1990) noted the characteristic occurrence of *Terebellina* traces in offshore muddy environments. As such, the partial infilling and crushing which have been used to determine *Terebellina* have nothing to do with the behaviour of the trace maker, and thus should not be used as taxonomic criteria; *Terebellina* where present as single burrows may be considered to be partly infilled and crushed *Palaeophycus heberti*, and where present in clusters may be considered to be partly infilled and crushed *Schaubcylindrichnus* traces. All Bulldog Shale *Terebellina* material exists as single tubes.

Ichnogenus THALASSINOIDES Ehrenberg, 1944

Diagnosis. Extensive burrow systems with vertical, inclined and horizontal components. Burrows cylindrical with diameter of 2cm-20cm, burrow dimensions are variable within a system. Branching regular, characterised by Y-shaped bifurcations, may be swollen at point of branching. Horizontal elements join to form polygons and are connected to the sediment-water interface by vertical or steeply inclined shafts (Kennedy, 1967).

Thalassinoides suevicus (Rieth, 1932)

For detailed synonymy of the ichnospecies *Thalassinoides suevicus*, see Kennedy (1967).

Horizon/locality. Relatively common component of Bulldog Shale trace fossil assemblages. Particularly well defined in cored material from the following depth intervals: Finniss 2, 37.20-37.00m, 28.82-28.71m; CBH 2, 329.60-329.50m; SPH 1, 387.90-387.80m, 385.10-385.00m, 384.90-384.80m, 307.80-307.70m

Diagnosis. *Thalassinoides* with tunnel diameters between 2cm-5cm. Lacks wall ornamentation (Kennedy, 1967).

Description. Preserved as endichnia, oblique and normal cross-sections in core and field material. Cylindrical burrows, predominantly horizontal or shallowly inclined, but vertical and steeply inclined tunnels are by no means rare. Tunnel diameter is constant in individual burrows, but varies between burrows from 7mm to 17mm. Burrows are unlined, though the wall is sharply defined. Burrow infill typically siltier than the host sediment, and in some cases has been re-bioturbated by *Anconichnus horizontalis*, and in such cases the re-bioturbator rarely penetrates the *Thalassinoides* wall. Branching is only uncommonly observed in cored material, but follows a downwards Y pattern without swelling at the nodes (Fig.3.18).

Discussion. *Thalassinoides* is distinguished from *Ophiomorpha* on the basis of its unlined wall; both traces have similar burrow geometry and, along with the spiral burrow *Gyrolithes*, are considered to be the work of various decapod crustaceans, particularly callianassid and thalassinidean shrimp, as reviewed by Bromley and Frey (1974) and Myrow (1995). Environmental parameters determine which burrow-type is

produced, and thus which burrow-building behaviour is deployed by the trace maker. All three types of burrow can intergrade (Bromley and Frey, 1974). For instance, Kern and Warme (1974) described burrow systems that comprise *Thalassinoides* in muddy interbeds where a structurally reinforcing wall lining is not required, and which attain a pelleted lining and thus form *Ophiomorpha* burrows in siltier interbeds where structural support for the burrow boundaries is required. Bromley (1990) noted similar features in modern burrows inhabited by *Callianassa biformis* shrimp.

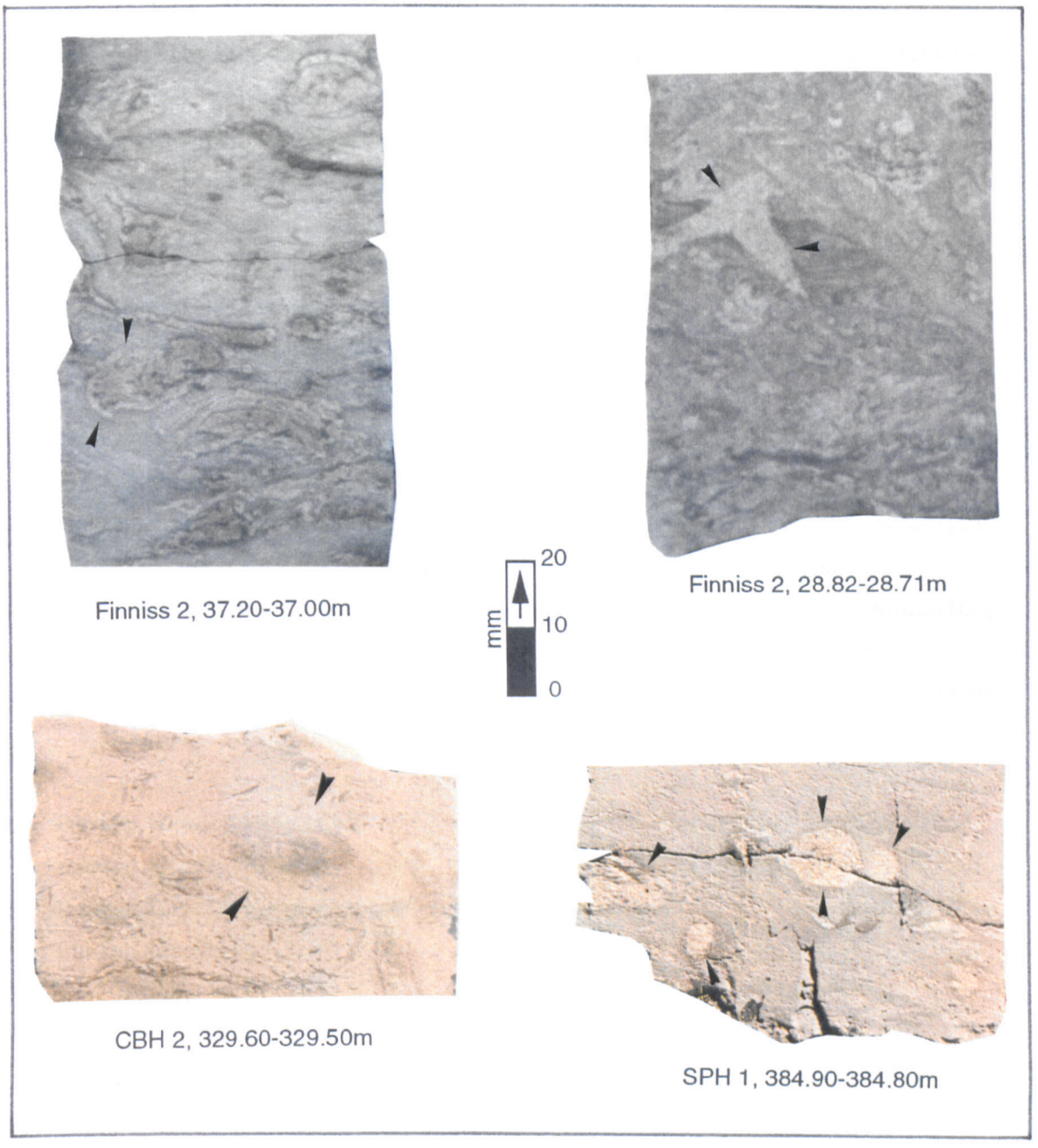

Fig.3.18 *Thalassinoides suevicus*, marked by arrows, in vertically sectioned core material.

3.3 A key to the Bulldog Shale trace fossils

A key has been constructed to provide a means for easy identification of trace fossils in core and field material of the Bulldog Shale (table 3.1), though it will also be useful in earlier and later marine Mesozoic trace fossil assemblages from the Eromanga Basin.

Table 3.1 A key to the trace fossils of the Bulldog Shale. Bold numbers in right column indicate which row to go to.

1a.	Traces predominantly vertically oriented, straight, cylindrical to subcylindrical, rarely inclined or curved, lined or unlined----------	*Skolithos verticalis* (Hall, 1843) **(2)**
1b.	Traces produced by migration of horizontal cylindrical to subcylindrical burrows in the vertical plane, producing stacked array of previous burrows----------	**(3)**
1c.	Traces with both vertically and horizontally oriented cylindrical to subcylindrical components----------	**(5)**
1d.	Traces predominantly horizontally oriented----------	**(8)**
2a.	Structureless pale silty fill; thin (approximately 0.25x thickness of silty fill), smooth, dark muddy lining----------	*Skolithos verticalis* (Hall, 1843) var. B
2b.	Structureless pale silty fill; thick (approximately 0.5-1.0x thickness of silty fill), smooth, dark muddy lining----------	*Skolithos verticalis* (Hall, 1843) var. C
2c.	Structureless dark muddy fill; thick (approximately 0.5x thickness of muddy fill), pale silty lining----------	*Skolithos verticalis* (Hall, 1843) var. D
2d.	Structureless pale silty fill, unlined----------	*Skolithos verticalis* (Hall, 1843) var. F
3a.	Previous burrow positions represented by vertically stacked, slightly concave upwards, horizontal to slightly inclined spreite----------	*Teichichnus* Seilacher, 1955 **(4)**
3b.	Previous burrows vertically compressed, but individual walls and fills still discernible----------	*Ophiomorpha nodosa* var. *spatha* Hester and Pryor, 1972
4a.	Straight form, little lateral shift; distinct growth stages occasionally visible----------	*Teichichnus rectus* Seilacher, 1955
	Considerable lateral shift in vertical stack----------	*Teichichnus zigzag* Frey and Bromley, 1985

5a.	Unbranched, small diameter (<3mm), faecal mud fill, diffuse silty halo, orientation variable, irregular "frog spawn" appearance---------	*Anconichnus horizontalis* Kern, 1978
5b.	Regular diameter, downwards Y and T branching----------	(6)
6a.	Large diameter (>5mm), structureless pale silty fill, dark muddy pelleted wall----------	*Ophiomorpha* Lundgren, 1891 (7)
6b.	Small diameter (<2mm), structureless pale silty fill, unlined----------	*Chondrites* von Sternberg, 1833
6c.	Large diameter (>5mm), structureless pale silty fill, unlined----------	*Thalassinoides suevicus* (Rieth, 1932)
7a.	Thick (0.5-2.0mm), single-pelleted, occasionally incomplete lining with nodulose outer surface and smooth inner surface----------	*Ophiomorpha nodosa* Lundgren, 1891
7b.	Thin (<0.5mm), sparsely nodulose, irregular, often incomplete lining----------	*Ophiomorpha irregulaire* Frey, Howard and Pryor, 1978
8a.	Horizontal to slightly inclined, cylindrical to sub-cylindrical traces--	(9)
8b.	Large (>5mm) U-tube spreiten burrows. Limbs parallel to slightly oblique to bedding plane and parallel to each other in the horizontal plane. Well-developed spreiten between the arms, typically protrusive, is normally all that is observed in core - limbs typically not sampled----------	*Rhizocorallium irregulare* Mayer, 1954
9a.	Traces with lining----------	(10)
9b.	Traces without lining----------	(17)
10a.	Dark, predominantly muddy lining, pale structureless silty fill--------	(11)
10b.	Pale, predominantly silty lining, dark structureless muddy fill--------	(13)
11a.	Lining pelleted----------	*Ophiomorpha* Lundgren, 1891 (12)
11b.	Lining non-pelleted, smooth, thin (diameter of lining + fill <2x that of fill alone)----------	*Palaeophycus tubularis* Hall, 1847
12a.	Thick (0.5-2.0mm), single pellet wall construction with nodulose outer surface and smooth inner surface, occasionally incomplete-----	*Ophiomorpha nodosa* Lundgren, 1891

12b.	Thin (<0.5mm), sparsely nodulose, irregular, often incomplete lining----------	*Ophiomorpha irregulaire* Frey, Howard and Pryor, 1978
13a.	Small diameter (<3mm), unbranched, faecal mud fill and diffuse silty halo, variable orientation, irregular "frog spawn" appearance---	*Anconichnus horizontalis* Kern, 1978
13b.	Large diameter (>5mm), regular silty lining, cylindrical to subcylindrical traces----------	**(14)**
14a.	Diameter of entire trace (lining + fill) less than 3x that of fill alone--	**(15)**
14b.	Large diameter (>10mm), diameter of entire trace (lining + fill) greater than 3x that of fill alone, frequently clustered----------	*Phoebichnus* Bromley and Asgaard, 1972
15a.	Traces generally solitary, low density----------	**(16)**
15b.	Generally clustered, high density----------	*Schaubcylindrichnus* Frey and Howard, 1981
16a.	Cylindrical to slightly subcylindrical----------	*Palaeophycus heberti* Saporta, 1872
16b.	Very subcylindrical, vertically compressed, muddy fill rectangular in cross-section----------	*Terebellina* Ulrich, 1910
17a.	Cylindrical to slightly subcylindrical, structureless silty or muddy fill, fill differs from matrix----------	*Planolites montanus* Richter, 1937
17b.	Very sub-cylindrical, vertically compressed; bilobed upper margin, m-form in cross-section; fill similar to matrix----------	*Gyrochorte comosa* Heer, 1865

Chapter 4

Palaeoenvironmental Fabric Type Analysis

4.1 Bioturbation and ichnofabrics: an overview

This chapter concerns the development of the Palaeoenvironmental Fabric Type (PFT) methodology, and the application of this new scheme to the rock fabrics of the Bulldog Shale. To set the scene an overview of bioturbation and ichnofabrics is provided, along with details of their environmental implications. In addition, previous schemes for the measurement and classification of bioturbation and ichnofabrics are discussed and evaluated. Problems with these schemes are defined, and the ability to solve those problems through the use of the PFT methodology is assessed.

4.1.1 Trace Fossil Tiering

As in modern marine sediments, organisms living in comparable ancient marine deposits were tiered (Ausich and Bottjer, 1982; Bottjer and Ausich, 1986). Tiering, in this instance, is defined as the vertical distribution of taxa at different depths within the sediment.

Vertical profiles of modern marine sediments illustrate the existence of two important layers, a result of differences in sediment and water content. These layers, originally defined by Ekdale *et al.* (1984), comprise the surface layer and transition layer. The surface layer, or mixed layer, ranges from a few centimetres to a decimetre in thickness and does not preserve trace fossils well due to a relatively high water content. Directly underlying the mixed layer is the transition layer, which ranges from one decimetre to several decimetres in thickness and is characterised by a tiered array of organisms that live or feed at various depths within the sediment column; the sediments of the transition layer have less water content than those of the surface layer and thus trace fossils are better preserved. With accretion of the sediment and consequent upward migration of the actively bioturbated zone, the burrows become part of the historical layer, which directly underlies the transition layer, and in which no further burrowing occurs. This process produces a composite record of the tiered traces, in which burrows from the deeper tiers cross-cut burrows of the originally shallower tiers (Fig.4.01). Where this assemblage contains an association of traces produced in a stable environment by a single community of organisms it is termed an ichnocoenosis,

originally defined by Lessertisseur (1955). In situations where there is a changing environment, a succession of communities may occupy the same sediment. These produce a series of superimposed ichnocoenoses, termed "composite ichnofabrics" by Bromley and Ekdale (1986) and Ekdale and Bromley (1991). Detailed analysis of the cross-cutting relationships in ichnocoenoses and composite ichnofabrics enables the reconstruction of the original tiered community structure.

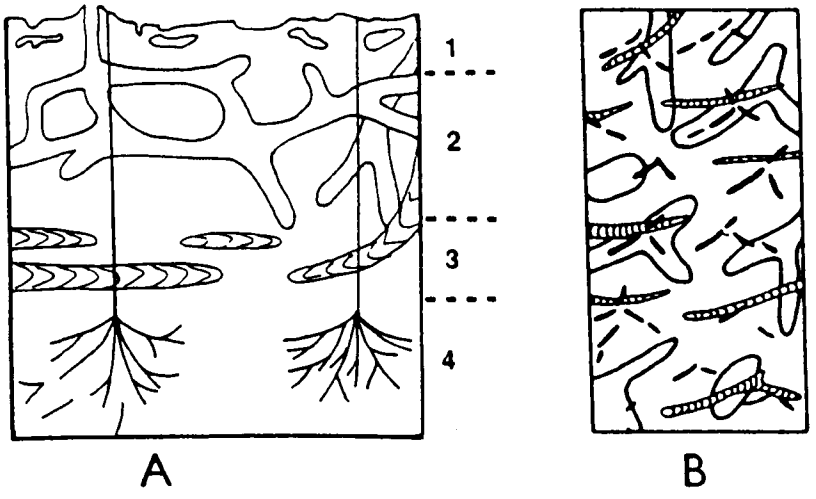

Fig.4.01 Tiering of infauna as recognised from the study of trace fossils.
(A) Schematic vertical profile of modern marine sediments with four tiers. Tier 1 contains poorly preserved burrows of the mixed layer, tier 2 *Thalassinoides*, tier 3 *Zoophycos*, tier 4 *Chondrites*; tiers 2-4 are in the transition layer. Thickness of the actively bioturbated mixed and transition layers varies, but in this example it is 15cm.
(B) Schematic illustration of the composite record of tiering (transition layer burrows only) that is produced with sediment accretion and subsequent upward migration of trace fossil tiers 2, 3 and 4. Tier 4 cross-cuts tiers 3 and 2, tier 3 cross-cuts tier 2, and tier 2 cross-cuts none of the preserved burrows.
From Droser and Bottjer (1993).

4.1.2 Ichnofabric defined

Ichnofabric was first defined by Ekdale and Bromley (1983) (Pg. 110) as "those aspects of the texture and internal structure of a sediment resulting from all phases of bioturbation". Thus, ichnofabric represents the totality of bioturbation structures in a sedimentary rock, including both identifiable traces and unidentifiable mottled traces

(Droser and Bottjer, 1989; 1991; Droser and O'Connell, 1992; Droser and Bottjer, 1993; 1994). Taylor and Goldring (1993) (pg. 141) went further, with their interpretation of Ekdale and Bromley's (1983) definition of ichnofabric by describing it as "a record of the primary sedimentary conditions, original endobenthic community structure, and subsequent history of one or more phases of biogenic activity".

4.1.3 Controlling factors on ichnofabric

Trace fossils are, by definition, *in-situ* records of their maker's behaviour. As such, the preserved ichnofabric ultimately relates to the local environment during sediment deposition. Bromley and Ekdale (1986) stated that, in the marine realm, the most important controlling factors on ichnofabric are water depth, salinity, substrate character and oxygen content of the bottom and interstitial waters. Wetzel (1991) also considered organic matter content of the sediment, and sediment accumulation rate, to be important.

Variation of Bulldog Shale ichnofabrics may be considered to be the result of variations in substrate character and its accumulation rate, and bottom water oxygenation levels. Variation due to water depth, as portrayed in Seilacher's (1964, 1967) ichnofacies concept, can be discarded since, according to the scheme, all Bulldog Shale trace fossil assemblages were deposited in shallow marine environments, and no further resolution can be made. In any case, the bathymetrically-controlled ichnofacies scheme has largely been rejected, for water depth itself is not perceived to be a determining factor (Byers, 1982; Goldring, 1993, 1995). Salinity as a factor may also be discarded, since the effects of salinity variation on the behaviour of organisms, as expressed in trace fossils, represents only minor modifications to typical marine assemblages (Pemberton and Wightman, 1992). Furthermore, as revealed by organic carbon analysis (§5.2.4), organic matter content exhibits no statistically significant variation throughout the Bulldog Shale succession, and thus it is unlikely that organic matter content of the sediment played a part in the variation of its ichnofabrics.

Substrate character

Goldring (1995) reported that the nature of the substrate affects trophism, and the attachment and penetration of benthic organisms. As such, substrate character may be considered an important control on resultant ichnofabric.

Wetzel (1991) stated that bioturbation is affected by grain size due to variations in the permeability and consistency of the sediment. In addition substrate consistency has important affects, not only on the burrow-types emplaced, but also on their style of preservation (Goldring, 1995). Coarse silty and sandy deposits are less stable than fine-grained sediments at tunnel boundaries and so if burrows are to be kept open in these coarser deposits the wall has to be structurally reinforced with a lining. Of particular relevance to the present study, Kern and Warme (1974) described interconnected burrow networks penetrating both sandy and muddy horizons in an interbedded sequence. Those burrows of the network penetrating the sandier beds were of the taxon *Ophiomorpha* with its strengthening pelleted burrow walls, while in the muddier interbeds the burrow wall was absent and the burrows, despite obviously being formed by the same organism, were of the taxon *Thalassinoides*. Frey *et al.* (1978), also working on *Ophiomorpha*, noted that horizontal burrows occasionally have a thickly-walled roof and a thinly-walled floor. This morphology usually occurs at lithological interfaces, and reflects the need for a stronger retaining wall above the burrow than below it.

Sediment accumulation rate

As Wetzel (1991) stated, infaunal activity is greatly influenced by the amount of sediment deposited per unit time and its rate of change. Wetzel (1991) distinguished two end members of sedimentation rate variation: slight changes with a low rate of change and a short to long period; and event sedimentation with a large rate of change and a relatively short period.

Slight changes in sedimentation rate indirectly affect benthic infauna through the resulting change in burial rate of organic material, and therefore, benthic food availability is altered. Low sedimentation rates usually correspond to low numbers of tiers within a thin transition layer, the result of low inputs of food in the form of organic matter. With increasing rate of sedimentation the input of food material increases, a larger number of tiers are produced, and therefore the transition zone becomes thicker.

Large increases in sedimentation rate result in less sediment reworking because the infaunal organisms have insufficient time to completely burrow a specific sediment layer. Thus, due to a reduction in the amount of cross-cutting and reworking of traces, the preservation potential of traces, particularly that of shallow forms most at risk from over-printing, increases (Wetzel, 1991). The opposite affect occurs with a large decrease in sedimentation rates.

Bottom-water oxygenation levels

As summarised by Allison *et al.* (1995), fully oxygenated modern marine waters contain approximately 8ml O_2/l H_2O. Studies of benthic life inhabiting modern basins in which bottom-water oxygenation levels vary (Rhoads and Morse, 1971; Byers, 1977; Savrda *et al.*, 1984; Edwards, 1985; Thompson *et al.*, 1985) has allowed marine waters to be divided into three categories of dissolved oxygen concentration: aerobic (fully oxygenated), where oxygen concentrations exceed 1.0ml O_2/l H_2O; dysaerobic (poorly oxygenated), oxygen concentrations between 1.0 and 0.1ml O_2/l H_2O; and anaerobic (anoxic), oxygen concentrations lower than 0.1ml O_2/l H_2O. With such a decline in oxygen levels there are corresponding changes in the benthic infauna and thus in the traces produced. These trends, along with those for benthic epifauna, are summarised in two separate models: the "Rhoads/Morse/Byers (RMB) model", and the shelf model, both discussed by Wignall (1994).

From the two models, the variation of two features under declining bottom-water oxygenation levels are in agreement:
1) trace fossil species diversity, and that of benthic organisms in general, declines with oxygen levels to become zero at the dysaerobic/ anaerobic boundary;
2) depth and size of burrows decrease until, in the lowest dysaerobic conditions, burrows become too small to disrupt millimetre-scale lamination. Therefore there is a transition from burrowed to laminated sediment.
In addition, the RMB model predicts a change in life strategies of the benthos; deposit feeding increases while suspension feeding decreases.

These oxygen-related ichnological trends have subsequently been used to develop models that enable the reconstruction of palaeo-oxygenation conditions. Two such models are discussed here: the trace fossil tiering/oxygen-related biofacies scheme of Savrda and Bottjer (1986; 1987a; 1987b; 1991), and the behavioural model of Ekdale and Mason (1988).

Trace fossil tiering/oxygen-related biofacies model

As discussed previously (§4.1.1), under well-oxygenated conditions trace makers produce a complex tiered burrow system. In such situations, burrowers of the deepest tier commonly excavate anaerobic sediments beneath the redox potential discontinuity, yet they survive through the active irrigation of their burrows (Wetzel 1991). As bottom-water oxygen levels decline, either along lateral sea-floor oxygenation gradients or through time, it becomes increasingly difficult to oxygenate these deep burrows, and

so the burrows of the deepest tiers, produced by organisms most adapted to low oxygen levels, become shallower whilst the burrows of the shallower tiers, created by organisms less adapted to low oxygen levels, are lost. In addition to this decline in the penetration depth of transition layer burrows there is also a reduction in the diversity of traces, the size of the trace makers, and thus in the mean burrow diameter (Fig.4.02) (Savrda and Bottjer 1987b).

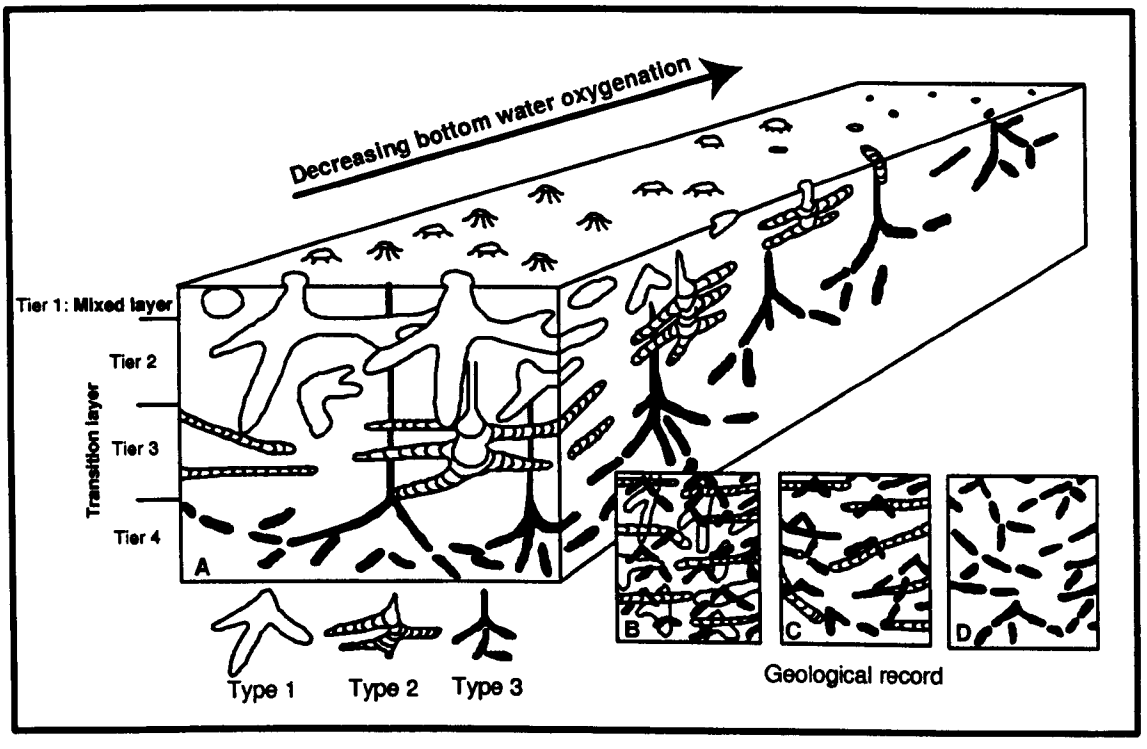

Fig.4.02 Changes in burrow size, bioturbation depth, and tiering structure associated with a declining oxygen gradient (A), and expected trace fossil cross-cutting relationships in strata deposited at various sites along the gradient (B, C, and D). Tiering as in Fig.4.01.
Redrawn from Savrda and Bottjer (1987b).

Savrda and Bottjer's (1986; 1987b; 1991) scheme is largely concerned with defining "oxygen-related ichnocoenoses" or ORIs. Examples of predicted ORIs under a declining oxygen gradient are given in Figs.4.02B, C, and D, and were produced by the upward migration of a tiered array of trace making organisms keeping pace with sedimentation (§4.1.1).

Variations in these ORIs have been used by Savrda and Bottjer (1986; 1987b; 1989; 1991) to define temporal changes, and variations in the rapidity of those changes in

oxygenation levels; in addition, through detailed vertical sequence analysis the model has been utilised to reconstruct palaeo-oxygenation histories of stratigraphic sequences.

The behavioural model

Ekdale and Mason (1988) presented a model in which the control of oxygenation levels on ichnofabric is expressed in changing behavioural strategies, particularly with regard to feeding methods.

With an increase in oxygenation levels from the non-bioturbated anaerobic state Ekdale and Mason's (1988) model predicts the successive dominance of three distinctive feeding strategies (Fig.4.03); those of domichnia, pascichnia and fodinichnia. These terms form part of Seilacher's (1953) ethological classification of ichnocoenoses.

In the lowest dysaerobic environment fodinichnia are dominant. Fodinichnial traces are the product of non-vagile deposit feeders, systematically mining the sediment for food. Theirs is an opportunistic lifestyle, eking out a living in anaerobic sediment with permanent connections to the sediment surface and the poorly oxygenated bottom waters.

With increasing bottom-water oxygenation interstitial waters become partially oxygenated. With this increase in oxygen levels there is an associated change in trace maker feeding strategies and a pascichnia assemblage is formed. Pascichnia are produced by vagile detritus and deposit feeders, feeding either on the sediment surface or endobenthically, in the search for digestible organic matter. The presence of such unoxidised digestible organic matter within the sediment is an indication of oxygen depletion within the interstitial waters; however some oxygen must be present for these endobenthic animals, which maintain no open connection to the surface and must take their oxygen from the interstitial water.

With further oxygenation, the bottom waters and the interstitial waters become fully oxygenated. Organic matter is rapidly decomposed and thus deposit feeders cannot survive in these conditions. Domichnial assemblages tend to form in these environments, comprising the permanent dwelling structures of suspension feeding animals.

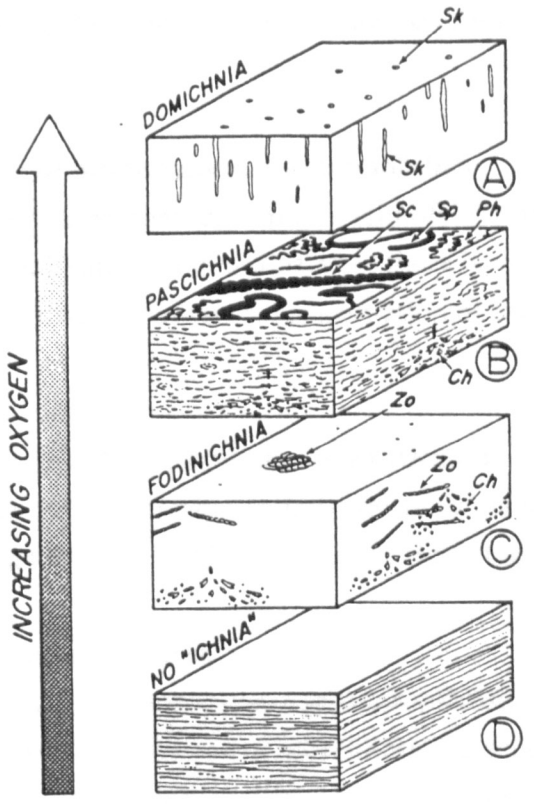

Fig.4.03 Model for oxygen-controlled ichnofabric composition based on dominant trace maker feeding behaviour.
(A) Domichnia-dominated trace makers, occurring where bottom water and interstitial water is fully oxygenated (aerobic).
(B) Pascichnia-dominated trace makers, occurring where bottom water is aerobic or dysaerobic, and the interstitial water is dysaerobic.
(C) Fodinichnia-dominated trace makers, occurring where bottom water is aerobic, or more probably dysaerobic, and the interstitial water is anaerobic.
(D) The abiotic state with no trace makers, occurring where the bottom water and the interstitial water is anaerobic.
Sk. = *Skolithos*, *Sc.* = *Scalarituba*, *Sp.* = *Spirophyton*, *Ph.* = *Phycosiphon*, *Ch.* = *Chondrites*, *Zo.* = *Zoophycos*.
From Ekdale and Mason (1988).

Each of the two models presented here can be used independently as a tool to reconstruct palaeo-oxygenation trends and curves. Used together, however, they act as a more powerful descriptor of palaeoenvironment, being records of independent behavioural responses to a single environmental forcing. Under any apparent oxygenation or deoxygenation, with the associated gain or loss of tiers and ichnotaxa,

the replacement of traces representative of one feeding strategy with traces representative of another should be included in the analysis for reasons of completeness and accuracy.

4.1.4 Index measurements of bioturbation and ichnofabric

In order to advance from the subjective reporting of ichnofabric data (e.g. poorly bioturbated, moderately bioturbated, well bioturbated) there have been a number of proposed models for standardised analysis and presentation of trace fossil assemblage data.

Arguably the most popular model for ichnofabric classification is the 'ichnofabric index', first proposed by Droser and Bottjer (1986) and subsequently modified in a series of papers (Droser and Bottjer, 1989; 1991; 1993; Bottjer and Droser, 1991).

Droser and Bottjer's ichnofabric index

Based on studies of Cambrian and Ordovician carbonates Droser and Bottjer (1986) produced a "semiquantitative classification of ichnofabric", a scheme which allows the ranking of extent of bioturbation, as reflected by ichnofabric, in six categories. These categories, termed ichnofabric indices (ii), are based on the extent of bioturbation, regarding the degree to which the original sedimentary structures have been biogenically disrupted, and were defined from planimeter studies of 50cm by 35cm vertical cross-sectional areas. The six ichnofabric indices are:

(1) No bioturbation recorded; all original sedimentary structures preserved.

(2) Discrete, isolated trace fossils; up to 10% of original bedding disturbed.

(3) Burrows generally isolated, but locally overlap; approximately 10 to 40% of original bedding disturbed.

(4) Burrows overlap and are not always well defined, only last vestiges of bedding discernible; approximately 40 to 60% of original bedding disturbed.

(5) Discrete burrows still present, though bedding completely disturbed.

(6) No discrete burrows; bedding nearly or totally homogenised.

These six ichnofabric indices were presented in a "flash card" form to enable rapid estimation of ichnofabric index in stratigraphic sequences at various scales in the field or in the laboratory. However, as Droser and Bottjer (1986) stated, these specific diagrams are directly applicable only to the rocks from which they were defined. For other types of strata different sets of diagrams are required to reflect dissimilar primary physical structures, bed thicknesses, and trace fossil assemblages; if, however, these are

constructed using the same definitions for ichnofabric indices as proposed by Droser and Bottjer (1986) the data will be comparable.

To meet this requirement, Droser and Bottjer (1989) and Droser (1991) applied their scheme to sandstones deposited in high-energy nearshore environments. They presented flash card series for strata dominated by *Skolithos* traces, and those dominated by *Ophiomorpha* traces.

Further additions to the environments and strata covered by the ichnofabric index scheme were made by Droser and Bottjer (1991) in a study of deep sea sediments of Cretaceous and Tertiary age. Somewhat surprisingly, given the need for environment-specific adaptations of the model, these same flash cards were also used by Droser and O'Connell (1992) in a study of Triassic shallow water and marginal marine sediments.

Another development of the ichnofabric index scheme is the use of "ichnograms" (Bottjer and Droser 1991). These involve the tallying of ichnofabric index data over a given thickness, which is then normalised in terms of percent of the total measured thickness. These data are then plotted on histograms, or "ichnograms", which provide a summary of ichnofabric index data when computed from data collected from sediments deposited in a single defined sedimentary environment. In addition, to further characterise a succession, an average ichnofabric index can be calculated and used for comparative purposes.

Despite their wide use, index measurements of ichnofabric are not without problems. Frey and Wheatcroft (1989) and Wheatcroft and Frey (1990) noted that measurements of the percentage area of disturbed sediments are not the best way to quantify bioturbation for they exclude too much information inherent within the sediments and the trace fossil assemblages, and they are too dependent on variations in sedimentation rates. Consequently, such index measurements do not provide well for comparison between different sedimentary environments. Rather, information regarding trace maker abundance, or the amount of sediment moved per unit time by the trace makers, would give more accurate results. Wheatcroft and Frey (1990) produced a statistical methodology based on spatial autocorrelation to address these problems. However, Taylor and Goldring (1993) pointed out that such studies are difficult and time consuming to perform, and suggested a more utilitarian methodology based more on description than quantification.

Taylor and Goldring's ichnofabric analysis model

Taylor and Goldring (1993) argued that the measurement of the degree of bioturbation only assesses the rate of biogenic activity which is controlled by sedimentation, erosion and diagenetic variables. As such, the ichnofabric indices, which as Taylor and Goldring (1993) accurately stated should be termed bioturbation indices, do not adequately reflect parameters such as the ichnotaxa present, diversity, density, and cross-cutting relationships that interact to produce an ichnofabric. In addition, as Ekdale and Bromley (1991) explained, where a succession of infaunal communities produce a series of super-imposed ichnocoenoses it is virtually impossible to characterise the assemblage by a single index number.

Taylor and Goldring (1993) thus presented their own model as an alternative to the solely index-based schemes. They also utilised a "bioturbation index", but preferred a modified version of a seven category percentage bioturbated model first proposed by Reineck (1963) (Table 4.1).

Table 4.1 Bioturbation Index (BI) where each grade is described in terms of the sharpness of the primary sedimentary fabric, burrow abundance and amount of burrow overlap. From Taylor and Goldring (1993).

Grade	Percent bioturbated	Classification
0	0	No bioturbation
1	1-4	Sparse bioturbation, bedding distinct, few discrete traces and/or escape structures
2	5-30	Low bioturbation, bedding distinct, low trace density, escape structures common
3	31-60	Moderate bioturbation, bedding boundaries sharp, traces discrete, overlap rare.
4	61-90	High bioturbation, bedding boundaries indistinct, high trace density with overlap common
5	91-99	Intense bioturbation, bedding completely disturbed (just visible), limited reworking, later burrows discrete
6	100	Complete bioturbation, sediment reworking due to repeated overprinting

In Taylor and Goldring's (1993) model, absence of bioturbation is represented by a zero grade. Sparse and low levels of bioturbation are referred to in grades 1 and 2, where the physical sedimentary structures dominate over biogenic structures and the trace fossils represent the behaviour of opportunistic colonisers of the substrate, a more mature community being precluded from developing due to high levels of environmental stress. Moderate to high levels of bioturbation, represented in grades 3 and 4, are defined by an increase in the density of bioturbation and/or diversity to an extent that the primary sedimentary structure is destroyed. Intense to complete bioturbation, grades 5 and 6, reflect the dominance of biogenic structures.

While Taylor and Goldring's (1993) bioturbation index is slightly more detailed than that of Droser and Bottjer (1986), in essence it provides little further insight into ichnofabrics. In order to record the other parameters integral to the ichnofabric concept, i.e. the ichnotaxa present, diversity of the traces, density and size of the traces, and the order of emplacement, Taylor and Goldring (1993) have proposed the use of the "ichnofabric constituent diagram" (ICD). This diagram graphically incorporates a record of the ichnotaxa present, their order of emplacement, cross-section dimensions, and percentage area occupied by the primary sedimentary structures and the secondary biogenic structures.

4.1.5 Problems with these schemes, and a solution

Palaeoenvironmental studies should involve the pulling together of disparate strands of evidence to produce as complete and accurate an interpretation as is possible. Biogenic structures are, through their presence or absence, morphology, ichnocoenoses, and ichnofabrics, an important palaeoenvironmental indicator. Indeed, in the Bulldog Shale they are unequivocally the most important indicator. However, they are but one factor in several that may, or may not, be contingent in a particular setting.

Index measurements of bioturbation, both those proposed by Droser and Bottjer (1986) and Taylor and Goldring (1993), are elegantly simple, quick and easy to use, but they provide only an incomplete account of ichnofabric. They can work well as palaeoenvironmental descriptors in situations where benthic faunas have changed in response to the variation of a single environmental factor and where all other environmental conditions remain approximately stable. Such situations are rare, however, for anthropogenically defined environmental parameters do not represent closed systems, and their variation in response to larger-scale environmental or climatic

forcing is associated with, and may result in, changes in other associated environmental factors. These complex environmental changes result in sedimentary facies and fabric variations, and/or associated changes in trace making taxa and their behaviour, all of which affect the subsequent trace fossils and the preserved ichnofabrics. Such complicated changes in the preserved sediments and ichnofabrics cannot be summarised in the single numerical terms that index measures provide. In addition, the use of ichnograms and average bioturbation index values, as advocated by Bottjer and Droser (1991), should be treated with caution, because their application can result in the concealment of important variation, and therefore can result in considerable error.

Taylor and Goldring (1993) considered these arguments in the proposition of their methodology for more thorough analysis of trace fossil communities through the use of ICDs. However, this methodology, while providing vivid analysis and classification of biogenic sedimentary structures and communities, still omits much information regarding sediments and sedimentary environments, and body fossils are not considered. Indeed, as advocated by Goldring (1995), an integrated approach that incorporates all appropriate aspects of a facies, including ichnological, sedimentological, palaeontological and diagenetic data, is required. In addition, the time-consuming and complicated nature of the ICD approach severely curtails its use in the field, and its reliance on quantification is problematic in cases of severe overprinting of traces and sedimentary structures, and where traces are blurred either by preservation or preparation of the material. This last point is particularly important when small traces of only several millimetres diameter are considered. As Taylor and Goldring (1993) argued, a pragmatic method that is descriptive rather than quantitative, would be more useful. For correlation between sections the usefulness of ICDs is also limited, for it is not possible to plot them as continuous records alongside core logs in the way that bioturbation index data can be plotted.

The Bulldog Shale contains both variable amounts and types of bioturbation, and sediments of different facies. In some cases, changes in the sedimentary environment have little or no effect on the bioturbation, while in other situations sedimentary conditions do exert some control on the presence or absence of traces and on those types of traces produced. In addition, bioturbation in the Bulldog Shale frequently varies where there is no discernible sedimentary change. These complex permutations are clearly not the response to changes in a single environmental parameter, rather they reflect the response of trace makers to variations in two or more such factors.

In order to address these concerns, I propose the "palaeoenvironmental fabric type" (PFT) methodology for the analysis and classification of depositional environments within the Bulldog Shale, through the use of its trace fossils and associated sedimentary fabrics. This scheme is based on the ichnofabric concept, as defined by Taylor and Goldring (1993) (§4.1.2), but expressly tailored to the present study. It combines an index measurement of bioturbation, to provide a standardised measure to enable comparison with other studies, with an appreciation of those factors that define an ichnofabric (§4.1.4), the inclusion of sedimentary facies data, and an appreciation of macrofaunal changes. The term ichnofacies is avoided here as it is usually applied at basin-scale resolution and has connotations and problems unconnected with this methodology. Likewise, the term ichnofabric is not used, for it forms only a part, albeit an important one, of the PFT analytical procedure, and in some palaeoenvironmental fabrics trace fossils may be absent.

4.2 Palaeoenvironmental fabric type methodology

Palaeoenvironmental fabric types are constructed on the basis of those macroscopic biogenic, physical, and palaeontological criteria that yield information regarding the environment of deposition of the strata under study, and which can be discerned both in field and in cored material. As such the analysis of palaeoenvironmental fabric types represents an integrated approach to palaeoenvironmental analysis.

Those criteria used in the definition of palaeoenvironmental fabrics in the Bulldog Shale are as follows (Fig.4.04):

1) Percentage bioturbation. That is the degree to which the original sedimentary structures have been disrupted by biogenic activity (§4.1.4), and includes both distinct and mottled trace fossils. Taylor and Goldring's (1993) bioturbation index is used here rather than that of Droser and Bottjer (1986), as it forms part of a comprehensive ichnofabric evaluation scheme, and it includes seven rather than six grades of bioturbation, thus offering finer control on the classification of bioturbation intensity.

2) The diversity and types of trace fossils present, and their cross-cutting relationships. The analysis of trace fossil cross-cutting relationships provides information for the reconstruction of the original tiering profile (§4.1.1). This, along with analysis of those other factors that make up an ichnofabric (§4.1.2), provides the basis for palaeoenvironmental reconstruction.

3) Grain size. The Bulldog Shale largely comprises silty claystone material, and therefore grain size is expressed as the percentage of silt, and the presence or absence of sand-grade material.
4) Physical sedimentary structures. Where not obliterated by bioturbation, these tell us much about bathymetry and environmental energy levels.
5) Body fossils. Macrofaunal and floral remains, their diversity, and relationship with the surrounding sediment, must be included in an analysis of palaeoenvironmental fabrics, largely for reasons of completeness. Such studies however, are considered of only secondary importance to those involving trace fossil and sedimentary analyses for they can be less reliable indicators of palaeoenvironments at the place of deposition. Sediments and their physical and biogenic structures are, by their nature, in-situ records of environmental conditions. Macrofossil remains can be in-situ, however they are also often ex-situ, and as such can provide misleading information.

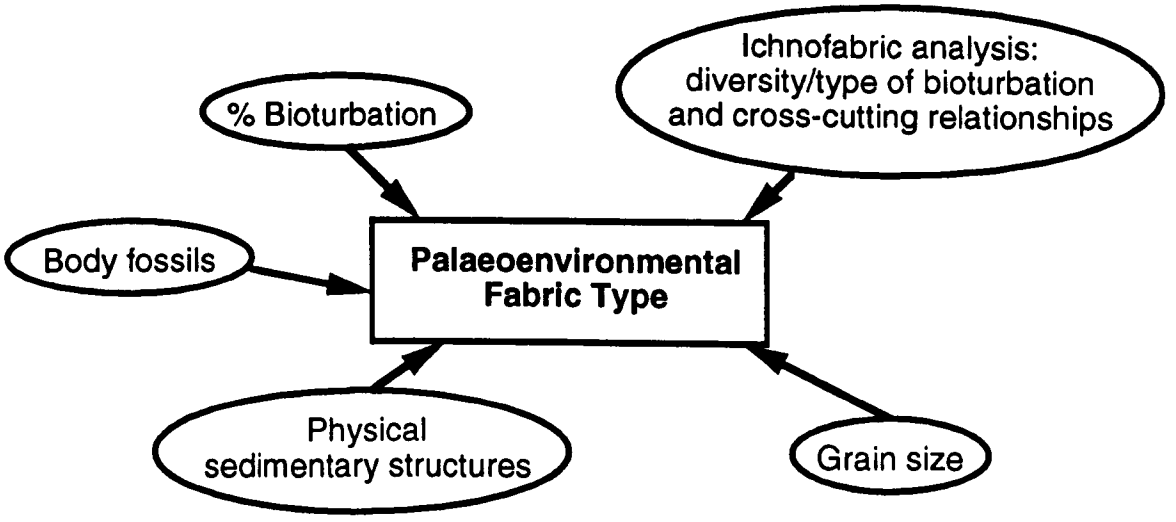

Fig.4.04 Criteria used to define palaeoenvironmental fabric types in the Bulldog Shale.

4.3 Palaeoenvironmental fabric types of the Bulldog Shale

Using the approach outlined above, seven palaeoenvironmental fabric types (A to G) have been defined from Bulldog Shale material.

On any scale, the palaeoenvironmental fabric of a section of rock, from core or field material, is unique, and is the result of the interplay between a multitude of basin-wide and local factors which define the environment of deposition in any location. Thus, no two sections of rock are exactly the same, and this variety can be considered to be

infinite. Palaeoenvironmental fabric types provide the basis for the division of this infinite variation into a series of broad, set regions or classes. By definition, therefore, palaeoenvironmental fabric types encompass considerable variation. Such division is necessary to provide for correlation and comparison of sections both within and between studies; and to distinguish the large scale (basin-wide) environmental variations, the effects of which produce the large-scale trends in the preserved sedimentary record on which the PFT divisions are based, from the smaller-scale (local) environmental variations responsible for local environmental heterogeneity, which are reflected in the sedimentary record as variations within each PFT

Variation within defined palaeoenvironmental fabric types, as outlined above, is a feature of Bulldog Shale material, particularly where bioturbation predominates over physical sedimentary structures. In cored material, the limited lateral extent of the rock (usually 4 to 6cm diameter) prevents an appreciation of the local lateral variations and heterogeneity of the palaeoenvironmental fabrics. In this case, variations within the defined palaeoenvironmental fabric types probably reflects the vertical sampling of such lateral heterogeneity through the core.

For each described example each of the factors outlined in §4.2 is considered. Photographs and interpretive diagrams are given. In addition, the original community tiering structure is defined from observed cross-cutting relationships, as described in §4.1.1 and presented in a reconstruction of the tiering profile.

The characteristic features used to define and identify each palaeoenvironmental fabric type are summarised in a palaeoenvironmental fabric type table (table 4.2).

PFT	% Silt (remainder = clay-grade)	B.I.	Dominant trace fossil taxa	Subsidiary trace fossil taxa	Sedimentology	Macropalaeontology
A	0-10	0-1	NO DOMINANTS	*An., Pl.*	Planar lamination	Broken and complete thin shelled bivalve material. Rare gastropods and scaphopods. Macerated plant matter.
B	10-20	2-3	*An.*	*Pl., O. nod., P. heb.*	Irregular planar lamination, occasional small ripples and scours	Broken and complete thin shelled bivalve material. Macerated plant matter.
C	10-50	3	*An.*	*Pl., O. nod., P. heb., P. tub.*	Irregular planar lamination, occasional small ripples, scours and 1-2mm thick silty interbeds	Broken thin shelled bivalves. Macerated plant matter.
D	20-60	3-5	*An., Pl., O. nod.*	*P. heb., P. tub., Te., Sk.*	Irregular planar lamination, with common 1-5mm thick silty interbeds and associated small ripples and scours	Broken thin and thick shelled bivalve material. Macerated plant matter.
E	20-95 (+ occasional minor sand fraction)	5-6	*An, Pl., O. nod., Te.*	*P. heb., P. tub., Ph., O. irr., O. nod.* var. *spatha, Rh., Th., Sk., Sch., Tb.*	NONE PRESERVED	Broken thick shelled bivalve and rarer belemnite material. Macerated plant matter.
F	50-100 (+ minor sand fraction)	2-4	*An.*	*Pl., P. heb., P. tub., O. nod., Te., Ch., Sk.*	Interbedded silt and clay dominated horizons, both with planar lamination. Silty interbeds also bear erosively scoured bases, ripples, cross lamination and HCS.	Indeterminate shelly material. Macerated and structured plant matter.
G	100 (+ sand fraction)	0-1	NO DOMINANTS	*An.* Very occasionally *Pl., O. nod., Sk.*	Planar and cross lamination, and HCS.	Broken bivalve material, occasional echinoids and starfish. Macerated and structured plant matter.

Table 4.2 Palaeoenvironmental fabric type table for the Bulldog Shale. Annotations: *An.* = *Anconichnus*, *Ch.* = *Chondrites*, *O. irr.* = *Ophiomorpha irregulaire*, *O. nod.* = *Ophiomorpha nodosa*, *P. heb.* = *Palaeophycus heberti*, *P. tub.* = *Palaeophycus tubularis*, *Ph.* = *Phoebichnus*, *Pl.* = *Planolites*, *Rh.* = *Rhizocorallium*, *Sch.* = *Schaubcylindrichnus*, *Sk.* = *Skolithos*, *Tb.* = *Terebellina*, *Te.* = *Teichichnus*, *Th.* = *Thalassinoides*, HCS = hummocky cross-stratification.

4.3.1 Palaeoenvironmental fabric type A

General characteristics

Silty claystone, composed of 90 to 100% clay-grade material, the remainder being silt-grade. Physical rather than biogenic sedimentary structures predominate, and comprise planar lamination. Bioturbation is non-existent to very sparse (B.I.0-1). Where trace fossils do exist the assemblage is of low diversity with very occasional *Anconichnus* and silt-filled *Planolites* (Fig.4.05). Cross-cutting relationships between the two ichnotaxa are uncertain owing to their rarity. Preserved shelly macrofauna are only occasionally present and typically comprise probable autochthonous broken, and more rarely unbroken, thin-shelled bivalve remains. Assorted allochthonous material, including gastropod and scaphopod remains may also be present.

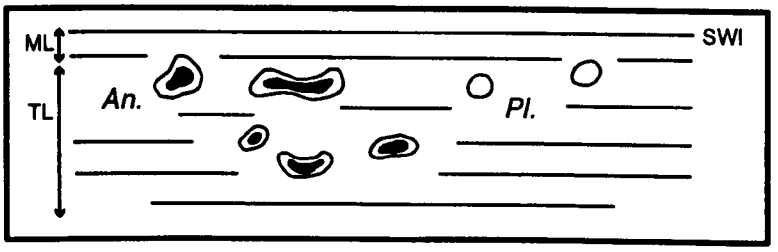

Fig.4.05 Palaeoenvironmental fabric type A, schematic trace fossil tiering diagram. Annotations as before, plus: SWI = sediment water interface, ML = mixed layer, TL = transition layer. Not to scale.

Example: Finniss 2, 84.60 - 84.45m

Silty claystone, composed of an estimated 90% clay and 10% silt-grade material. Some diagenetic pyrite growth. Physical rather than biogenic sedimentary structures predominate, and comprise slightly irregular planar laminations (Fig.4.06). Bioturbation is very sparse (B.I.1) and of low diversity with only two ichnotaxa represented. The trace fossil assemblage consists of occasional *Anconichnus*, and silt-filled *Planolites* (Fig.4.06). Cross-cutting relationships between the two ichnotaxa are uncertain. Preserved shelly macrofauna are absent.

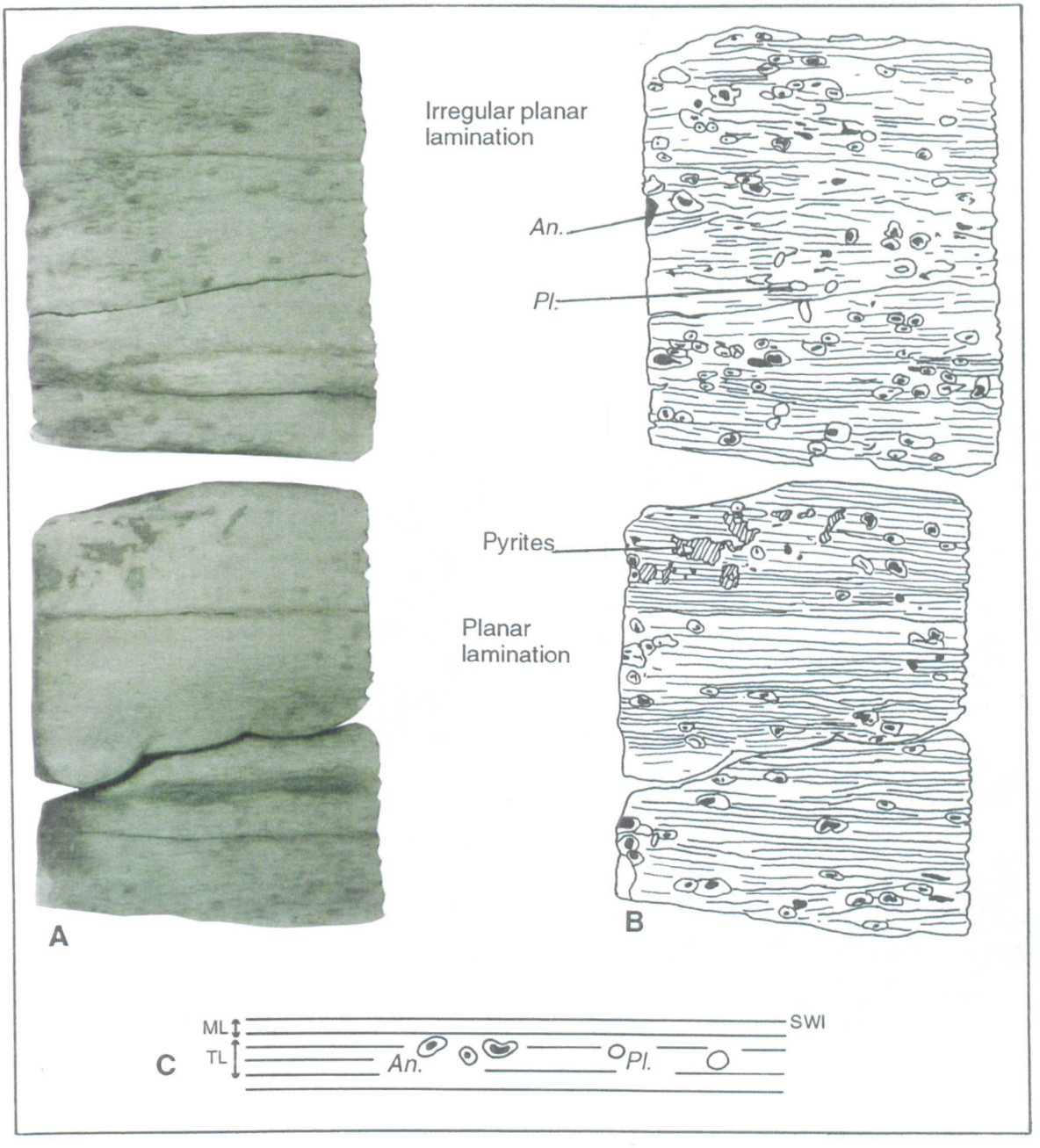

Fig.4.06 Finniss 2, 84.60 - 84.45m. (A) Photograph of the core, cut surface, actual size. (B) Sketch of the photograph. (C) Schematic trace fossil tiering diagram, not to scale. Annotations as before

Example: CBH 2, 366.80 - 366.70m

Silty claystone, composed of an estimated 95% clay and 5% silt-grade material. Physical rather than biogenic sedimentary structures predominate, and comprise planar laminations (Fig.4.07). Bioturbation is very sparse (B.I.1), and of low diversity, with only two ichnotaxa represented. The trace fossil assemblage consists of occasional

Anconichnus, and very occasional silt-filled *Planolites* (Fig.4.07). Cross-cutting relationships between the two ichnotaxa are uncertain. An unusual macrofossil assemblage is present, including indeterminate thin-shelled bivalve material, allochthonous scaphopod remains and probably allochthonous, possibly ice-rafted, gastropod material.

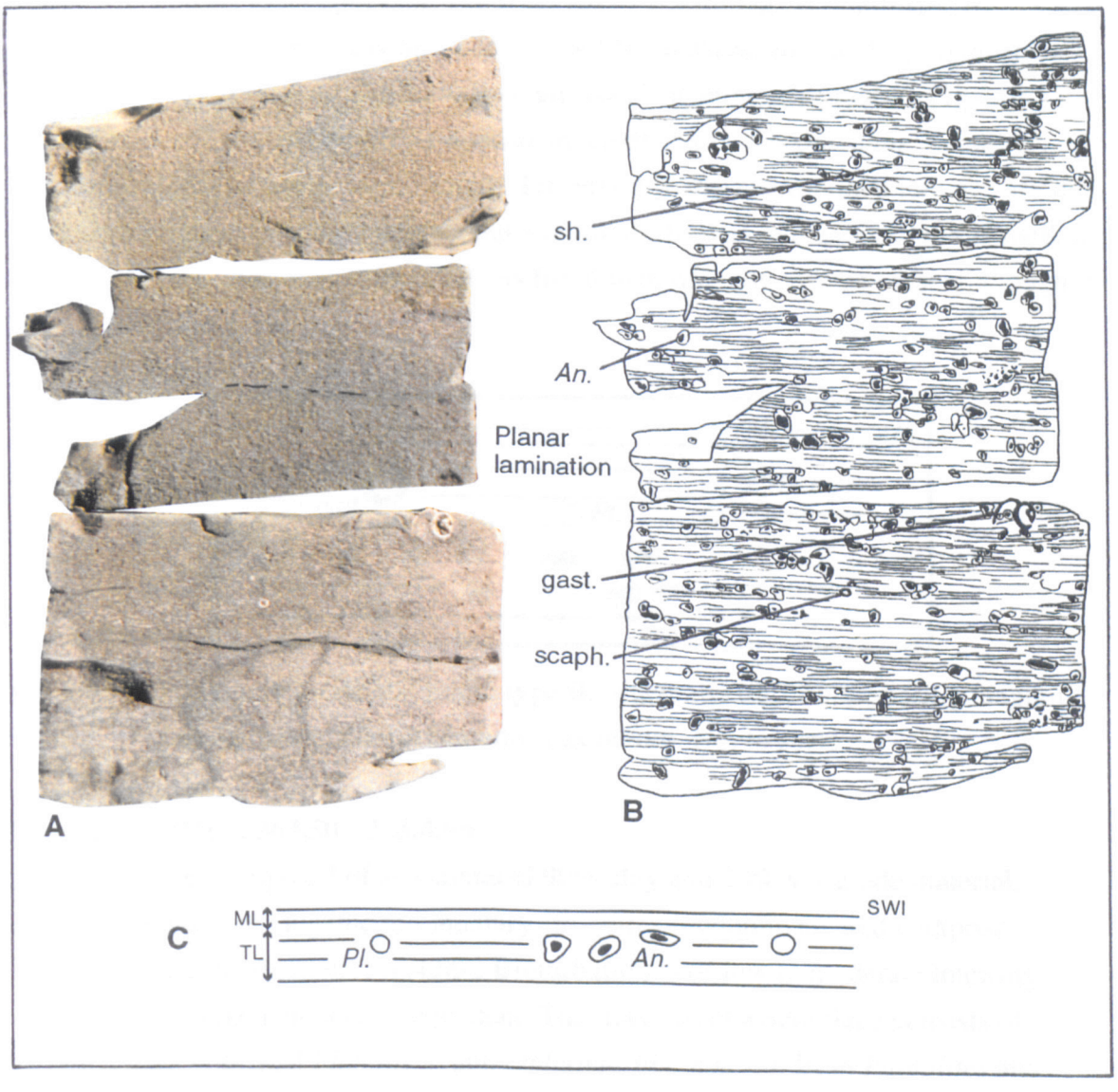

Fig.4.07 CBH 2, 366.80 - 366.70m. (A) Photograph of the core, cut surface, actual size. (B) Sketch of the photograph. (C) Schematic trace fossil tiering diagram, not to scale. Annotations as before, plus: sh. = indeterminate shelly material; gast. = gastropod, scaph. = scaphopod.

4.3.2 Palaeoenvironmental fabric type B

General characteristics

Silty claystone, composed of 80 to 90% clay-grade material, the remainder being silt-grade. Physical rather than biogenic sedimentary structures predominate, and comprise irregular planar lamination with uncommon small ripples and scours. Bioturbation is of low intensity (B.I.2-3), with up to four ichnotaxa represented, though the occurrence of just two or three is more common. The trace fossil assemblage is dominated by *Anconichnus*, with more occasional silt- or mud-filled *Planolites*, and *Ophiomorpha nodosa*. In addition *Palaeophycus heberti* are very uncommonly present (Fig.4.08). Both *Planolites* and *Ophiomorpha nodosa* are cross-cut by *Anconichnus*, but other cross-cutting relationships are uncertain. Preserved shelly macrofaunal remains are rare, but where present comprise probable autochthonous broken and unbroken thin-shelled bivalve material. Assorted autochthonous fossil material may also be present, though it has not been observed.

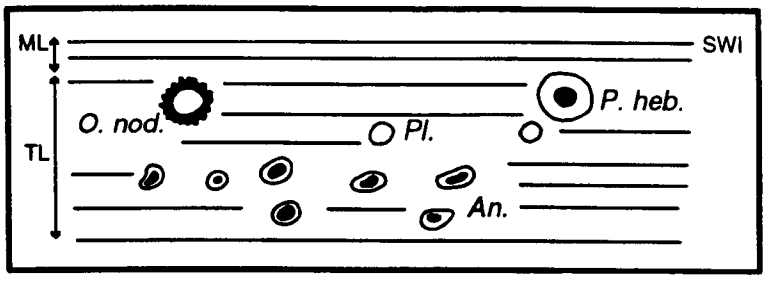

Fig.4.08 Palaeoenvironmental fabric type B, schematic trace fossil tiering diagram and reconstruction. Annotations as before. Not to scale.

Example: CBH 2, 363.50 - 363.40m

Silty claystone, composed of an estimated 90% clay and 10% silt-grade material. Physical rather than biogenic sedimentary structures predominate, and comprise irregular planar lamination (Fig.4.09). Bioturbation is of low to moderate intensity (B.I.2-3), and three ichnotaxa are present. The trace fossil assemblage consists of *Anconichnus*, silt-filled *Planolites*, and *Ophiomorpha nodosa*. Both *Planolites* and *Ophiomorpha nodosa* are cross-cut by *Anconichnus* (Fig.4.09). Cross-cutting relationships between *Planolites* and *Ophiomorpha nodosa* are not clear. Small amounts of indeterminate shelly material, probably thin-shelled bivalve, is present.

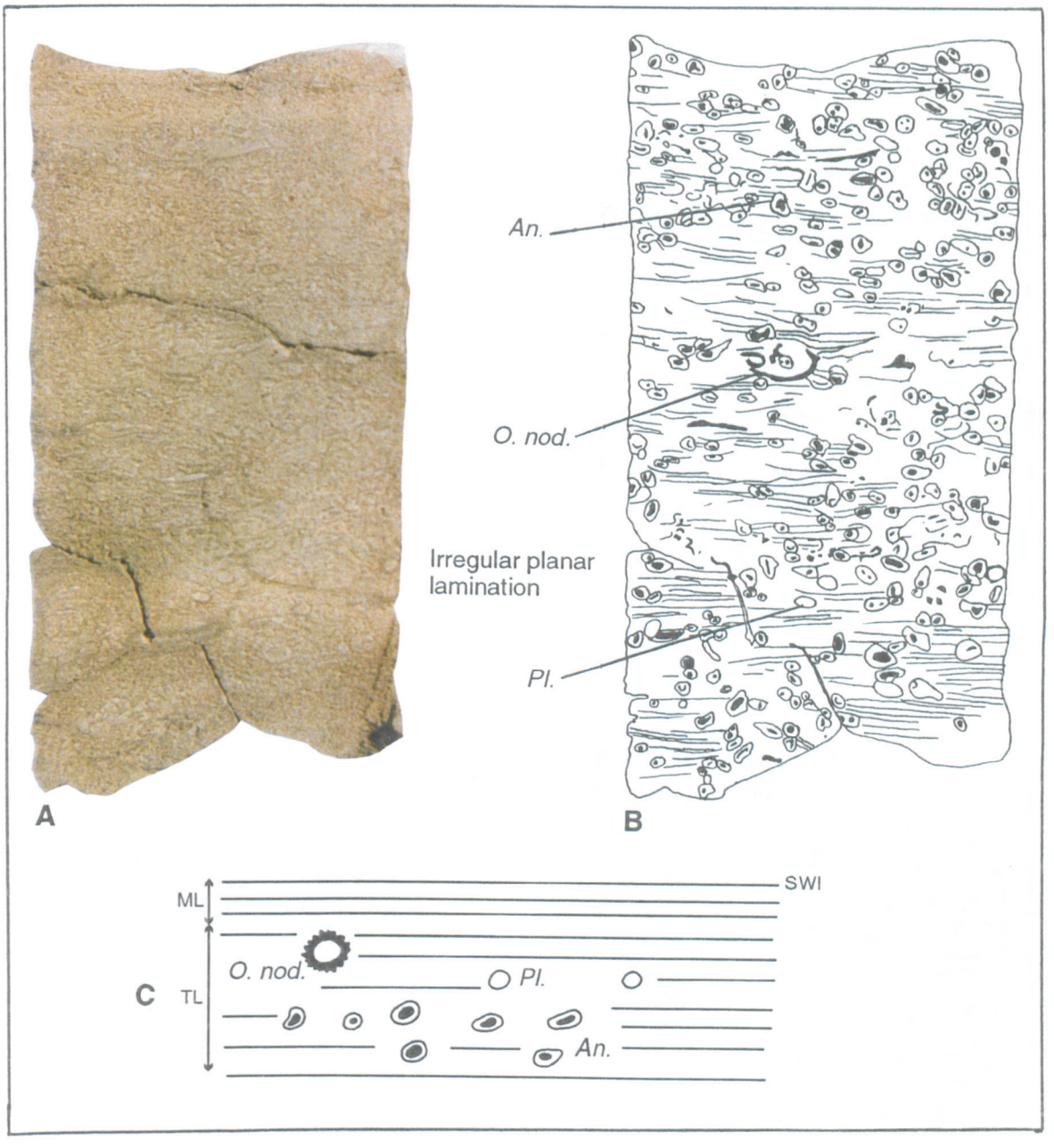

Fig.4.09 CBH 2, 363.50 - 363.40m. (A) Photograph of core, cut surface, actual size. (B) Sketch of the photograph. (C) Schematic trace fossil tiering diagram, not to scale. Annotations as before.

Example: SPH 1, 413.40 - 413.30m

Silty claystone, composed of an estimated 90% clay and 10% silt-grade material. Physical rather than biogenic sedimentary structures predominate, and comprise planar lamination (Fig.4.10). Bioturbation is of low to moderate intensity (B.I.2-3) and very low diversity. The trace fossil assemblage consists solely of large *Anconichnus*

(Fig.4.10). Cross-cutting relationships between the ichnotaxa are uncertain. Preserved shelly macrofauna are absent.

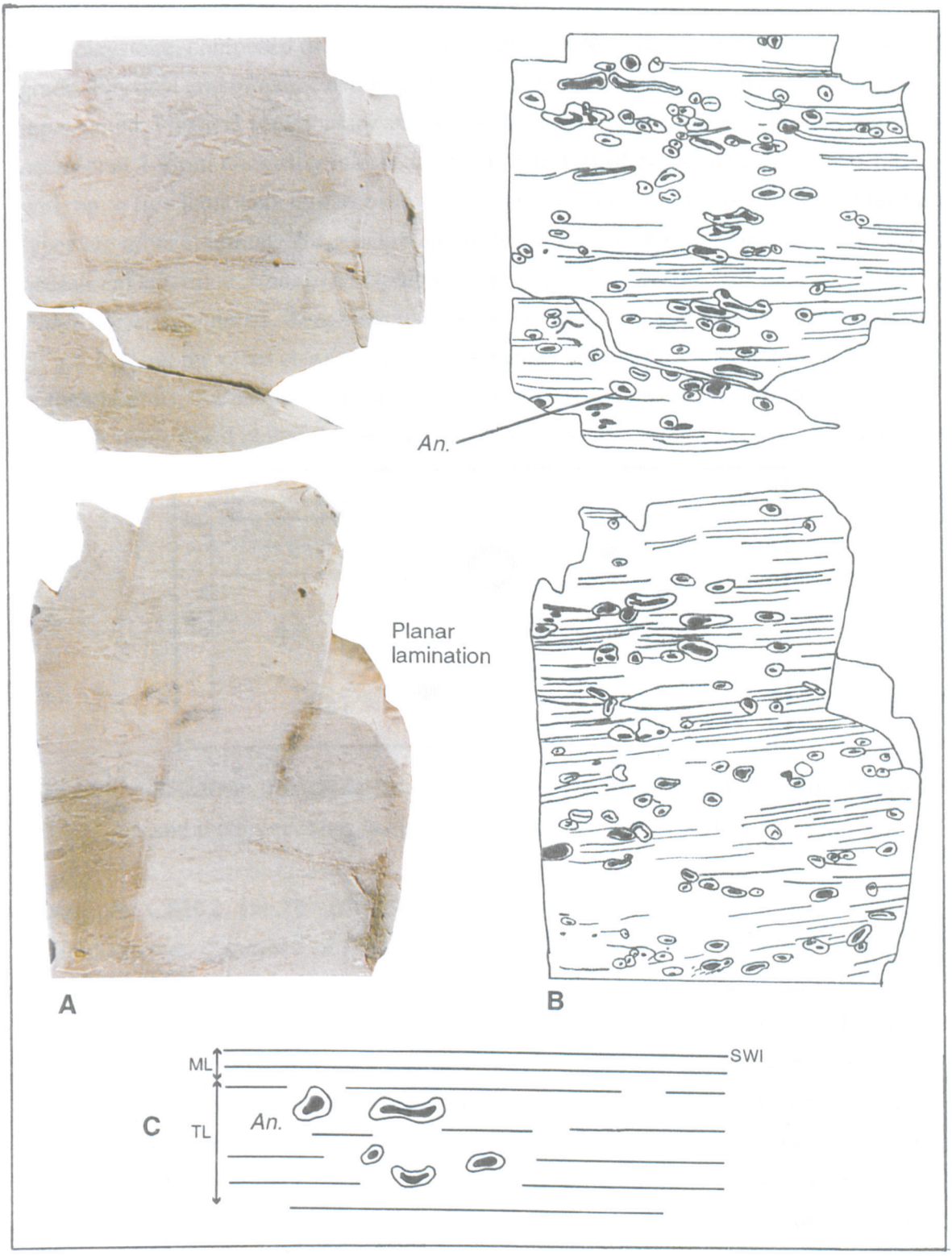

Fig.4.10 SPH 1, 413.40 - 413.30m. (A) Photograph of the core, cut surface, 1.5x actual size. (B) Sketch of the photograph. (C) Schematic trace fossil tiering diagram, not to scale. Annotations as before.

4.3.3 Palaeoenvironmental fabric type C

General characteristics

Silty claystone, composed of 50 to 90% clay-grade material, the remainder being silt-grade. Physical and biogenic sedimentary structures are approximately equally represented. Physical sedimentary structures comprise irregular planar lamination with occasional 1-2mm thick silty interbeds. Bioturbation is of moderate intensity (B.I.3) with up to five ichnotaxa represented, though assemblages containing three or four trace types are more common. The assemblage is dominated by *Anconichnus*, with more occasional silt-filled *Planolites*, *Ophiomorpha nodosa*, *Palaeophycus heberti*, and *Palaeophycus tubularis*. *Anconichnus* cross-cuts *Planolites* and *Ophiomorpha nodosa* (Fig.4.11), but the other cross-cutting relationships are unknown. Probable autochthonous, occasional thin-shelled bivalve material is present. Assorted allochthonous fossil material may also be present, though it has not been observed.

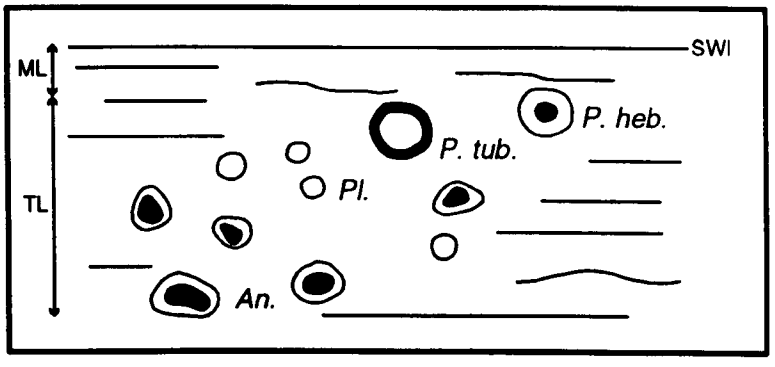

Fig.4.11 Palaeoenvironmental fabric type C, schematic trace fossil tiering diagram and reconstruction. Annotations as before. Not to scale.

Example: CBH 2, 356.70 - 356.60m

Silty claystone, composed of an estimated 80% clay and 20% silt-grade material. Biogenic sedimentary structures predominate slightly over physical sedimentary structures which, where apparent, are limited to irregular planar lamination (Fig.4.12). Bioturbation is of relatively high intensity (B.I.4), but low diversity, with three ichnotaxa represented. The trace fossil assemblage is dominated by *Anconichnus* and silt-filled *Planolites*, with very occasional *Ophiomorpha nodosa*. *Anconichnus* cross-cuts both *Planolites* and *Ophiomorpha nodosa* (Fig.4.12), other cross-cutting relationships are uncertain. Occasional indeterminate shelly material, probably from thin-shelled bivalves, is present.

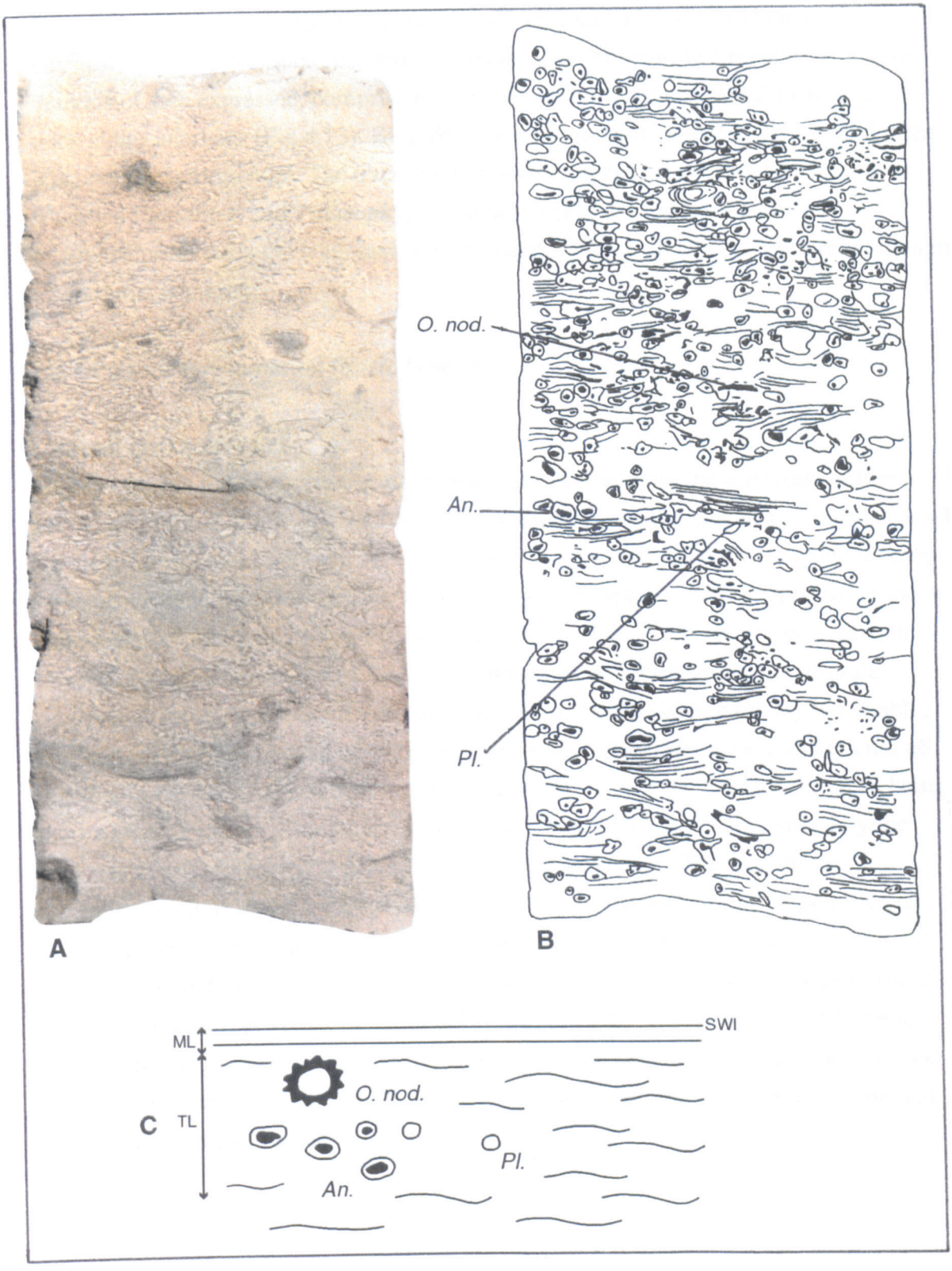

Fig.4.12 CBH 2, 356.70 - 356.60m. (A) Photograph of the core, cut surface, actual size. (B) Sketch of the photograph. (C) Schematic trace fossil tiering diagram, not to scale. Annotations as before.

Example: SPH 1, 404.50 - 404.40m

Silty claystone, composed of an estimated 85% clay and 15% silt-grade material. Physical sedimentary structures, which roughly equal biogenic sedimentary structures in terms of area expressed, comprise planar lamination with occasional 1mm to 2mm thick siltier interbeds (Fig.4.13). Bioturbation is of moderate intensity (B.I.3) and three ichnotaxa are represented. The trace fossil assemblage consists of large *Anconichnus*, silt-filled *Planolites*, and *Palaeophycus tubularis* (Fig.4.13). Cross-cutting relationships between the ichnotaxa are uncertain. Thin-shelled bivalve material, though uncommon, is present

4.3.4 Palaeoenvironmental fabric type D

General characteristics

Highly variable palaeoenvironmental fabric type, representing the transition between PFT/C and PFT/E. Silty claystone or clayey siltstone, sometimes with a minor fine sand fraction, composed of between 40% and 80% clay-grade material, the remainder being largely silt-grade. Biogenic sedimentary structures are approximately equal to, or more commonly predominate over, physical sedimentary structures in their representation. Physical sedimentary structures comprise irregular planar lamination, small-scale ripples and scours, and 1-2mm thick silty interbeds. Bioturbation intensity is variable, between B.I.3 and B.I.5, and up to seven ichnotaxa may be represented, though not all together in the same assemblage, the presence of four or five different trace types being more typical. Palaeoenvironmental fabric type D is particularly characterised by the appearance of *Teichichnus* and *Skolithos* within a succession. The trace fossil assemblage is dominated by *Anconichnus*, with *Planolites* and *Ophiomorpha nodosa* important components also; *Palaeophycus heberti*, *Palaeophycus tubularis*, *Teichichnus*, and *Skolithos* are more minor constituent traces. *Planolites*, *Ophiomorpha nodosa*, and *Palaeophycus heberti* are all cross-cut by *Anconichnus* (Fig.4.14). Other cross-cutting relationships are uncertain. Preserved shelly macrofauna are uncommon, but where present comprise largely broken, autochthonous and allochthonous thin and thick shelled bivalve material.

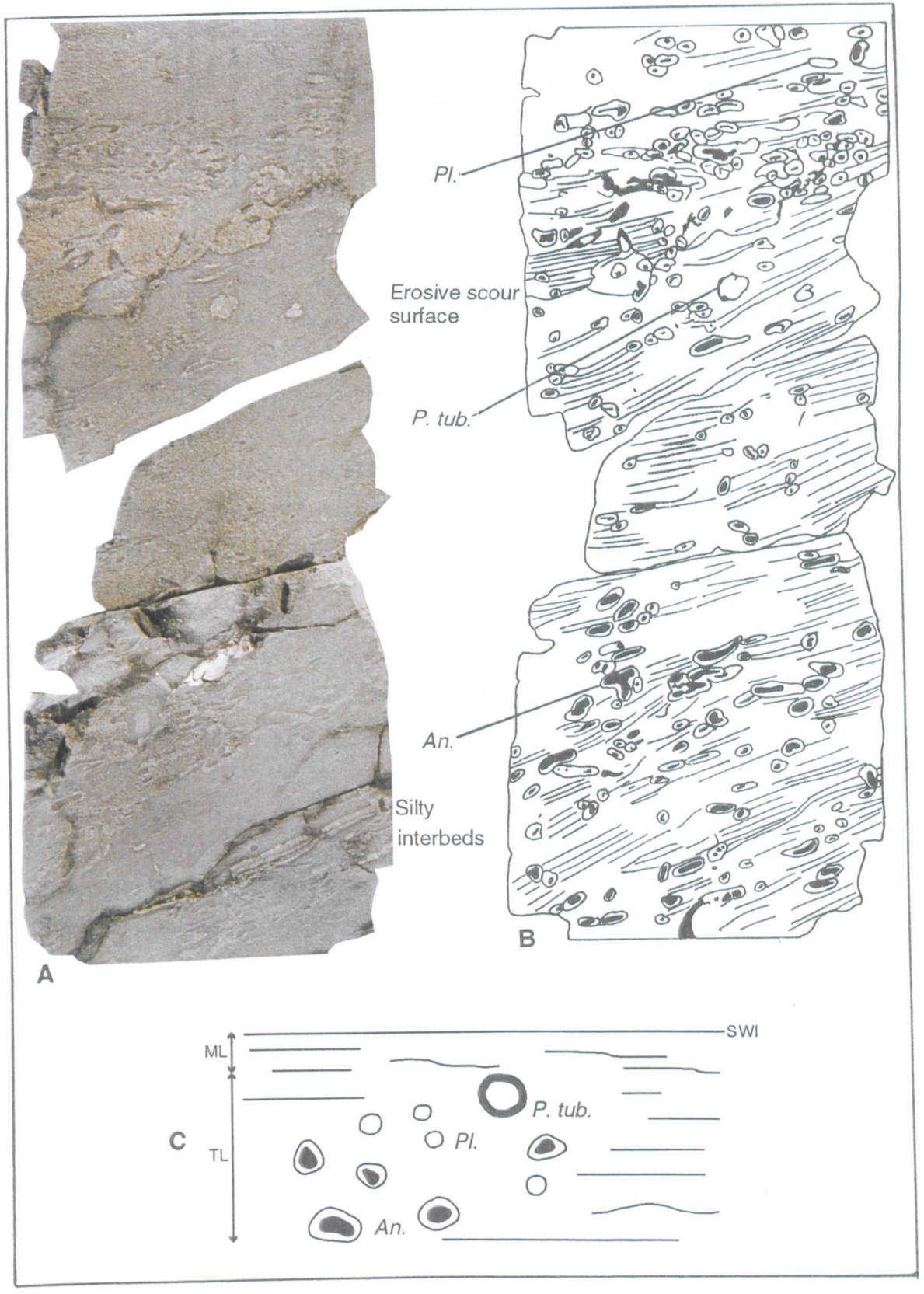

Fig.4.13 SPH 1, 404.50 - 404.40m. (A) Photograph of the core, cut surface, 1.5x actual size. (B) Sketch of the photograph. (C) Schematic trace fossil tiering diagram, not to scale. Annotations as before.

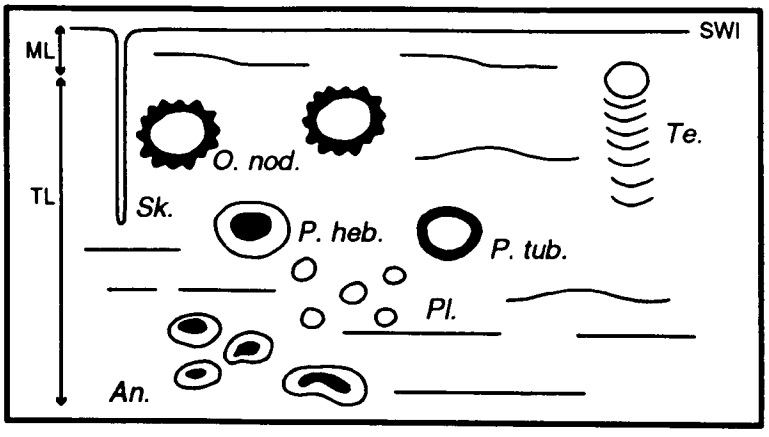

Fig.4.14 Palaeoenvironmental fabric type D, schematic trace fossil tiering diagram and reconstruction. Annotations as before. Not to scale.

Example: Alford 1, 53.20 - 53.10m

Clayey siltstone, composed of an estimated 65% silt and 35% clay-grade material, with a minor fine sand fraction. Biogenic sedimentary structures predominate over physical sedimentary structures which, where apparent comprise irregular planar lamination and small ripples (Fig.4.15). Bioturbation generally reaches B.I.3, and B.I.4 in places. Four ichnotaxa are represented. The trace fossil assemblage consists of *Anconichnus*, silt-filled *Planolites*, *Palaeophycus tubularis*, and occasional *Teichichnus*. In addition, *Thalassinoides* may also be present. *Planolites* are cross-cut by *Anconichnus* (Fig.4.15); other cross-cutting relationships are uncertain. Broken bivalve remains are present.

Example: SPH 1, 385.70 - 385.60m

Silty claystone, composed of approximately 75% clay and 25% silt-grade material. Biogenic sedimentary structures predominate over physical sedimentary structures which, where apparent comprise irregular planar and rippled lamination (Fig.4.16). Bioturbation intensity varies between B.I.3 and B.I.4, and four ichnotaxa are represented. The trace fossil assemblage is dominated by *Anconichnus*, with more occasional silt-filled *Planolites*, *Palaeophycus heberti*, and *Ophiomorpha nodosa*. Both *Palaeophycus heberti* and *Ophiomorpha nodosa* are cross-cut by *Anconichnus* (Fig.4.16). Other cross-cutting relationships are uncertain. A fragment of thick-shelled bivalve material is present.

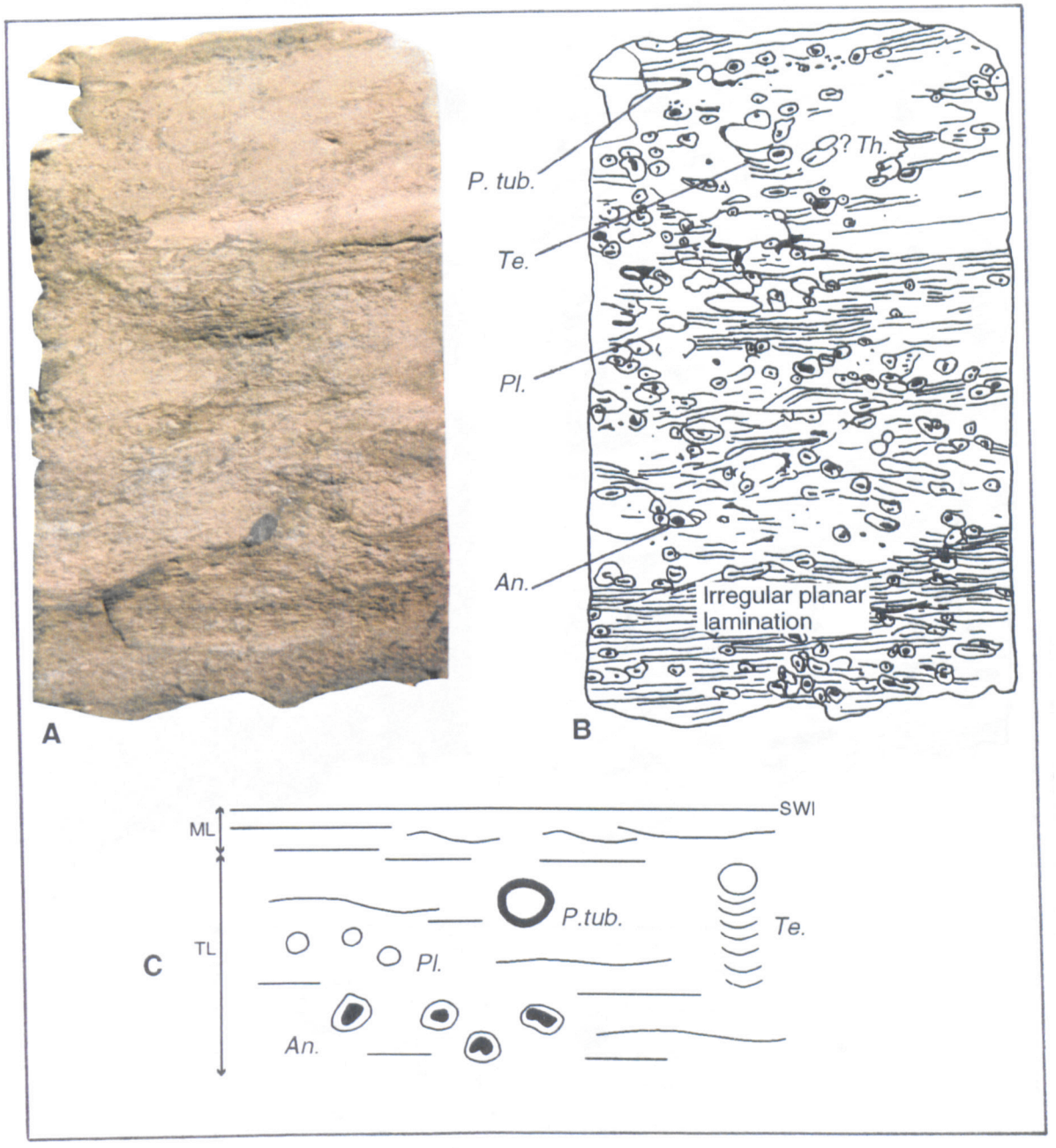

Fig.4.15 Alford 1, 53.20 - 53.10m. (A) Photograph of the core, cut surface, actual size. (B) Sketch of the photograph. (C) Schematic trace fossil tiering diagram, not to scale. Annotations as before.

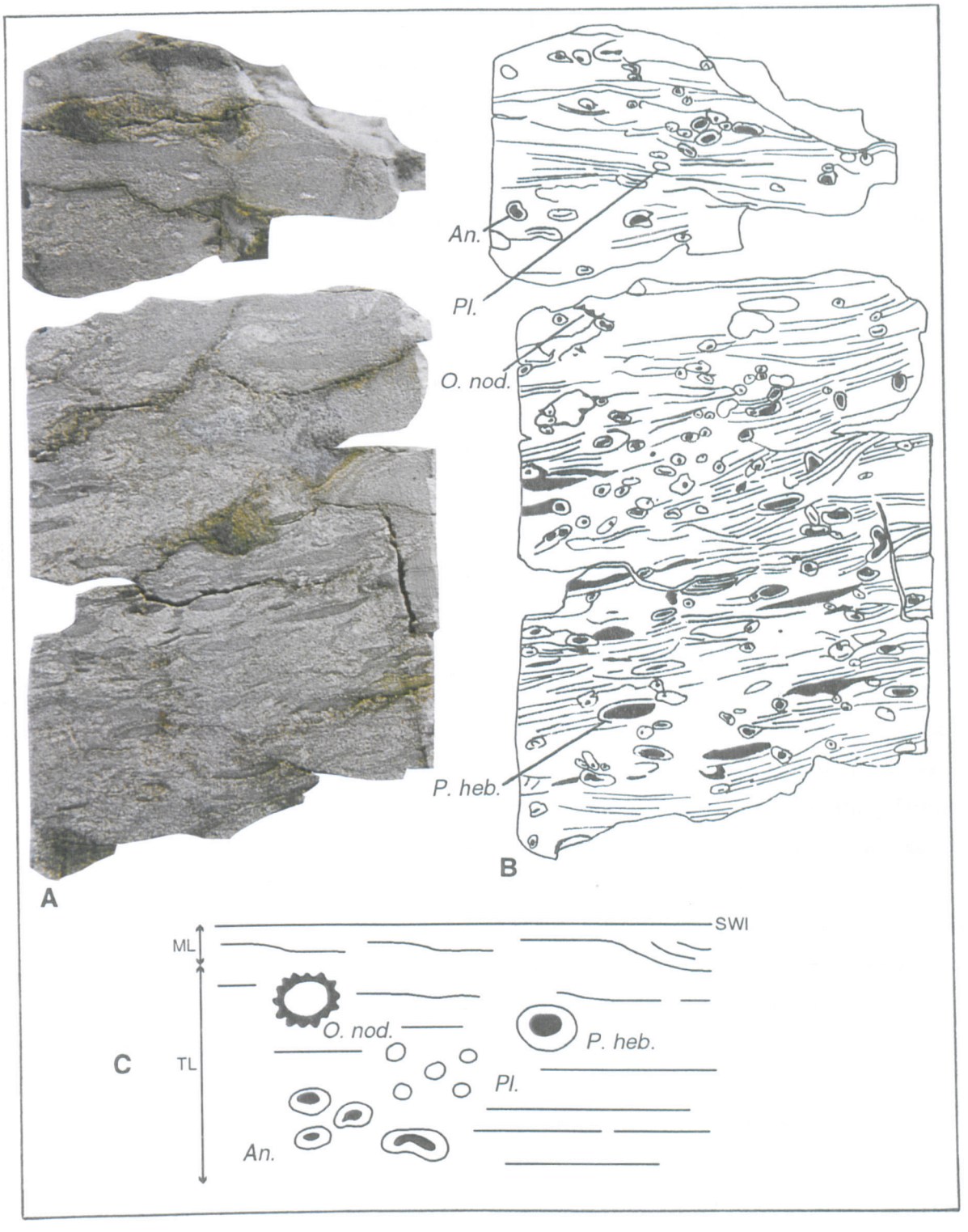

Fig.4.16 SPH 1, 385.70 - 385.60m. (A) Photograph of the core, cut surface, 1.5x actual size. (B) Sketch of the photograph. (C) Schematic trace fossil tiering diagram, not to scale. Annotations as before.

Example: SPH 1, 350.00 - 349.90m

Silty claystone, composed of an estimated 80% clay and 20% silt-grade material. Physical sedimentary structures consist of irregular planar and slightly rippled laminae, largely clay dominated, but with occasional 1-2mm thick silty interbeds (Fig.4.17). Bioturbation is of moderate intensity (B.I.3), and four ichnotaxa are represented. The trace fossil assemblage is dominated by *Anconichnus*, silt-filled *Planolites*, and *Ophiomorpha nodosa*, with possible occasional *Skolithos* (var.F) (Fig.4.17). Cross-cutting relationships are uncertain. Preserved shelly macrofauna are absent.

4.3.5 Palaeoenvironmental fabric type E

General characteristics

Highly variable palaeoenvironmental fabric type, characterised by the totality or near totality of bioturbation in a generally high diversity assemblage. Silty claystone or clayey siltstone composed of 5 to 80% clay grade material, sometimes with a minor fine sand fraction, the remainder being largely silt-grade. Generally, no physical sedimentary structures are preserved and bioturbation is complete at B.I.6. However, where bioturbation is of high intensity, but is not quite complete (B.I.5), some remnant of the physical sedimentary structures remains, comprising mm to cm thickness silty interbeds with associated erosive scours, irregular planar lamination, cross-lamination, and possible hummocky cross-stratification. Trace fossil diversity is high with twelve ichnotaxa represented, though any one assemblage typically consists of anything from four to nine trace fossil types. In the idealised assemblage, with all twelve ichnotaxa present, the assemblage is dominated by *Anconichnus*, silt-filled *Planolites*, *Ophiomorpha nodosa*, and *Teichichnus*. Important, though more secondary components to the assemblage are *Palaeophycus heberti*, *Palaeophycus tubularis*, *Phoebichnus*, *Ophiomorpha irregulaire*, *Terebellina*, *Rhizocorallium*, *Thalassinoides*, *Skolithos* (var.F), and *Skolithos* (var.D) (Fig.4.18). It should be noted, that such high trace fossil diversity, particularly where *Thalassinoides* and/or *Skolithos* are present in an overprinting form, may represent composite ichnofabrics (§4.4.3). Cross-cutting relationships between the ichnotaxa are well-constrained, though in the case of rarely represented traces, namely *Palaeophycus heberti*, *Palaeophycus tubularis*, *Ophiomorpha irregulaire*, and *Terebellina* the appreciation of cross-cutting relationships is not complete. However, in such cases the limited evidence available is usually sufficient to reasonably infer a tiering position for that ichnotaxon. In addition, mutual cross-cutting by trace types indicates the overlapping or even co-occurrence of

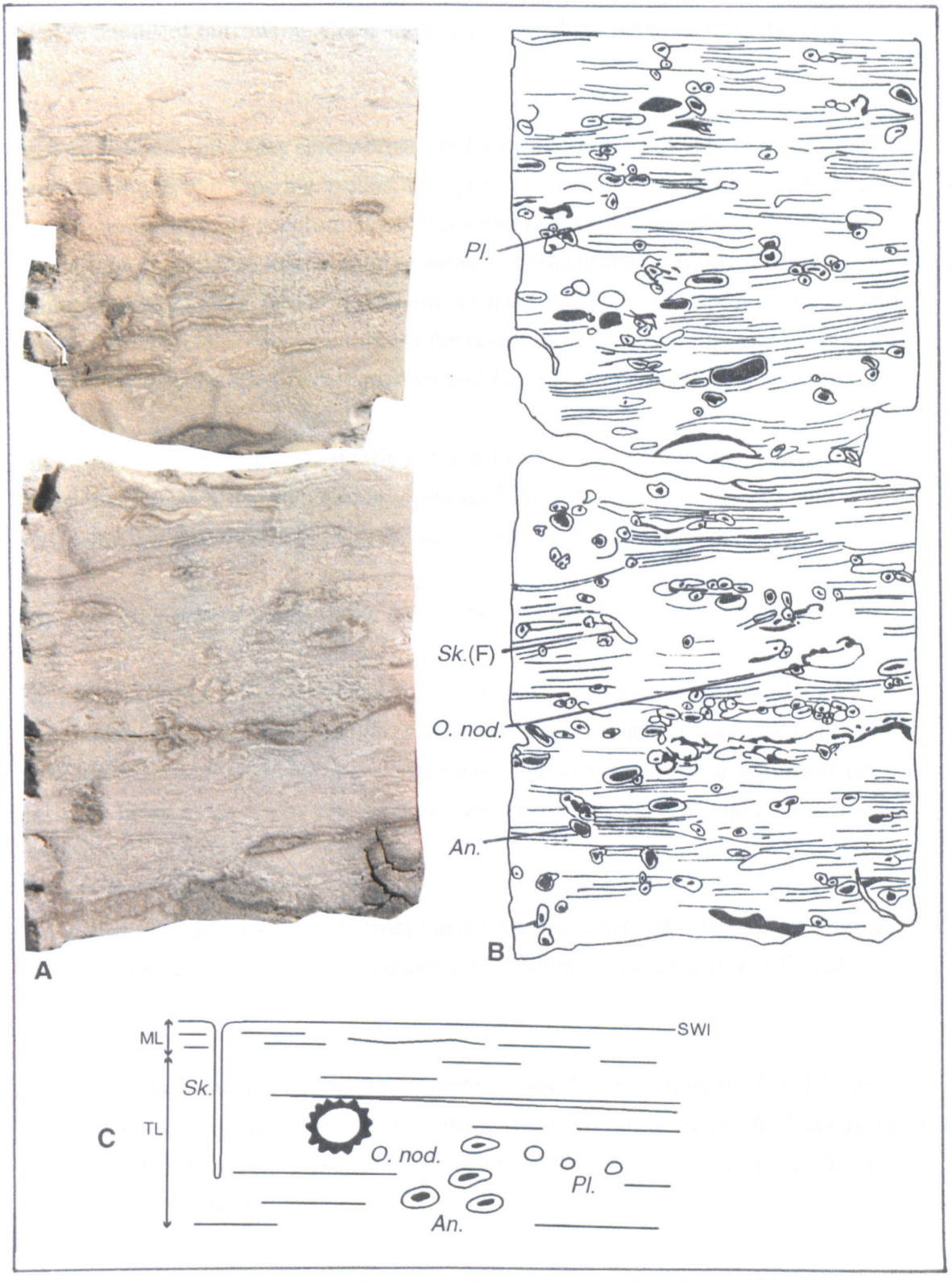

Fig.4.17 SPH 1, 350.00 - 349.90m. (A) Photograph of the core, cut surface, 1.5x actual size. (B) Sketch of the photograph. (C) Schematic trace fossil tiering diagram, not to scale. Annotations as before.

tiers. In such cases the dominant cross-cutting relationship is that used to define the relative depths of burrowing. Cross-cutting relationships between trace-types are as follows:

Anconichnus are only very rarely cross-cut by other trace types. These cross-cutting traces belong to two separate groups. The primary cross-cutters of *Anconichnus* are those representative of generations of traces emplaced subsequently to the original assemblage in response to alteration of sediment constituency during a break in sedimentation, namely *Skolithos* (variants D and F) and *Thalassinoides*. The second group of *Anconichnus* cross-cutters are the result of tier overlapping and occur only very rarely, they are silt-filled *Planolites* and *Ophiomorpha nodosa*.

Silt-filled *Planolites* are consistently cross-cut only by *Anconichnus*. However, occasional cross-cutting by *Ophiomorpha nodosa*, *Palaeophycus heberti*, and *Teichichnus* is also evident, and is the result of tier overlapping.

Palaeophycus heberti are recorded only to be consistently cross-cut by *Anconichnus*.

Phoebichnus has a fairly variable tier position. In some cases it is cross-cut by *Anconichnus* and silt-filled *Planolites* only, a situation in which it cross-cuts *Ophiomorpha nodosa*. In other cases however, it clearly occupies a shallower tier position, being cross-cut by *Anconichnus*, *Palaeophycus heberti*, and *Ophiomorpha nodosa*.

Rhizocorallium are consistently cross-cut by *Anconichnus*, silt-filled *Planolites*, and *Ophiomorpha nodosa*, and less frequently by *Skolithos* (variants D and F) and *Thalassinoides*.

Ophiomorpha nodosa are consistently cross-cut by *Anconichnus*, silt-filled *Planolites*, *Ophiomorpha irregulaire*, and *Phoebichnus*, and more rarely by *Teichichnus* as a result of tier overlap. In addition, some cross-cutting by *Skolithos* (variants D and F) and *Thalassinoides* also occurs.

Teichichnus are consistently cross-cut by *Anconichnus*, silt-filled *Planolites*, *Ophiomorpha nodosa*, *Phoebichnus*, and *Rhizocorallium*, and more rarely by *Skolithos* (var.D and F) and *Thalassinoides*.

Skolithos (variants D and F) are cross-cut by *Anconichnus*, *Ophiomorpha nodosa*, and *Rhizocorallium.*

Thalassinoides are cross-cut by *Anconichnus*, *Ophiomorpha nodosa*, *Teichichnus*, *Terebellina*, and *Rhizocorallium.* In addition, the silty infill of *Thalassinoides* burrows are frequently reworked by *Anconichnus* traces.

Preserved shelly macrofauna are, in general, absent, though occasional broken thick-shelled bivalve and very rare belemnite material is present.

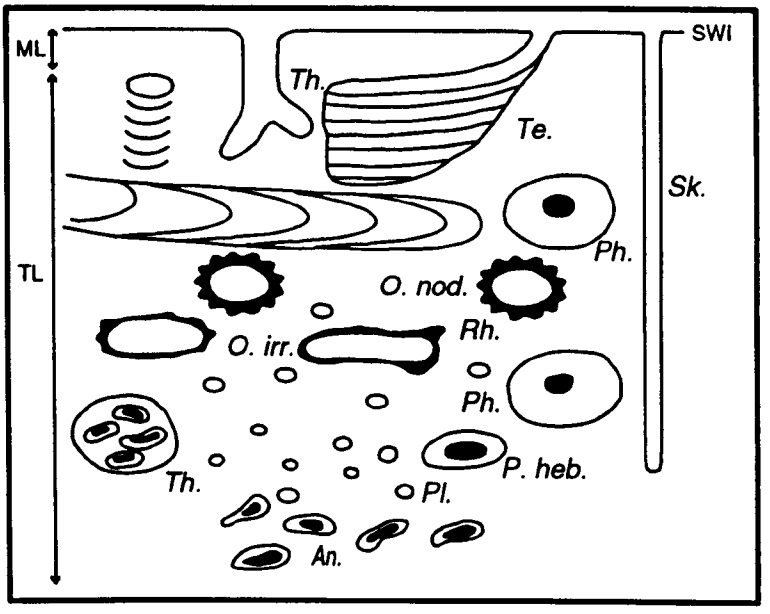

Fig.4.18 Palaeoenvironmental fabric type E, schematic trace fossil tiering diagram and reconstruction. Annotations as before. Not to scale.

Example: Finniss 2, 53.43 - 53.28m

Silty claystone, composed of an estimated 75% clay and 25% silt-grade material. No physical sedimentary structures are preserved, bioturbation is complete at B.I.6. Trace fossil diversity is high with seven ichnotaxa represented. The trace fossil assemblage is dominated by *Anconichnus*, silt-filled *Planolites*, *Ophiomorpha nodosa*, and *Teichichnus*, with occasional *Thalassinoides*, *Phoebichnus*, and *Terebellina* traces (Fig.4.19). Cross-cutting relationships are well constrained: *Anconichnus* and *Planolites* are not cross-cut by any other trace-type; *Ophiomorpha nodosa* are cross-cut by *Anconichnus*, *Planolites*, *Teichichnus*, and *Thalassinoides*; *Teichichnus* are cross-cut by *Anconichnus* and *Ophiomorpha nodosa* (*Teichichnus* also more rarely cross-cut *Ophiomorpha nodosa.* This mutual cross-cutting relationship is indicative of

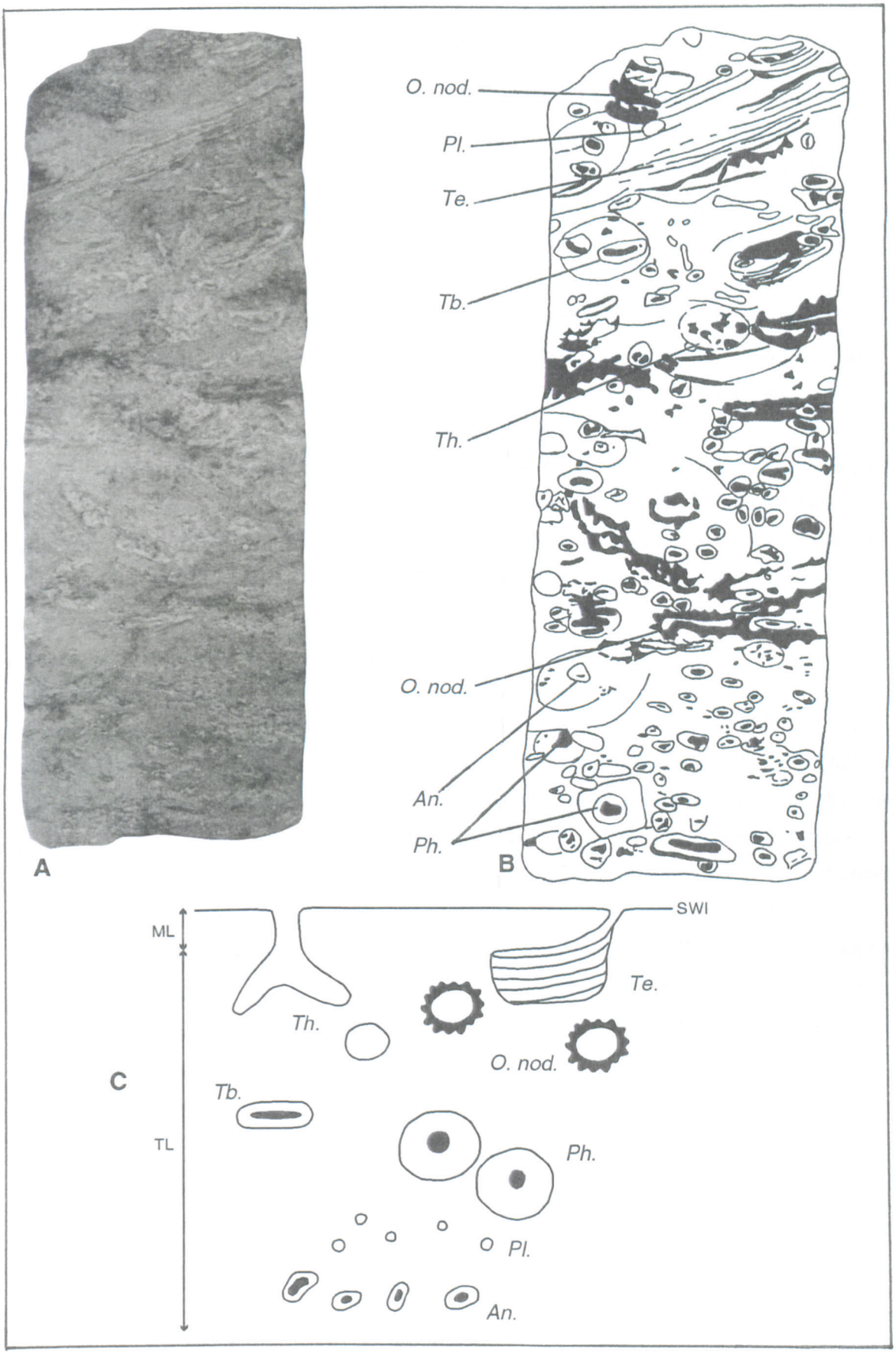

Fig.4.19 Finniss 2, 53.43 - 53.28m. (A) Photograph of the core, cut surface, actual size. (B) Sketch of the photograph. (C) Schematic trace fossil tiering diagram, not to scale. Annotations as before.

overlapping tiers (§4.4.3)); *Thalassinoides* are cross-cut by *Anconichnus*, *Ophiomorpha nodosa*, and *Terebellina*; and *Phoebichnus* are apparently only cross-cut by *Planolites* (Fig.4.19). Preserved shelly macrofauna are absent, though bivalve and belemnite remains are present in otherwise similar neighbouring regions of core.

Example: Finniss 2, 37.20 - 37.00m

Silty claystone, composed of an estimated 60% clay and 40% silt-grade material. No physical sedimentary structures are preserved, bioturbation is complete at B.I.6. Trace fossil diversity is moderate with three ichnotaxa represented. The trace fossil assemblage is dominated by *Anconichnus* and the stacked *Ophiomorpha nodosa* var. *spatha*, with less common silt-filled *Planolites* (Fig.4.20). Cross-cutting relationships are well constrained: *Anconichnus* are not cross-cut by any other ichnotaxa; *Planolites* are cross-cut by *Anconichnus* only; while *Ophiomorpha nodosa* are cross-cut by both *Anconichnus* and *Planolites* (Fig.4.20). Preserved shelly macrofauna are absent.

Example: Finniss 2, 30.25 - 30.08m

Silty claystone, composed of an estimated 60% clay and 40% silt-grade material. No physical sedimentary structures are preserved, bioturbation is complete at B.I.6. Trace fossil diversity is high with seven ichnotaxa represented. The trace fossil assemblage is dominated by *Anconichnus*, silt-filled *Planolites*, and *Ophiomorpha nodosa*, with more occasional *Teichichnus*, *Phoebichnus*, *Rhizocorallium*, and *Skolithos* (var. F) traces (Fig.4.21). Cross-cutting relationships are well constrained: *Anconichnus* are not cross-cut by any other ichnotaxa; *Planolites* and *Skolithos* are both cross-cut only by *Anconichnus*; *Ophiomorpha nodosa*, *Phoebichnus* and *Rhizocorallium* are cross-cut by *Anconichnus* and *Planolites*; while the poorly preserved *Teichichnus* are cross-cut by *Anconichnus*, *Planolites*, and *Ophiomorpha nodosa* (Fig.4.21). Preserved shelly macrofauna are absent.

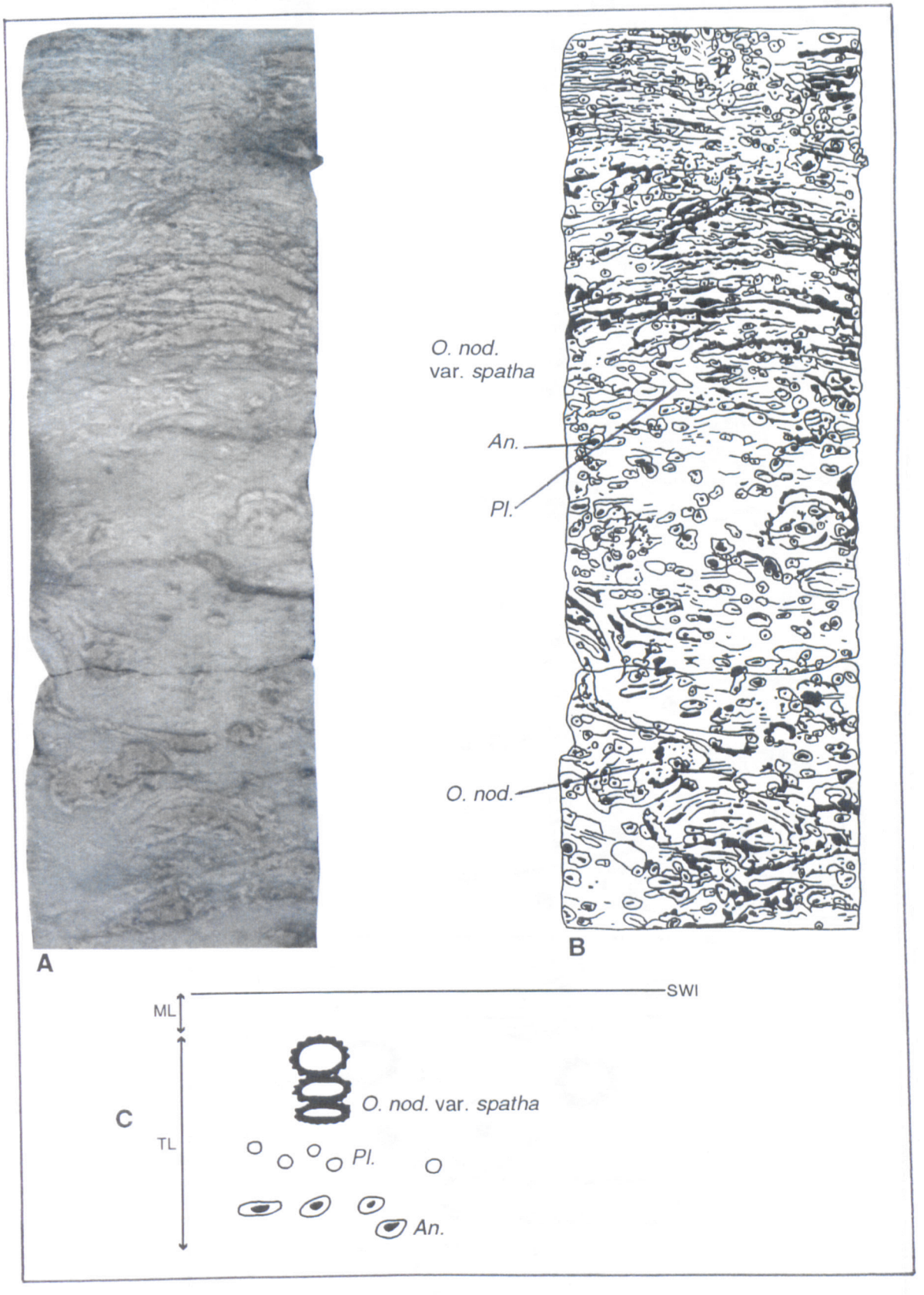

Fig.4.20 Finniss 2, 37.20 - 37.00m. (A) Photograph of the core, cut surface, actual size. (B) Sketch of the photograph. (C) Schematic trace fossil tiering diagram, not to scale. Annotations as before.

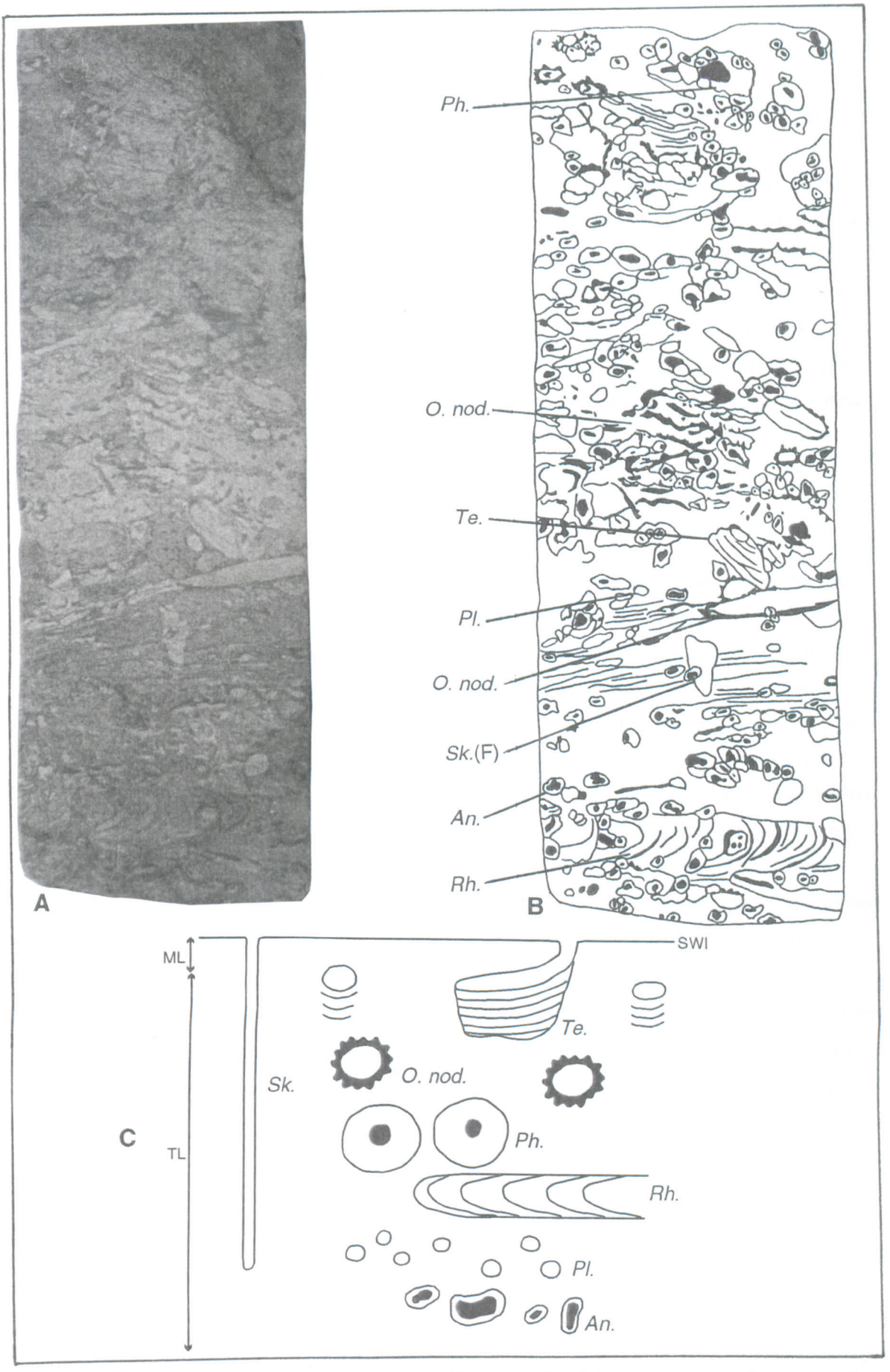

Fig.4.21 Finniss 2, 30.25 - 30.08m. (A) Photograph of the core, cut surface, actual size. (B) Sketch of the photograph. (C) Schematic trace fossil tiering diagram, not to scale. Annotations as before.

Example: Finniss 2, 29.25 - 29.15m

Clayey siltstone, composed of an estimated 90% silt and 10% clay-grade material. No physical sedimentary structures are preserved, bioturbation is complete at B.I.6. Trace fossil diversity is high with seven ichnotaxa represented. The assemblage is dominated by *Anconichnus*, silt-filled *Planolites*, *Ophiomorpha nodosa*, and *Teichichnus*, with less common *Ophiomorpha irregulaire*, *Palaeophycus heberti*, and *Phoebichnus* (Fig.4.22). Cross-cutting relationships are well constrained: *Anconichnus* are not cross-cut by any other ichnotaxa; *Planolites* and *Palaeophycus heberti* are both cross-cut only by *Anconichnus*; *Ophiomorpha nodosa* are cross-cut by *Anconichnus* and *Ophiomorpha irregulaire*; *Teichichnus* are cross-cut by *Anconichnus*, *Planolites*, and *Ophiomorpha nodosa*; and *Phoebichnus* are cross-cut by *Anconichnus*, *Palaeophycus heberti*, and *Ophiomorpha nodosa* (Fig.4.22). Preserved shelly macrofauna are absent.

Example: Finniss 2, 29.15 - 29.00m

Clayey siltstone, composed of an estimated 95% silt and 5% clay-grade material. No physical sedimentary structures are preserved, bioturbation is complete at B.I.6. Trace fossil diversity is high with seven ichnotaxa represented. The trace fossil assemblage consists of *Anconichnus*, silt-filled *Planolites*, *Ophiomorpha nodosa*, *Teichichnus* (possibly two generations, the younger generation considerably better preserved than the older generation, and with different cross-cutting relationships); *Palaeophycus heberti*, *Phoebichnus*, and *Skolithos* (var. F) (Fig.4.23). In addition, transitional forms between *Ophiomorpha nodosa* and *Palaeophycus heberti* are present. Cross-cutting relationships are reasonably well constrained, though in part they vary from those recorded elsewhere: *Anconichnus* are cross-cut only by *Skolithos*; *Planolites* are cross-cut by *Palaeophycus heberti*, and very occasionally by the younger generation of *Teichichnus*; *Ophiomorpha nodosa* are cross-cut by *Anconichnus*, *Planolites* and *Phoebichnus*; *Teichichnus* (older generation) are cross-cut by *Anconichnus*, *Planolites*, *Ophiomorpha nodosa*, *Teichichnus* (younger generation), *Palaeophycus heberti*, and *Skolithos*; and *Teichichnus* (younger generation) are cross-cut by *Anconichnus* and *Ophiomorpha nodosa* (Fig.4.23). Preserved shelly macrofauna are absent.

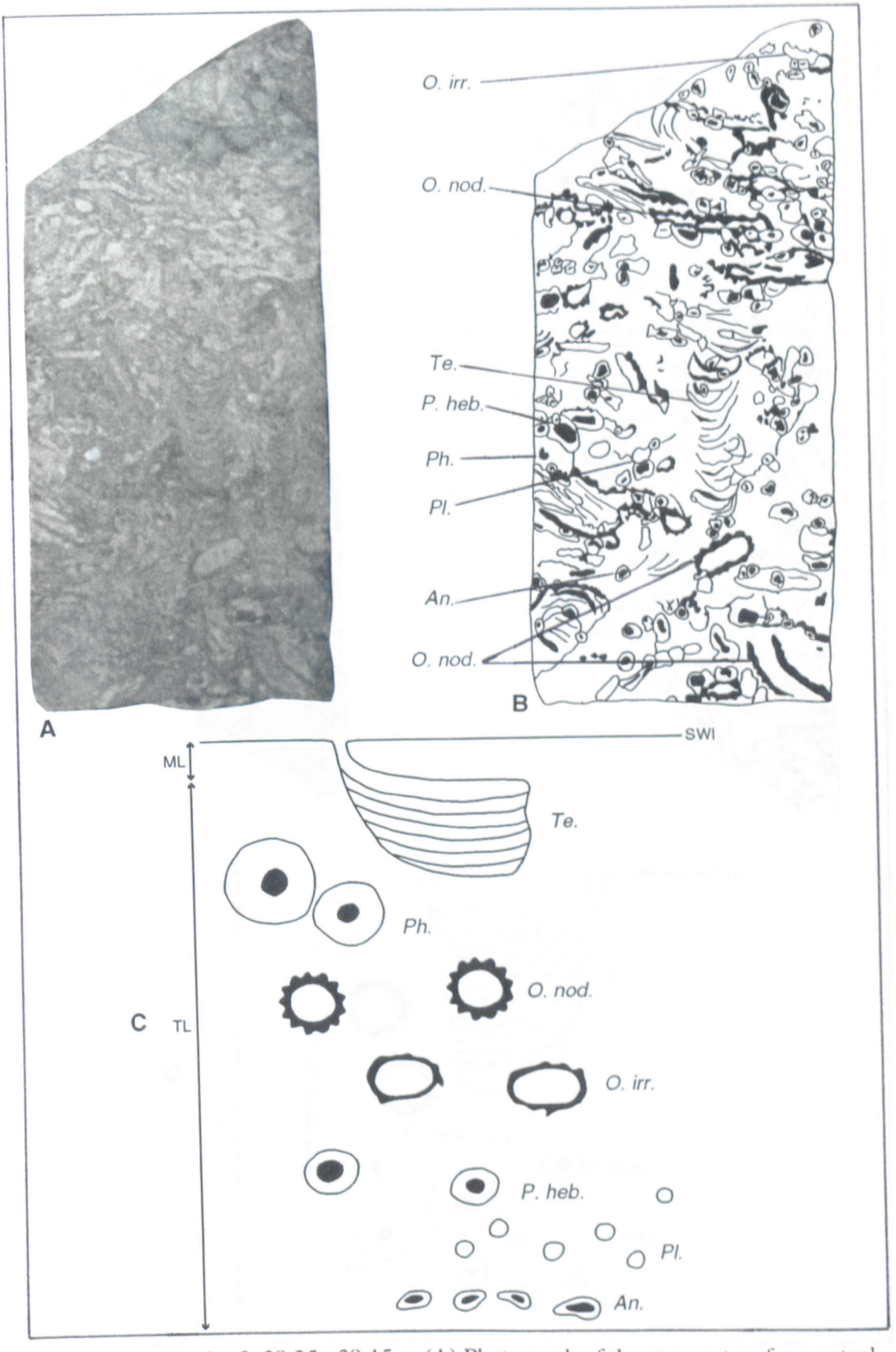

Fig.4.22 Finniss 2, 29.25 - 29.15m. (A) Photograph of the core, cut surface, actual size. (B) Sketch of the photograph. (C) Schematic trace fossil tiering diagram, not to scale. Annotations as before.

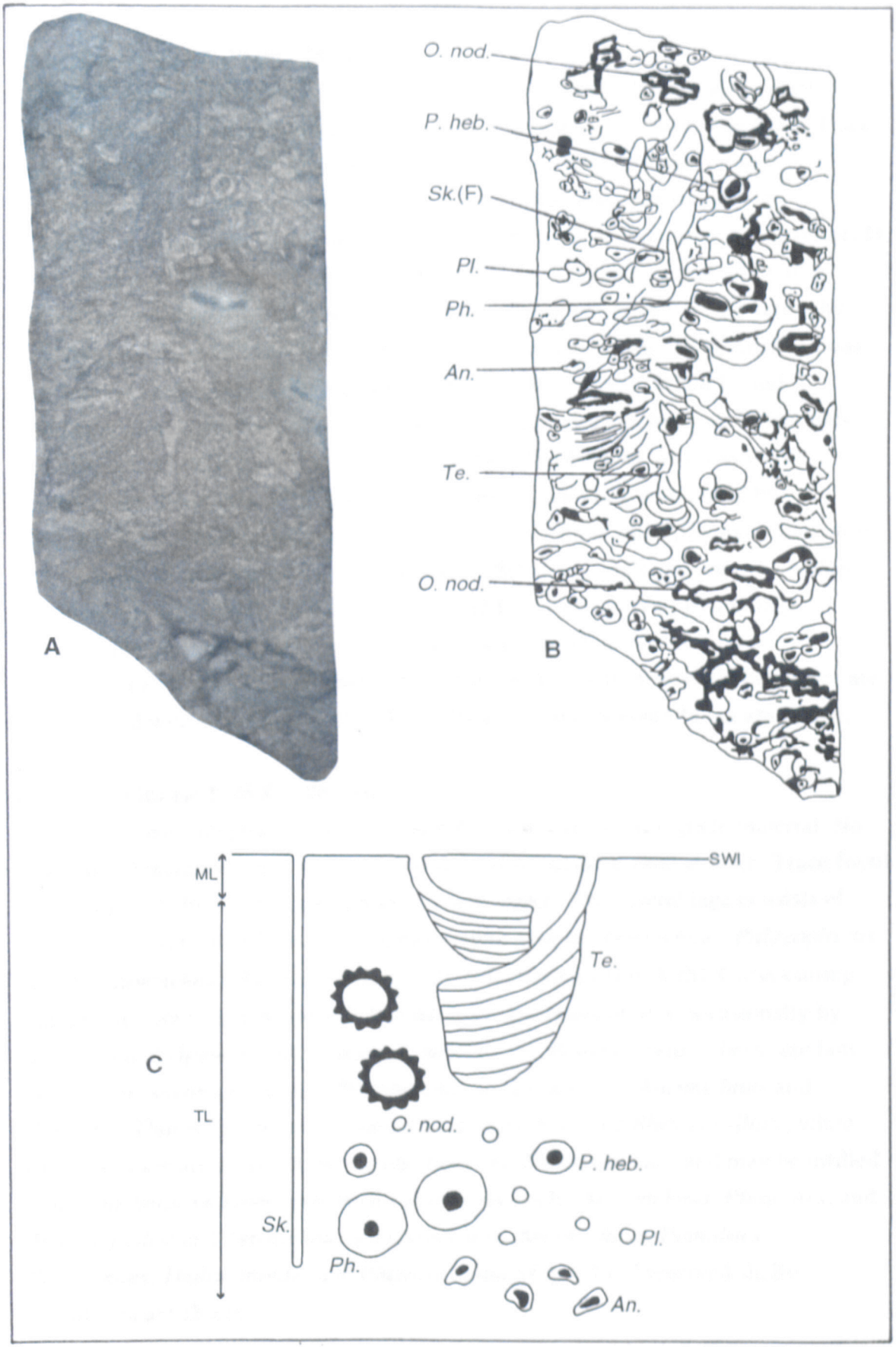

Fig.4.23 Finniss 2, 29.15 - 29.00m. (A) Photograph of the core, cut surface, actual size. (B) Sketch of the photograph. (C) Schematic trace fossil tiering diagram, not to scale. Annotations as before.

Example: Finniss 2, 29.00 - 28.82m

Clayey siltstone, composed of an estimated 95% silt and 5% clay-grade material. No physical sedimentary structures are preserved, bioturbation is complete at B.I.6. Trace fossil diversity is very high with nine ichnotaxa represented. The assemblage is dominated by *Anconichnus*, silt-filled *Planolites*, *Ophiomorpha nodosa*, and *Teichichnus*, with more occasional *Phoebichnus, Rhizocorallium*, *Skolithos* (variants D and F), and possible *Thalassinoides* (infilled with *Anconichnus*) (Fig.4.24). Cross-cutting relationships are well constrained: *Anconichnus* are cross-cut only rarely by *Skolithos* (var. D and F) and *Thalassinoides*; *Planolites* are cross-cut by *Anconichnus* and very occasionally by *Ophiomorpha nodosa*, *Skolithos* (var. D and F) and *Thalassinoides*; *Ophiomorpha nodosa* are cross-cut by *Anconichnus*, and Planolites, and very occasionally by *Skolithos* (var. D and F); *Teichichnus* are cross-cut by *Anconichnus*, *Planolites*, and *Ophiomorpha nodosa*, and only very rarely by *Thalassinoides*; *Phoebichnus* are cross-cut by *Anconichnus* and *Ophiomorpha nodosa*, *Rhizocorallium* are cross-cut by *Anconichnus*, *Planolites*, and *Ophiomorpha nodosa*, and more occasionally by *Skolithos* (var. D and F); *Skolithos* (var. F) are only occasionally cross-cut by *Anconichnus*; *Skolithos* (var. D) are cross-cut by *Rhizocorallium* only. *Thalassinoides* tend not to be cross-cut by any ichnotaxa, but are often infilled with *Anconichnus* (Fig.4.24). Preserved shelly macrofauna are absent.

Example: Finniss 2, 28.82 - 28.71m

Clayey siltstone, composed of an estimated 95% silt and 5% clay-grade material. No physical sedimentary structures are preserved, bioturbation is total at B.I.6. Trace fossil diversity is very high with eight ichnotaxa represented. The assemblage consists of *Anconichnus*, silt-filled *Planolites*, *Ophiomorpha nodosa*, *Teichichnus*, *Palaeophycus heberti*, *Phoebichnus*, *Rhizocorallium*, and *Thalassinoides* (Fig.4.25). Cross-cutting relationships are well constrained: *Anconichnus* are cross-cut only occasionally by *Planolites* and *Ophiomorpha nodosa*; *Planolites* and *Palaeophycus heberti* are both cross-cut by *Anconichnus* only; *Phoebichnus* are cross-cut by *Anconichnus* and *Planolites*; *Thalassinoides* are cross-cut by *Anconichnus* and *Rhizocorallium*, while *Rhizocorallium* are cross-cut by *Anconichnus* and *Thalassinoides*, and may be infilled by *Anconichnus*; *Ophiomorpha nodosa* are cross-cut by *Anconichnus*, *Planolites*, and *Thalassinoides*; and *Teichichnus* are cross-cut by *Anconichnus*, *Planolites*, *Phoebichnus*, *Thalassinoides* and *Rhizocorallium* (Fig.4.25). Preserved shelly macrofauna are absent.

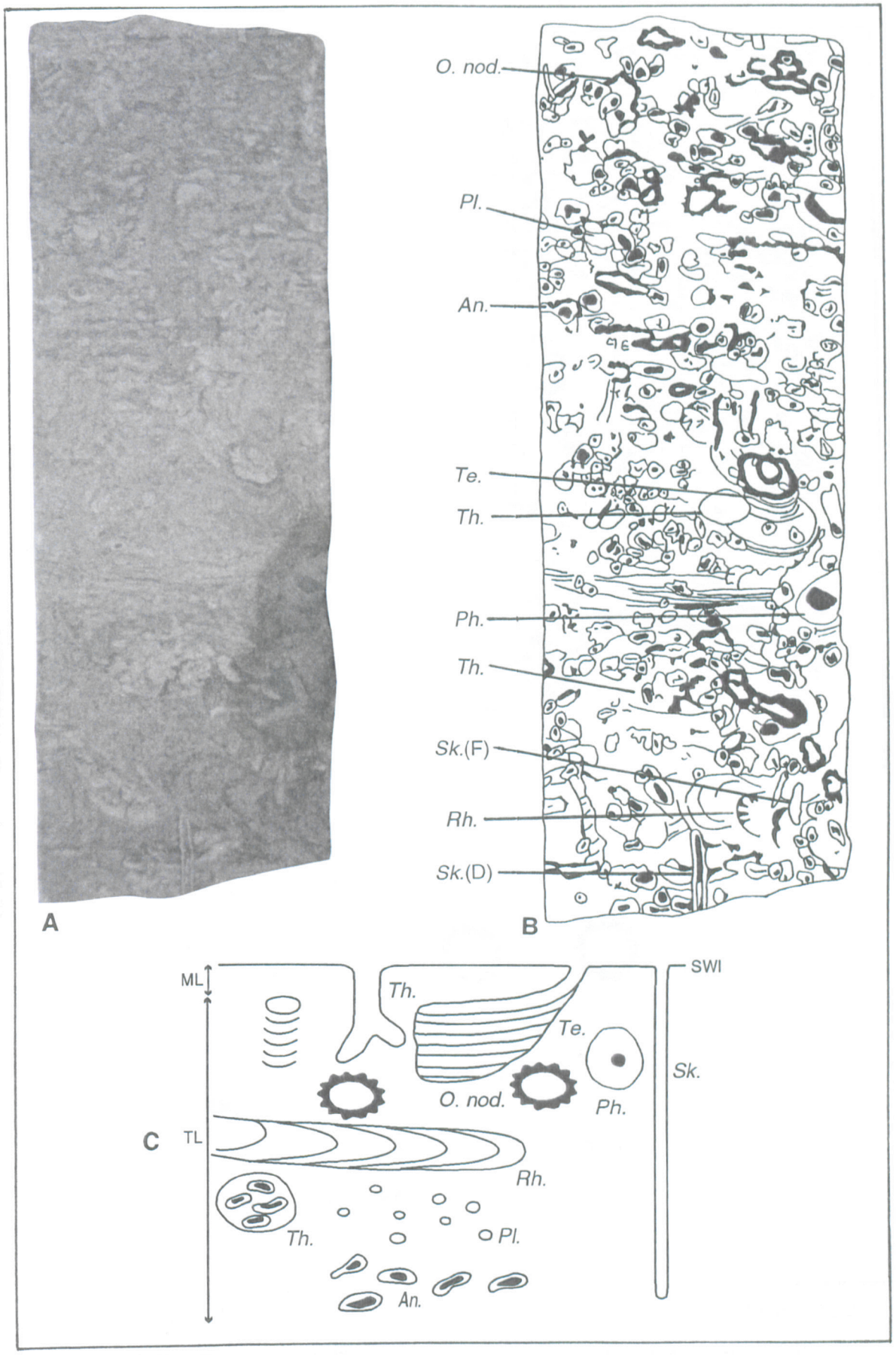

Fig.4.24 Finniss 2, 29.00 - 28.82m. (A) Photograph of the core, cut surface, actual size. (B) Sketch of the photograph. (C) Schematic trace fossil tiering diagram, not to scale. Annotations as before.

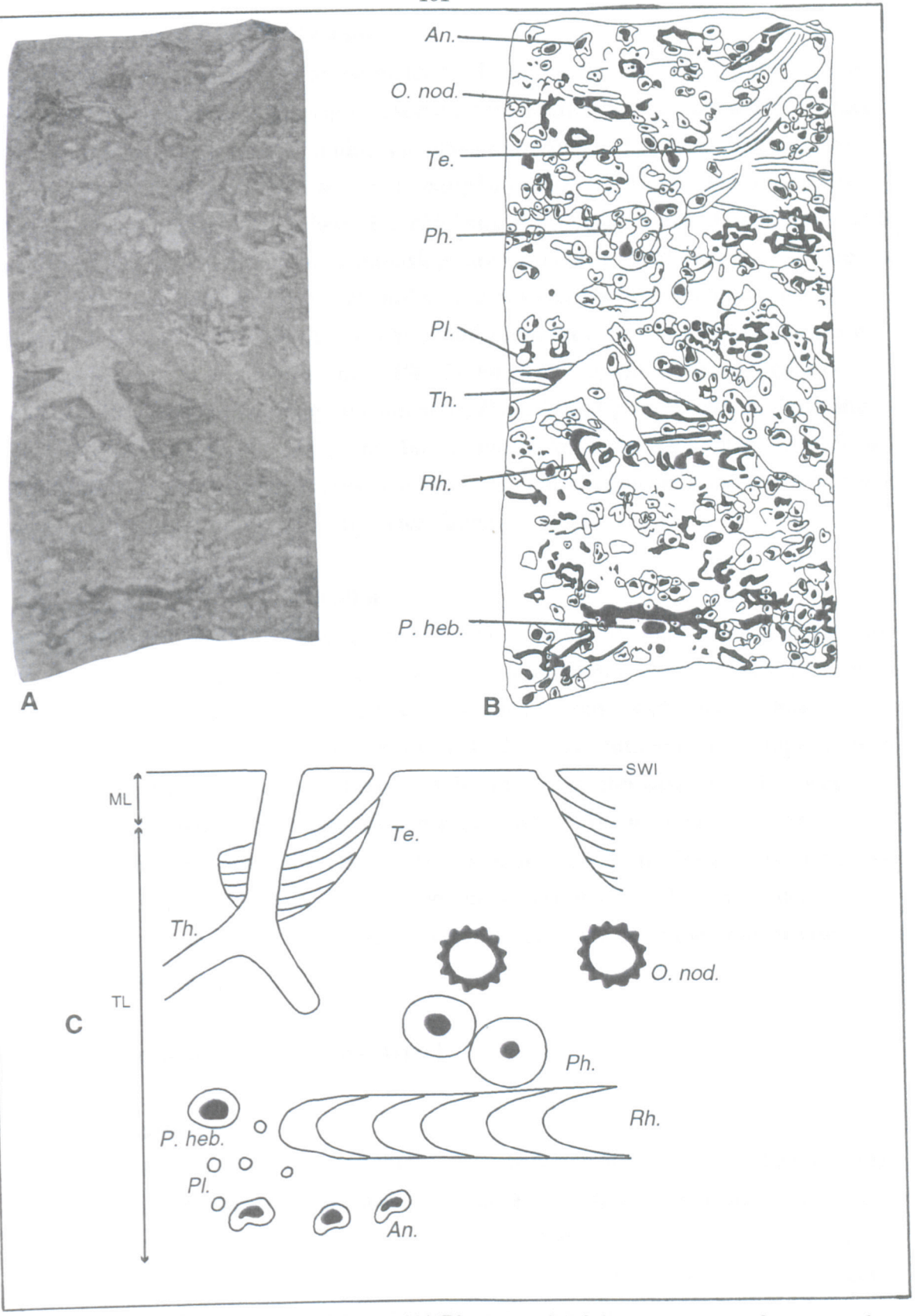

Fig.4.25 Finniss 2, 28.82 - 28.71m. (A) Photograph of the core, cut surface, actual size. (B) Sketch of the photograph. (C) Schematic trace fossil tiering diagram, not to scale. Annotations as before.

Example: Finniss 2, 28.66 - 28.48m

Clayey siltstone, composed of an estimated 95% silt and 5% clay-grade material. No physical sedimentary structures are preserved, bioturbation is complete at B.I.6. Trace fossil diversity is very high with nine ichnotaxa represented. The assemblage contains *Anconichnus*, silt-filled *Planolites*, *Ophiomorpha nodosa*, *Ophiomorpha irregulaire*, *Teichichnus*, *Palaeophycus heberti*, *Phoebichnus*, *Rhizocorallium*, and *Skolithos* (var.B and F) (Fig.4.26). Cross-cutting relationships are well constrained: *Anconichnus* are not cross-cut by any other trace type; *Planolites* are cross-cut by *Anconichnus* only; *Phoebichnus* are cross-cut by *Anconichnus* and *Planolites*; *Ophiomorpha nodosa* are cross-cut by *Anconichnus*, *Planolites*, *Phoebichnus*, and *Ophiomorpha irregulaire*; *Rhizocorallium* are cross-cut by *Anconichnus*, *Planolites*, *Ophiomorpha nodosa*, and *Skolithos*; *Teichichnus* is cross-cut by *Anconichnus*, *Planolites*, *Ophiomorpha nodosa*, and *Skolithos*; and *Skolithos* is cross-cut by occasional *Anconichnus* and *Ophiomorpha nodosa* (Fig.4.26). Preserved shelly macrofauna are absent.

Example: Alford 1, 60.40 - 60.30m

Clayey siltstone, composed of an estimated 60% silt and 40% clay-grade material. No physical sedimentary structures are preserved, bioturbation is complete at B.I.6. Three ichnotaxa are represented, the trace fossil assemblage consists of *Anconichnus*, *Ophiomorpha nodosa*, and *Teichichnus* (Fig.4.27). Cross-cutting relationships are well constrained: *Anconichnus* are not cross-cut by any other ichnotaxa, though newer *Anconichnus* appear to overprint an older generation of *Anconichnus* mottling; *Ophiomorpha nodosa* are cross-cut by *Anconichnus* only; while *Teichichnus* are cross-cut by both *Anconichnus* and *Ophiomorpha nodosa* (Fig.4.27). Preserved shelly macrofauna are absent, though broken bivalve remains are common in otherwise similar neighbouring regions of core.

4.3.6 Palaeoenvironmental fabric type F

General characteristics

Clayey siltstone in which the silt content varies between 50% and 80%, the remainder being clay grade material, with a minor fine sand-grade fraction in places. Physical sedimentary structures comprise cm scale interbedded clay-rich and more silt-rich horizons, cm to dm scale fining-upwards sequences, both with occasional basal scour surfaces, planar silty lamination, aggradational ripples, cross-lamination, and hummocky cross-stratification (Fig.4.28). Bioturbation intensity is variable between B.I.2 and B.I.4 with up to five trace fossil types in any one assemblage, though eight

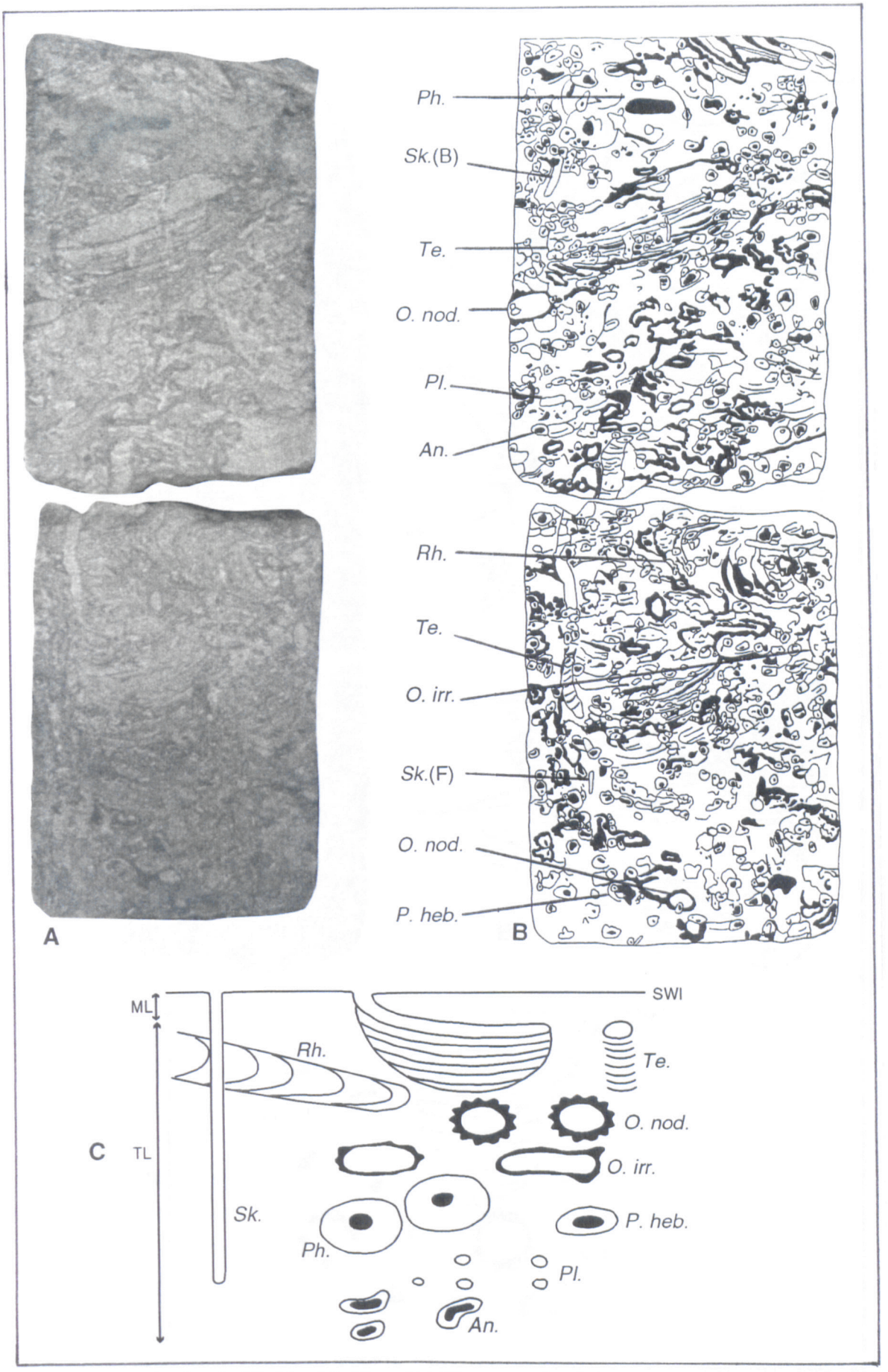

Fig.4.26 Finniss 2, 28.66 - 28.48m. (A) Photograph of the core, cut surface, actual size. (B) Sketch of the photograph. (C) Schematic trace fossil tiering diagram, not to scale. Annotations as before.

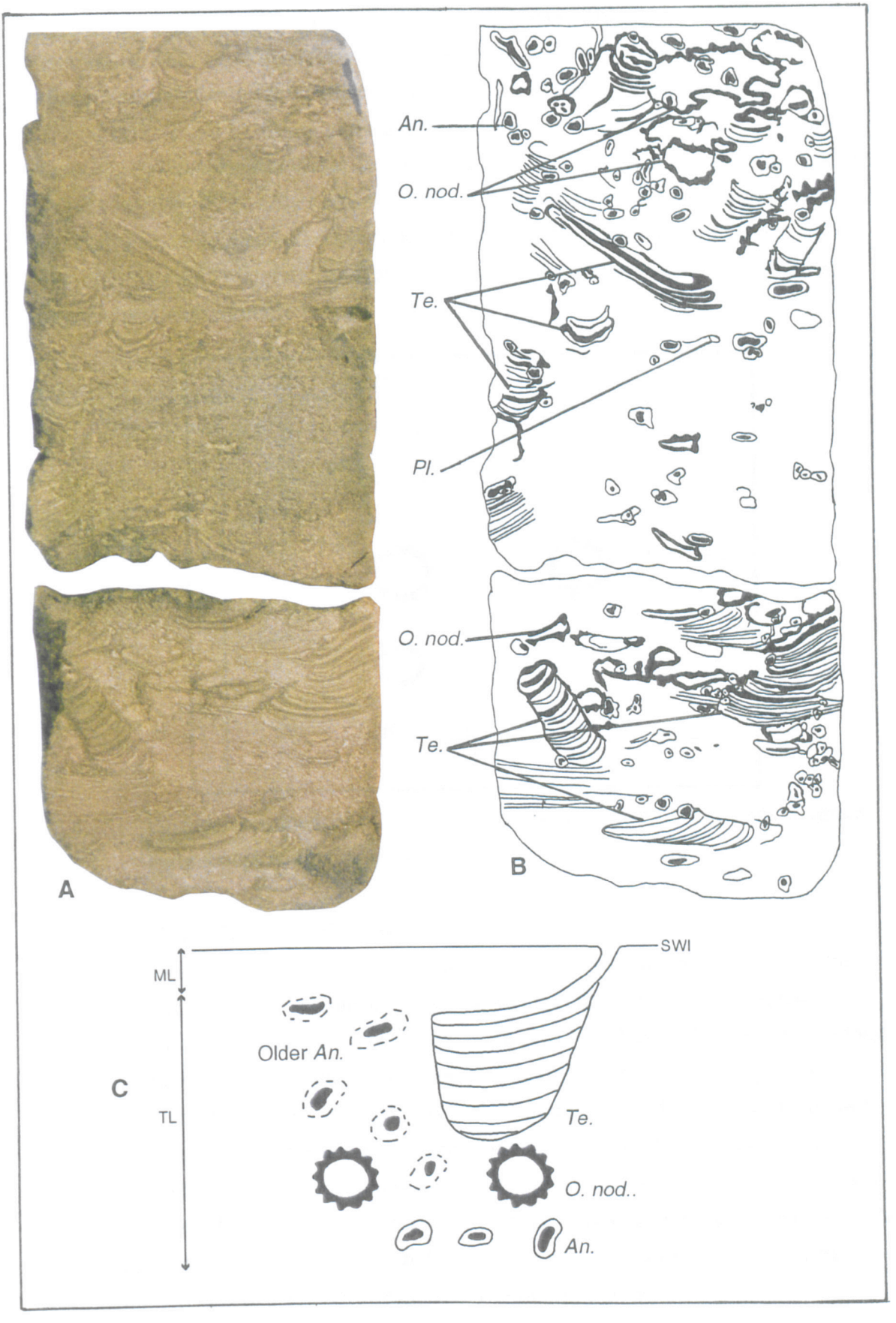

Fig.4.27 Alford 1, 60.40 - 60.30m. (A) Photograph of the core, cut surface, actual size. (B) Sketch of the photograph. (C) Schematic trace fossil tiering diagram, not to scale. Annotations as before.

ichnotaxa have been recorded from PFT/F material. Assemblages are dominated by *Anconichnus*, with more occasional silt-filled *Planolites*, *Palaeophycus heberti*, *Palaeophycus tubularis*, *Ophiomorpha nodosa*, *Teichichnus*, silt-filled *Chondrites*, and *Skolithos* (var. B and F). Cross-cutting relationships are poorly constrained, though *Planolites*, *Ophiomorpha nodosa*, *Teichichnus*, and *Skolithos* (var. B) are cross-cut by *Anconichnus* (Fig.4.28). Other cross-cutting relationships are probably as previously described. Preserved macrofauna is generally absent, though broken and fragmented indeterminate shelly material, probably with both autochthonous and allochthonous components, is occasionally present.

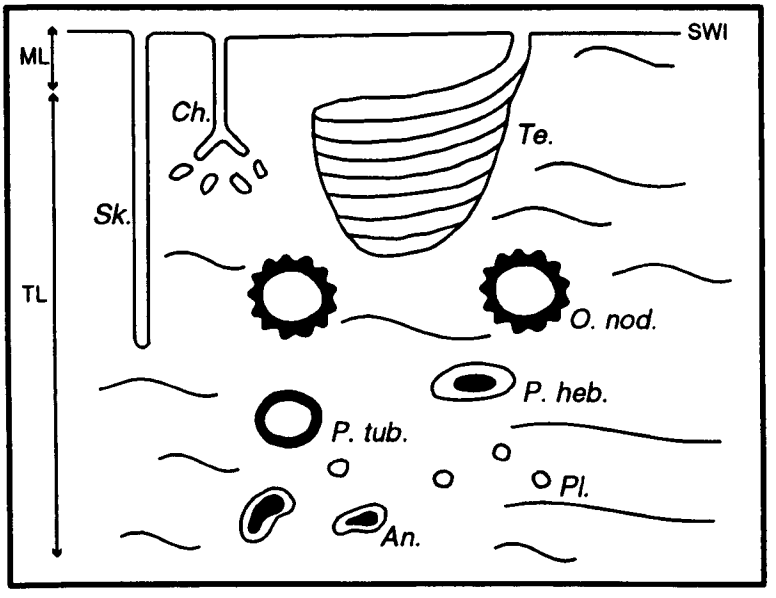

Fig.4.28 Palaeoenvironmental fabric type F, schematic trace fossil tiering diagram and reconstruction. Annotations as before. Not to scale.

Example: Alford 1, 57.90 - 57.80m

Clayey siltstone in which the estimated silt content varies between 60 and 80%, the remainder being clay-grade material. Physical sedimentary structures comprise occasional cm thickness, silt-rich horizons, often erosively based along scour surfaces. These silty horizons bear planar lamination and aggradational ripples (Fig.4.29). Bioturbation reaches B.I.4-5 in more clay-rich material below the scour surface, and B.I.3 in the siltier sediments deposited after the erosive event. Four ichnotaxa are represented. The assemblage is dominated by *Anconichnus*, with more occasional silt-filled *Planolites*, *Teichichnus*, and *Skolithos* (var. B). Cross-cutting relationships are not particularly well constrained, but both *Teichichnus* and *Skolithos* are cross-cut by *Anconichnus* (Fig.4.29). Indeterminate shelly material is present.

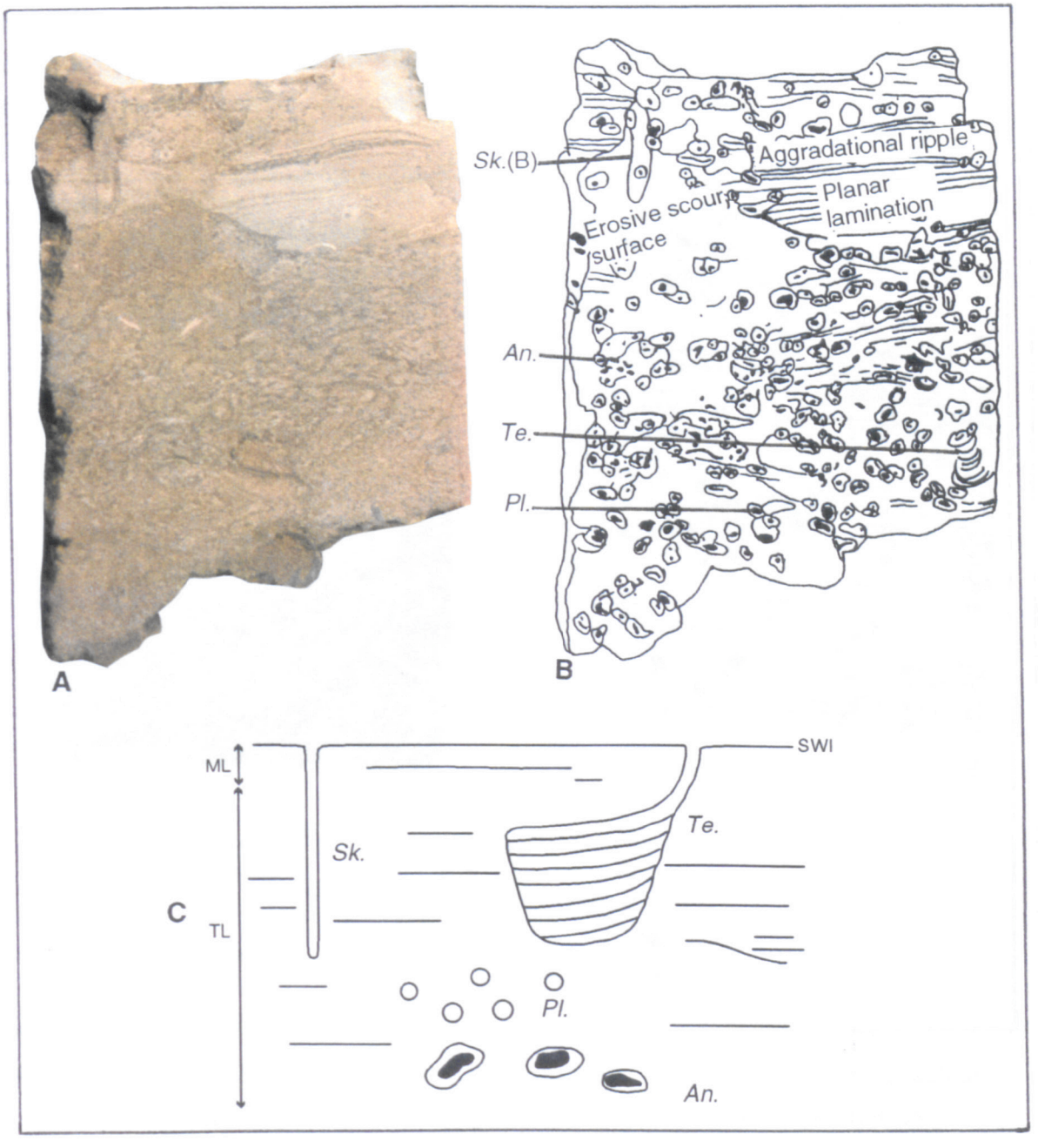

Fig.4.29 Alford 1, 57.90 - 57.80m. (A) Photograph of the core, cut surface, actual size. (B) Sketch of the photograph. (C) Schematic trace fossil tiering diagram, not to scale. Annotations as before.

Example: CBH 2, 342.40 - 342.30m

Clayey siltstone, composed of an estimated 90% silt and 10% clay-grade material. Physical sedimentary structures are well-preserved and consist of fining-upwards successions of cm to 1 dm thickness, cross-lamination and hummocky cross-stratification (Fig.4.30). Bioturbation varies in intensity between B.I.2 and B.I.3. Trace

fossil diversity is low with only two ichnotaxa represented. The trace fossil assemblage consists of *Anconichnus* and silt-filled *Chondrites* (Fig.4.30). Cross-cutting relationships are uncertain. Preserved shelly macrofauna are absent.

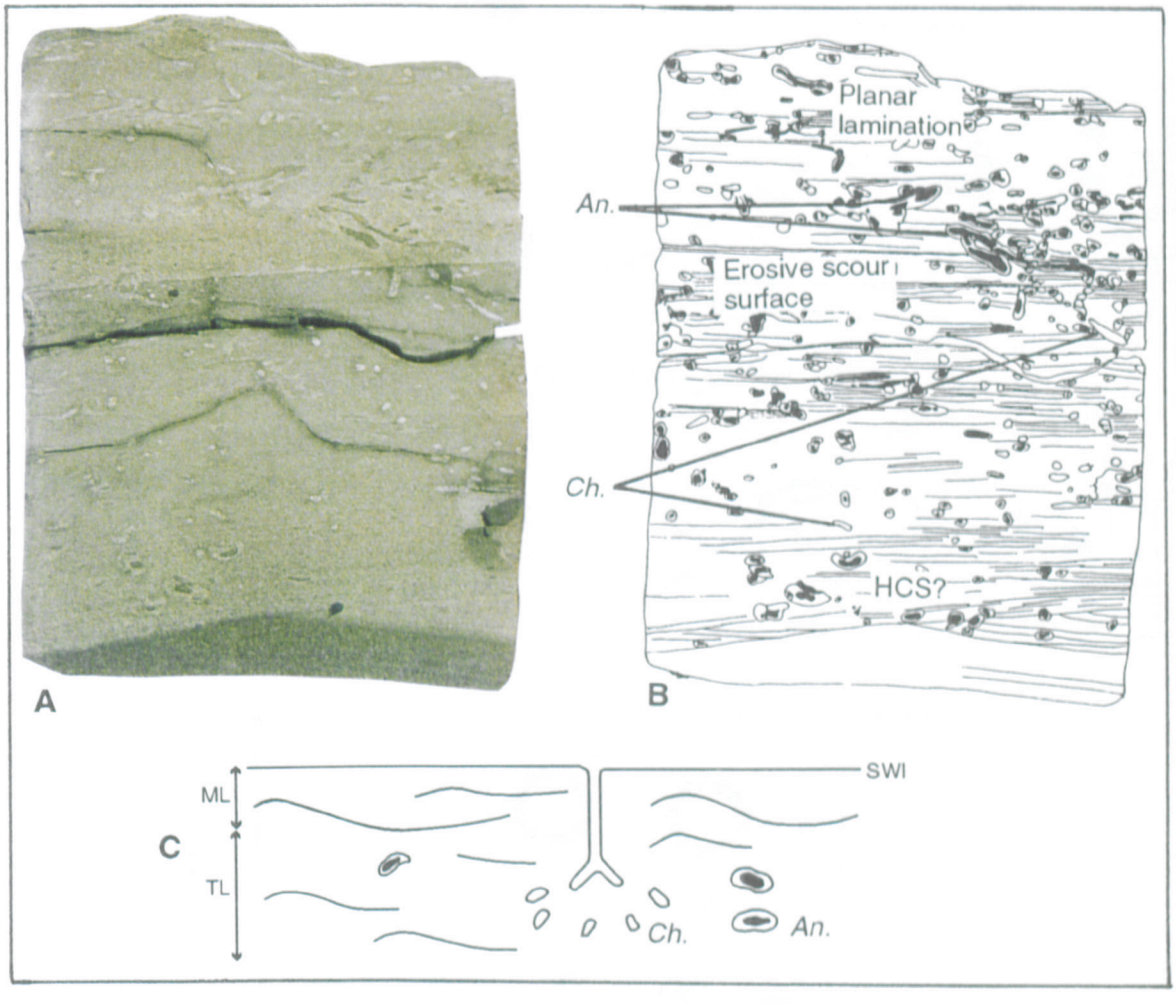

Fig.4.30 CBH 2, 342.40 - 342.30m. (A) Photograph of the core, cut surface, actual size. (B) Sketch of the photograph. (C) Schematic trace fossil tiering diagram, not to scale. Annotations as before.

Example: SPH 1, 291.80 - 291.70m

Clayey siltstone, composed of an estimated 50% (at the base) to 80 % (at the top) silt grade material, the remainder being clay-grade material. Physical sedimentary structures are well-preserved and are dominated by fining-upwards sequences of cm to 1dm thickness, often erosively based across scour surfaces, and bearing planar lamination (Fig.4.31). Bioturbation intensity varies between B.I.2 and B.I.3. Three trace fossil taxa are present. The trace fossil assemblage is dominated by *Anconichnus*, with more occasional silt-filled *Planolites* and *Ophiomorpha nodosa* (Fig.4.31). *Planolites*

are cross-cut by *Anconichnus*; other cross-cutting relationships are uncertain. Preserved shelly macrofauna are absent.

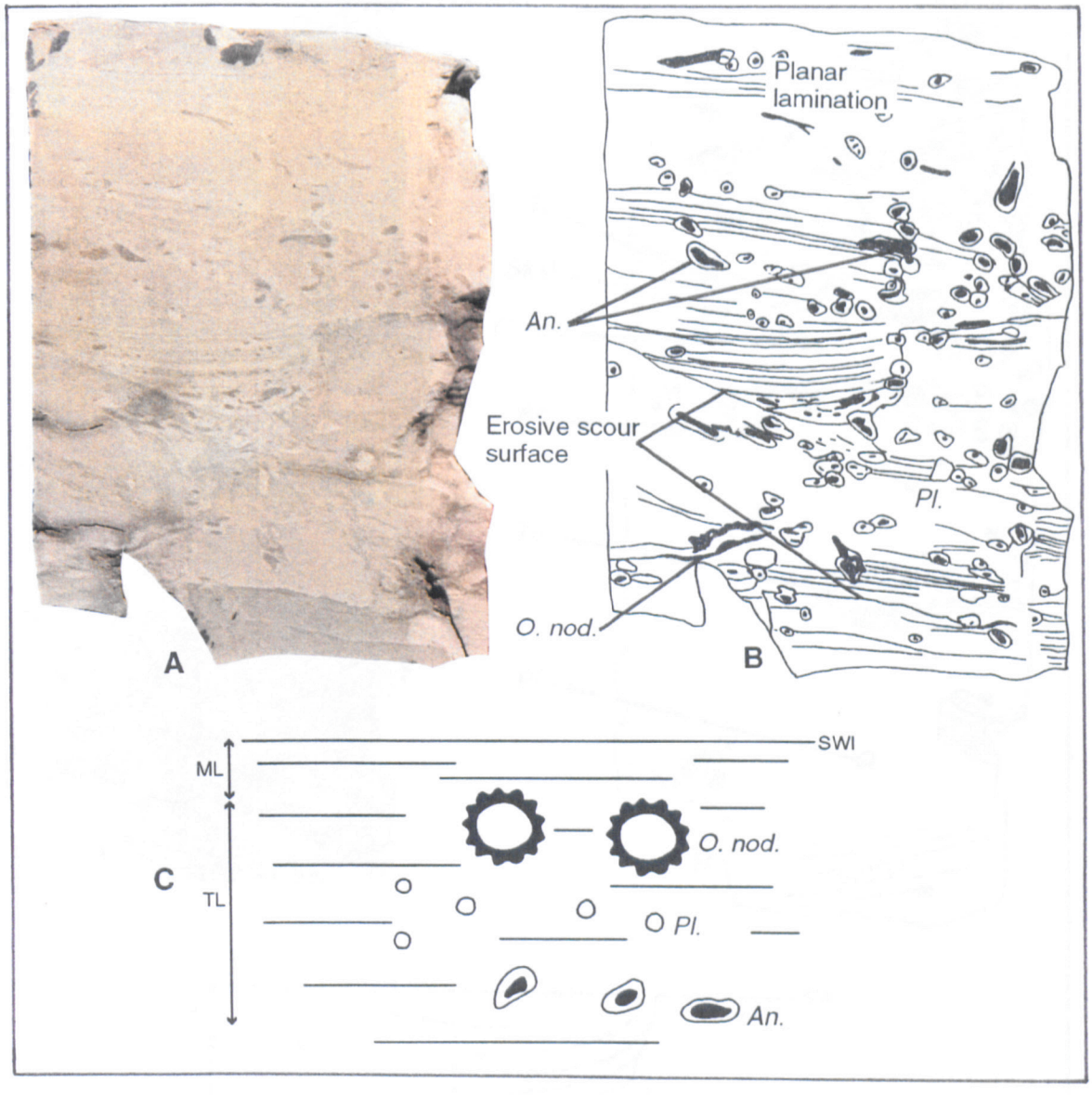

Fig.4.31 SPH 1, 291.80 - 291.70m. (A) Photograph of the core, cut surface, 1.5x actual size. (B) Sketch of the photograph. (C) Schematic trace fossil tiering diagram, not to scale. Annotations as before.

Example: SPH 1, 290.40 - 290.30m

Clayey siltstone, composed of an estimated 80% silt and 20% clay-grade material, with a minor fine sand fraction. Physical sedimentary structures are well preserved and are dominated by interbedded horizons of variable silt content and of several cm thickness, bearing planar lamination with possible hummocky cross-stratification (Fig.4.32). Bioturbation intensity varies between B.I.2 and B.I.3. Five trace fossil taxa are present

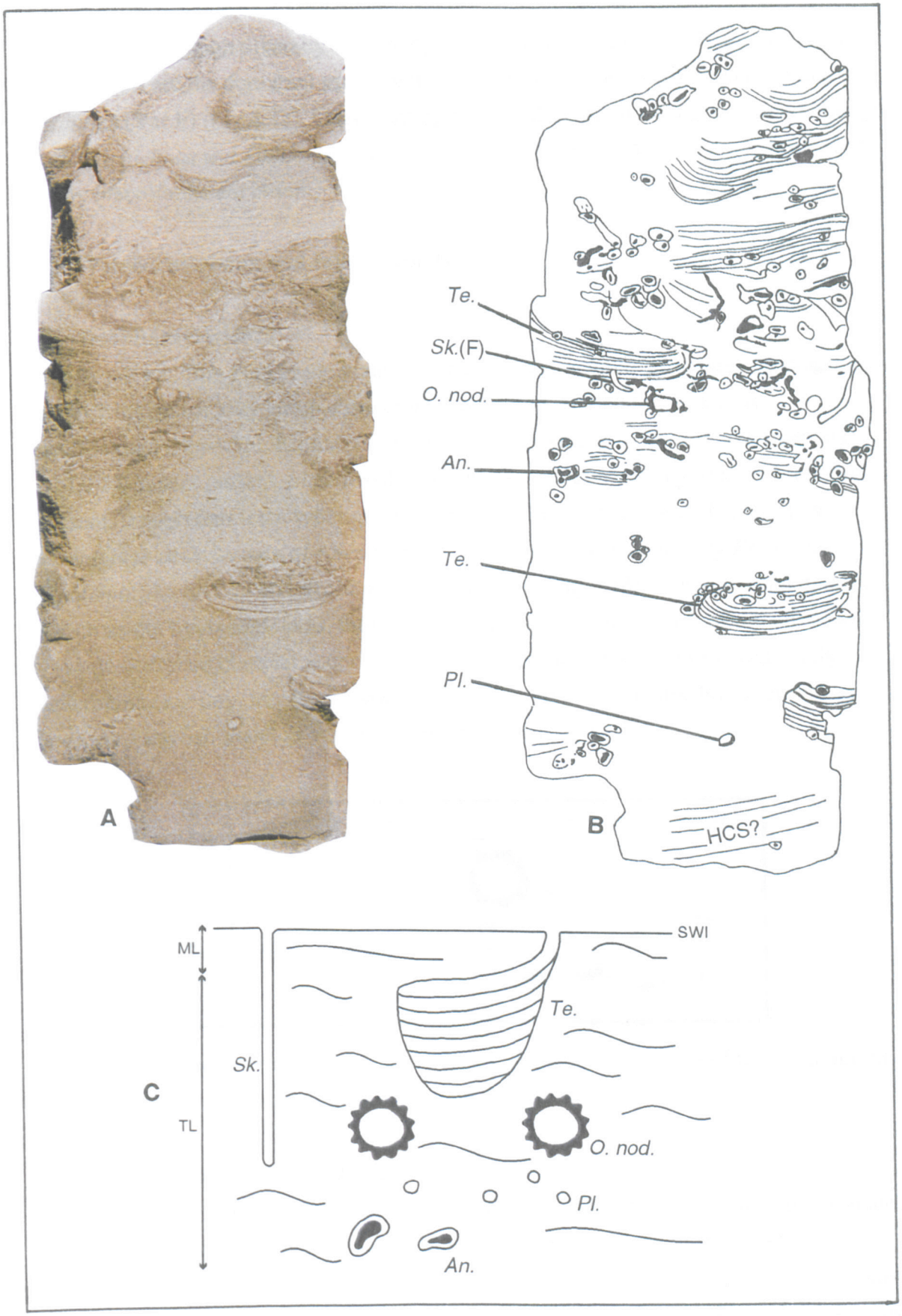

Fig.4.32 SPH 1, 290.40 - 290.30m. (A) Photograph of the core, cut surface, 1.5x actual size. (B) Sketch of the photograph. (C) Schematic trace fossil tiering diagram, not to scale. Annotations as before.

in this relatively high diversity assemblage: *Anconichnus*, silt-filled *Planolites*, and *Teichichnus* are the dominant traces, with less common *Ophiomorpha nodosa* and *Skolithos* (Var.F) (Fig.4.32). Cross-cutting relationships are poorly constrained, though both *Teichichnus* and *Ophiomorpha nodosa* are cross-cut by *Anconichnus*. Preserved shelly macrofauna are absent.

4.3.7 Palaeoenvironmental fabric type G

General characteristics

Coarse silt and fine sand grade material. Physical sedimentary structures predominate, comprising planar silty lamination, cross-lamination, and hummocky cross-stratification (Fig.4.33). Bioturbation is either non-existent or of very low intensity (B.I.0-1). Where present, trace fossils form an assemblage with up to three ichnotaxa present, though four trace types are evident from different samples. Typically the assemblage consists only of *Anconichnus* , however very occasionally *Planolites*, *Ophiomorpha nodosa* and *Skolithos* can be present (Fig.4.33). *Ophiomorpha nodosa* are cross-cut by *Anconichnus*, though other cross-cutting relationships are unknown. Fragmented plant material is concentrated along some horizons. Preserved shelly macrofauna are rare, largely consisting of broken bivalve remains, however one well preserved starfish skeleton has also been recovered.

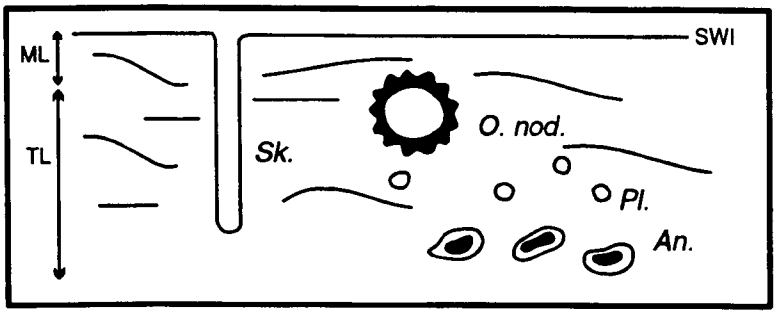

Fig.4.33 Palaeoenvironmental fabric type G, schematic trace fossil tiering diagram and reconstruction. Annotations as before. Not to scale.

Example: Alford 1, 40.45 - 40.35m

Coarse silt and fine sand-grade material. Physical sedimentary structures predominate, comprising planar lamination and hummocky cross-stratification (Fig.4.34). Bioturbation intensity is very low at B.I.1. Three trace types are present: *Anconichnus*, *Ophiomorpha nodosa*, and *Skolithos* (var.F) (Fig.4.34). *Ophiomorpha nodosa* are cross-

cut by *Anconichnus*, other trace fossil cross-cutting relationships are uncertain. Preserved shelly macrofauna are absent.

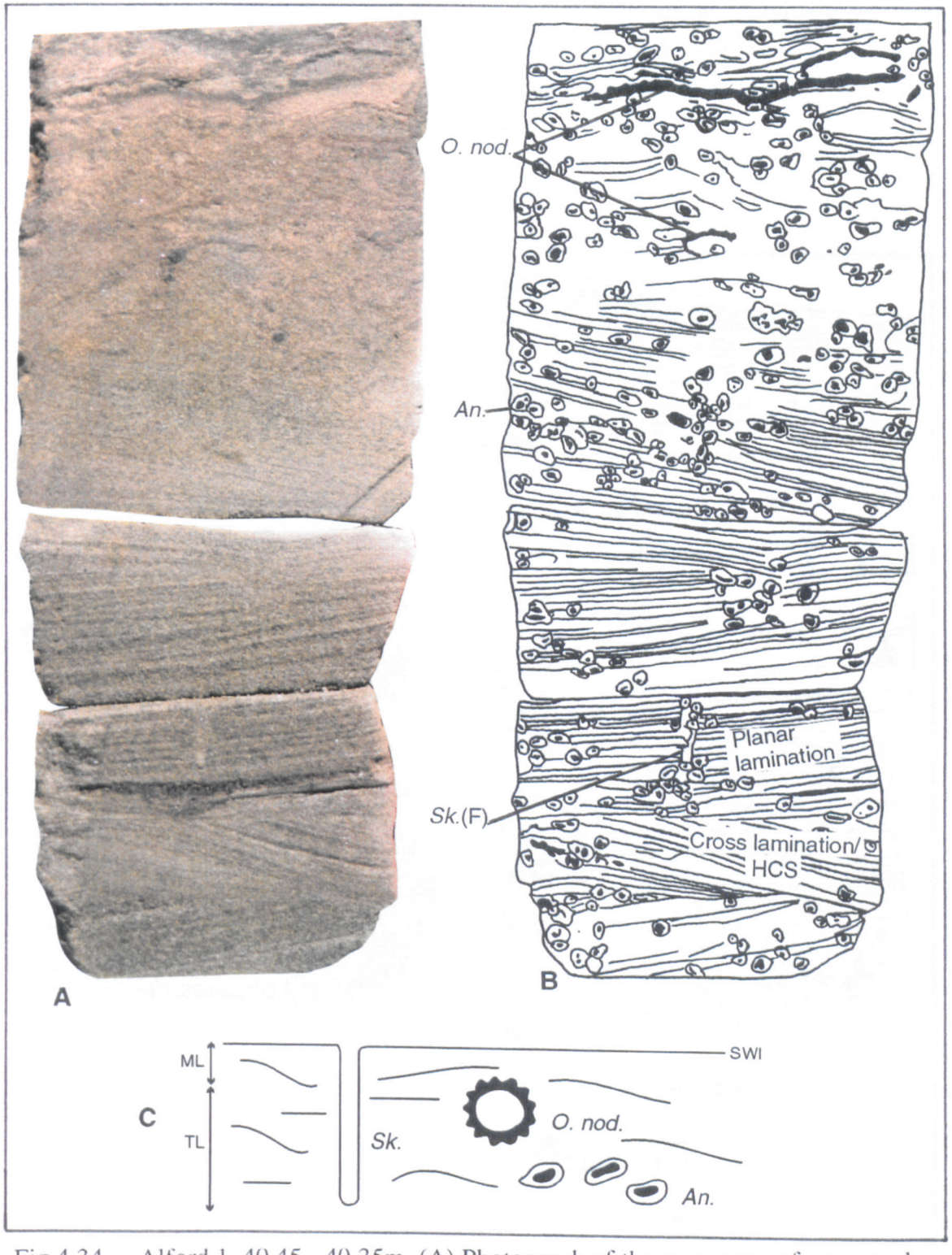

Fig.4.34 Alford 1, 40.45 - 40.35m. (A) Photograph of the core, cut surface, actual size. (B) Sketch of the photograph. (C) Schematic trace fossil tiering diagram, not to scale. Annotations as before.

Example: CBH 2, 350.80 - 350.70m

Coarse silt and fine sand-grade material. Physical sedimentary structures predominate, comprising planar lamination, cross-lamination with clay drapes, and hummocky cross-stratification (Fig.4.35). Bioturbation intensity is very low, and varies between B.I.0 and B.I.1. *Anconichnus* is the only trace present, and these tend to be isolated and small (Fig.4.35). Preserved shelly macrofauna are absent.

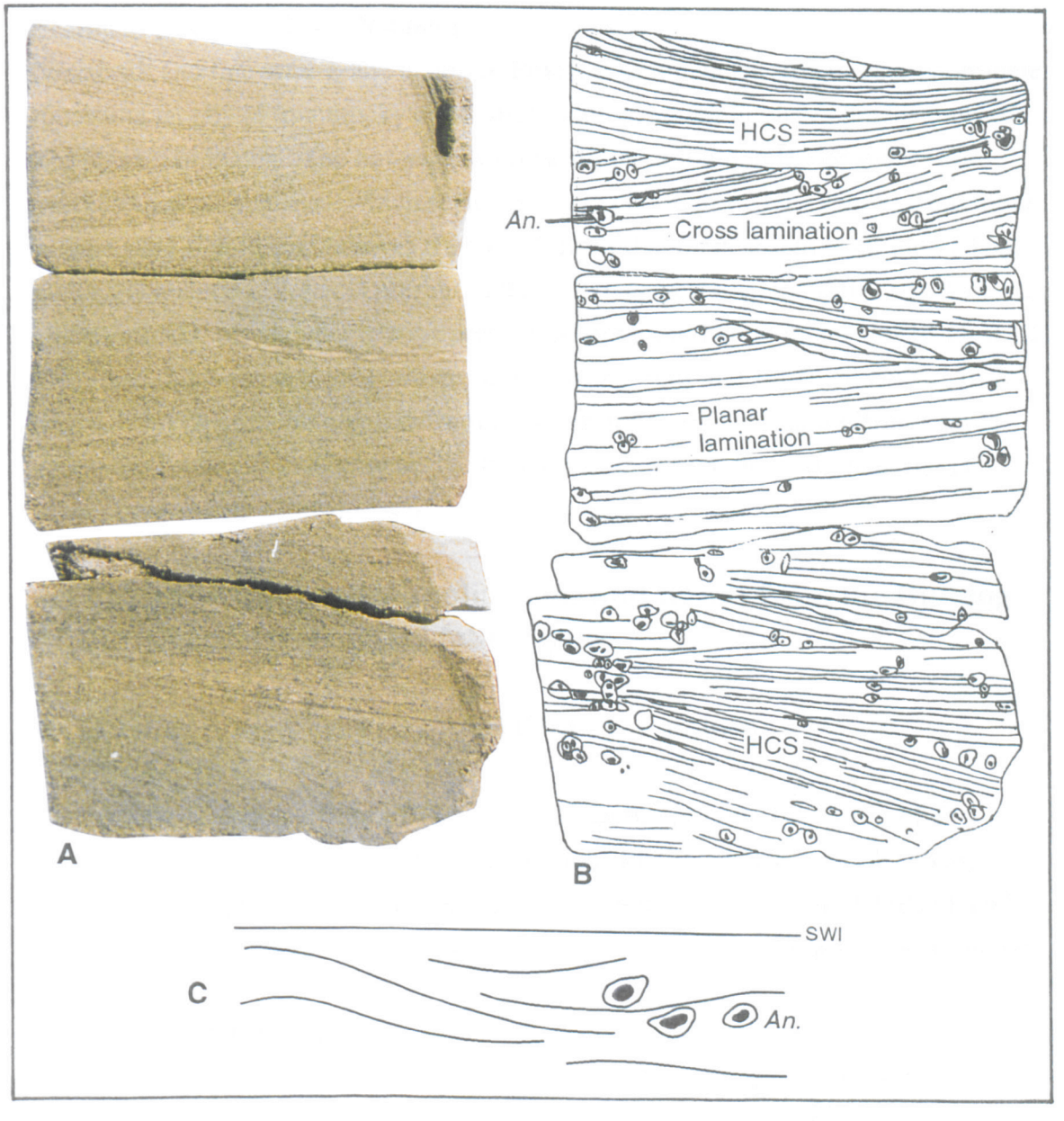

Fig.4.35 CBH 2, 350.80 - 350.70m. (A) Photograph of the core, cut surface, actual size. (B) Sketch of the photograph. (C) Schematic trace fossil tiering diagram, not to scale. Annotations as before.

Example: CBH 2, 339.15 - 339.05m

Coarse silt and fine sand grade-material. Physical sedimentary structures predominate, consisting of planar and cross-lamination, and hummocky cross-stratification (Fig.4.36). Bioturbation intensity is very low and varies between B.I.0 and B.I.1. *Anconichnus* is the only trace present, and these tend to be isolated and small (Fig.4.36). A starfish is well preserved on an erosive surface, one arm is cross-sectioned in the cut core (Fig.4.36) (§4.4.2, Fig.4.39), the presence of which testifies to the rapidity of deposition of the overlying sediment.

Example: SPH 1, 304.70 - 304.60m

Coarse silt and fine sand-grade material. Physical sedimentary structures predominate, consisting largely of hummocky cross-stratification, which in places grades upwards into planar lamination. The hummocky cross-stratification dominated succession overlies an erosive surface which separates more clay-rich PFT/F (below) from more silt and sand-rich PFT/G (above) (Fig.4.37). Bioturbation is absent from the PFT/G sandy siltstone (B.I.0), but is present in the PFT/F clayey siltstone (80% silt, 20% clay grade material) beneath the erosive surface, where bioturbation intensities reach B.I.2. This trace fossil assemblage contains large *Anconichnus* and silt-filled *Chondrites* (Fig.4.37). The cross-cutting relationship between *Anconichnus* and *Chondrites* is uncertain. Preserved macrofaunal shelly material is absent, but plant material is concentrated along some horizons.

4.4 Palaeoenvironmental implications and trends from the Bulldog Shale palaeoenvironmental fabric types

4.4.1 Tiering changes in an idealised PFT/A - G transition

The idealised transition from PFT/A - PFT/G can be split into two parts: PFT/A - PFT/E; and PFT/E - PFT/G. In these successions PFT/A, PFT/E, and PFT/G are considered to represent key depositional environmental states, with PFT/B, PFT/C, PFT/D, and PFT/F delineating transitional states between these marker environments.

Transition: PFT/A - PFT/E

In response to palaeoenvironmental changes (§4.4.2), the transition from PFT/A - PFT/E (Figs.4.05, 4.08, 4.11, 4.14, 4.18) involves an increase in the suitability of the environment to trace making organisms. Those trace-makers, or types of trace maker behaviour, e.g. *Anconichnus*, already present, and represented in PFT/A, are those for

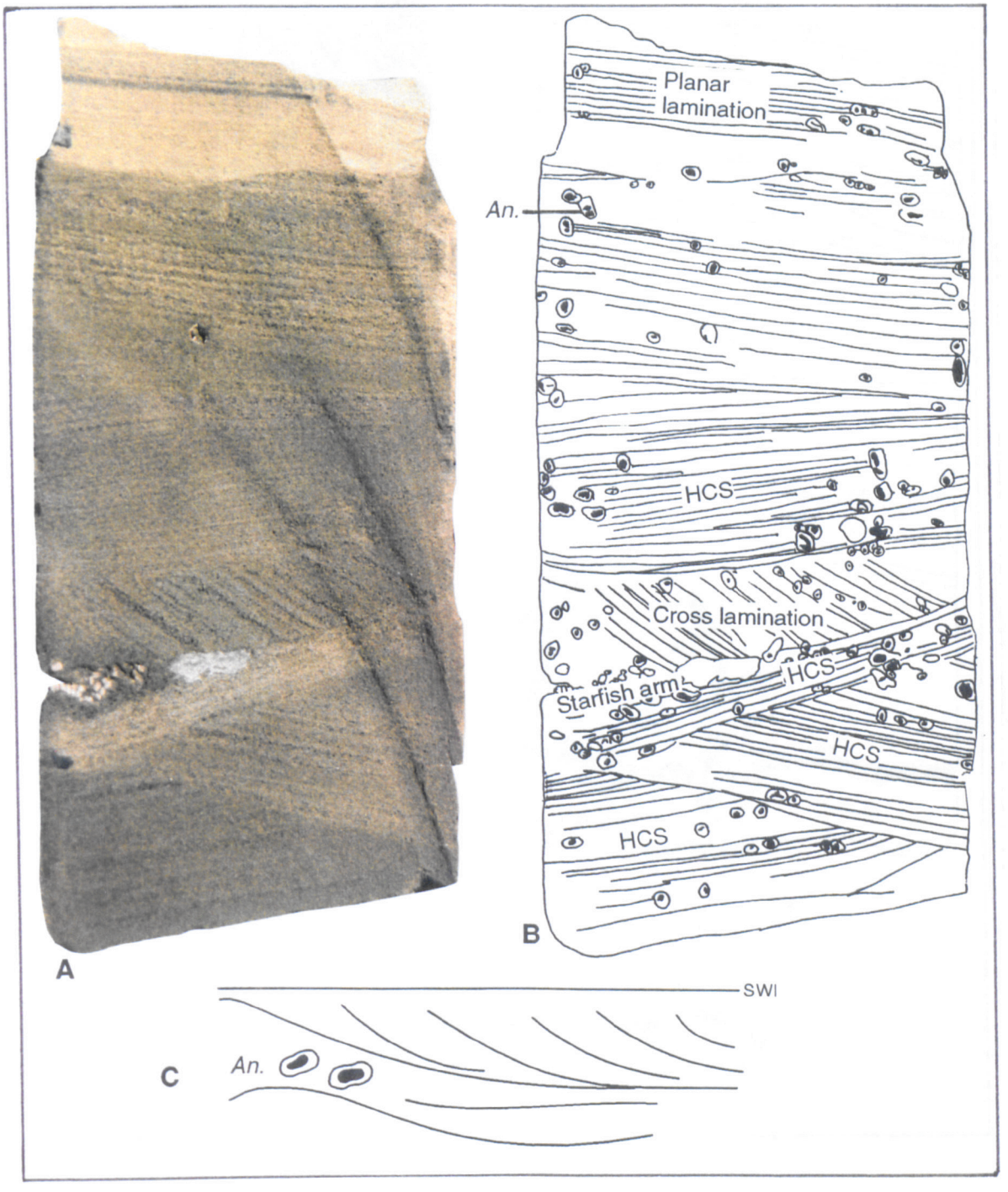

Fig.4.36 CBH 2, 339.15 - 339.05m. (A) Photograph of the core, cut surface, actual size. (B) Sketch of the photograph. (C) Schematic trace fossil tiering diagram, not to scale. Annotations as before.

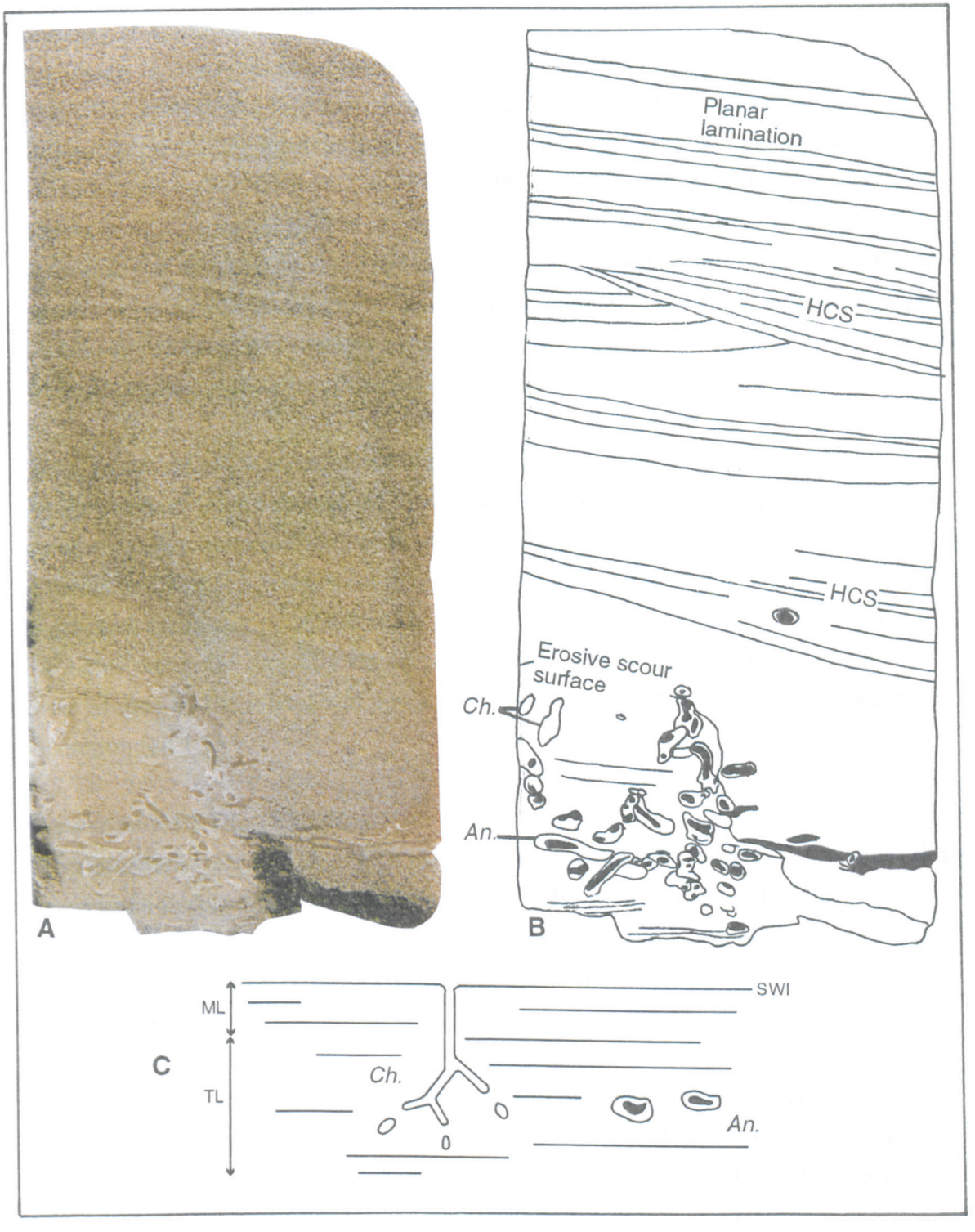

Fig.4.37 SPH 1, 304.70 - 304.60m. (A) Photograph of the core, cut surface, 1.5x actual size. (B) Sketch of the photograph. (C) Schematic trace fossil tiering diagram, not to scale. Annotations as before.

whom stressed environments are the optimum. With slight improvements in environmental conditions their rate of activity increases, resulting in an increase in intensity of bioturbation. Through necessity these trace makers utilise only the shallowest layer of sediment, producing a transition layer of only 1-2cm, conditions below this level precluding even their hardened existence. The transition from conditions precluding more general trace maker existence and activity to a state of increased optimality, from PFT/A - PFT/B, PFT/C, PFT/D, and eventually PFT/E, results in the downward shift of those conditions optimal to *Anconichnus*, and the acquisition of new trace makers and new trace making behaviours in the shallower tier previously occupied by *Anconichnus*. As environmental conditions continue to improve so the acquisition of new trace types and the associated downward shift in pre-existing tiers proceeds, resulting in a complex multi-tiered profile.

Such processes might be expected to produce ichnocoenoses in which the traces of the shallower tiers cross-cut traces of the deeper tiers. Such cross-cutting relationships are however rarely observed, and where they are noted they are more likely to represent tier overlap or sharing. It is apparent that the effects of downward tier migration with their associated cross-cutting relationships are almost entirely lacking in preservation, probably due to the typically very gradual nature of such environmental change, and overprinting by the subsequent upward migration of tiers in response to sediment accretion (§4.1.1).

Transition: PFT/E - PFT/G

The transition from PFT/E - PFT/G (Fig.4.18, 4.28, 4.33) is, in part, a reversal of those trace fossil tiering trends noted in the transition from PFT/A - PFT/E. The environmental variations producing this reversal are, however, different from those responsible for the PFT/A - PFT/E transition, and the resultant fabric types are very different (§4.4.2).

The transition from PFT/E - PFT/G is the result of palaeoenvironmental changes that act to reduce the environmental optimality to the trace makers. This results in the progressive loss of tiers, upward migration of ichnotaxa, associated reduction in trace type diversity and a drop in bioturbation intensity.

4.4.2 The control on tiering changes: palaeoenvironmental trends and variation

In an idealised transition from PFT/A - PFT/G specific trends are defined in intensity of bioturbation, diversity of bioturbation, grain size (% silt), and frequency and thickness of storm-derived interbeds (from mm thick silty interbeds to hummocky cross-stratified horizons). These variations in the fabric of the rock can be related to two important basin-wide environmental parameters, namely: bottom water oxygenation levels and environmental energy levels, both of which are controlled by relative sea level and its variation (Fig.4.38).

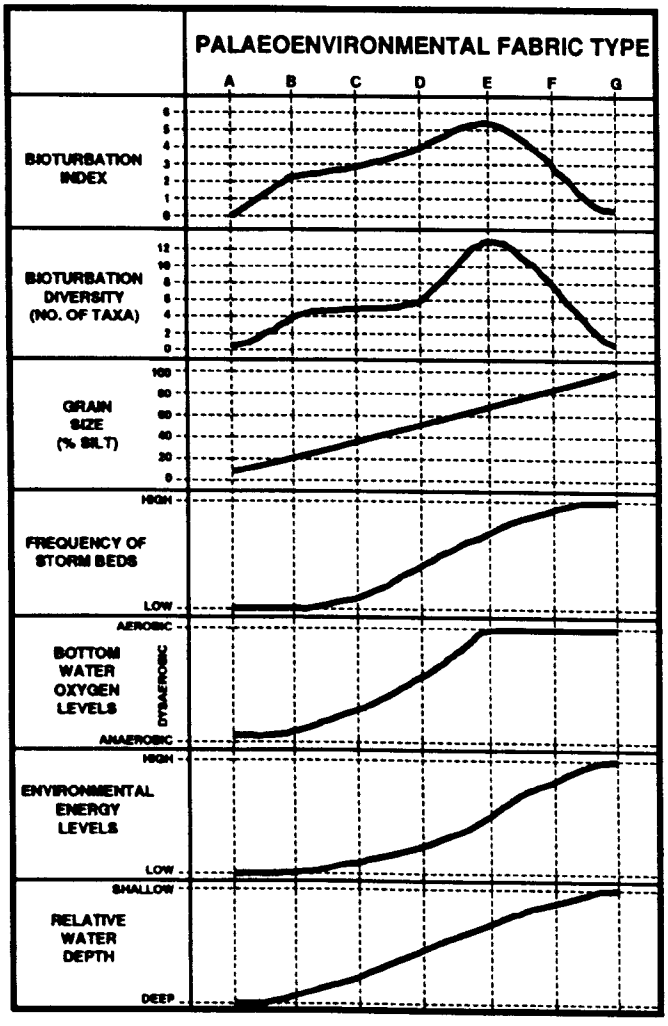

Fig.4.38 Trends in bioturbation intensity, bioturbation diversity, grain size as expressed by percentage silt content, and the frequency of storm-derived beds, and the variations in their controlling factors: bottom water oxygenation levels, environmental energy levels, and ultimately sea level.

In essence, a transition from PFT/A - PFT/G represents a relative shallowing of sea level. This shallowing is particularly well exhibited in a comparison of the three key palaeoenvironmental types.

Palaeoenvironmental fabric type A

Palaeoenvironmental fabric type A represents relatively deep basinal clay-dominated laminated muds deposited in low energy, strongly dysaerobic to anaerobic conditions. Such conditions were not conducive to trace maker existence, hence the extremely low values and diversity of bioturbation. The transition through PFT/B, PFT/C, and PFT/D represents shallowing such that bottom water oxygenation levels increase as the dysaerobic waters and the pycnocline recede basinwards. As such, in this transition, oxygen levels restrict the existence of trace makers less and less.

Palaeoenvironmental fabric type E

Palaeoenvironmental fabric type E represents depositional conditions probably just above local storm wave base but below fair weather wave base, as inferred from the increased silt content of the material, and the predominance of biogenic over physical sedimentary structures. Bottom water oxygenation levels are no longer restrictive to the existence of trace makers, and a highly diverse trace fossil assemblage is produced, frequently obliterating all physical sedimentary structures.

Palaeoenvironmental fabric type G

In the transition to PFT/F, and subsequently to PFT/G, shallowing continues. Increased environmental hydraulic energy levels begin to restrict the activity of trace makers, until at PFT/G only occasional *Anconichnus*, the ubiquitous trace, coloniser of stressful environments, is left. Palaeoenvironmental fabric type G is silt and sand dominated, deposited under waning storm conditions as indicated by the high frequency of hummocky cross-stratified material. Such conditions, with rapid erosion and deposition, provided far too unstable a substrate for the majority of trace makers, and trace fossils are for the most part absent. The potential for remarkable preservation in such storm-dominated successions with their associated rapid sedimentation, is evident from a starfish skeleton deposited on an erosive surface in the CBH 2 core (339.15 - 339.05m interval (§4.3.7; Fig.4.36) (Fig.4.39), which must have been buried rapidly before decay destroyed the soft parts and allowed each skeletal element to separate and be scattered.

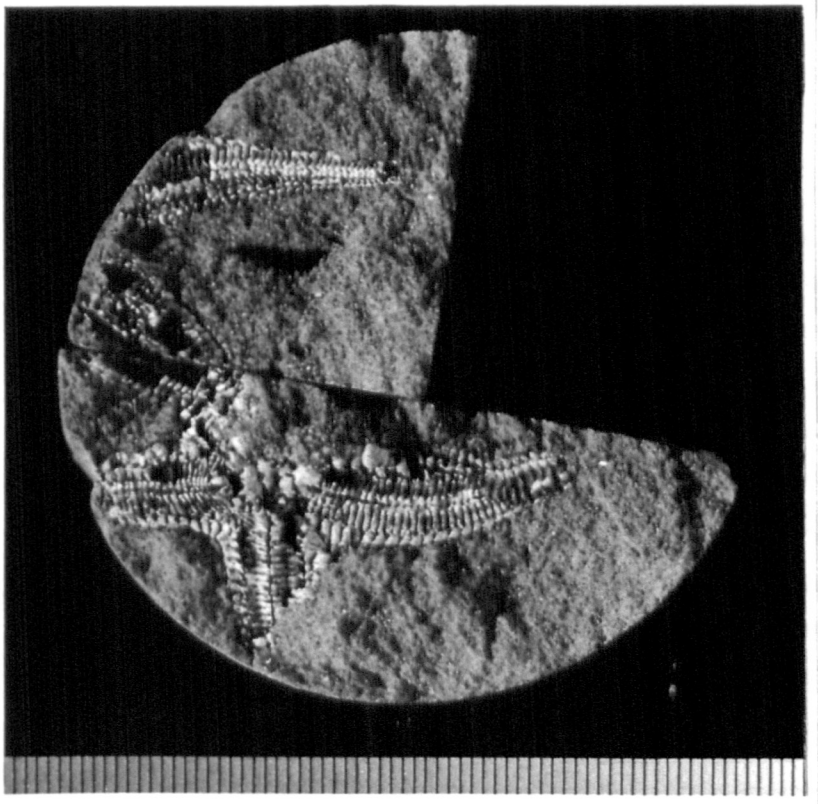

Fig.4.39 Starfish skeleton from within PFT/G material from CBH 2 339.15-339.10m. Scale bar divisions in mm.

Water depth, the primary control on PFT

Analyses of foraminiferal faunas from the Bulldog Shale equivalent Wallumbilla Formation by Haig and Lynch (1993) have determined maximum water depths during deposition of these sediments as being in the region of 50m. As described above, within the PFT scheme presented here, PFT/A represents deposition within the deepest conditions, with the transition from PFT/A to G occurring in response to a decrease in relative sea depth and associated increased proximity to the palaeoshoreline, with corresponding changes in bottom water oxygenation and environmental energy levels.

Relative sea depths can be defined within such a shallowing transition through analysis of the nature of storm deposited silt and sand levels (Aigner and Reineck, 1982). Storm sands and silts are transported from coastal sands and are spread out across the shelf by offshore-flowing currents as storms abate. Four storm-derived silt and sand facies have been defined, the deposition of which is controlled by water depth and associated proximity to the shoreline, from sediments of the Helgoland Bight of the south east North Sea in water depths of 3m to 50m. The characteristics of each of these storm facies is summarised in table 4.3.

Table 4.3 Characteristics of Aigner and Reineck's (1982) storm derived silt and sand facies.

Facies name	Water depth	Composition
Shoreface storm layers	3-10m	Several dm of hummocky cross-stratification (HCS) dominated, amalgamated sand bodies. Lack of reworking by fair-weather processes, therefore deposited below fair weather wave base.
Proximal storm sands	7-15m	Up to dm scale, sand and silt layers with erosive base commonly paved with shell lags. Overlain by parallel lamination or HCS, and subsequently by wave-ripple lamination, with final typically unbioturbated mud drape layer.
Distal storm layers	15-40m	Laminated sands and silts of mm-scale, within thicker shelf mud deposits. Decrease in thickness and grain size away from coast.
Mud tempestites	40m+	Typically unbioturbated mud erosively cut through underlying muds.

It is evident, in comparison with the characteristics of the PFTs derived for Bulldog Shale material (table 4.2), that the general pattern of storm-generated sand facies, from shoreface storm layers to mud tempestites, is that represented in a PFT/G to B transition.

It is likely that the hummocky cross-stratified, planar laminated and cross laminated silts and sands of PFT/G represent shoreface storm layers. Furthermore, the silt and sand-dominated interbedded silt-rich and more clay-rich material of PFT/F probably represents proximal storm sands. Storm sands cannot be determined from PFT/E material owing to the intensity of bioturbation, though the complete reworking of these sediments by bioturbation indicates that storm derived deposition was not dominant. In turn, the 1-2mm thick, typically planar laminated silty horizons within thick clay-dominated sediments of PFT/D, and less commonly PFT/C, represent progressively deeper and more distal deposits of distal storm sands. Palaeoenvironmental fabric type B is marked by a general lack of discrete siltier storm-derived horizons, however occasional scour and cross-lamination within clay-dominated successions represents comparable material to the mud tempestite facies. Palaeoenvironmental fabric type A exhibits no discernible storm-influenced deposition.

Palaeobathymetric implications

The similarities in maximum water depths recorded for the Helgoland Bight and inferred for the Eromanga Basin from other sources, both less than 50m, and the similarities in the storm-derived deposits from both settings, enables application of water depths defined from the modern case for each of the storm-derived facies to those of the ancient example. Thus, approximate water depths can be assigned to Bulldog Shale PFTs.

Palaeoenvironmental fabric type A represents sediments deposited in the deepest basinal environment prevailing during deposition of the Bulldog Shale, probably between 40 and 50m water depth. The transition from PFT/A to E represents a shallowing, with sediments of PFT/E deposited within non-storm dominated conditions at or below 15m water depth. Palaeoenvironmental fabric type F represents sediments deposited in a narrow depth zone between approximately 10m and 15m water depth, while PFT/G represents sediments of amalgamated storm events deposited at water depths less than 10m deep, though deeper than the influence of fair-weather processes.

4.4.3 Discrepancies and variation in tiering profiles

Mutual cross-cutting relationships and sediment character

Trace fossil cross-cutting relationships in the Bulldog Shale are remarkably consistent, a result of the inexorable upward movement of the trace fossil tiers keeping pace with sediment aggradation. Discrepancies in this tidy situation do occur, where certain trace types have apparently mutually cross-cutting relationships, e.g. *Teichichnus* and *Ophiomorpha nodosa* in Finniss 2, 53.43-53.28m (Fig.4.19) (§4.3.5). In such cases the mutuality of the cross-cutting relationship is due to overlapping and partial sharing of the tier positions of the two trace types. Such shared tier regions are considered to be relatively narrow compared to the depth ranges occupied by the two ichnotaxa, for the majority of cross-cutting relationships concur with those observed elsewhere in situations where cross-cutting relationships are non-mutual.

Mutual cross-cutting relationships can also occur where more than one assemblage of trace fossils is represented in a composite ichnofabric, due to changing substrate consistency at a depositional hiatus (§4.1.1, 4.1.3). A fine example of such an occurrence is evident in the cored interval Finniss 2, 29.00 - 28.82m (§4.3.5) (Fig.4.24) and Finniss 2, 28.82 - 28.71m (§4.3.5) (Fig.4.25), in which up to three communities of trace makers existed. The key to such an occurrence is given by the existence of

Ophiomorpha nodosa and *Thalassinoides* in the same composite ichnofabric. As described in §4.1.3 Kern and Warme (1974) noted that *Ophiomorpha nodosa* and *Thalassinoides* are produced by the same trace maker, *Ophiomorpha nodosa* representing the response of the organism to unconsolidated sediments where a burrow wall is required to maintain an open burrow, and *Thalassinoides* representing the organism's response to more consolidated sediments in which burrow walls are not required to keep the burrow open. In the example under consideration, an initial trace fossil assemblage of which *Ophiomorpha nodosa* was an integral part, has been cross-cut by *Thalassinoides* burrows. A period of depositional hiatus is therefore inferred, in which the sediment compacted and became sufficiently consolidated to allow *Thalassinoides* type burrows to be used. Thus, the first trace fossil community comprises that in which *Ophiomorpha nodosa* was an integral part, the second community comprises that in which firmer sediment allowed *Thalassinoides* burrows to be produced, while the third comprises *Anconichnus* burrows which have reworked the structureless passive silty infill of the *Thalassinoides* burrows. It should be noted that, while the trace fossils changed from the first to the second community, the trace maker very probably did not.

In addition, it is evident that in diverse tiered trace fossil assemblages, particularly of PFT/E (§4.3.5; Fig.4.18), with increased sediment compaction and consolidation with depth, there is a progressive downward change from domichnial traces with thick walls (*Teichichnus*, *Ophiomorpha nodosa*) to domichnial traces with thinner walls (*Ophiomorpha irregulaire*), to non-maintained fodinichnial traces without walls (*Planolites*, *Anconichnus*). It is also evident from this generalised section that deeper tiers comprise smaller traces than shallower tiers, a response to the declining pore-water oxygen concentration with increased depth (Fig.4.18).

Sudden shifts in palaeoenvironmental fabric type

Gradual change is the normal situation in Bulldog Shale successions. This feature of palaeoenvironmental variation at the time of Bulldog Shale deposition provides for the delineation of several transitional palaeoenvironmental fabric types. Occasionally however, sudden shifts in PFT are evident, and are the result of erosion and subsequent deposition. Such features are most common where the erosional surface, produced during storm conditions, is overlain by PFT/G material, deposited as hydraulic energy levels declined as the storm waned. A fine example of such a transition is observed in Fig.4.37, where PFT/G erosively overlies PFT/F.

4.5 Internal independent tests

The palaeoenvironmental fabric type methodology provides an integrated framework for the analysis of sedimentary rocks, in which both physical and biogenic sedimentary structures are significant, though varying, components. Such an integrated study is safeguarded from error resulting from incorrect analysis of any particular factor, or through study of an unrepresentative sample, by the inclusion of several complementing and supporting factors that act as internal independent tests within the scheme.

Chapter 5

Palaeoenvironmental fabric types: application to logged sections and further analyses

5.1 Palaeoenvironmental fabric types in logged sections

With reference to the PFT scheme described and illustrated in Chapter 4 (Table 4.2), PFTs can be plotted as continuous records alongside each of the logged sections described in Chapter 2 (§2.1.1) (Figs.5.01; 5.02; 5.03; 5.04; 5.05). This is a major advantage of the PFT scheme over the ICD approach advocated by Taylor and Goldring (1993) (§4.1.4).

5.2 Further analysis of the palaeoenvironmental fabric types

To further investigate the nature of the individual palaeoenvironmental fabric types and the different palaeoenvironments represented by them, analyses of macropalaeontology, thin-sectioned material, clay mineral composition and organic carbon geochemistry have been conducted.

An appreciation of the macropalaeontology and its palaeoenvironmental implications forms an integral part of the PFT methodology (Fig.4.04; table 4.2). However, its usefulness is more evident in the field than in cored material. In core the laterally limited nature of the material provides only frequently incomplete material of unknown representability. Therefore, both field and core observations are included here.

Analyses of Bulldog Shale in thin section, and of its clay mineral suites and organic carbon geochemistry, are not included in PFT determination, since the scheme is intended to be a tool for rapid palaeoenvironmental analysis in the field or in the core library, and these further analyses are time consuming to conduct. However, accounts of these studies are included here in order to define further differences or similarities between individual PFTs.

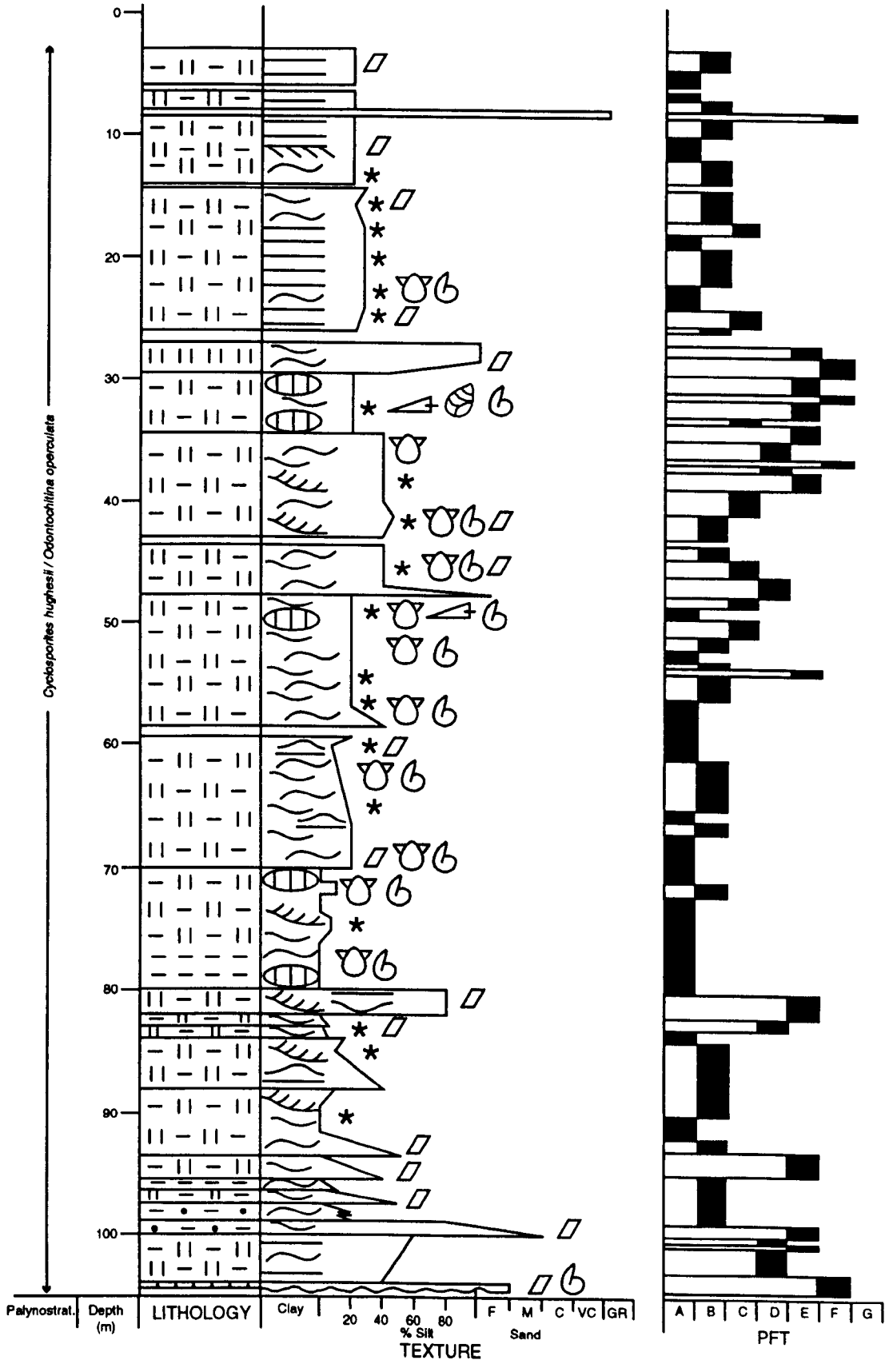

Fig.5.01 Finniss 2 Bulldog Shale log, with PFT plot. For key to symbols, see Fig.2.08.

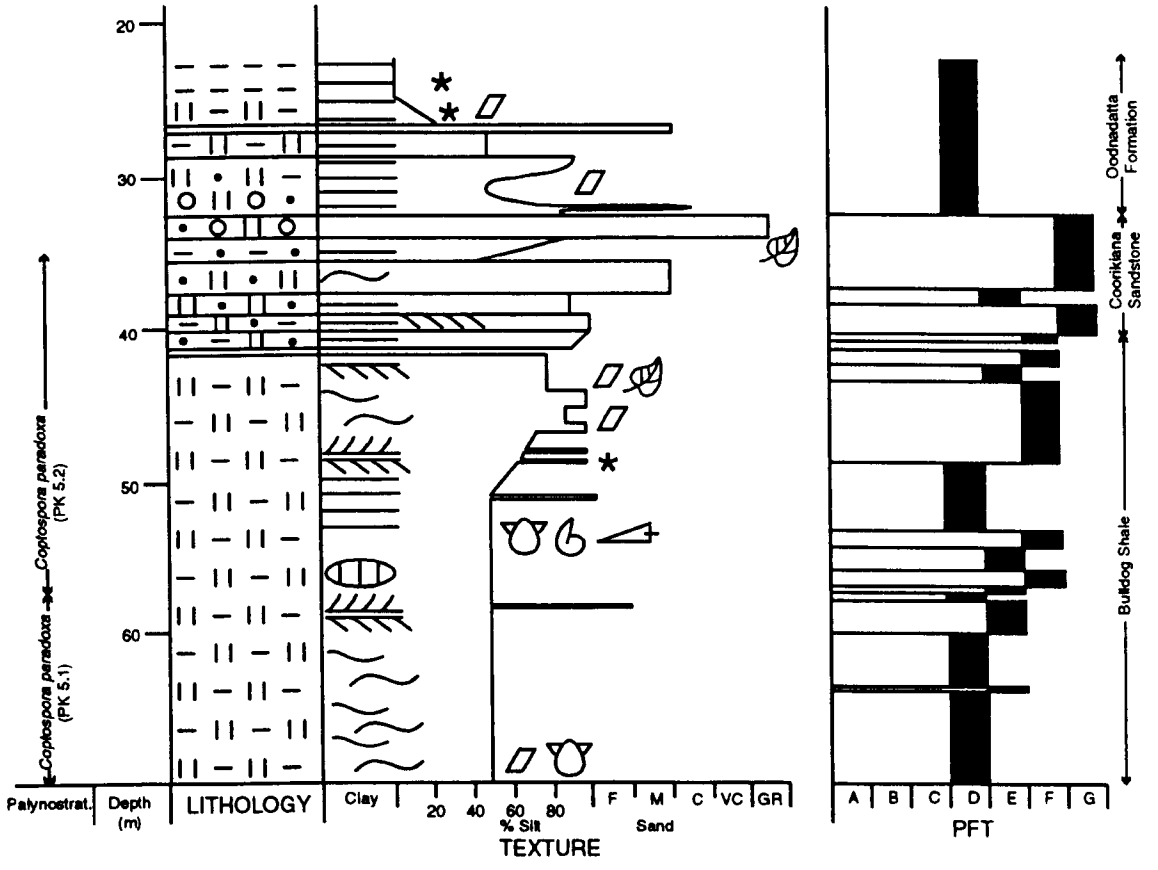

Fig.5.02 Alford 1 Bulldog Shale log, with PFT plot. For key to symbols, see Fig.2.08.

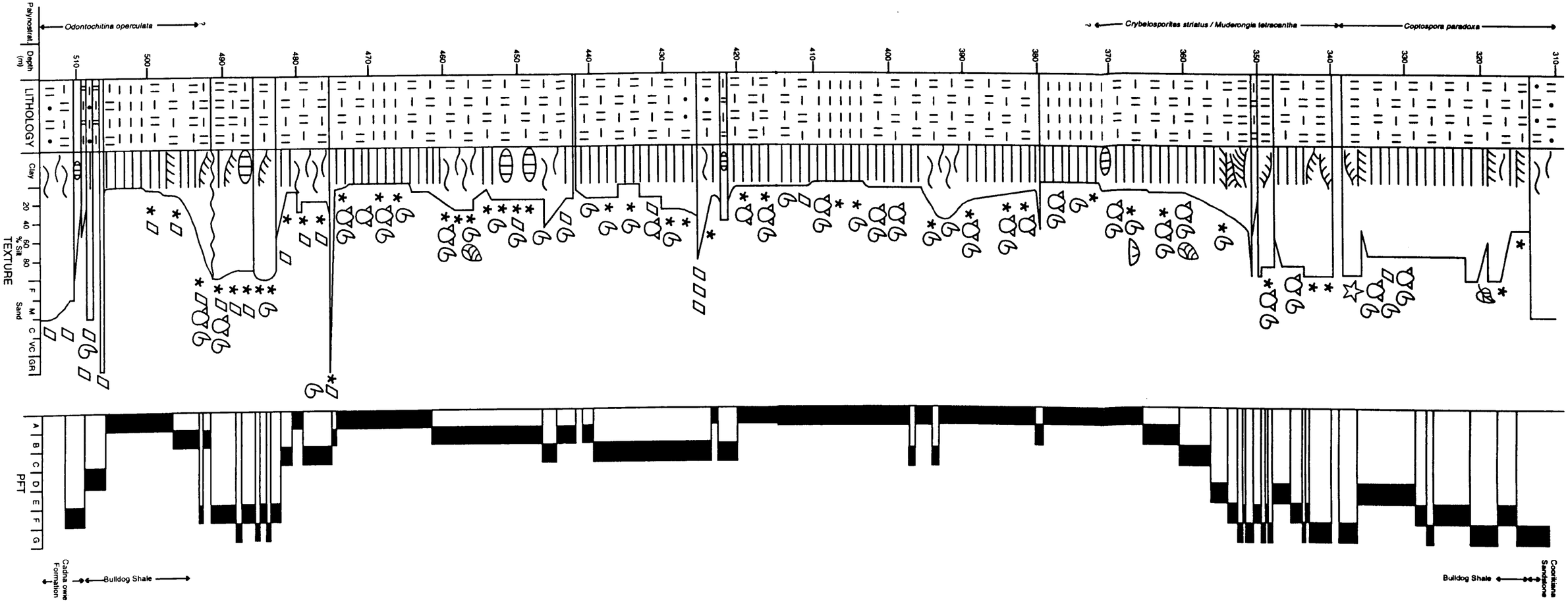

Fig.5.03 CBH 2 Bulldog Shale log, with PFT plot. For key to symbols, see Fig.2.08.

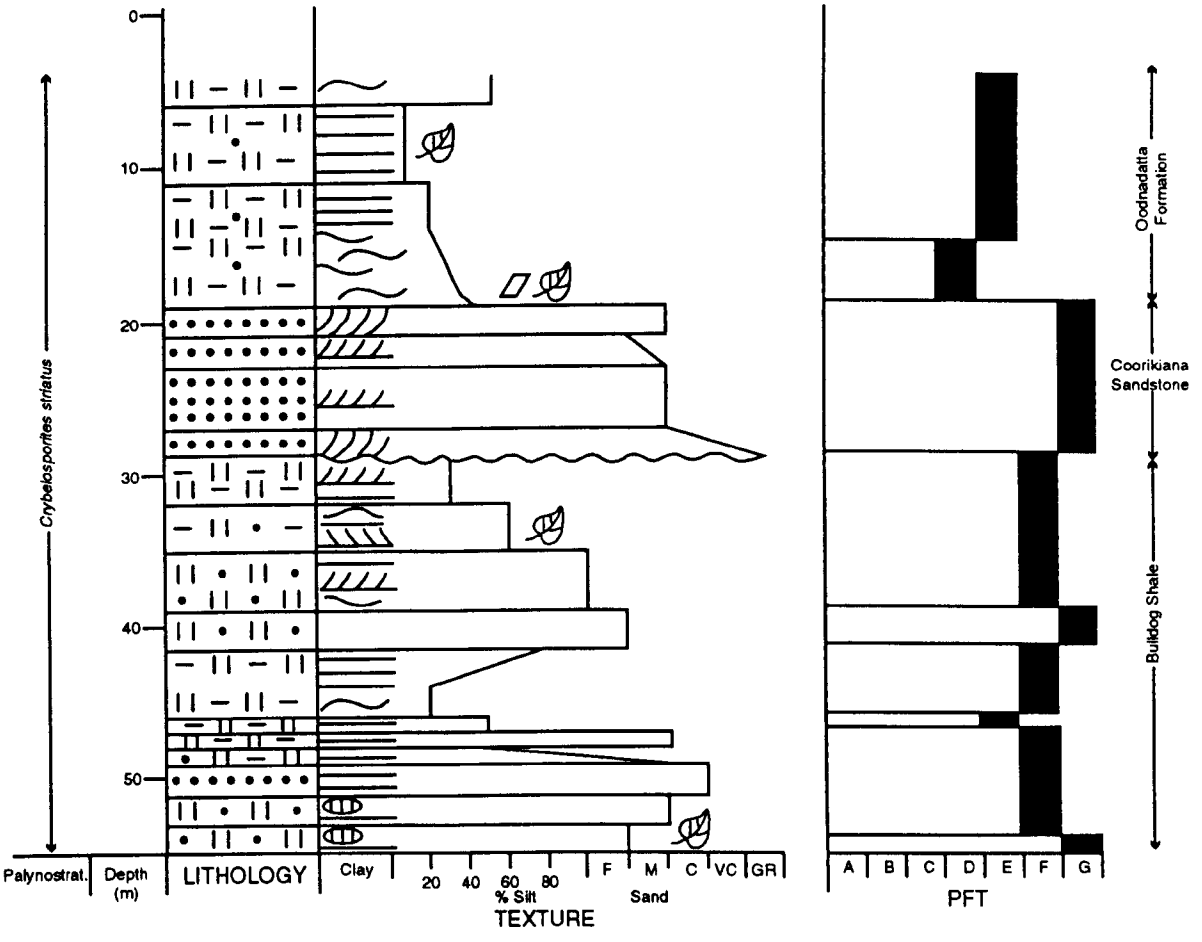

Fig.5.04 Mt. Yerila Bulldog Shale log, with PFT plot. For key to symbols, see Fig.2.08.

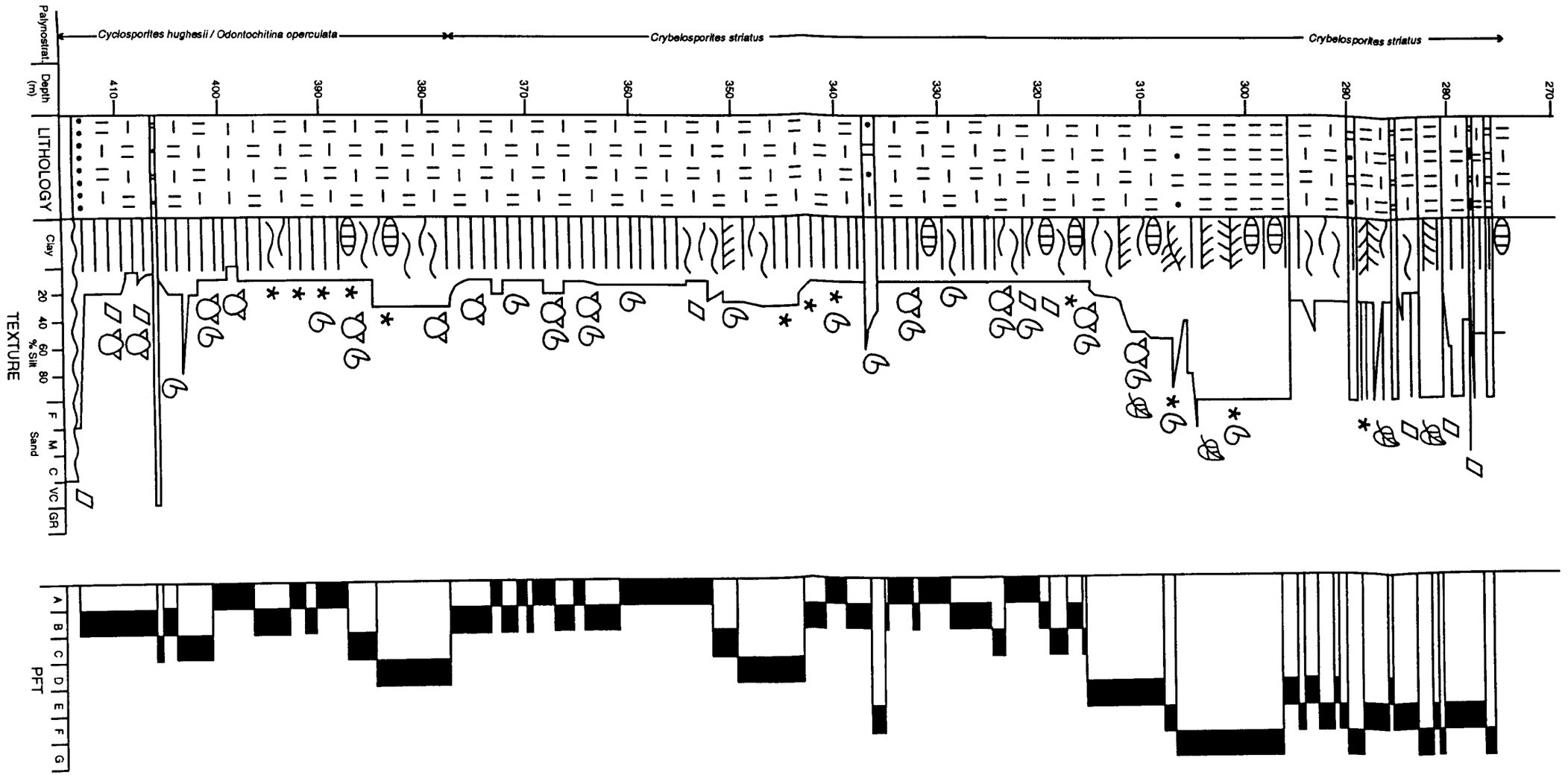

Fig.5.05 SPH 1 Bulldog Shale log, with PFT plot. For key to symbols, see Fig.2.08.

5.2.1 Macropalaeontology of the PFTs

Allochthonous material

Allochthonous fossil components of the Bulldog Shale include: pyritised wood from the basal Bulldog Shale at Petermorra Creek sites VII and VIII (Fig.2.05); structured plant material of PFT/F-G; generally fragmented and often abraded bivalve material and indeterminate shelly material from all PFTs; belemnite guards (e.g. from: upper Bulldog Shale at Mt. Yerila (Fig.2.06) (PFT/F-G); Finniss 2, 50.96m (PFT/C); Alford 1, 53.00m (PFT/D); CBH 2, 454.10m (PFT/B); SPH 1, 330.50m (PFT/A)); gastropod shells (e.g. from: CBH 2, 366.80m (PFT/A); CBH 2, 455.70m and 359.90m (PFT/B)); and scaphopod shells (e.g. from: basal Bulldog Shale at Petermorra Creek site VIII (Fig.2.05) (PFT/C); Finniss 2, 103.79m (PFT/C); CBH 2, 417.20 (PFT/A) and 367.60m (PFT/A)). Of much rarer occurrence is the single observation of an abraded echinoid test at CBH 2, 368.40m (PFT/A/B), and a well preserved starfish skeleton at CBH 2, 338.90 (Fig.4.36; 4.39) (PFT/G), transported and dumped by a high energy offshore waning storm current.

Of particular importance to palaeoenvironmental analysis, the presence of calcified wood and structured plant material may be used to imply periods of relative proximity to the palaeoshoreline. Thus, both the wood-rich basal regions of the Bulldog Shale, and those deposited in the relatively high energy conditions of PFT/F and G, i.e. the uppermost part of the Bulldog Shale and the overlying Coorikiana Sandstone, may be considered to have been deposited in close proximity to the palaeoshoreline.

Elsewhere, lags of lonestones have been utilised to infer periods of reworking. In addition, bivalve shell lags are evident in PFT/D cored material from Alford 1, depth intervals 68.05m, 66.10m and 64.70m, in which almost all the valves are convex upwards, and which indicate periods of winnowing and reworking.

Autochthonous material

Autochthonous material, principally bivalves in which both valves occur together, often still articulated, is recorded from PFT/A-E, though it is most common in PFT/A-C. In PFT/D-E allochthonous material is more common, and degradation of autochthonous material by bioturbation activity is more marked. Bivalves are generally thin shelled, though thick shelled forms (shell in excess of 1.0mm thick) become more common in PFT/D-E, both as autochthonous and allochthonous components. In field exposures, shelly fossils occur often as moulds, the carbonate material having dissolved away

(Fig.5.06A). Shelly material is commonly preserved however (Fig.2.30C) in carbonate concretions (Fig.2.27A) and in cores (Fig.5.06B).

A

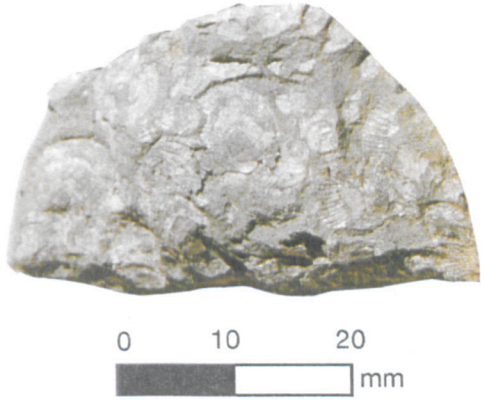

Fig.5.06 A: Moulds of articulated and open bivalves in PFT/C material from Petermorra Creek site VIII. B: *Pecten*-like small and thin-shelled bivalves covering a bedding plane in PFT/B material from SPH 1, 376.20m.

Autochthonous bivalve material occasionally occurs in laterally persistent beds colonised by large numbers of limited taxonomic diversity, and may represent colonisation of organisms during limited oxygenation events which punctuated dysoxic

conditions. Such a horizon is evident in the core SPH 1, at depth 376.20m, where one bedding plane is covered in small and thin shelled *Pecten*-like bivalves within PFT/B material (Fig.5.06B). Such horizons may represent either the "exaerobic biofacies" of Savrda and Bottjer (1987a), and taken to indicate the operation of organisms in low oxygen levels through specialised physiological adaptations, or simple opportunistic colonisation during brief periods of oxygenation, termed "episodically dysaerobic" by Wignall and Myers (1988) or "poikiloaerobic" by Oschmann (1991). The exact nature of what these terms relate to is currently the subject of debate, see recent discussions in Allison *et al.* (1995) and Bottjer *et al.* (1995). What is certain is that bedding planes of the Bulldog Shale covered in autochthonous bivalve material represent brief colonisation events in response to specific variations in bottom-water conditions; whether this involves only a brief rise in bottom-water oxygenation, or a more complex combination of increased oxygenation and physiological specialisation (probably some form of symbiosis with sulphur-reducing bacteria) is uncertain.

5.2.2 Thin section analyses of the Bulldog Shale

In thin section the main components of the Bulldog Shale are: clay minerals, quartz grains, glauconite grains, organic material and opaque minerals. Rarer, though still important, components include shelly fossil remains, micas and assorted lithic fragments.

The nature and relative proportions of each of these components varies between palaeoenvironmental fabric types, and also according to proximity to the basal part of the unit which tends to be more poorly sorted than the rest. However, certain generalisations can be made for each of these component parts of the Bulldog Shale, and variations are noted where they occur. Trace fossils are occasionally evident in thin sectioned material, and are described where appropriate.

Clay minerals

Clay minerals form much of the matrix throughout the Bulldog Shale. Individual crystals are characteristically lath-shaped, with high birefringence. Detailed clay mineralogy is not attempted here and is addressed in §5.2.3.

Quartz grains

Quartz grains from the Bulldog Shale (Fig.5.07, 5.08) are typically silt to fine sand grade (less than 250μm diameter), though exceptionally grains of medium sand grade

up to 375μm are present. Individual grains are generally angular to very angular, more occasionally with a subangular to subrounded component, also common are sharp triangular grains, which may be "glass shards" (Fig.5.07). Under cross polars almost all grains exhibit wavy extinction, and some show probable mechanical twinning, both features indicative of a volcanogenic origin, or derivation from locally outcropping metamorphic rocks. Both potential sources are probably implicated in the sourcing of these quartz grains, for various metasediments outcrop around the south-western Eromanga Basin margin, and "glass shards" are indicative of volcanogenic processes only and, as summarised in Veevers (1984), volcanogenic processes were operating to the east at the time of Bulldog Shale deposition. In addition, grains are occasionally polycrystalline; this and the angular nature of the majority of grains indicates low levels of transport prior to deposition. Sorting is variable.

Where the rock is non-bioturbated, and where high energy current/wave flow is not responsible for deposition (regions of PFT/A-E), the quartz grains are typically scattered and disseminated throughout the fine-grained matrix (Fig.5.07), a distribution for which dropping from melting ice-rafts may be invoked as the transport mechanism. Elsewhere, quartz grains are concentrated at the base of laminae and in silty trace fossil burrow fills, though in the same samples away from these regions of concentration, dissemination is the rule.

Much of the variation in Bulldog Shale lithology involves proportions of quartz grains and clay mineral-dominated matrix, a feature utilised in the palaeoenvironmental fabric type methodology as %silt content (§4.1).

The presence of occasional micas and lithic fragments confirms the generally immature nature of the Bulldog Shale as a whole, and provides further evidence in favour of low levels of transport for Bulldog Shale sediments.

Glauconite grains

Glauconite grains of the Bulldog Shale are well rounded and of coarse silt to medium sand grade (up to 375μm diameter) (Fig. 5.07, 5.08); they are scattered throughout the sediment, though in places they are concentrated within silty burrow fills, in silt-dominated interbeds and along lamination planes (Fig.5.08).

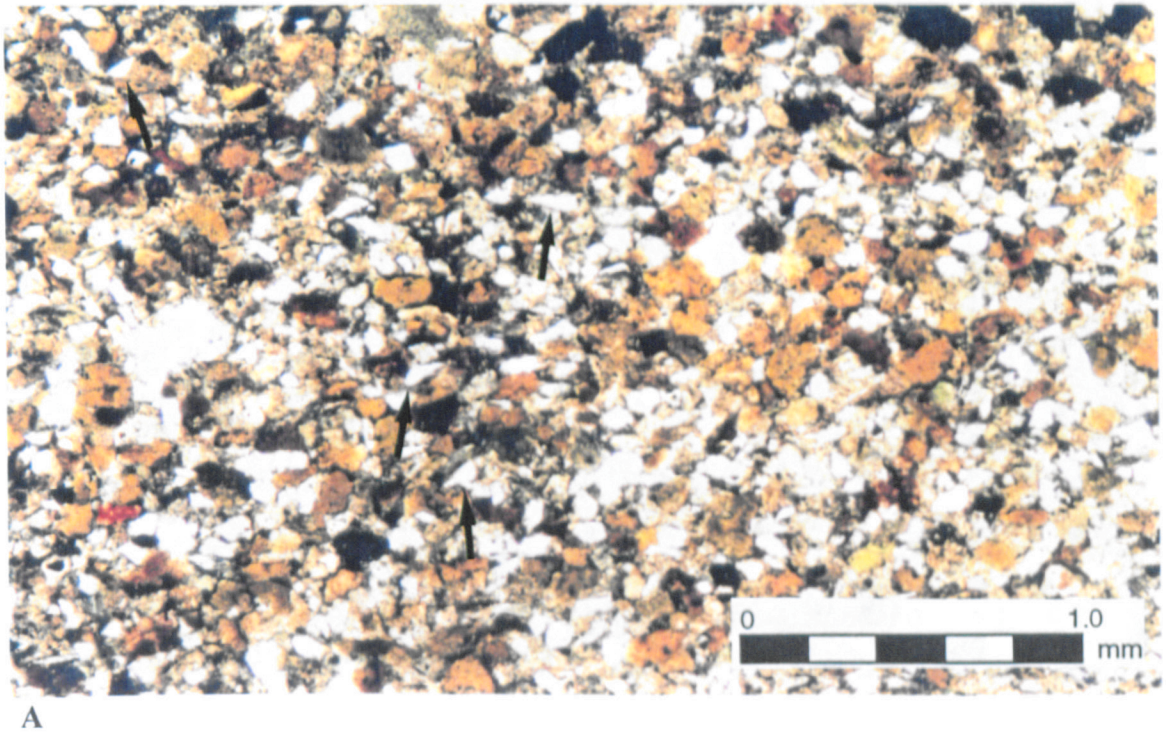

A

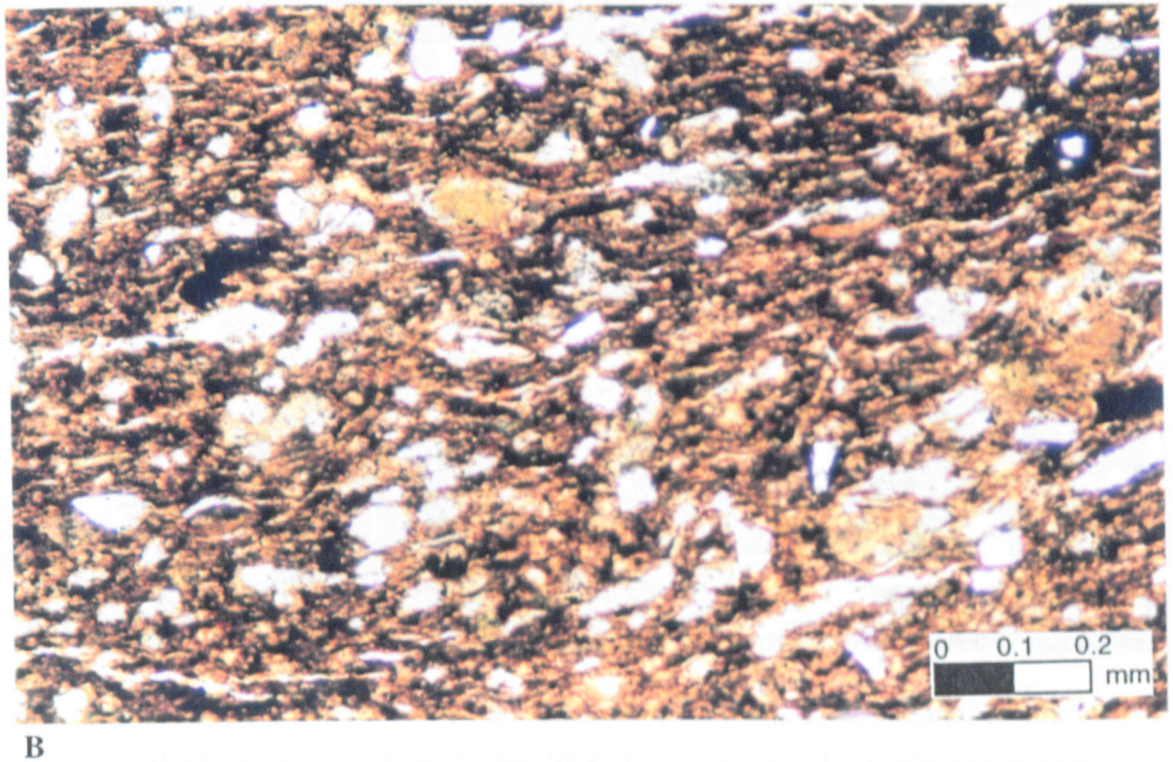

B

Fig.5.07 A: CBH 2, 350.70m, PFT/G. Quartz and glauconite grain dominated Bulldog Shale.. Arrows indicate potential glass shards. B: Finniss 2, 103.40m, PFT/B. Quartz and glauconite grains in a matrix rich in aligned organic matter.

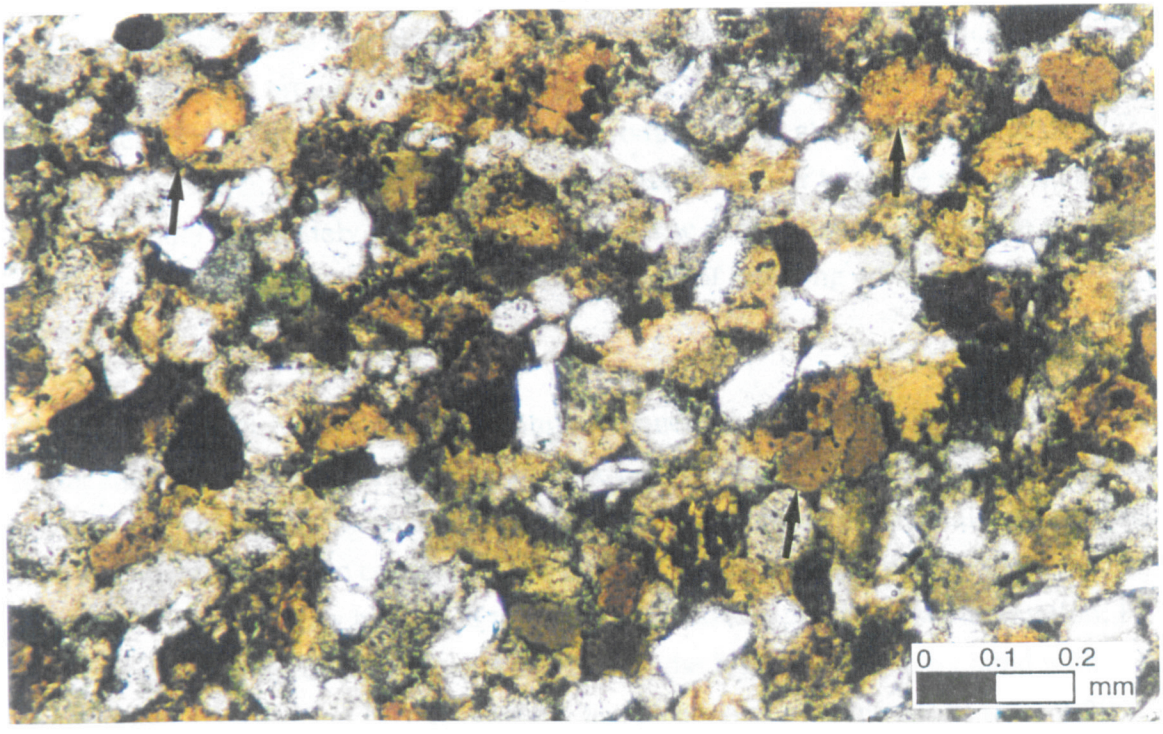

A

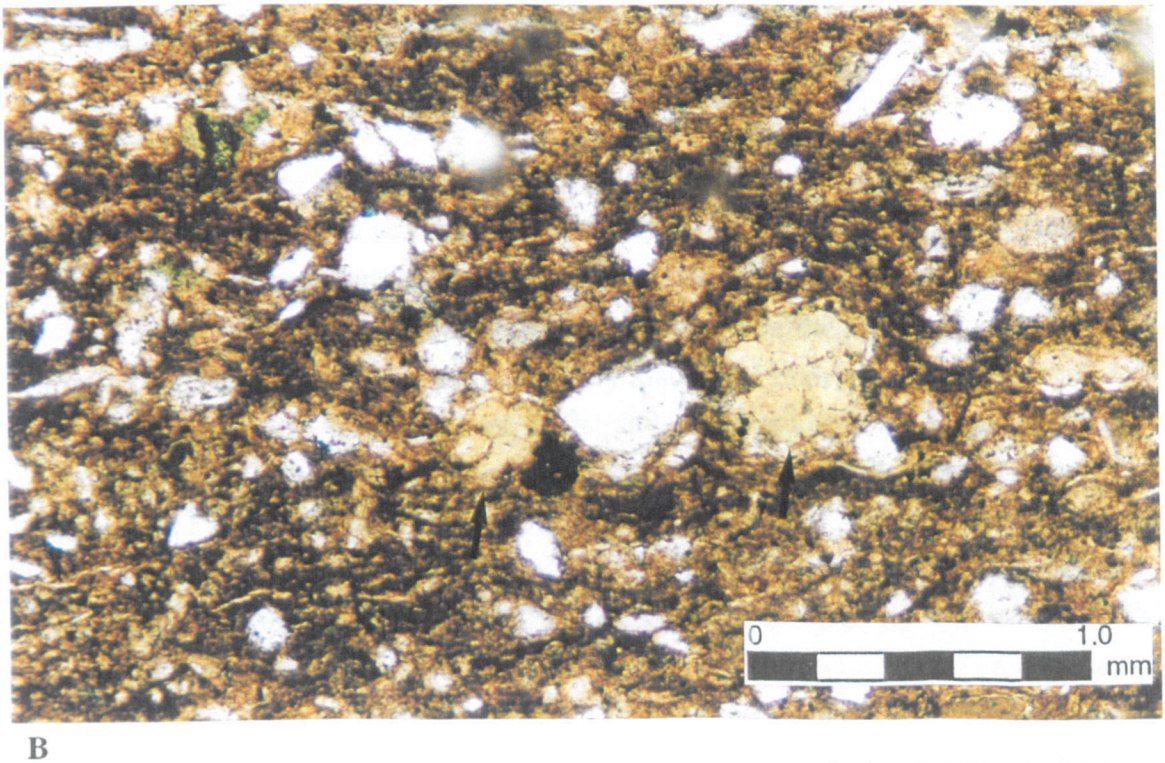

B

Fig.5.08 A: CBH 2, 350.70m, PFT/G. Glauconite and quartz dominated Bulldog Shale. B: Finniss 2, 103.40m, PFT/B. Quartz and glauconite grains in a matrix rich in aligned organic matter. In A and B arrows indicate examples of glauconite grains

Deer *et al.* (1966) noted that glauconite can be considered to be both a mica and a clay mineral of the illite group (§5.2.3), typically taking the form of rounded fine-grained aggregates of ill-formed platelets. These are produced through marine diagenesis of various materials in shallow waters during periods of slow or negative sedimentation, typically under moderately reducing conditions. The association of glauconite with pyrite, Deer *et al.* (1966) also reported as indicative of reducing conditions during deposition.

Clearly, the presence of glauconite throughout much of the Bulldog Shale has important implications for deposition rates, and also for oxygen levels within the sedimentary column. Concentrations of glauconite vary between palaeoenvironmental fabric types: PFT A-D have glauconite concentrations from 0-5%, exceptionally 10%, these relatively low levels may be related to slow, yet relatively continual sedimentation; PFT E-F have glauconite concentrations from 2-15%, the higher values associated with depositional hiatuses; and PFT G typically has glauconite concentrations from 2-20%, and exceptionally 30%, though these high concentrations are predominantly the effect of reworking and/or depositional hiatuses.

Organic material

Organic material from the Bulldog Shale typically comprises two distinct types: indeterminate organic material macerated to varying degrees (amorphous organic matter); and structured plant material. The former is very common throughout the Bulldog Shale and can make up a significant proportion of the matrix in all PFTs. Some variation is observed however, with the finely macerated matrix component particularly common towards the base of the unit and much rarer in the mid-Bulldog Shale clay-dominated units. Variation between cores is also noted, with organic components being much more common in both Finniss 2 (Fig.5.07B, 5.08B) and Alford 1 than in CBH 2 and SPH 1, and thus reflecting different material sources. Structured plant material is virtually absent in PFTs A-E, though it is relatively common in PFTs F and G, a feature reflecting closer proximity to the palaeoshoreline at the time these fabric types were emplaced. In PFT/F and G, macerated organic matter is also very common. For example Alford 1, 43.15m PFT/F reaches up to 30% organic material (Fig.5.09), while Alford 1, 33.15m PFT/F in the basal Oodnadatta Formation has organic matter contents of between 5 and 25% and a particular layer rich in well preserved spore cases (Fig.5.09). Throughout the Bulldog Shale, and particularly in PFT/F and G, lamination is picked out by variations in the organic content of the matrix: where organic matter levels are low and clay minerals make up most if not

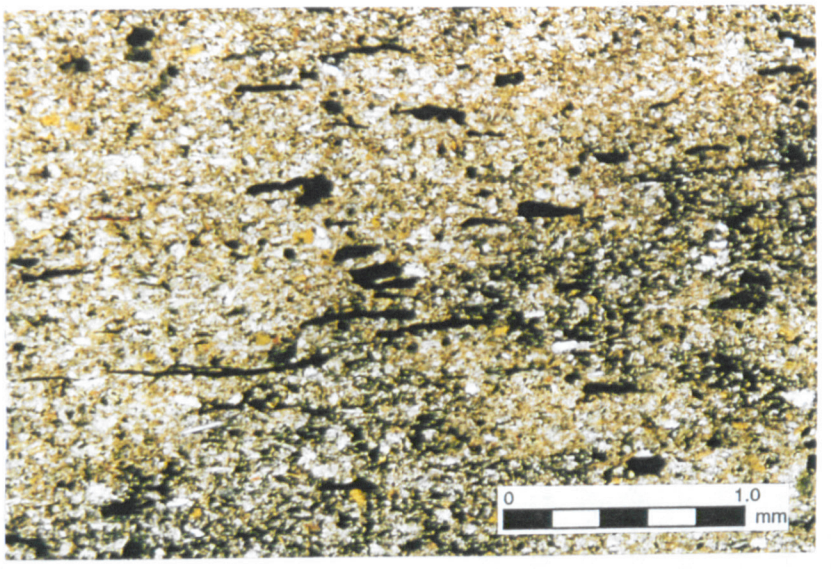

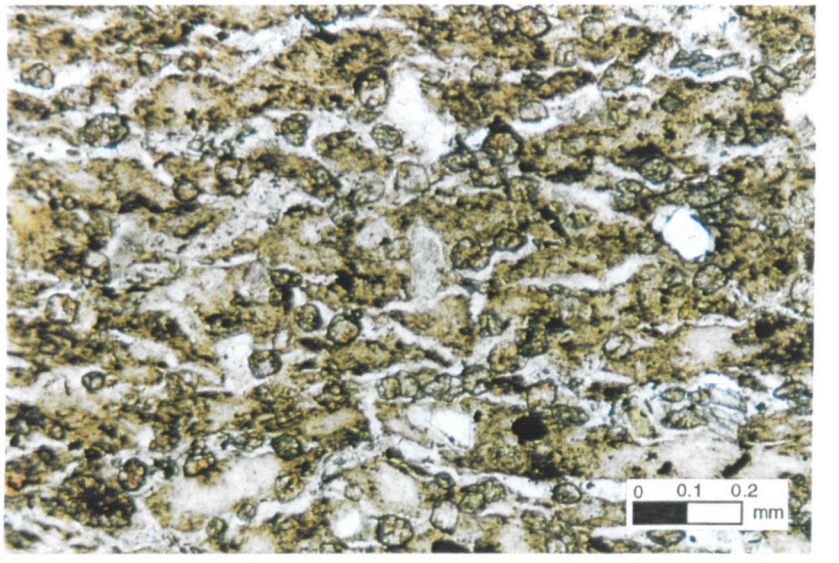

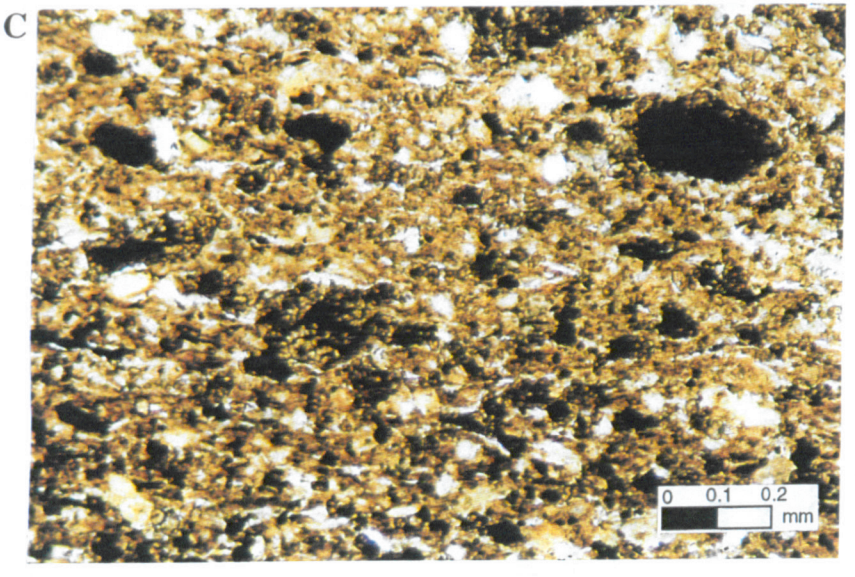

Fig.5.09 A: Alford 1, 43.15m, PFT/F. High levels of organic matter (Bulldog Shale). B: Alford 1, 33.15m, PFT/F. Well preserved spores in spore-rich layer (Oodnadatta Formation). C: Alford 1, 34.55m, PFT/G. Very high levels of organic matter (Coorikiana Sandstone). The Coorikiana Sandstone and Oodnadatta Formation overlie the Bulldog Shale, and were deposited in conditions only slightly different from it.

all of the matrix the material is grey in thin section; whereas where organic matter comprises a significant fraction of the clay mineral-dominated matrix the material is orange-brown in thin section (Fig.5.09). Indeed in Alford 1, 34.55m PFT/G Coorikiana Sandstone coarse silt to fine sand-rich material, organic matter makes up between 40 and 90% of the material in which laminations are picked out by macerated organic matter and aligned structured plant material (Fig.5.09).

Minerals opaque in cross section

For description of the macroscopic mineralogy of the Bulldog Shale see §2.7. Opaque minerals within the Bulldog Shale take either of two forms: cubic (pyrite) or granular. Variations between PFTs are minimal, though opaques are more common in PFT/E (0-10%) than in PFT/A-D (0-2%) or PFT/F-G (0-5%). Most opaque material is of coarse silt to fine sand grade, and is commonly scattered throughout the rock. However, concentrations of opaque minerals are often evident in silt-filled burrows, including *Planolites*, *Ophiomorpha nodosa*, *Thalassinoides* and *Skolithos* (Fig.5.10) in PFT/B-F.

In macroscopic observations (§2.7.1), pyrite is most common from the dark, well laminated and clay-dominated PFT/A-B, which represent deposition within the lower dysoxic realm. In addition, marcasite from Petermorra Creek site X (Fig.2.05) (§2.7.1), was also emplaced within PFT/B material. Pyrite is less common in more oxic PFT/C-E, where its presence is taken to infer growth below the redox discontinuity within the sediment, and is rare in the fully oxygenated higher energy PFT/F-G, where its occasional presence is most likely the result of reworked older material. Such macroscopic observations differ from those recorded from thin section analyses presented here, where opaque minerals, probably predominantly pyrite, attain apparently approximately equal concentrations in all PFTs, irrespective of palaeoenvironmental derivation, and are in some cases higher in the oxic PFT/E-G than in the more dysoxic PFT/A-D. This is probably the result of sampling effects, and the action of reworking and subsequent concentration within the silty and sandy shallow water sediments.

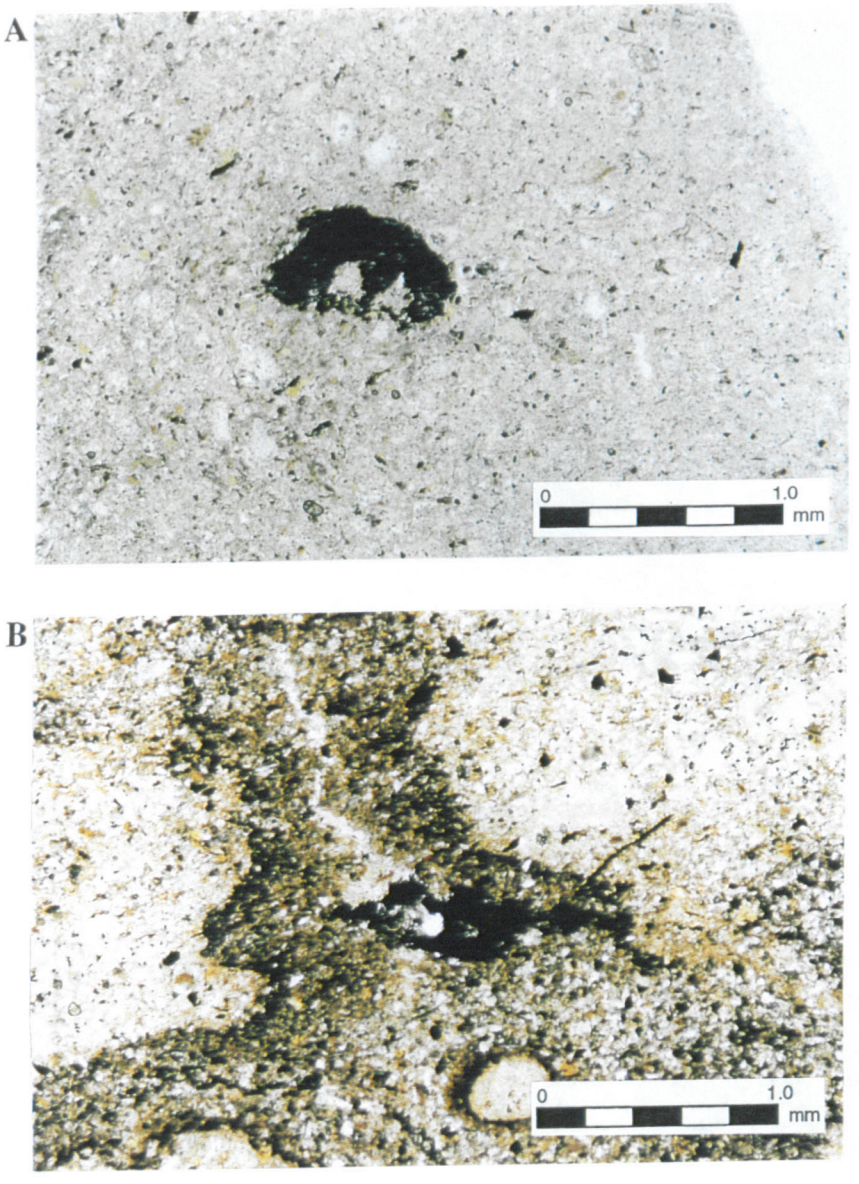

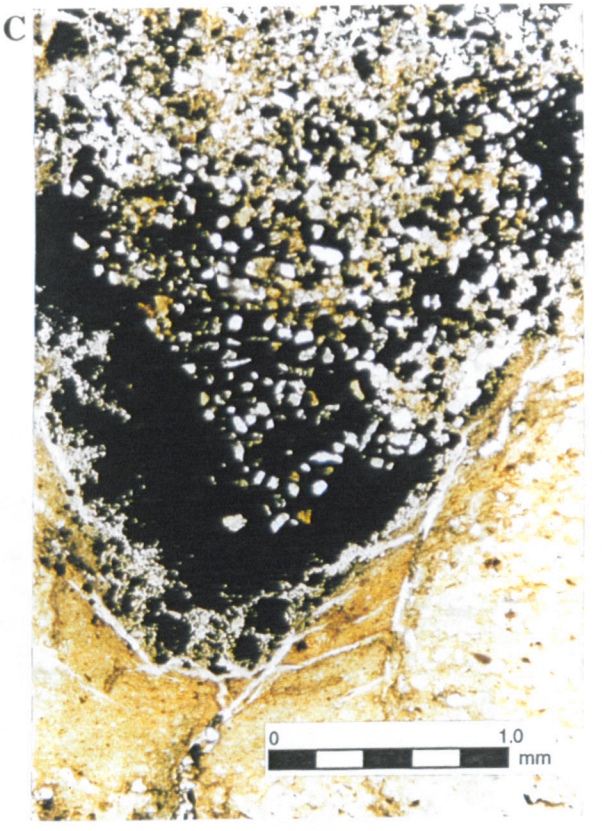

Fig.5.10 A: SPH 1, 328.60m, PFT/B. Opaque minerals within *Planolites* burrow fills. B: SPH 1, 309.70m, PFT/E. Opaque minerals within *Planolites* and *Thalassinoides* burrow fills. C: SPH 1, 385.60m, PFT/C. Pyrite growth around *Skolithos*.

Shelly fossil fragments

In thin section, shelly fossil material is rare and usually constitutes only indeterminate (possibly bivalve) allochthonous fragments. Occasional more complete allochthonous material is preserved however and constitutes scaphopod fragments (Fig.5.11A) and foraminiferal tests (Fig.5.11B).

A

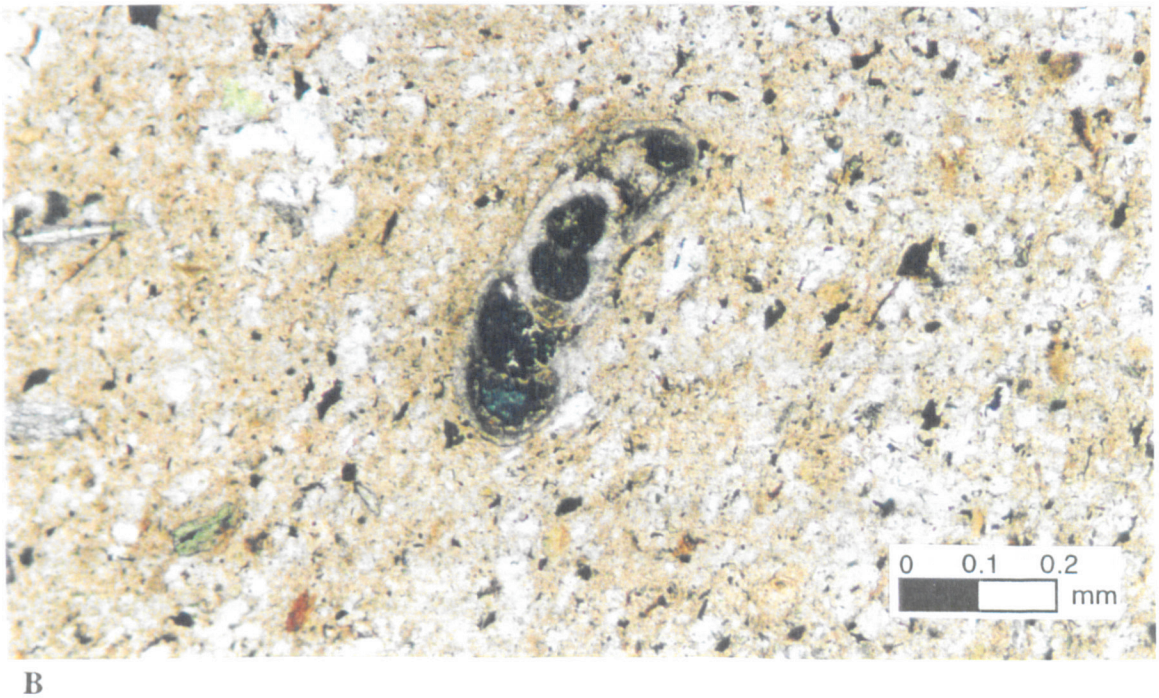

B

Fig.5.11 A: CBH 2, 366.80m, PFT/B. Scaphopod cross-section. B: SPH 1, 404.10m, PFT/C. Section through a foraminiferal test.

5.2.3 Clay mineralogy

X-ray diffraction has been used in order to qualitatively identify the clay minerals present within the Bulldog Shale, though no effort has been made at quantitative measurements of these minerals.

Methodology

Detailed accounts are given of the various methods of sample preparation for X-ray diffraction in Moore and Reynolds (1989), elements of which are combined for the standardised methodology used in the current study. The sample preparation methodology is summarised in Appendix 3.

Sample analysis

Each sample was run on a Philips Products PW 1840 X-ray diffractometer, utilising Philips Products ABD software. Initial mineral identification was made using Philips Products PCI Identify software.

Initial identification indicated the presence of the clay minerals smectite (montmorillonite), illite and kaolinite, with clay-grade quartz. To confirm these analyses representative samples of each palaeoenvironmental fabric type, including samples from all the cores, were given various treatments, and the resultant trace peaks were compared to those peaks obtained for standards of montmorillonite, illite, kaolinite and quartz. Three treatments were used:

1) Samples solvated in ethylene glycol vapour for one hour at approximately 60°C. This treatment has no effect on either kaolinite or illite, but the 001 reflection of montmorillonite shifts from about 6°2q (air-dried) to about 5.2°2q (glycolated). In addition, there is the appearance of a new peak at about 17°2q which confirms the presence of illite and smectite (Moore and Reynolds, 1989).

2) Samples heated at 300°C for 1 hour. This treatment has no effect on kaolinite, illite peaks become more intense, while the 001 peak of montmorillonite becomes about 9°2q.

3) Samples heated at 550°C for 1 hour. This treatment causes kaolinite to become amorphous and its peak collapses, illite peaks become more intense, while the 001 peak of montmorillonite remains at about 9°2q.

Results and analysis

The analysis of the effects of these treatments (Fig.5.12A), and the comparison of Bulldog Shale sample peaks with the peaks for standard material (Fig.5.12A) confirm the initial diagnosis. In all samples, from cores widely spaced around the Eromanga Basin margin (Fig.2.01) (Fig.5.12B), from throughout the Bulldog Shale, and from all its non-carbonate lithologies and palaeoenvironmental fabric types (Fig.5.12C), the clay mineral composition is unvarying, and comprises montmorillonite (smectite), kaolinite, and illite, with associated clay-grade quartz.

Fig.5.12 (page 203) A: X-ray diffraction lines for PFT/A sample SPH 1, 360.30m. Red line = air-dried sample, green line = glycolated sample, blue line = sample heated at 300°C, purple line = sample heated at 550°C. The individual lines are offset for clarity. Vertical lines represent peak positions of the standards: red = kaolinite; green = montmorillonite (solid = air-dried, dashed = glycolated, dotted = heated to 300°C/550°C); blue = illite; black = quartz.

B: X-ray diffraction lines for PFT/E from all four cores. Red line = Finniss 2, 29.20m, green line = Alford 1, 47.30m, blue line = CBH 2, 347.70m, purple line = SPH 1, 308.75m. Compare peak positions with standard lines given in A. Diffraction lines are vertically offset for clarity.

C: X-ray diffraction lines for PFT/A, E and G from the CBH 2 core. Red line = PFT/A 419.50m, green line = PFT/E 347.70m, blue line = PFT/G 339.10m. Compare peak positions with standard lines given in A. Diffraction lines have been offset for clarity. Changes in peak intensity should not necessarily be considered to represent variations in component abundance.

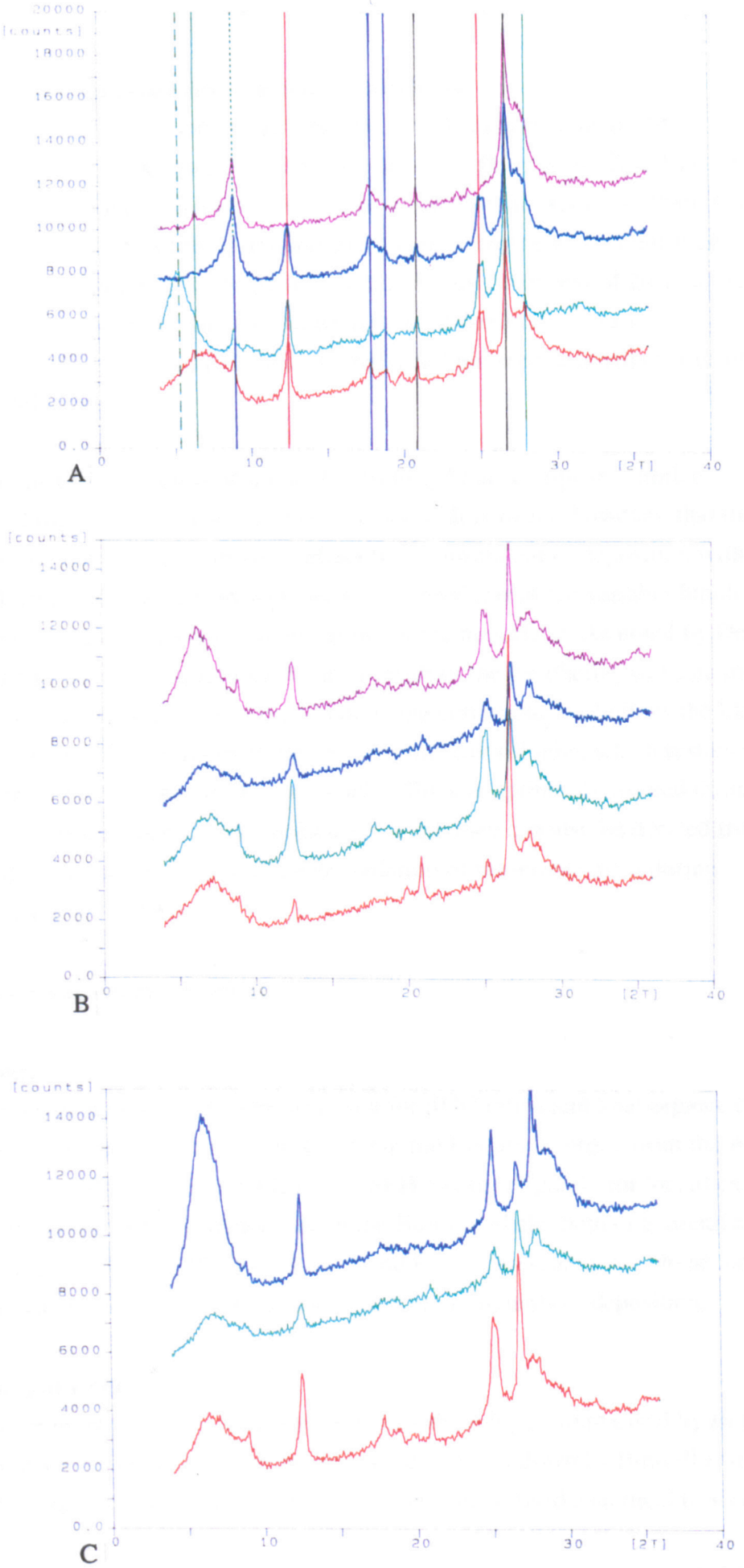

Fig.5.12 See page 202 for figure caption.

Other studies and palaeoenvironmental implications

The Skeleton 2 well completion report (Figs.2.01, 2.04 for core hole locality) (Callen *et al.*, 1990) contains eight X-ray diffraction analyses of Bulldog Shale 2μm fraction samples, covering an incomplete Bulldog Shale succession in excess of 300m. Each of the eight samples consists of the dominant component smectite with minor inter-stratification with illite; with kaolinite from subdominant (in excess of 20%) to trace (less than 5%) and rarely absent; clay-grade quartz subdominant to trace; montmorillonite from accessory (5-20%) to trace; and more occasionally traces of chlorite and feldspar.

It is apparent that the clay mineralogy of the Bulldog Shale comprises similar components throughout its vertical and lateral extent. It is likely, however, that these clay minerals do not, for the most part, reflect the environment of deposition within the Eromanga Basin, but instead represent weathering products of the variable lithologies and drainage conditions exposed and prevailing in the hinterland. As noted by Deer *et al.* (1966) the presence of smectites is a direct result of the weathering of basic rocks in conditions of poor drainage, while in good drainage conditions kaolinite is the likely weathering product. The smectite group includes montmorillonite, which results from the alteration of eruptive igneous rocks. Finally, illites are primarily formed through the weathering of silicates, particularly feldspars, though they can also be derived from the alteration of other clay minerals and the degradation of muscovite mica during diagenesis (Deer *et al.*, 1966).

5.2.4 Organic carbon geochemistry

Methodology

Thirty four whole rock samples were analysed for $\partial^{13}C$ ratios and total organic carbon (TOC) content. These samples included 19 from the Finniss 2 core, 2 from the Alford 1 core, 9 from the CBH 2 core, and 4 from the SPH 1 core, (Fig.2.01 for localities), and thus encompasses possible variation within the Bulldog Shale, both of a lateral and vertical nature. In addition, PFTs A, B, D, E and F are represented so as to account for variation in values with different lithologies and environments of deposition.

Sample preparation

Samples were prepared partly according to the methodology summarised by Boutton (1991a), and according to the experimental procedure laid down by Bottrell *et al.* (1991). However, idiosyncrasies occur within any standardised analytical procedure as

a result of specific tailoring of that procedure to the material undergoing analysis. Therefore, a brief methodology of sample preparation is given in Appendix 4.

Results

Figures 5.13 and 5.14 illustrate variation in TOC and $\partial^{13}C$ for Bulldog Shale material between palaeoenvironmental fabric types and between individual cores, respectively. It is evident from mean values and their error bars that significant variation in TOC or $\partial^{13}C$ does not occur between PFTs (Fig.5.13) or cores (Fig.5.14). Rather TOC and $\partial^{13}C$ vary about the mean in both cases. Mean TOC content for the Bulldog Shale = 1.52% (S.D.=0.957), varying from 0.34% to 4.64%; mean $\partial^{13}C$ values for the Bulldog Shale = -24.086‰ (S.D.0.958), varying from -26.21‰ to -22.23‰.

Palaeoenvironmental implications and previous work

Values of $\partial^{13}C$ from Bulldog Shale material (mean = -24.086‰) are those expected from a shallow marine environment with components of terrestrial plant material (the most common group of which has a $\partial^{13}C$ of -27‰) and marine organic material (most commonly phytoplankton, average $\partial^{13}C$ = -22‰), with possible accessory amounts of zooplankton (average $\partial^{13}C$ = -20‰) (Boutton, 1991b). Variation in $\partial^{13}C$ values from Bulldog Shale material reflects differing proportions of the individual organic components, though variation in sedimentation rate, microbial and bioturbation effects under varying oxygen levels, and diagenetic effects probably also play a part.

Previous work by McKirdy et al. (1986) confirms the diagnosis of TOC dominated by land plant material. McKirdy et al. (1986) studied TOC from the Bulldog Shale in the Toodla 1 core (Fig.2.01, 2.02), and concluded that significant stratigraphic variation in the composition of the organic matter was superimposed on a down-hole trend of increasing TOC, as a result of changes in sedimentation rate, *in situ* microbial activity, and the balance of the marine and terrestrial components. This organic matter, along with that of the underlying marine top of the Cadna-owie Formation and the lateral Bulldog Shale equivalent Wallumbilla Formation, McKirdy *et al.* (1986), noted as being largely of land plant origin, with a significant algal/bacterial component, as expected from shallow water mudrocks deposited in relative proximity to the basin margin.

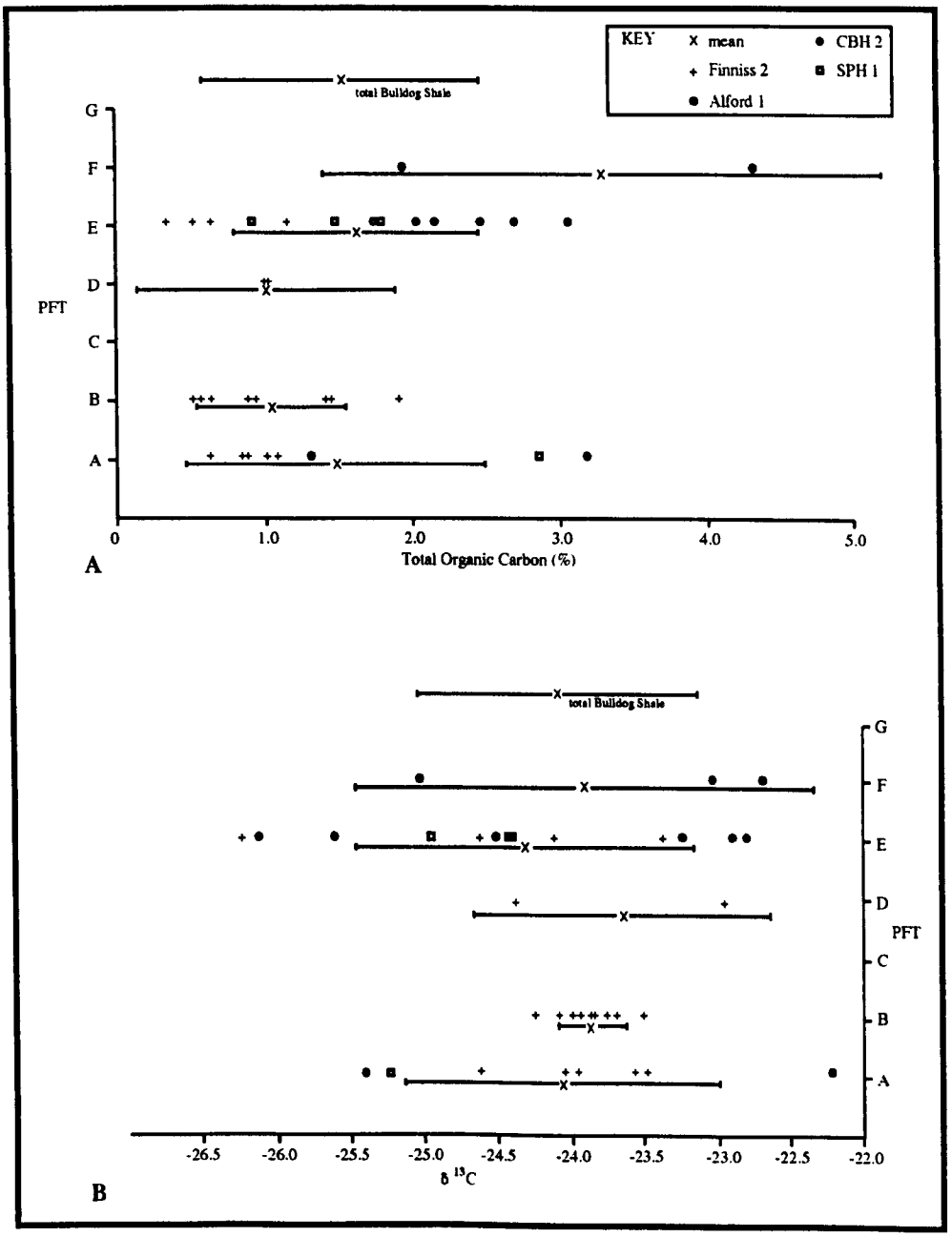

Fig.5.13 A: Graph of TOC for palaeoenvironmental fabric types A, B, D, E and F for all cores. Mean values and error bars also indicated; error bars = ± one standard deviation (S.D.). B: Graph of $\partial^{13}C$ for palaeoenvironmental fabric types A, B, D, E and F for all cores. Mean values and error bars also indicated; error bars = ± one S.D.

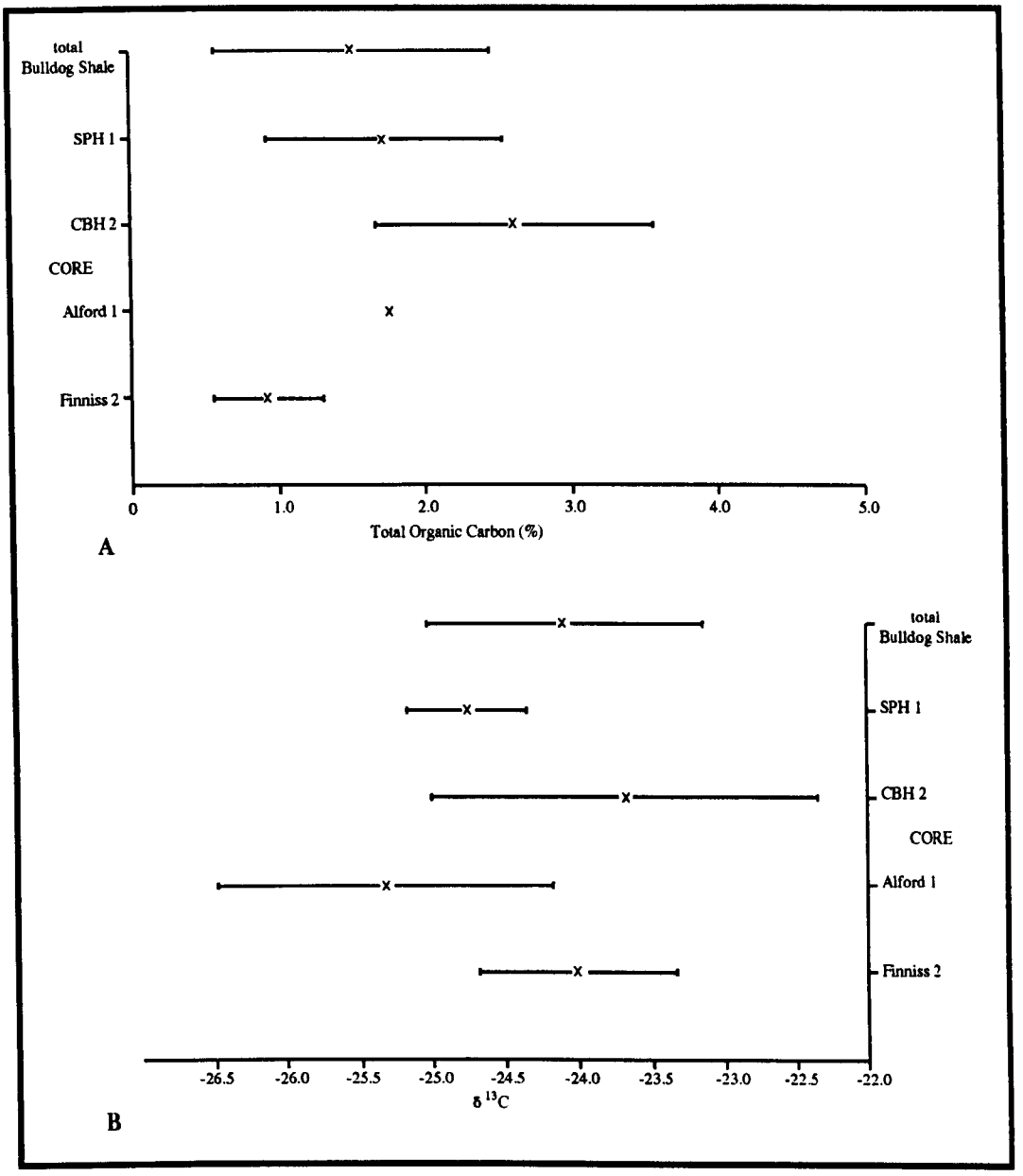

Fig.5.14 A: Graph of mean TOC values for all PFTs sampled in cores Finniss 2, Alford 1, CBH 2 and SPH 1. Mean for all Bulldog Shale samples also indicated; error bars = ± one S.D. B: Graph of mean $\partial^{13}C$ for all PFTs sampled in cores, as above. Mean for all Bulldog Shale samples also indicated; error bars as above.

Chapter 6

Correlation across the Eromanga Basin using the PFT scheme: a new approach

6.1 Sub-units of the Bulldog Shale

On the basis of the PFT log plots presented in Chapter 5 (§5.1), each Bulldog Shale section can be divided into a series of sub-units based on variation in dominant PFTs. In comparison between the five Bulldog Shale sections analysed herein (§2.2; 5.1), the same vertical sequence of sub-units is identified from each section. Therefore, these sub-units are laterally persistent entities of the Bulldog Shale, at least around the margin of the Eromanga Basin in South Australia, and thus they can be used as a correlative tool. Palynostratigraphic analyses indicate that corresponding sub-units in different sections are approximately coeval. Therefore, palynostratigraphy is included in sub-unit definition. Indeed, in cases where only part of the Bulldog Shale succession is present, palynostratigraphy proves extremely useful for it provides an independent means of identifying between different sub-units from high and low in the unit which bear similar PFT associations.

Variation does occur between sections in terms of sub-unit thickness. In addition, it should be noted that where a section incorporates only part of the Bulldog Shale succession, only the corresponding part of the sub-unit sequence is represented.

Ten sub-units are identified, denoted α through to κ, the characteristics of which, collated from all five sections, are summarised in Table 6.1. The information presented in this table is the tool for sub-unit identification and correlation.

Table 6.1 Summary table of the Bulldog Shale sub-units and their characteristics.

Sub-unit	Thickness variation	PFT (Bracketed types are rare)	Lithology	Palynostratigraphy
α	2.60m (CBH 2)-24.00m (Finniss 2)	(A-)B-D(-F)	Basal Bulldog Shale. Cm-m scale fining, and more rarely, coarsening upwards layers.	*Cyclosporites hughesii* *Odontochitina operculata*
β	13.00m (SPH 1)-41.00m (Finniss 2)	A-B(-C)	Clay-dominant, often near pure clay horizons; typically less than 20% silt.	*C. hughesii* *O. operculata*
γ	9.00m (CBH 2)-12.00m (Finniss 2)	(C-)E-G	More than 20% silt, often 90-100% silt, with occasional fine sand component.	*C. hughesii* *O. operculata*
δ	24.00m (Finniss 2) - 36.00m (CBH 2)	A-B(-C)	Clay-dominant, near pure clay horizons common; typically less than 30% silt.	*C. hughesii* *O. operculata*
ε	16.00m (SPH 1)-25.00m (CBH 2)	(A-)B-D(-F)	20-50% silt, occasional sandy component.	*Crybelosporites striatus*
ζ	21.00m (SPH 1)-55.50m (CBH 2)	A-B(-C)	Near pure clay-grade material; typically less than 10% silt; occasional thin siltier horizons.	*C. striatus*
η	8.00m (SPH 1)-20.00m+ (Alford 1)	(B-)D-E(-F) (upward transition)	Coarsening-upwards layer from 10-60% silt.	*C. striatus* / *C. paradoxa*
θ	11.00m (SPH 1)-17.50m (CBH 2)	(E-)F-G	Predominantly silty and sandy (up to coarse sand-grade); 100% silt and sand common; clay occasionally comprises up to 40% of sediment.	*C. striatus* *Muderongia tetracanthal* *Coptospora paradoxa*
ι	6.00m (SPH 1)-15.50m (CBH 2)	E-F(-G)	Interbedded cm-dm scale clay and silt-dominated horizons.	*C. striatus* / *C. paradoxa*
κ	6.00m (CBH 2)-14.00m+ (SPH 1)	(E-)F-G	Uppermost Bulldog Shale sub-unit. Interbedded cm-dm scale silt/sand and clay dominated horizons.	*C. striatus* / *C. paradoxa*

6.1.1 Sub-units of the Bulldog Shale in individual sections

CBH 2

CBH 2 represents a complete section through the Bulldog Shale succession, its base and its top (§2.2.3), and comprises all ten sub-units (Fig.6.01). As CBH 2 is the most complete and the thickest Bulldog Shale succession presented here, it can be regarded as the standard against which the other sections are compared. The characteristics of the sub-units from the CBH 2 section are summarised in Table 6.2.

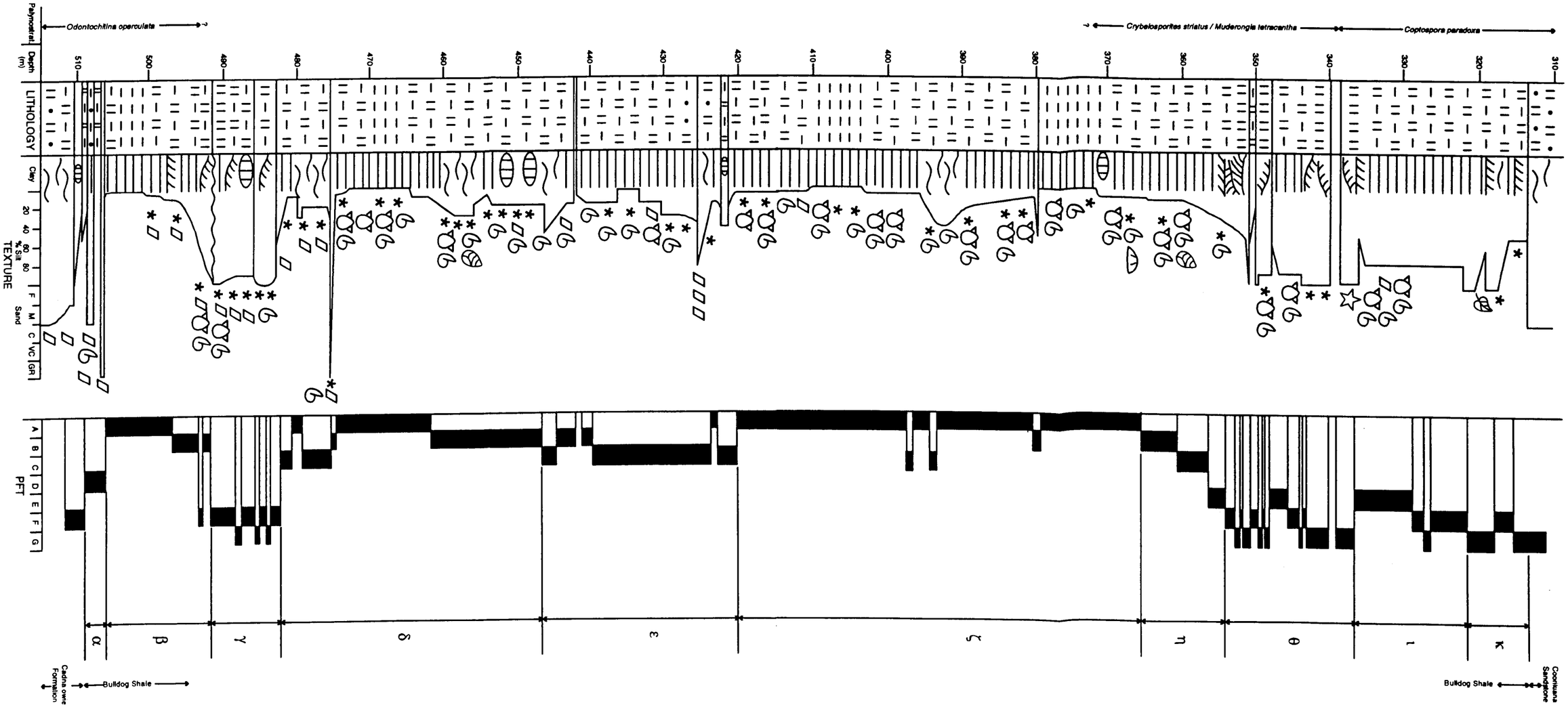

Fig.6.01 Summary log of the CBH 2 Bulldog Shale succession, with the sub-units delineated. For key to symbols see Fig.2.08.

Table 6.2 Characteristics of the sub-units from the CBH 2 Bulldog Shale succession.

Sub-unit	Depth interval	Thickness	Composition	Palynostratigraphy.
α	509.60-507.00m	2.60m	PFT variable, most commonly D. Basal sub-unit, overlying Cadna-owie Formation. Centimetre to dm scale fining-upwards layers and more occasional coarsening-upwards layers. Clay dominant, silt content highly variable.	*Odontochitina operculata* dinoflagellate zone (Harris, 1982).
β	507.00-492.00m	15.00m	PFT/A-B. Clay dominated. Horizons of near pure claystone are very common.	*O. operculata* dinoflagellate zone (Harris, 1982).
γ	492.00-483.00m	9.00m	PFT/F-G. Silt-dominant (90-100% silt).	*O. operculata* dinoflagellate zone (Harris, 1982).
δ	483.00-447.00m	36.00m	PFT/A-B. Clay-grade material dominant (silt typically less than 30%). Some horizons of near-pure claystone.	*O. operculata* dinoflagellate zone (Harris, 1982).
ε	447.00-420.50m	26.50m	PFT/C (occasionally B). Moderately silty (20-50% silt, exceptionally down to 10% and up to 80%), clay-dominated material. Distinct sand component evident in some horizons.	Palynostratigraphic data not available.
ζ	420.50-365.00m	55.50m	PFT/A. Near-pure claystone of less than 10% silt. Very occasional thin siltier horizons of PFT/B-C.	Palynostratigraphic data not available.
η	365.00-353.50m	11.50m	Up-section transition from PFT/B to E. Associated coarsening-upward trend from 10 to 50% silt in clay-dominated material.	Palynostratigraphic data not available.
θ	353.50-336.00m	17.50m	PFT/F-G (occasionally E). 90-100%sit. Lowermost of the upper Bulldog Shale silt and sand dominated horizons.	Sample depth 347.70m: *Crybelosporites striatus* spore-pollen zone; *Muderongia tetracantha* dinoflagellate zone. Sample depth 337.70m: *Coptospora paradoxa* spore-pollen zone, (Alley pers. comm. 1995).
ι	336.00-320.50m	15.50m	PFT/E-F (exceptionally G). Slightly finer than underlying and overlying sub-units. Silt-grade material dominates, typically 80% silt. Occasional clay-dominated interbeds.	*Coptospora paradoxa* spore-pollen zone, (Alley pers. comm. 1995).

Table 6.2 (continued).

Sub-unit	Depth interval	Thickness	Composition	Palynostratigraphy.
κ	320.50-314.50m	6.00m	PFT/F-G (occasionally E). Silt and sand dominated horizons, interbedded with occasional clay-rich horizons of only 20-30% silt. Overlain by Coorikiana Sandstone.	*Coptospora paradoxa* spore-pollen zone, (Alley pers. comm. 1995).

SPH 1

SPH 1 represents a near complete section through the Bulldog Shale succession, though the upper contact with the Coorikiana Sandstone has not been recovered (§2.2.5). However, all ten sub-units are present (Fig.6.02), as within the CBH 2 section. The characteristics of the sub-units from the SPH 1 section are summarised in Table 6.3.

Table 6.3 Characteristics of the sub-units from the SPH 1 Bulldog Shale succession.

Sub-unit	Depth interval	Thickness	Composition	Palynostratigraphy.
α	414.00-401.00m	13.00m	PFT/B-C. Basal unit overlying basement rock. Decimetre-scale fining and coarsening upwards layers, more clay-abundant than in CBH 2 or Finniss 2. Silt component rarely greater than 20%. Occasional sand fraction.	*Cyclosporites hughesii* spore-pollen zone; *Odontochitina operculata* dinoflagellate zone, (Alley pers. comm. 1994)
β	401.00-388.00m	13.00m	PFT/A-B. Clay-dominated sediments, typically less than 10% silt.	*C. hughesii* spore-pollen zone; *O. operculata* dinoflagellate zone, (Alley pers. comm. 1994)
γ	388.00-378.00m	10.00m	PFT/C-D. Moderately silty, up to 30% silt, clay-dominated sediments. Finer and with lower PFT values than equivalent sub-units from CBH 2 and Finniss 2.	*C. hughesii* spore-pollen zone; *O. operculata* dinoflagellate zone, (Alley pers. comm. 1994)
δ	378.00-352.00m	26.00m	PFT/A-B. Clay-dominated sediments, only slightly silty (less than 20% silt).	Palynostratigraphic data not available.
ε	352.00-336.00m	16.00m	PFT/B-D (exceptionally to A or F). Moderately silty (up to 30% silt) clay-dominated sediments with occasional sandy component.	Palynostratigraphic data not available.
ζ	336.00-315.00m	21.00m	PFT/A-B (occasionally C). Clay-dominated sediments, slightly silty (10% silt).	Palynostratigraphic data not available.
η	315.00-307.00m	8.00m	PFT/E (exceptionally F). Coarsening-upwards, clay-dominated succession in which silt content increases from approximately 10 to 50%.	Palynostratigraphic data not available.
θ	307.00-296.00m	11.00m	PFT/G. Near pure silt with occasional sand component.	Palynostratigraphic data not available.

Table 6.3 (continued).

Sub-unit	Depth interval	Thickness	Composition	Palynostratigraphy.
ι	296.00-290.00m	6.00m	PFT/E-F. Centimetre to dm scale interbedded near pure siltstones and more clay-dominated horizons (silt content down to 30% min.).	Palynostratigraphic data not available.
κ	290.00-276.00m	14.00m+	PFT/F-G (exceptionally E). Centimetre to dm scale interbedded near pure siltstones, occasionally with a sandy component, and less common clay-dominated horizons of 20-50% silt.	*Crybelosporites striatus* spore-pollen zone, (Alley pers. comm. 1994).

Finniss 2

Finniss 2 represents the basal part of the Bulldog Shale succession (§2.2.1), and comprises the four most basal sub-units: α, β, γ and δ (Fig.6.03). These are lateral equivalents to the basal sub-units defined from CBH 2 and SPH 1, and exhibit similar characteristics to them. The only major difference in the Finniss 2 sub-units is that they are considerably thicker than those elsewhere. The characteristics of the Finniss 2 sub-units are summarised in Table 6.4.

Table 6.4 Characteristics of sub-units α to δ from the Finniss 2 Bulldog Shale section.

Sub-unit	Depth interval	Thickness	Composition	Palynostratigraphy.
α	104.00-80.00m	24.00m	Highly variable PFT/A-F, most commonly PFT/C-D. Basal region. Thicker than at CBH 2, though its characteristics are very similar. Centimetre, dm and m scale fining and more occasional coarsening upwards layers dominate.	*Cyclosporites hughesii* spore-pollen zone; *Odontochitina operculata* dinoflagellate zone (Rogers *et al.*, 1989).
β	80.00m-39.00m	41.00m	PFT/A-B, exceptionally C. Lowest clay-dominant sub-unit, less than 40% silt, usually less than 20% silt, near pure clay common. Much thicker though less clay-dominated than at CBH 2.	*C. hughesii* spore-pollen zone; *O. operculata* dinoflagellate zone (Rogers *et al.*, 1989).
γ	39.00-27.00m	12.00m	PFT/D-G, most commonly E-G. High silt content (always more than 20%, typically more than 40%) with occasional fine sand component.	*C. hughesii* spore-pollen zone; *O. operculata* dinoflagellate zone (Rogers *et al.*, 1989).
δ	27.00m-3.00m	24.00m+	PFT/A-B, exceptionally C. Clay-dominated (less than 30% silt).	*C. hughesii* spore-pollen zone; *O. operculata* dinoflagellate zone (Rogers *et al.*, 1989).

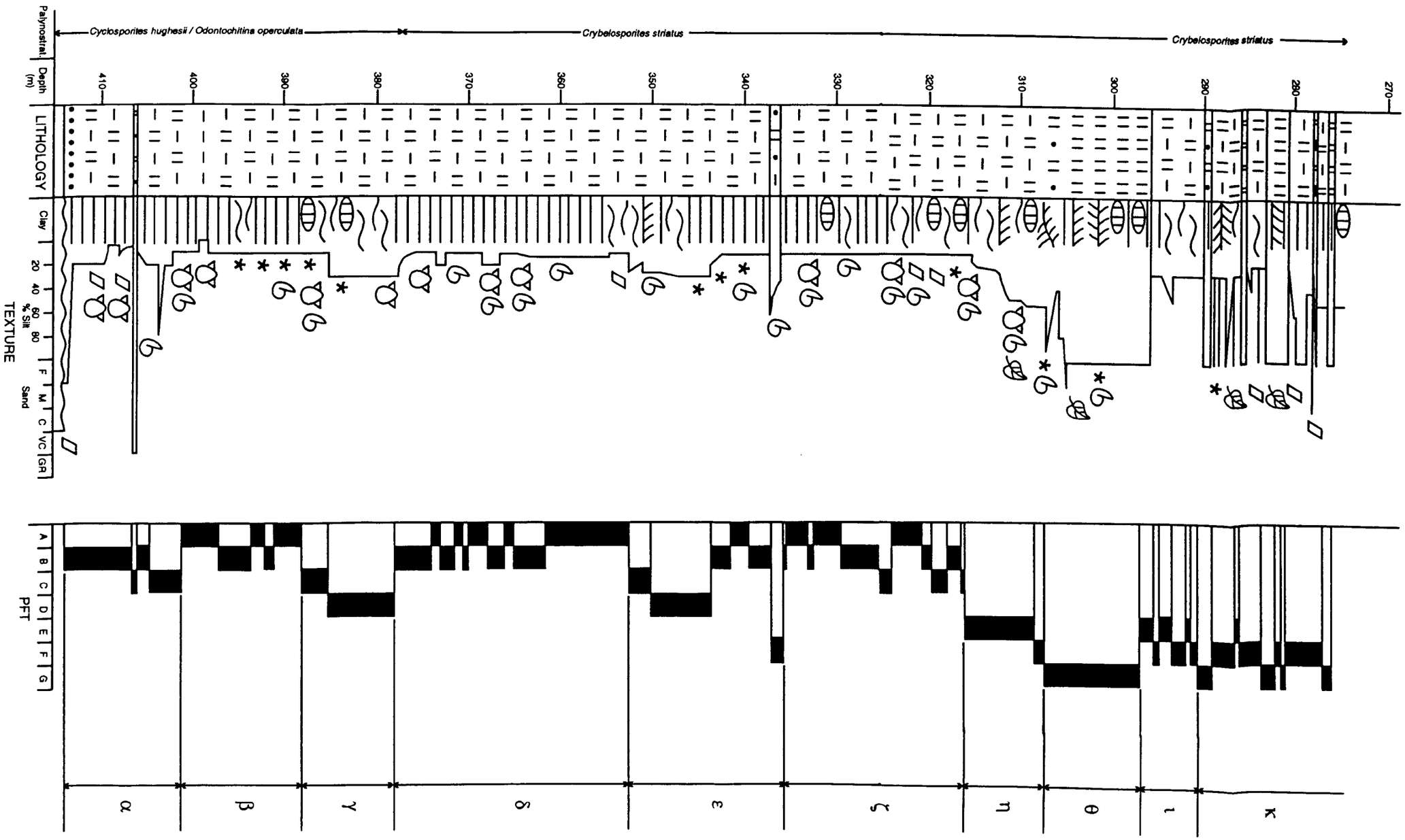

Fig.6.02 Summary log of the SPH 1 Bulldog Shale succession, with the sub-units delineated. For key to symbols see Fig.2.08.

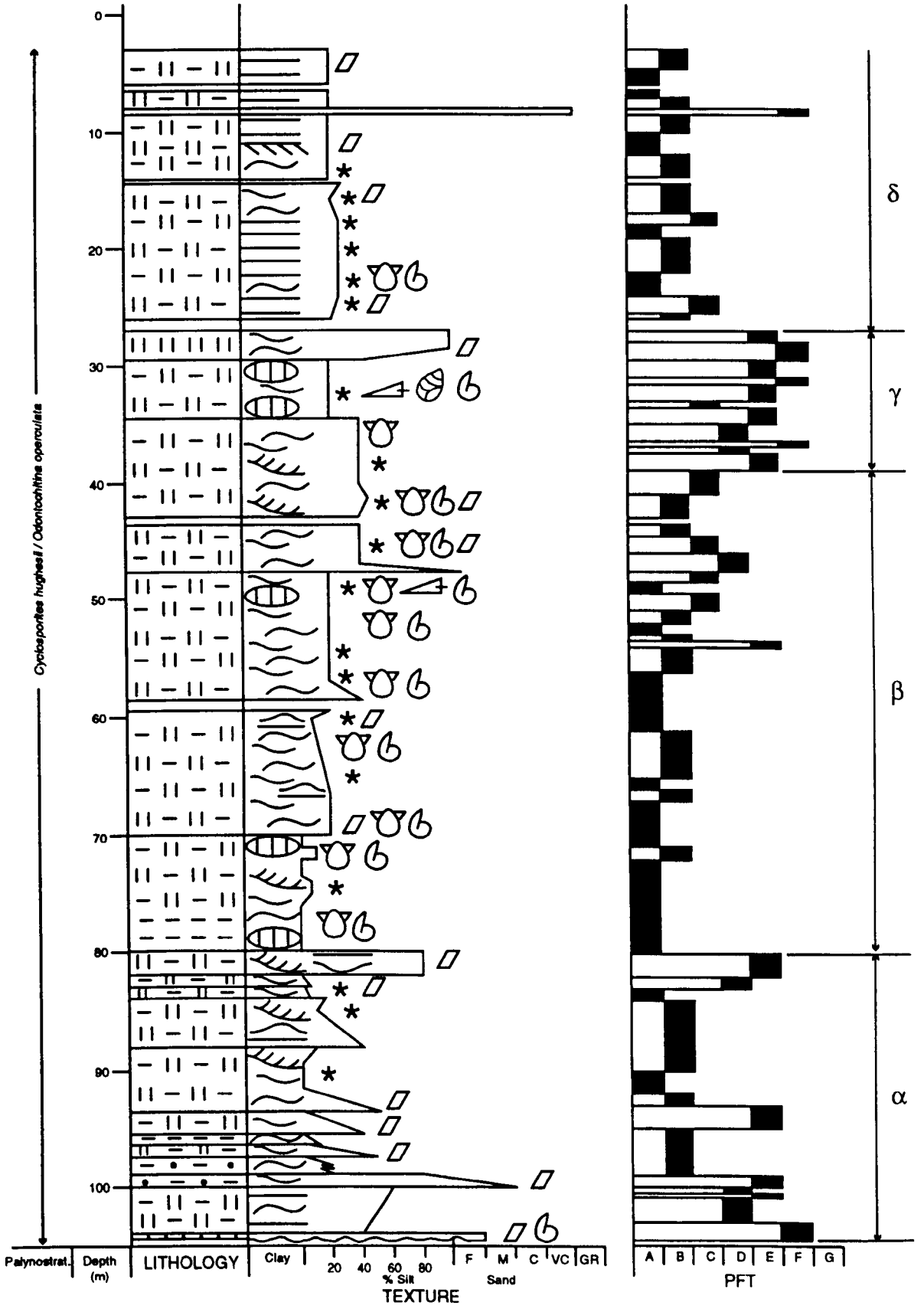

Fig.6.03 Summary log of the Finniss 2 Bulldog Shale succession, with sub-units α, β, γ and δ delineated. For key to symbols see Fig.2.08.

Alford 1

Alford 1 represents part of the upper Bulldog Shale succession (§2.2.2), and comprises the upper part of sub-unit η and the lower part of sub-unit θ (Fig.6.04). The characteristics of the sub-units from the Alford 1 section are summarised in Table 6.5.

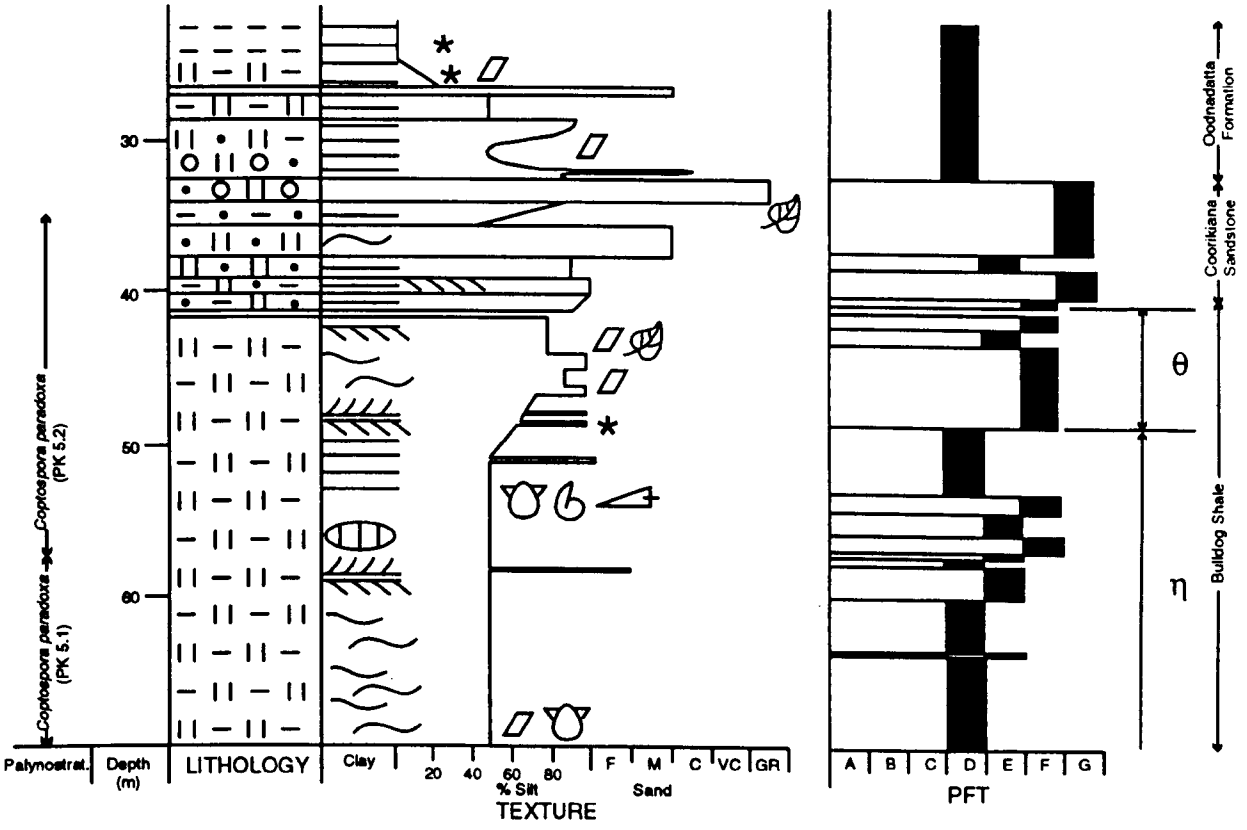

Fig.6.04 Summary log of the Alford 1 Bulldog Shale succession, with sub-units η and θ delineated. For key to symbols see Fig.2.08.

Stratigraphically higher Bulldog Shale sub-units (ι and κ) recorded from the three more easterly sections at CBH 2, Mount Yerila and SPH 1, are not present at Alford 1. In addition, sub-unit θ is considerably thinner, indicating that erosion occurring after Bulldog Shale deposition, and preceding that of the Coorikiana Sandstone may have been increasingly more severe and/or protracted to the west.

Table 6.5 Characteristics of sub-units η and θ from the Alford 1 Bulldog Shale succession.

Sub-unit	Depth interval	Thickness	Composition	Palynostratigraphy.
η	70.00-50.00m	20.00m+	PFT/D-E, exceptionally F. Increasingly silty (50-60% silt) coarsening-upwards horizon underlying silt- and sand-dominated horizons of uppermost Bulldog Shale. Very similar to sub-unit η from CBH 2.	*Coptospora paradoxa* spore-pollen zone, (Rogers *et al.*, 1989).
θ	50.00-41.60m	8.40m	PFT/E-G. Predominantly silty (60-100% silt).	*Coptospora paradoxa* spore-pollen zone, (Rogers *et al.*, 1989).

Mount Yerila section

The Mount Yerila Bulldog Shale section represents the uppermost part of the unit (§2.2.4), and comprises the three uppermost sub-units θ, ι and κ (Fig.6.05), which are very similar to the corresponding sub-units from the CBH 2 core. However, it is evident that Bulldog Shale sediments at Mount Yerila generally have a larger sand component than elsewhere. The characteristics of the sub-units from the Mount Yerila section are summarised in Table 6.6.

Table 6.6 Characteristics of the sub-units from the Mount Yerila Bulldog Shale succession.

Sub-unit	Thickness	Composition	Palynostratigraphy.
θ	13.50m+	PFT/F-G. Interbedded near pure siltstones and fine- to coarse-grade sandstone horizons of cm to dm thickness.	*Crybelosporites striatus* spore-pollen zone, (Alley pers. comm. 1994).
ι	5.50m	PFT/E-F. Coarsening-upwards succession from clay-dominated material with 20% silt content at the base, to silt-dominated sediments of 80% silt and 20% clay-grade material at the top.	*C. striatus* spore-pollen zone, (Alley pers. comm. 1994).
κ	12.50m	PFT/F-G. Units of dm thickness. Variable silt content, from near pure silt with distinct sand component, to only 30% silt material in clay-dominated sediment	*C. striatus* spore-pollen zone, (Alley pers. comm. 1994).

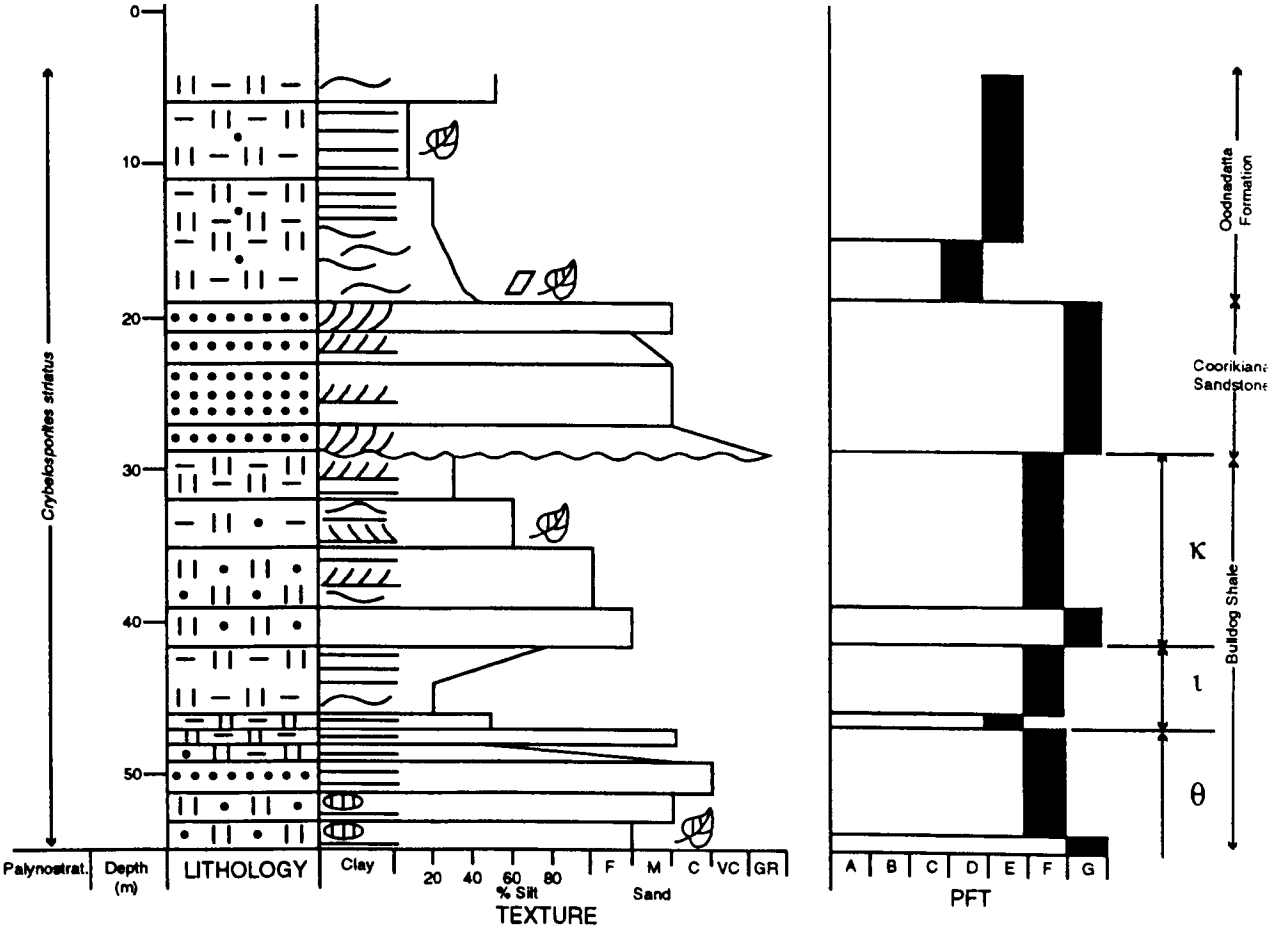

Fig.6.05 Summary log of the Mount Yerila Bulldog Shale succession, with sub-units θ, ι and κ delineated. For key to symbols see Fig.2.08.

6.1.2 Bulldog Shale sub-units: use as a tool

The establishment of the ten Bulldog Shale sub-units provides a new tool for future identification of stratigraphic position within the Bulldog Shale succession. This tool will be of most use in the analysis of isolated field exposures, and comparisons and correlations between them. It is important to note that the defined sub-units were correlated in a section essentially along strike. Correlations down dip into more basinal conditions must be made with care, though palynology can help determine relationships, and an appreciation of the variations in sub-unit thickness and PFT type in a transition from marginal to increasingly basinal conditions is required. Such a transition is briefly described for the marginal and more basinal core sections of SPH 1 and Skeleton 2 respectively (§6.3.3).

The detailed sub-division of the Bulldog Shale is important, for in previous studies this formation has merely been divided into two or three parts on the basis of its palynostratigraphy (see zones in Fig.2.09), or on the basis of its lithology. For example, in the Skeleton 2 well completion report, Callen *et al.* (1990) divided the Bulldog Shale into:

(i) a lower part characterised by clay-dominated material yielding *Cyclosporites hughesii* and *Diconodinium davidii* zone palynomorphs;

(ii) an un-named sandstone, and;

(iii) an upper part also characterised by clay-dominated material and yielding *Crybelosporites striatus* zone palynomorphs.

In the scheme utilised here, these subdivisions correspond to the sub-units α, β, γ and δ for the lower part, ε for the un-named sandstone, and ζ, η, θ, ι and κ for the upper part, as illustrated in the expanded correlation diagram (Fig.6.10).

6.2 Bulldog Shale section correlation

The identification of the same sub-unit succession, or parts thereof, from all the studied sections in a transect of approximately 276.00km around the south western Eromanga Basin, indicates that these sub-units are laterally very persistent, albeit with thickness variations. This lateral persistence is similar to that observed for the larger scale transitions from Bulldog Shale to Coorikiana Sandstone, and subsequently to Oodnadatta Formation and, as in the larger scale case, results from variations in palaeoenvironmental conditions, primarily sea level, which affected the entire region. Thus, the identification of the sub-units in a series of sections provides a new means for correlation between them. A correlation is made here for the south-western Eromanga Basin 276.00km transect, between the western-most section locality (Finniss 2) and the eastern-most section locality (SPH 1) (Fig.6.06), and is presented in Fig.6.07.

6.2.1 The value of geophysical logs

Various geophysical logs (caliper, short- and long-spaced density, magnetic susceptibility, gamma, neutron, short and long resistivity, point resistivity, and self-potential) were studied, where available, for the sections presented in Fig.6.07, but are

not used here for correlative purposes for they do not exhibit significant variation, and have a very subdued low response in all wells except where carbonate concretions are encountered. Carbonate concretions produce sharp peaks on density, magnetic susceptibility, neutron and self potential logs. However, the localised and isolated nature of many of these Bulldog Shale carbonate concretions (§2.5.3) signifies the lack of potential in using these as a basis for the correlation of sub-units.

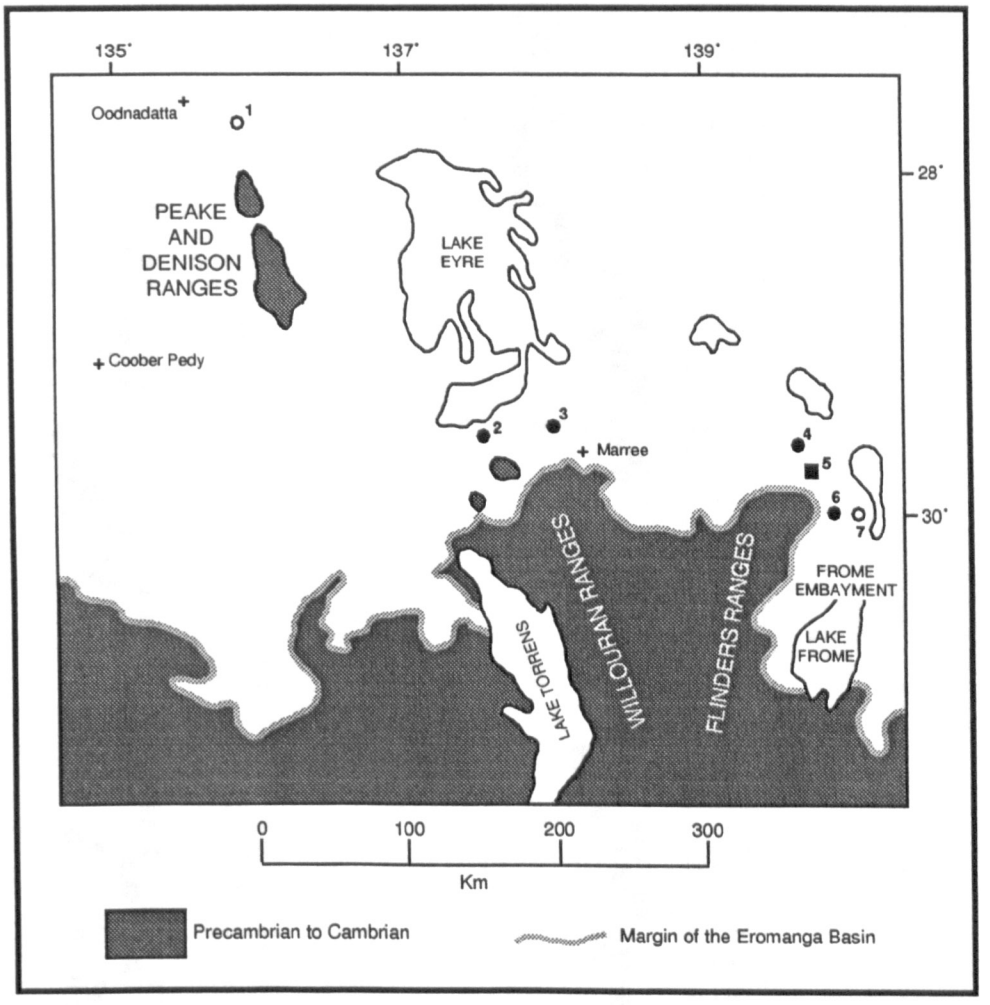

Fig.6.06 South western margin of the Eromanga Basin in South Australia, illustrating location of logged core and field sections included in the correlation of Bulldog Shale sub-units. 1 = Toodla 1, 2 = Finniss 2, 3 = Alford 1, 4 = CBH 2, 5 = Mt. Yerila, 6 = SPH 1 and 7 = Skeleton 2. Solid circles represent sections studied in detail; open circles represent sections logged by others and included in order to test and expand the correlation constructed here.

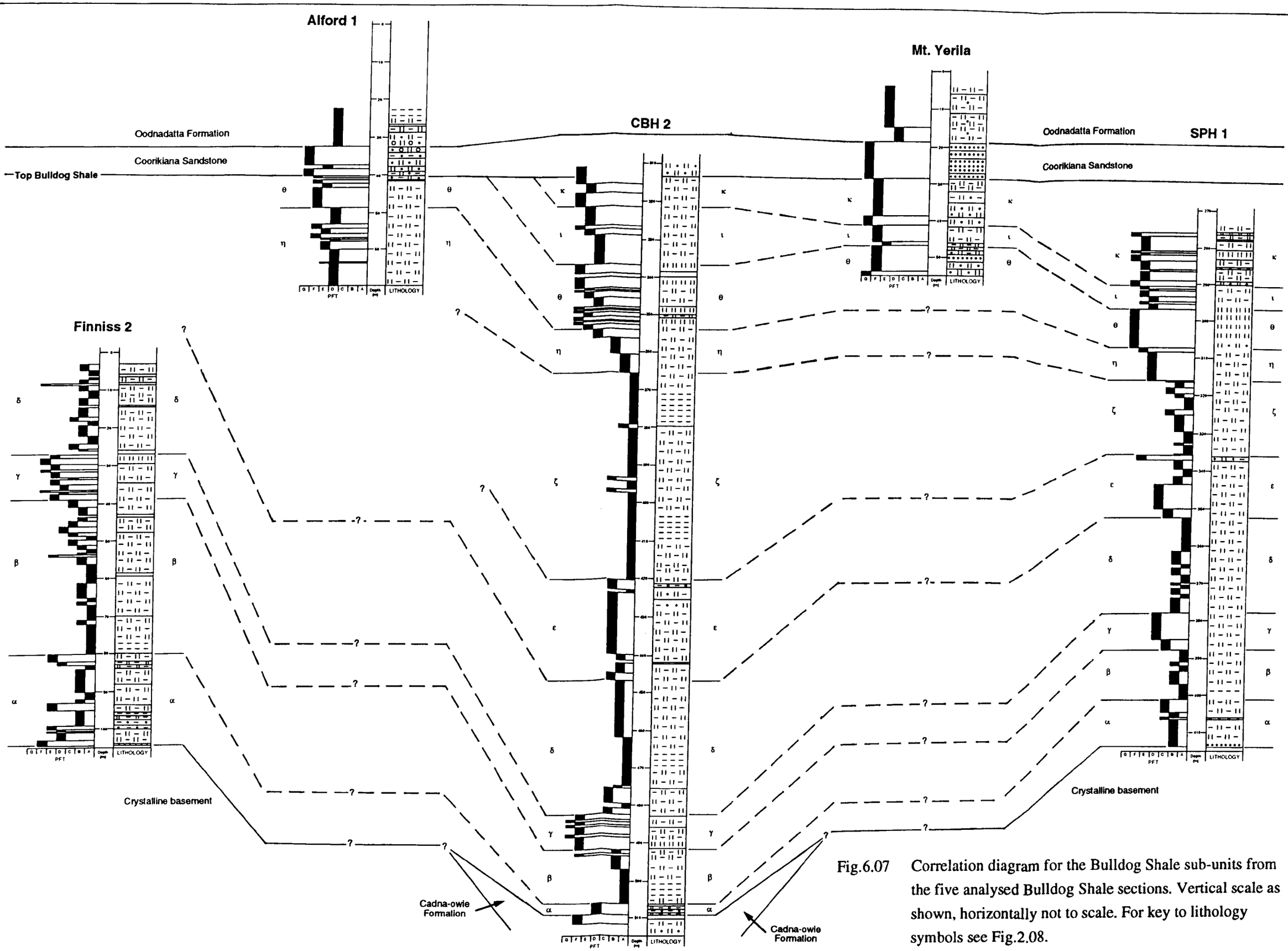

Fig.6.07 Correlation diagram for the Bulldog Shale sub-units from the five analysed Bulldog Shale sections. Vertical scale as shown, horizontally not to scale. For key to lithology symbols see Fig.2.08.

6.2.2 Variation between sections

Variation in the vertical position of the sections is related to their location, whether on relatively stable basement highs, or within basin depocentres. The sections from Finniss 2 and Mount Yerila were deposited on basement highs, and in these localities Bulldog Shale outcrops at the surface. The sections from CBH 2 and SPH 1, on the other hand, were deposited within basin depocentres which have experienced further subsidence since Bulldog Shale deposition. The section from CBH 2 was deposited within the Lake Eyre/Simpson Desert Basin (referred to as the Birdsville Basin by Veevers (1984)). The section from SPH 1 lies within the more easterly Callabonna sub-basin of the Lake Eyre depocentre (within the Frome Embayment (Fig.6.06)). In both the CBH 2 and SPH 1 sections the Bulldog Shale is overlain by younger Mesozoic and Cainozoic sediments, and does not outcrop at the surface.

Although the ten sub-units extend laterally throughout the study area, they exhibit some variation. This is expressed in terms of unit thickness and dominant grain size, which can largely be ascribed to the proximity to the palaeoshoreline (Table 6.7) and associated distance from sediment source. These variations are summarised below.

Table 6.7 Distance from palaeoshoreline (approximate) for the sections analysed in this study.

SECTION	DISTANCE FROM PALAEOSHORELINE
Finniss 2	5 km
Alford 1	20 km
CBH 2	25 km
Mt. Yerila	15 km
SPH 1	10 km

Of particular importance is the observation that in all sub-units, except θ and κ, the sediments of SPH 1 are generally finer grained than those of the other sections. This may reflect the location both distal from more westerly sediment sources and in relatively quiet conditions of the Frome Embayment (Fig.6.06).

The variations summarised here for each of the sub-units are illustrated in the section correlation diagram (Fig.6.07).

- Sub-unit α, the basal sub-unit of the Bulldog Shale has a noticeable thinning in the proximal to distal Finniss 2 - SPH 1 - CBH 2 offshore transition. Sub-unit thickness declines from 24.00m at Finniss 2 to 13.00m at SPH 1, and to only 2.60m in the more basinal CBH 2.

- Sub-unit β exhibits thinning from west to east, from 41.00m in Finniss 2 to 15.00m in CBH 2 and 13.00m in SPH 1.

- Sub-units γ and δ are both of relatively constant thickness throughout the correlated section.

- Sub-units ε and ζ are both thickest in the most basinal section of CBH 2.

- Sub-unit η both thins and fines to the east, from 20.00m+ at Alford 1 to 11.50m and 8.00m at CBH 2 and SPH 1 respectively.

- Sub-unit θ also thins to the east, though at Alford 1 it is truncated by an erosive boundary surface, overlain by the Coorikiana Sandstone. Thickness of this sub-unit decreases from 18.00m at CBH 2 to 13.50m and 6.00m at Mt. Yerila and SPH 1 respectively. In each of these sections sub-unit θ is overlain by further upper Bulldog Shale sub-units.

- Sub-unit ι again both thins (from 14.50m in CBH 2 to 5.50m and 6.00m at Mt. Yerila and SPH 1 respectively) and fines to the east.

- Sub-unit κ is incomplete in all analysed upper Bulldog Shale sections due to erosion preceding deposition of the overlying Coorikiana Sandstone. However, more of this sub-unit is preserved in the more easterly sections, from 6.50m thickness in CBH 2 to 12.50m and 14.00m+ in the Mt. Yerila and SPH 1 sections respectively.

6.3 Other cores containing Bulldog Shale

In order to expand and test the basinal correlation presented in Fig.6.07, two further logs have been constructed from summary logs and information given in well completion reports. These logs have been constructed for the cores Toodla 1 (Griffiths, 1980) (Fig.6.06) and Skeleton 2 (Callen *et al.*, 1990) (Fig.6.06). Palaeoenvironmental fabric types could not be constructed for these sections, owing to the lack of necessary

information regarding the presence/absence, amount and nature of bioturbation and detailed accounts of sedimentary structures. However, tentative correlation based on lithological variation and palynostratigraphy can be made with reference to the correlation presented in Fig.6.07. The inclusion of these additional sections provides an important test for the correlation scheme presented here, and considerably expands the distance covered in the correlation transect to nearly 550km.

6.3.1 Toodla 1

Location: Latitude 27°43'47"S; Longitude 135°50'55"E (Fig. 2.01).

Thickness

Total depth reached in Toodla 1 is 353.00m, from a ground elevation of +96.70m, in which the Mesozoic sequence overlies metamorphic basement rocks at 342.00m. Bulldog Shale conformably overlies the Cadna-owie Formation at 266.00m, is overlain by Coorikiana Sandstone at 99.50m, and thus comprises a sequence of 166.50m thickness (Fig.6.08).

Completeness

The section is fully cored from the base to 150.00m, though above this depth (including the uppermost 50.50m Bulldog Shale) cuttings only have been recovered.

Sub-unit description

Palynostratigraphy of the Toodla 1 Bulldog Shale section (Fig.6.08), as defined by Alley (1985), has identified a hiatus within the depth interval 197.00-194.00m. This hiatus shortens the section, and corresponds with a probable thinned sub-unit δ. On the basis of lithological characteristics and palynostratigraphy a full basal succession of sub-units α, β and γ are identified beneath the thinned sub-unit δ. This basal region represents the *Cyclosporites hughesii* spore-pollen zone and the *Odontochitina operculata* dinoflagellate zone. Sub-unit δ in Toodla 1 appears slightly younger than observed elsewhere, and represents the basal *Crybelosporites striatus* spore-pollen zone. Above the hiatus, sub-units ε and ζ have been tentatively identified, both representative of the *Crybelosporites striatus* spore-pollen zone. Resolution and detail are lacking in the cuttings of the upper Bulldog Shale section, such that delineation of the sub-units η to κ cannot be made. However, the thickness of this part of the section (50.50m) is similar to that observed elsewhere (31.00-67.00m), such that it is likely that all the upper Bulldog Shale sub-units are represented. Samples from this region yielded

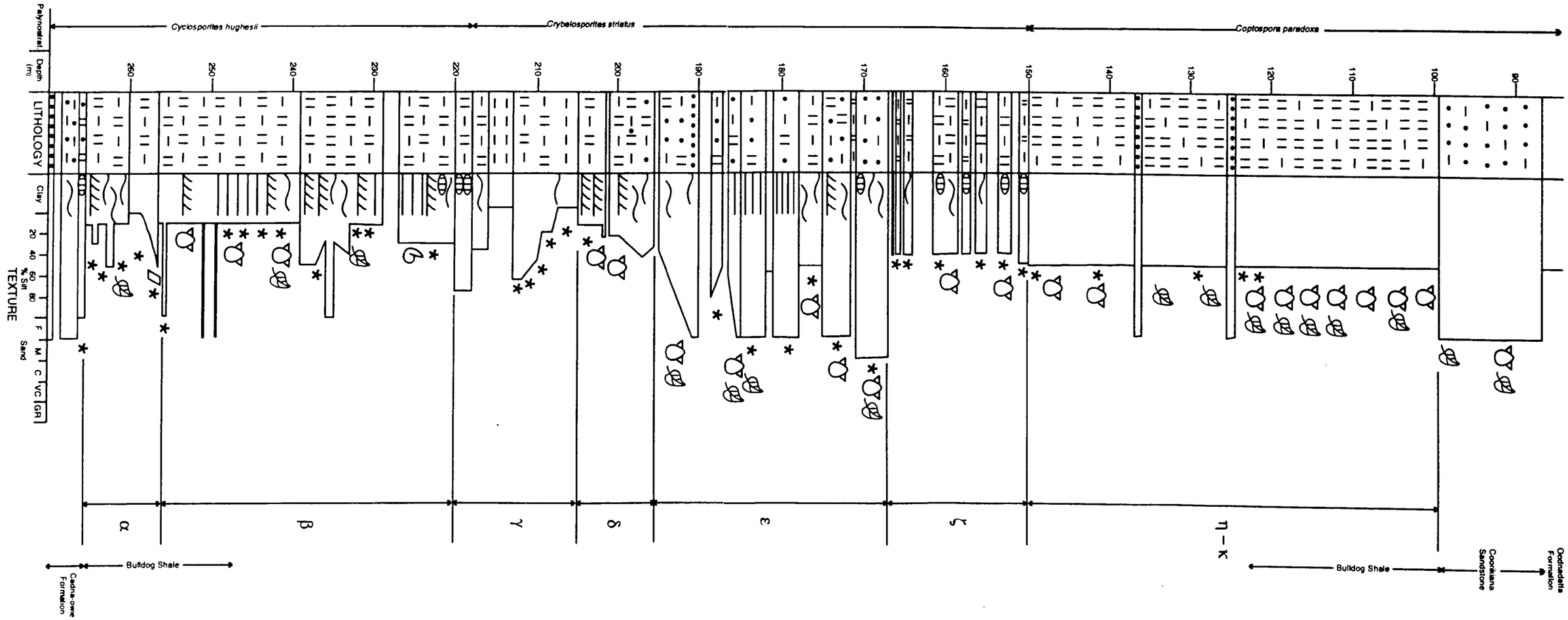

Fig.6.08 Summary log of the Toodla 1 Bulldog Shale succession. For key to symbols see Fig.2.08. Palynostratigraphy from Alley (1985). Redrawn from Griffiths (1980).

Coptospora paradoxa spore-pollen zone palynomorphs, as in the CBH 2 and Alford 1 sections.

The inclusion of Toodla 1 in the correlation diagram extends the section 255.00km NNE from Finniss 2 into a more basinal area. Care should be taken however in viewing the Toodla 1 locality in a deep basinal context, for the core locality resides on the slope of the Mount Dutton basement high which outcrops approximately 20km to the WSW. Therefore, more shoreline-proximal conditions may have prevailed, such as those at Finniss 2, during Bulldog Shale deposition at this locality.

6.3.2 Skeleton 2

Location: Latitude 29°54'30"S; Longitude 140°00'54"E (Fig.2.04).

Thickness

Skeleton 2 reaches a total depth of 591.75m, from a ground elevation of +27.72m, in which the Mesozoic sequence overlies probable Adelaidean age metasediments at 537.00m. Within the Mesozoic section, Bulldog Shale overlies Cadna-owie Formation at 520.40m, and is unconformably overlain by the Tertiary Eyre Formation at 187.20m, and thus comprises a total thickness of 333.20m (Fig.6.09).

Completeness

The recovered section of Bulldog Shale largely comprises cuttings and thus much detail is lost. However, most of the Bulldog Shale sub-units can be tentatively identified in this core on lithological and palynostratigraphic evidence; problems do occur in the uppermost 50m though, where much of the core was not recovered (Fig.6.09).

Sub-unit description

Uppermost Cadna-owie Formation and basal Bulldog Shale represent the *Cyclosporites hughesii / Odontochitina operculata* zone. Sediments of sub-unit δ at depths 440.10m and 443.60m produced probable *Cyclosporites hughesii / Diconodinium davidii* zone palynomorphs. Uppermost Bulldog Shale sediments (probably sub-units θ and ι) produced palynomorphs of the *Crybelosporites striatus* zone (Callen *et al.*, 1990; Alley pers. comm. 1994).

Sub-units α, β, γ, δ, ε, ζ, η and θ can be identified from the Skeleton 2 section (Fig.6.09). This identification is made on the basis of similarities between the

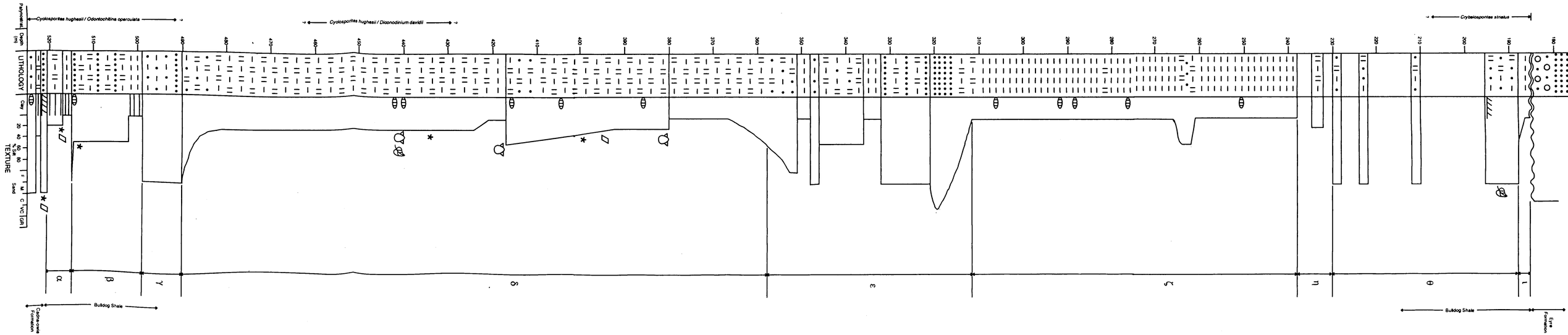

Fig.6.09 Summary log of the Skeleton 2 Bulldog Shale succession. For key to symbols see Fig.2.08. Redrawn from Callen *et al.* (1990).

lithological variation and the palynostratigraphy recorded for the Skeleton 2 section, and that exhibited in the sections studied in detail. Core loss from the upper part of the section, together with the lack of PFT information, and the uncertainty regarding the extent of Bulldog Shale erosion prior to deposition of the Eyre Formation, make identification of the sub-units in this region more difficult. However, it is likely that the thin clay-dominated Bulldog Shale unit upon which the Eyre Formation rests (Fig.6.09) is the remnant of sub-unit ι. If this is the case, most of this sub-unit, and all of the younger Bulldog Shale (sub-unit κ) and Cretaceous sediments were eroded prior to Eyre Formation deposition.

The inclusion of Skeleton 2 into the basin correlation expands the transect 18.00km to the east from SPH 1, directly into the more basinal setting of the Frome Embayment (Fig.6.06).

6.3.3 Correlation with the other five sections

From the summary logs presented here (Fig.6.08; 6.09), it is evident that the sub-units defined on the basis of PFT and palynostratigraphy can be identified, albeit with some caution, from other sections elsewhere in the basin on the basis of their lithology and palynostratigraphy only. Thus, these additional sections can be included within the basin correlation diagram (Fig.6.10).

Problems in sub-unit identification and correlation arise through the lack of detail and resolution. These difficulties are particularly apparent in the upper 50.50m of the succession in Toodla 1, from which only cuttings were studied, and definition between sub-units η, θ, ι and κ cannot be safely made (Fig.6.10).

Skeleton 2 is less problematical, despite much of the Bulldog Shale succession originally being described from cuttings only. The section from the Skeleton 2 well is strikingly similar to that from SPH 1. The primary difference between the two sections is that the mid-Bulldog Shale sub-units δ, ε and ζ exhibit considerable thickening in the more basinal and distal Skeleton 2, while underlying and overlying sub-units maintain relatively similar thicknesses (Fig.6.10). In addition, sediments in each of the sub-units are typically more finer grained in Skeleton 2 than in SPH 1 (Fig.6.10), another indicator of its more distal position.

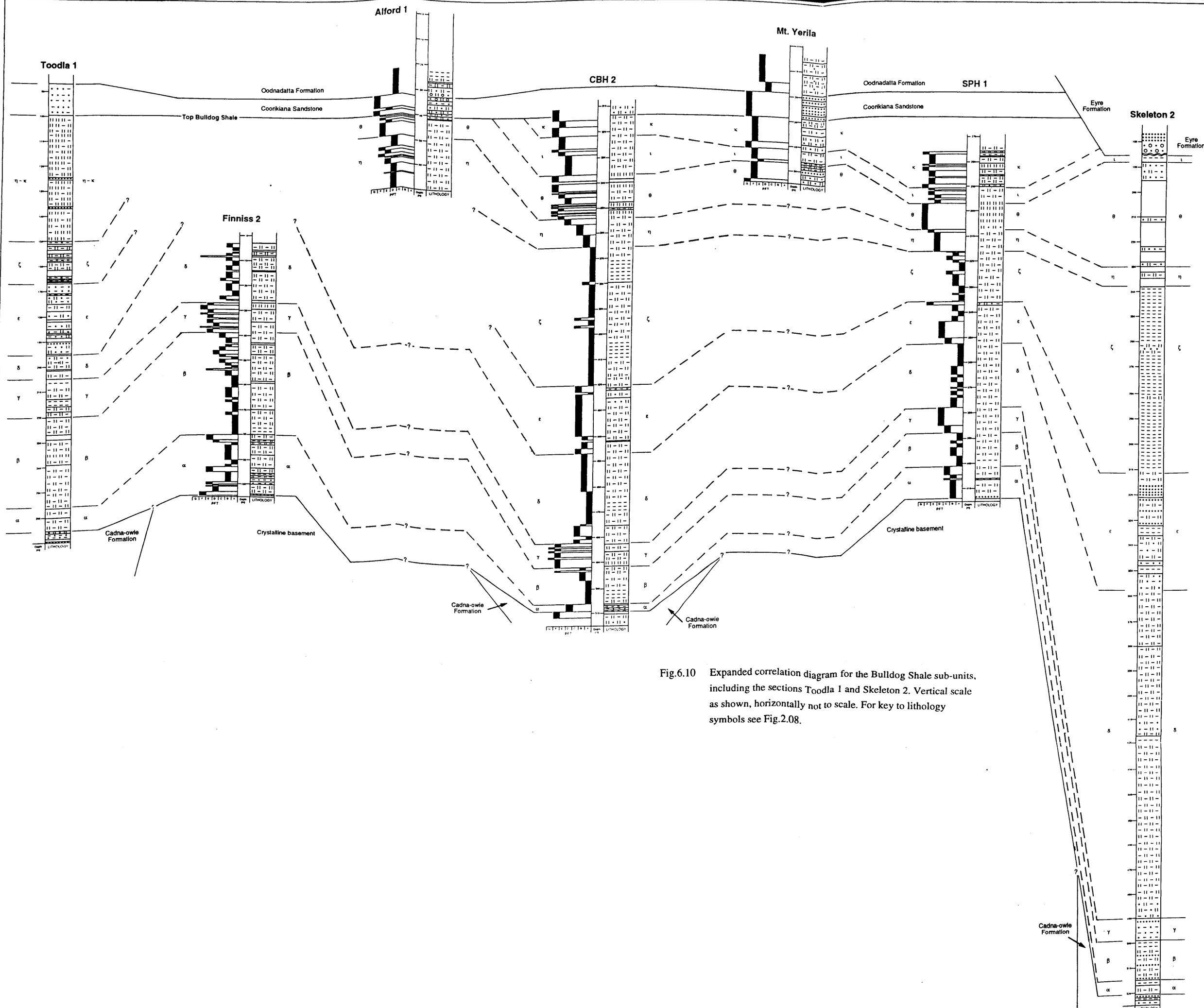

Fig.6.10 Expanded correlation diagram for the Bulldog Shale sub-units, including the sections Toodla 1 and Skeleton 2. Vertical scale as shown, horizontally not to scale. For key to lithology symbols see Fig.2.08.

Problems are also incurred in the upper Bulldog Shale of Skeleton 2, largely as a result of core loss. It is likely that sub-units θ and ι are present, though much of ι has been eroded along with all of sub-unit κ prior to deposition of the Eyre Formation (Fig.6.10).

It is evident that detailed PFT analysis of the Toodla 1 and Skeleton 2 Bulldog Shale successions is required in order to confirm or refute the speculative correlations suggested here, and in order to solve those problems defined above.

6.4 Palaeoenvironmental Interpretation

Probable water depths have been inferred for each of the palaeoenvironmental fabric types (§4.4.2). Therefore, with the chief palaeoenvironmental constraint of sea level clearly expressed by PFTs and their broader scale associations, as recorded in defined Bulldog Shale sub-units, a curve of relative sea level, or palaeobathymetry, can be drawn up for the Bulldog Shale succession of the south western Eromanga Basin (Fig.6.11; 6.12).

It is evident from Fig.6.11 that the palaeobathymetric curves generated from each of the sections are very similar. This is expected however, for they are derived from the same sub-unit succession in each case, the lateral persistence of which is a result of the basin-wide nature of relative sea level change. Of these five sections, CBH 2 is the most complete, and therefore produces the most complete palaeobathymetric curve (Fig.6.12). Furthermore the similarity between the five palaeobathymetric curves allows CBH 2 to be taken as a valid standard for description and discussion.

From the palaeobathymetric curves presented in Fig.6.11 and Fig.6.12 it is evident that the Bulldog Shale contains a record of fluctuating sea levels.

- The commencement of Bulldog Shale deposition occurred in response to the major marine transgression recorded as sub-unit α. In the Finniss 2 and SPH 1 sections where the Bulldog Shale was the first of the Mesozoic Eromanga Basin sediments to be deposited, the transgression occurred over previously terrestrial or very shallow water conditions. Water depths approaching 50m were rapidly attained. Elsewhere, in the sections Toodla 1, CBH 2 and Skeleton 2, in which the Bulldog Shale conformably overlies the Cadna-owie Formation and shallow (less than 20m depth) marine conditions were already in existence, the transgression increased sea level to deeper basinal conditions (up to 50m depth).

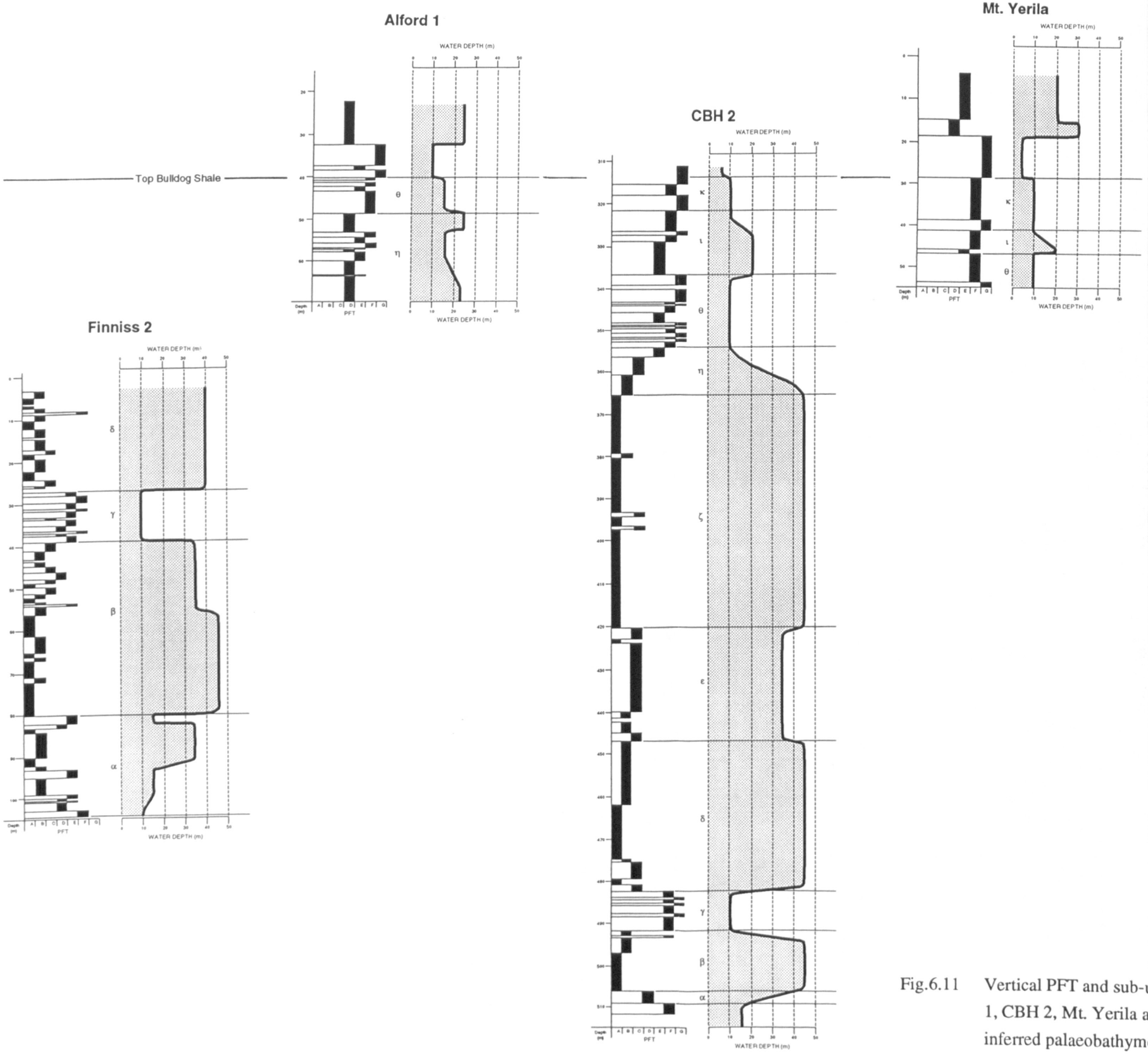

Fig.6.11 Vertical PFT and sub-unit successions for the Finniss 2, Alford 1, CBH 2, Mt. Yerila and SPH 1 Bulldog Shale sections, with inferred palaeobathymetric curves.

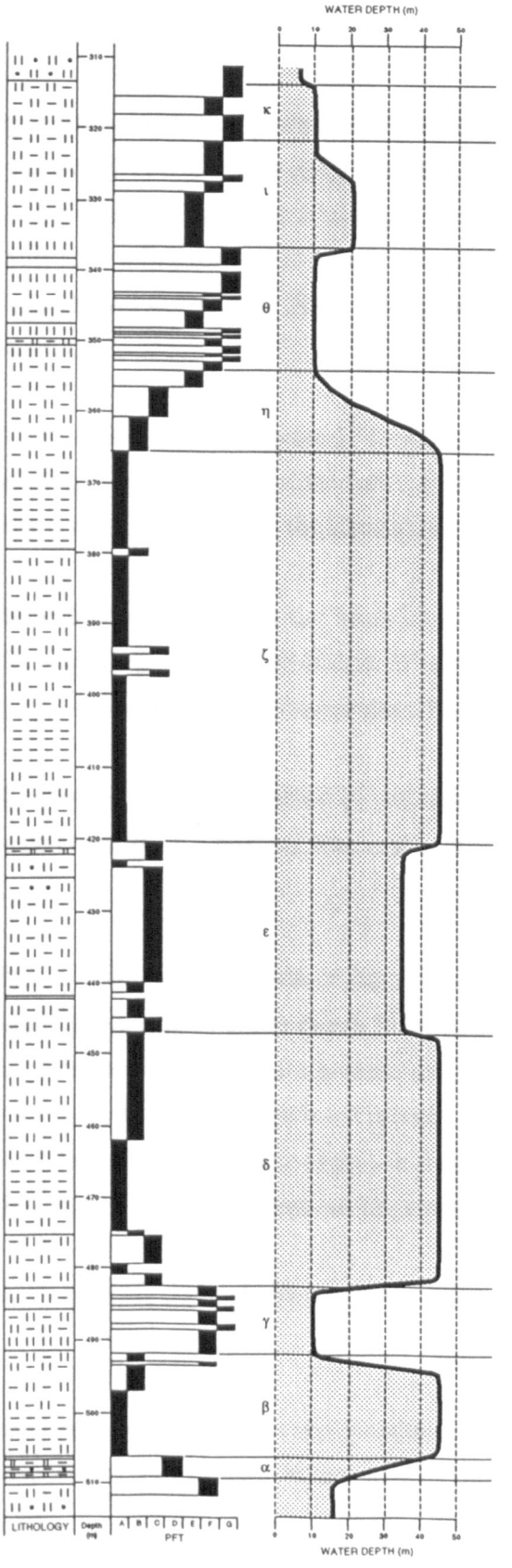

Fig.6.12 Palaeobathymetric curve for the CBH 2 Bulldog Shale succession.

- Sub-unit β marks deposition during the subsequent high sea levels which followed the major transgression.

- Subsequently, deposition of sub-unit β was terminated by a major regression which is marked by the boundary between sub-units β and γ. This regression lowered sea levels from up to 50m depth to less than 20m depth, and enabled the deposition of the sediments of sub-unit γ. Regression is favoured here rather than gradual sediment progradation and associated shallowing due to the sharpness of change in the sedimentation patterns.

- The deposition of sub-unit γ was subsequently terminated by a further major transgression marked by the boundary of sub-units γ and δ, which signalled the return to water depths of up to 50m and the deposition of sub-unit δ.

- A further slight regression is marked by the boundary between sub-units δ and ε, and was responsible for the deposition of sub-unit ε. Water depths were still in excess of 20m, though probably considerably shallower than 50m.

- The deposition of sub-unit ε was terminated by another slight transgression, with a return to deeper water conditions close to 50m depth, and the subsequent deposition of sub-unit ζ.

- The later deposition of sub-unit η terminated deposition of sub-unit ζ, and was in response to a gradual reduction in water depth from close to 50m to approximately 10m. This regression formed the start of a general regression recorded in the sediments of sub-units η, θ, ι and κ, which eventually resulted in the deposition of the Coorikiana Sandstone. While eustatic regression undoubtedly played a part here, sediment progradation may also have been an important factor.

- Sub-unit θ represents deposition in shallow water conditions, typically less than 20m depth.

- The boundary between sub-units θ and ι was produced by a slight transgression with the subsequent deposition of sub-unit ι. Water depths increased from less than 20m to approximately 20m.

- The conditions in which sub-unit ι was deposited were reversed with a subsequent slight regression which is marked by the boundary between sub-units ι and κ. This regression resulted in a return to very shallow (typically less than 20m water depth) conditions.

- A further slight regression brought the water depth down to within fair weather wave base, and the Coorikiana Sandstone (§1.2.2) was deposited, exhibiting signs of tidal action not observed within the Bulldog Shale. Within the enclosed Eromanga Sea, it is possible that tidal ranges and currents were minimal, and thus it is expected that only those deposits formed within the shallowest, possibly intertidal zone, should exhibit these effects.

6.4.1 Comparison of the Bulldog Shale palaeobathymetric curve with other studies and relative sea level curves

Palaeoenvironmental interpretations from palynomorph studies

The palaeobathymetric curve for the Bulldog Shale succession presented in Fig.6.11 and Fig.6.12 largely agrees with the palaeoenvironmental interpretations based on palynomorph studies of parts of the sequence from each cored succession. These interpretations are summarised in Table 6.8.

Table 6.8 Summary table of palaeoenvironmental interpretations of Bulldog Shale sub-unit material from palynomorph analyses, and their relevance to this study.

Sub-unit, core	Palaeoenvironmental interpretation and author	Notes and comparisons with palaeobathymetric curves of this study (Fig.6.11; Fig.6.12)
α CBH 2	Very shallow water Harris (1982)	Harris' (1982) interpretation provides the only note of dissent from the open marine consensus. However, it seems likely that Harris' (1982) sample, given as originating from core depth 507.00m, was taken from a thin (only 5cm thick) granule-rich horizon, and as such is not representative of this sub-unit.
α Finniss 2	Open marine Rogers *et al.* (1989)	See above
α SPH 1	Open marine Alley (pers. comm. 1994)	See above
α Skeleton2	Open marine Alley (pers. comm. 1994)	See above

Table 6.8 (continued).

Sub-unit, core	Palaeoenvironmental interpretation and author	Notes and comparisons with palaeobathymetric curves of this study (Fig.6.11; Fig.6.12)
β Finniss 2	Below 68.00m core depth: deep open marine conditions. Above 68.00m: considerably shallower conditions. Rogers *et al.* (1989)	These observations tie in well with the sea level curves presented in Fig.6.11 and Fig.6.12, with the deep open marine conditions resulting from the basal transgression recorded in sub-unit α, and with the subsequent regression resulting in the shallow water conditions of sub-unit γ.
γ Finniss 2	Shallow marine conditions, probably with water depths little in excess of 10m. Rogers *et al.* (1989)	This palaeoenvironmental interpretation fits in well with the sea level curve for sub-unit γ presented in Fig.6.11 and Fig.6.12.
γ CBH 2	As above. Harris (1982)	As above.
γ SPH 1	As above. Alley (pers. comm. 1994)	As above.
δ Finniss 2	Shallow marine. Rogers *et al.* (1989)	Samples taken from Finniss 2 come from near the base of the sub-unit, while samples taken from Skeleton 2 originate from the middle of the sub-unit. Such observations fit in well with the sea level curves presented in Fig.6.11 and Fig.6.12, with the samples towards the base of the sub-unit representing shallow water conditions prevailing during the transgression, and the samples taken from the middle of the sub-unit representing deeper water conditions (approaching 50m depth) prevailing once the transgression had occurred. Palaeogeography may also play a part here, with the Skeleton 2 section occupying a more basinal location than SPH 1 or Finniss 2 (Fig.6.06).
δ Skeleton2	Deep open marine Alley (pers. comm. 1994)	See above
η Alford 1	Shallowing-upwards trend from shallow conditions to very shallow conditions. Rogers *et al.* (1989)	Such interpretations fit in well with the sea level curves presented in Fig.6.11 and Fig.6.12, which interpret sub-unit η as resulting from a gradual regression from water depths of near 50m to less than 20m and probably nearer 10m.
θ Alford 1	Shallow waters. Rogers *et al.* (1989)	These interpretations fit in well with the sea level curves in Fig.6.11 and Fig.6.12, in which water depths of little more than 10m are inferred.
θ CBH 2	Open marine conditions. Alley (pers. comm. 1995)	As above
θ Skeleton2	Open marine conditions. Alley (pers. comm. 1994)	As above
ι Skeleton2	Marine. Alley (pers. comm. 1994)	Such an interpretation is consistent with the sea level curves presented for this sub-unit in Fig.6.11 and Fig.6.12, which indicated a transgressive and subsequently regressive nature of the sub-unit. Sea levels apparently rose rapidly from 10m to approximately 20m at the boundary between sub-units θ and ι, and more gradually lowered back to approximately 10m just below the sub-unit ι - κ boundary.

Table 6.8 (continued).

Sub-unit, core	Palaeoenvironmental interpretation and author	Notes and comparisons with palaeobathymetric curves of this study (Fig.6.11; Fig.6.12)
κ CBH 2	Marginal marine. Alley (pers. comm. 1995)	Such interpretations fit in well with the sea level curves presented in Fig.6.11 and Fig.6.12, in which sub-unit κ is interpreted to represent deposition within water depths little in excess of 10m, and forms the last part of the gradual upper Bulldog Shale regression. A further minor regression terminated deposition of sub-unit κ, and resulted in the deposition of the Coorikiana Sandstone. Such an interpretation is based on the assumption that, while deposition of the Coorikiana Sandstone was preceded by erosion into the top of the Bulldog Shale, particularly in the more westerly sections, sub-unit κ represents the true topmost Bulldog Shale sub-unit.
κ SPH 1	Very shallow marine. Alley (pers. comm. 1994)	As above

Comparison with Morgan's relative sea level curve

Morgan (1980) attempted a correlation of the Mesozoic sediments of the Eromanga Basin on the basis of lithostratigraphy, palaeontology and palynostratigraphy. However, this work did not incorporate detailed trace fossil and ichnofabric analysis. From his analyses Morgan (1980) produced a relative sea level curve for the Eromanga Basin Mesozoic section which included the Bulldog Shale (Fig.1.01).

Morgan's (1980) relative sea level curve depicts three transgression - regression couplets occurring during the deposition of the Bulldog Shale, and he termed these gamma, delta and epsilon. A direct comparison of Morgan's (1980) relative sea level curve with the one constructed in this study is presented in Fig.6.13.

As is evident from Fig.6.13 the CBH 2 palaeobathymetric curve exhibits a similar, though more detailed, succession of transgressions and regressions as that of Morgan (1980):

(i) sub-units α and β correspond to Morgan's (1980) initial transgression and highstand gamma;

(ii) the boundary between sub-units β and γ corresponds to Morgan's (1980) minor regression gamma, while sub-unit γ corresponds to Morgan's (1980) lowstand gamma;

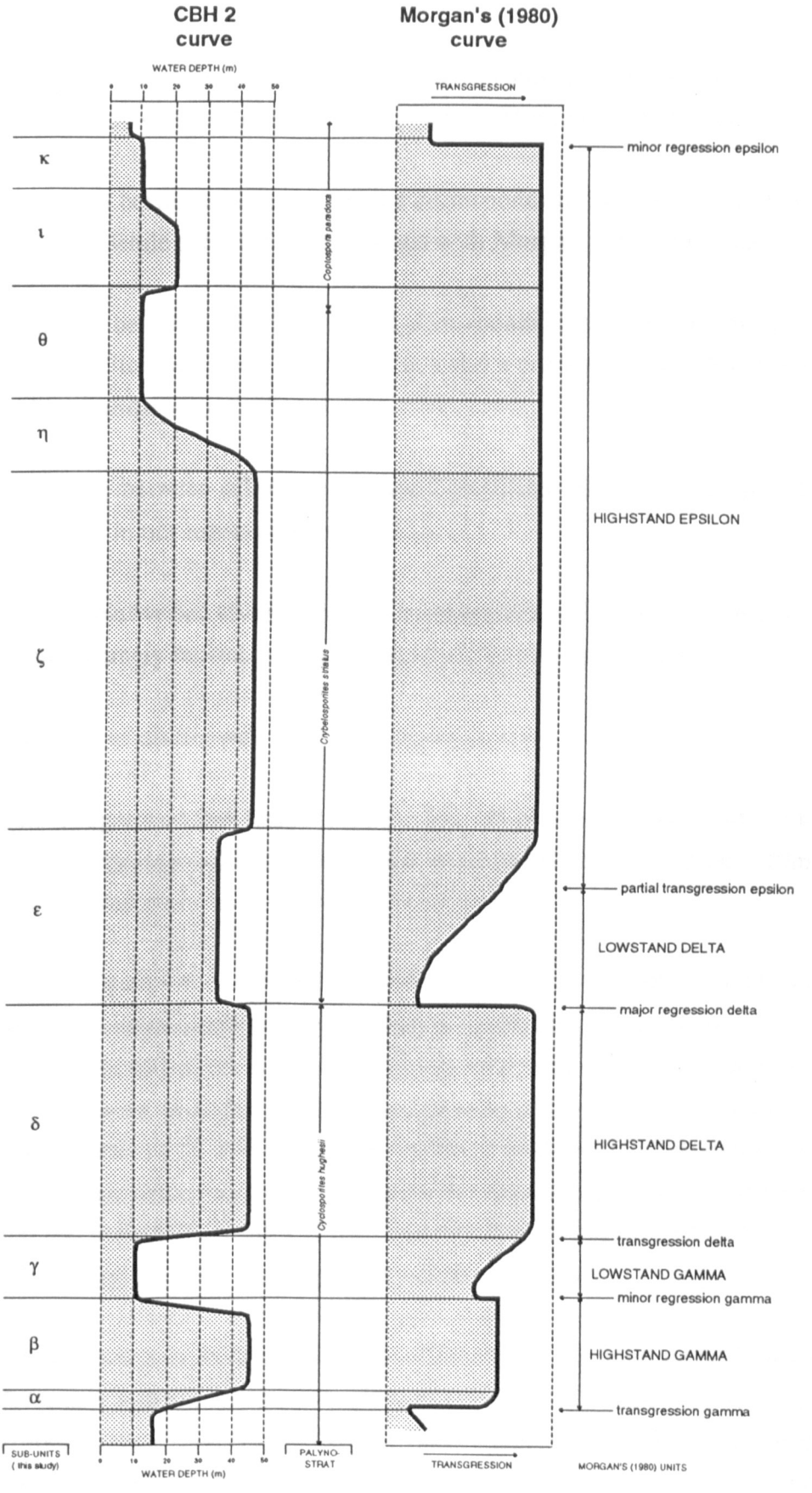

Fig.6.13 Comparison of the Bulldog Shale CBH 2 section palaeobathymetric curve with that of Morgan (1980).

(iii) the boundary between sub-units γ and δ corresponds to Morgan's (1980) transgression delta, while sub-unit δ corresponds to Morgan's (1980) highstand delta;

(iv) the boundary between sub-units δ and ε corresponds to Morgan's (1980) major regression delta, while sub-unit ε corresponds with Morgan's (1980) lowstand delta;

(v) the boundary between sub-units ε and ζ corresponds to Morgan's (1980) partial transgression epsilon, while sub-units ζ, η, θ, ι and κ correspond with Morgan's (1980) supposed highstand epsilon, and;

(vi) the boundary between sub-unit κ and the Coorikiana Sandstone corresponds to Morgan's (1980) minor regression epsilon.

While the two relative sea level curves fit together fairly well, there are certain discrepancies, namely between defined magnitude of events and dating.

The prime cases of discrepancy in event magnitude come at:

(i) The major regression that marks the boundary between sub-units β and γ, and which represents a shallowing event from near 50m water depth to approximately 10m depth, Morgan (1980) described as being only a minor event.

(ii) The minor regression that marks the boundary between sub-units δ and ε, and which represents only a slight shallowing event from a maximum of 50m depth to approximately 40-30m depth, Morgan (1980) defined as being a major event. However, Morgan (1980) went on to describe the transgression which marks the boundary between sub-units ε and ζ as being only a "partial transgression". Yet within the Bulldog Shale this transgression brought about the re-establishment of marine mud deposition and deposition of the thickest and most basinal Bulldog Shale sub-unit ζ, and clearly marks the reversal of an earlier minor regression.

(iii) Sub-unit ζ contains the thickest and most basinal of the Bulldog Shale mudstones, with PFT/A very much in dominance. However, Morgan (1980) considered that these were shallow water mudrocks, and that the lower mudstones of what is herein termed sub-unit δ represented the most open marine conditions of deposition during Bulldog Shale formation. In addition, the upper Bulldog Shale, that is to say sub-units ζ, η, θ, ι and κ, remain unresolved in Morgan's (1980) scheme, and thus this part of his sea level

curve does not contain details of the gradual regression of sub-unit η, the shallow water deposits of sub-unit θ, the transgression and more gradual regression of sub-unit ι, or the very shallow water deposits of sub-unit κ. Thus, Morgan's (1980) shallow water mudstone unit is in part deep water, and in part truly shallow water in its formation. Sub-unit κ is truncated by the overlying Coorikiana Sandstone, and it is likely that deposition of this resulted from a further minor regression, a description also used by Morgan (1980).

Discrepancies between the palaeobathymetric curves can also occur as a result of diachroneity in sub-unit deposition between sections. Morgan (1980) noted that all but one of the transgressions and regressions of the Bulldog Shale were at least slightly diachronous, with only the regression marked here by the boundary of Bulldog Shale sub-units δ and ε being isochronous.

Measurement of diachroneity of transgressions, regressions and the emplacement of certain sub-units is hampered by the lack of extensive palynostratigraphic sampling for each section. However, from those sections studied here it appears likely that the regression marked by the boundary of sub-units δ and ε was indeed isochronous throughout the studied section and roughly coincides with the *Cyclosporites hughesii* / *Crybelosporites striatus* palynostratigraphic boundary, though in no sections is this palynostratigraphic boundary exactly defined.

In addition, diachroneity is also evident within the upper Bulldog Shale of the section correlation presented here (Figs.6.01 to 6.05). In the eastern sections of Mount Yerila, SPH 1 and Skeleton 2, all of the upper sub-units (ε to κ) are representative of the *Crybelosporites striatus* spore-pollen zone. However, in the more westerly CBH 2 section, the boundary between sub-units θ and ι lies approximately at the boundary of the *Crybelosporites striatus* and *Coptospora paradoxa* spore-pollen zones, and thus both sub-units ι and κ originate from the younger zone. Furthermore, in the even more westerly Alford 1 section, both the sub-units η and θ are representative of the *Coptospora paradoxa* spore/pollen zone. Thus, it would appear that these upper Bulldog Shale sub-units were deposited progressively later towards the west of the basin. This observation indicates a diachroneity of sea-level change at this time within the basin, a feature probably related to distance from the link with the open ocean through the Carpentaria Basin, and associated basinal circulation patterns.

Finally, discrepancies between the palaeobathymetric curves presented herein and that of Morgan (1980) are likely to be at least partly due to the differing criteria used in their construction. It is evident from Fig.6.13 that the curves generated through integrated PFT analyses offer considerably more detailed insight into both local and regional sea level fluctuations and subsequent palaeoenvironmental changes, than those generated from broader and more disparate analyses.

Chapter 7

Discussion

7.1 Introduction

At the present time the Australian landmass covers in excess of 7 600 000 square km of the Earth's surface. During Aptian and Early Albian times up to approximately one third of this area was submerged beneath high global sea levels, which inundated a connected series of marginal and intracratonic basins (Fig.1.04). Largest of these basins was the Eromanga Basin of central Australia, in the south west of which the organic-rich argillaceous Bulldog Shale was deposited. At this time Australia was much further south than today, and the Eromanga Basin occupied palaeolatitudes between 65°S and 75°S.

In the following section the nature and implications of Bulldog Shale deposition are considered with reference to published models of organic-rich sediment deposition. In particular, sedimentation of those rocks within epeiric seas and under transgressive conditions is discussed, since the Bulldog Shale was deposited within the epeiric Eromanga Basin partly under transgressive conditions. Furthermore, the relevance of Bulldog Shale deposition to purportedly global events of organic-rich sediment deposition is considered. Section 7.3 considers the palaeoclimatic indicators of the Bulldog Shale, while section 7.4 deals with the changes in palaeobathymetry represented by the Bulldog Shale, and their local and global significance. Finally, section 7.5 compares the Eromanga Basin and Bulldog Shale deposition with other high palaeolatitude Cretaceous basins.

7.2 The Bulldog Shale: a black shale

The Bulldog Shale can be considered to be a black shale for it fulfils, at least in part, each of the two definitions of the term. Arthur *et al.* (1990, p.75) and Arthur and Sageman (1994) defined black shales as "sequences of variable lithology containing numerous beds with organic carbon (C_{org}) contents in excess of 1% by weight". As described earlier (§5.2.4), the Bulldog Shale has a mean C_{org} content of 1.52%. Another definition of the term black shale, originally proposed by Tyson (1987, p.52), and preferred by Wignall (1994), described black shales as "dark-coloured, fine grained mudrocks having the sedimentological, palaeoecological and geochemical

characteristics associated with deposition under oxygen-deficient or oxygen-free bottom waters". Large regions of the Bulldog Shale, namely those of PFT/A-E, fulfil these criteria.

In the current study the Bulldog Shale itself is observed to comprise variable lithology and C_{org} content. Some parts of the unit meet the criteria of both definitions of black shales, some regions meet just one definition's criteria, while others meet the criteria of neither definition. With such potential for confusion the term black shale is dropped from this study and more directly lithologically descriptive terms have been used. However, it should be recognised that the prerequisites required for, and the processes involved in deposition of black shale lithologies, as defined by various workers, provide important palaeoenvironmental implications regarding deposition of the Bulldog Shale. Of particular relevance are those factors promoting and encouraging black shale deposition within silled epeiric seas, in consideration of the fact that the Bulldog Shale was deposited in the silled and epeiric Eromanga Basin.

7.2.1 Black shale deposition: processes and implications

Black shales are typically, though not always, enriched in organic matter, and so some enhancement of organic matter preservation is required for their deposition. As defined by Tyson (1987), and later reviewed by Wignall (1994), there are five main factors controlling the preservation of organic matter: sediment texture and grain size, water depth and associated water column transit times for sinking organic matter, sedimentation rates, primary productivity and the rate of organic matter supply to the sediment, and bottom water oxygenation levels.

The only common theme in all published models of black shale formation is the presence of dysoxic to anoxic bottom waters, produced as a result of excessive oxygen demand and/or deficient oxygen supply (Wignall, 1994). Indeed, PFT analyses of the Bulldog Shale have indicated that considerable thicknesses of the unit were deposited under such low oxygen levels. There are two principle models which differently address the role of dysoxia/anoxia in black shale deposition. These are termed the preservation model and the productivity model.

Within the preservation model organic-rich sediments accumulate as a result of enhanced preservation of organic material in anoxic environments developed within a density stratified water column.

The productivity model, particularly championed by Pedersen and Calvert (1990), also involves low bottom water oxygen conditions, but in this case the dysoxia/anoxia is the result of high oxygen demand, unrelated to how much organic carbon is preserved. This high demand for oxygen is caused by enhanced biological productivity within the water column.

Opinion is still divided as to which of these models is correct, though it is likely that both may prevail in different places and at different times. It is certain, however, that the two models are incompatible, for high productivity requires large amounts of upwelling nutrients, a feature that does not occur with enhanced preservation beneath a stratified water column. In addition, the preservation model requires slow sedimentation rates while sedimentation rates for the productivity model are generally considered to be higher (Wignall 1994).

7.2.2 Black shale deposition within epeiric seas

The identification of the prevailing processes which lead to the deposition of black shales within silled basins such as the Eromanga Basin is relatively easy, for the restricted nature of the basins facilitates development of a density stratified water column and thus for enhanced preservation of organic matter. No increase in biological productivity need be inferred.

Density interfaces, or pycnoclines, are formed by the vertical separation of the water mass either into bodies of different temperature, in which case the density interface is termed a thermocline, or into bodies of different salinity, in which case the density interface is termed a halocline.

Bacterial decomposition of organic material that sinks from the surface waters and which reaches the sea bed uses oxygen. The development of a density interface within the water column prevents vertical mixing of the water body and the replenishment of the oxygen deficit from the surface, while the existence of the silled connections with the open ocean prevent the lateral movement of oxygen-rich water into the basin (Demaison and Moore, 1980). The Eromanga Basin was silled, with the Nebine Ridge separating the Eromanga Basin from the more easterly Surat Basin, and the Euroka Arch separating the Eromanga Basin from the more northerly Carpentaria Basin and the connection with the open ocean (Fig.1.01). With continued aerobic degradation of the organic material the oxygen in the restricted bottom waters is entirely utilised and

degradation proceeds via anaerobic bacterial respiratory pathways. Low oxygen levels prevent metazoan scavengers from utilising the organic matter, and it is their absence that leads to enhanced C_{org} preservation.

In addition to its silled nature, a basin must have a positive water balance for a pycnocline to be developed. For this, temperate climatic conditions with high annual amounts of precipitation are required (Demaison and Moore, 1980), features which may be inferred for the Australian Aptian-Albian climate (§7.3)

Shallow waters and seasonal anoxia

Tyson and Pearson (1991) noted that water depths in temperate shallow shelf and epeiric seas rarely achieved depths deeper than the mixing effects of winter storm waves. Indeed, during deposition of the Bulldog Shale, water depths are unlikely to have exceeded 50m. In modern settings winter waves act to break up any density stratification of the water column generated during the summer months. Black shale lithologies can be deposited within such settings however, for repeated annual development of a pycnocline and bottom water anoxia/dysoxia for 4 to 7 months precludes successful or long-term colonisation by benthic faunas and results in their elimination. The most likely pycnoclines in these settings are thermoclines developed at between 10-40m depth (Tyson and Pearson, 1991). These density interfaces form as a result of the heating of the surface waters by spring and summer warmth, and degrade due to autumn and winter cooling and increased wind stress. The development of haloclines, which are inherently stronger than thermoclines, are not considered to be the dominant type of density interface, for low salinity water does not usually spread out across an entire basin, but occurs in discrete plumes around the locations of freshwater inflow, causing localised effects only. Thermoclines can therefore be inferred for the Eromanga Basin during Bulldog Shale deposition since those parts of the formation apparently deposited under low oxygen levels, those of PFT/A-D, are laterally extensive around the basin and are not local features.

The Bulldog Shale exhibits evidence of having been deposited in conditions of varying and episodic dysoxia, in water depths of less than 50m and under considerable storm influence. Thus, Tyson and Pearson's (1991) seasonal anoxia model explains well the depositional conditions and their affect on the subsequent nature of the Bulldog Shale. In addition, black shale deposition within the Eromanga Basin was favoured by its silled nature, and through the probable presence of a positive water balance.

7.2.3 Transgressive black shales

Of direct relevance to the Bulldog Shale is a model presented by Wignall (1991) for the deposition of thick black shale successions within an epicontinental setting and under transgressive conditions. Bulldog Shale sub-units α, β, δ and ζ, which comprise the black shale-like material dominated by PFT/A-B and were therefore deposited under strongly dysoxic bottom-water conditions, were all deposited under transgressive conditions. Wignall's (1991) model proposed that black shales from these settings were deposited beneath a "puddle" of dysoxic to anoxic bottom water in the deepest parts of the basin as a result of pycnocline formation (Fig.7.01). Progressing from this situation, rapid sea level rise results in sediment starvation in the basin due to sediment entrapment in flooded river valleys. This decreased supply of sediment input, coupled with basin subsidence and sea level rise, results in rapid deepening of the water column, and thus a lateral expansion of the area covered by the oxygen-deficient bottom waters. Black shale deposits are thus laid down over previously shallow water or terrestrial sediments, the two sediment types separated by a basal transgressive lag or an unconformity. With a re-establishment of sediment influx aggradation of the sea bed occurs which outstrips any further sea level rise and thus results in relative shallowing of the basin and associated retreat of the oxygen-deficient bottom waters.

7.2.4 Anoxic oceanic events

The Aptian and Albian were times of widespread global deposition of black shales (Schlanger and Jenkyns, 1976; Frakes *et al.*, 1992; Francis and Frakes, 1993). This observation is of direct relevance to this study, since the Bulldog Shale was also deposited during the Aptian and Early Albian. The Aptian-Albian global black shale deposits arise from one of several such Cretaceous depositional events, with a similar distribution of black shales exhibited from sediments of Cenomanian-Turonian age. Of primary importance are the observations by Schlanger and Jenkyns (1976) and Arthur *et al.* (1990) that, during the Aptian and Albian and later during the Cenomanian and Turonian, black shale deposition was not limited to silled basins, but occurred over a variety of palaeobathymetric settings, including oceanic plateaux and basins, continental margins and shelf seas. This widespread nature of the deposits indicates that their deposition was not controlled by local basin geometry, but were the products of "oceanic anoxic events" (OAEs) (Schlanger and Jenkyns, 1976, p.179). In order to prevent confusion, Arthur *et al.* (1990, p.78) refined the term oceanic anoxic event to mean "time envelopes, during which the global ocean conditions were favourable for

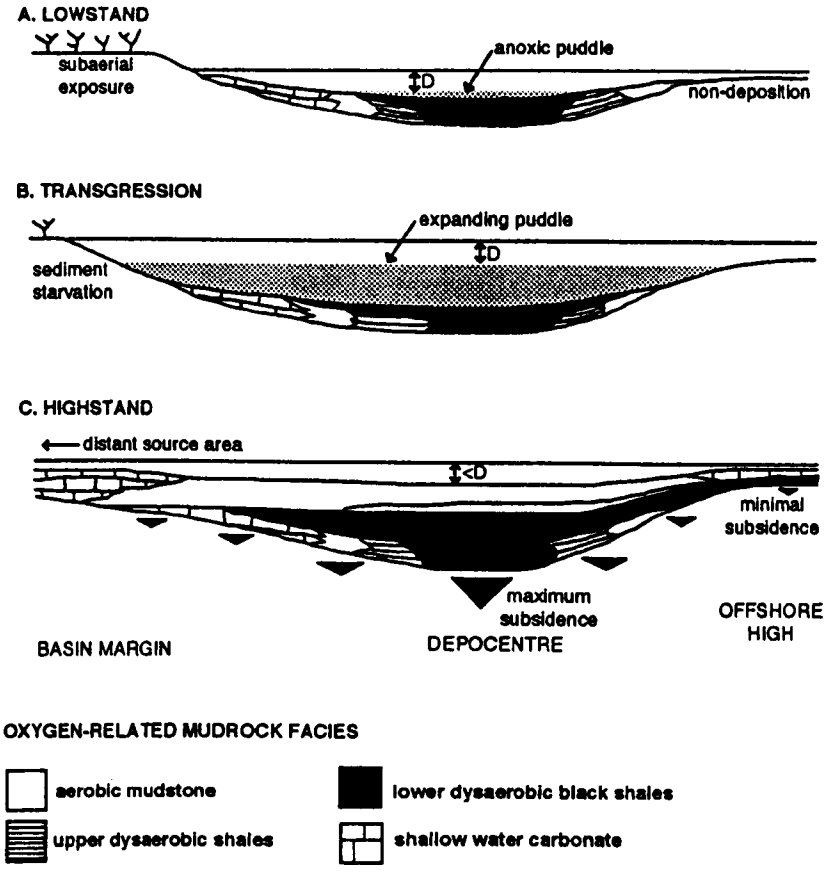

Fig.7.01 Model for the deposition of transgressive black shales in an epicontinental basin setting. D = critical water depth at which a permanent pycnocline is developed, with dysoxic to anoxic water trapped beneath it. A) During lowstand conditions, black shales only accumulate in the depocentres. In the Eromanga Basin this represents pre-Bulldog Shale deposition. B) A combination of sea level rise and associated sediment starvation, and continuing subsidence during the transgression causes marked expansion of the area of deep water and thus black shale deposition. In the Eromanga Basin these conditions are represented by Bulldog Shale sub-units α, β, δ and ζ. C) During highstand, marine conditions reach their maximum extent, but re-establishment of sediment influx causes shallowing of the water column. In the Eromanga Basin these conditions are represented by Bulldog Shale sub-units γ, ε, and η-κ. Redrawn from Wignall (1991).

the deposition of organic carbon-rich sediments (but not implying global total anoxia of deep water masses)". Implicit in this is the acceptance that either the preservation or the productivity models for black shale deposition may have prevailed, and this question has engendered considerable debate.

The Aptian-Albian OAE lasted approximately 22 million years (Arthur *et al.*, 1990), though it did not comprise a single coherent sequence of black shale deposition spanning this entire time. Rather, it comprised two separate oceanic anoxic sub-events (OASEs), namely one in the lower Aptian (correlative with the *Cyclosporites hughesii* spore-pollen zone in the Eromanga Basin (Fig.1.02)), and a second event later in the lower Albian (correlative with the *Crybelosporites striatus* spore-pollen zone in the Eromanga Basin (Fig.1.02)). A third OASE defined from the latest Albian occurred later than deposition of the Bulldog Shale. The time envelopes during which OASE black shale deposition occurred were very narrow, of perhaps less than 1 million years duration (Arthur and Sageman, 1994). Furthermore, the early Aptian OASE probably comprised a brief period of peak dysoxia/anoxia lasting less than 1 million years, within a longer 2-3 million year interval of intermittent oxygen deficiency which began in the late Barremian (Bralower *et al.*, 1994). This event may have been related to changes in climate, ocean chemistry and circulation, and sea level, possibly brought about by increased production of oceanic crust at mid-plate boundaries.

Causative factors for the OASEs may be invoked via both the productivity and preservation models (Frakes *et al.*, 1992; Francis and Frakes, 1993). In favour of the productivity model is the idea that higher rainfall and temperatures in a global climate of increased humidity would have led to a higher rate of nutrient supply to the oceans, thus aiding to increase productivity. Conversely, in favour of the preservation model is the assertion that the organic matter was preserved as a result of unusually low oxygen levels within bottom waters, which were only sluggishly mixed as a result of reduced circulation due to a low equator to pole temperature difference, and a lack of cold oxygenated bottom water flow from polar ice caps which were very restricted or non-existent at this time.

The temporal position of Arthur *et al.*'s (1990) lower Aptian and lower Albian OASEs are plotted on Haq *et al.*'s (1988) global sea level curve in Fig.7.02. This in turn is correlated with variations in the Bulldog Shale palaeobathymetric curve (§7.4.3), and it is evident that the lower Aptian OASE may be correlated with sub-units α and β of the Bulldog Shale, while the lower Albian OASE correlates with sub-units δ and ε. Of

particular importance is the fact that both sub-units β and δ represent thick successions of clay-dominated sediments, deposited in relatively deep dysoxic basinal conditions in response to sea level rise. Therefore, the deposition of these sub-units appears to be related to global patterns of sea level change. However, the invocation of a mechanism for global black shale deposition, as proposed by Schlanger and Jenkyns (1976) and Arthur *et al.* (1990), is not required to explain the deposition of the Bulldog Shale. Such an opinion was also taken by Haig and Lynch (1993) regarding deposition of the Toolebuc Formation, in response to Arthur *et al.*'s (1990) consideration that this unit was deposited as a result of a late Albian OASE. Rather, deposition of the Bulldog Shale, and those parts of it that represent deposition within dysoxic basinal conditions, can be explained simply through the silled and epeiric nature of the Eromanga Basin, and the affect of marine transgression on depositional processes within the basin, as described in Wignall's (1991) model for black shales deposited under transgressive regimes. In essence, deposition of the Bulldog Shale occurred in response to local conditions, mediated by both global and local controls on sea level.

7.3 Bulldog Shale climatic indicators

As noted in §1.1, Aptian and Albian climates of high palaeolatitude areas, such as the Eromanga Basin, were likely to have experienced at least seasonal freezing conditions. Two important features of the Bulldog Shale have important implications, not only for local palaeoenvironments and palaeoclimates, but also for the regional and even global palaeoenvironments and palaeoclimates prevailing during the Aptian and Albian. These components are lonestones (§1.2.2; 2.6) and glendonite nodules (§2.8).

7.3.1 Lonestones

Large exotic pebbles, cobbles and boulders occur in both the Cadna-owie Formation and the Bulldog Shale, reaching their maximum abundance and greatest dimension in the basal Bulldog Shale (Krieg *et al.*, 1991). Many of the Bulldog Shale boulders reach up to 1m across, with some attaining longest dimensions in excess of 3m. These boulders are mainly of locally derived Adelaidean quartzite, but other lithologies are present. Indeed, Flint *et al.* (1980) recorded fossiliferous Lower Devonian quartzite boulders with probable source areas to the east in New South Wales, with transportation to South Australia by ice in the Permian glaciation. In addition, Ambrose and Flint (1981) recorded small numbers of acid porphyry boulders, probably derived from the Gawler Ranges, and boulders of banded chalcedony.

Four potential mechanisms have been proposed for emplacement of the lonestones within typical Bulldog Shale material (Ambrose and Flint, 1981). Perhaps the most convincing argument, and certainly the most popular, is that the exotic clasts were rafted into the basin encased within, or resting on, ice, which subsequently melted allowing the rock material contained within it to fall to the sea bed. This theory has been proposed several times, namely by Brown (1905), Jack (1915), Woolnough and David (1926) and most recently and persuasively by Frakes and Francis (1988). Whereas the earlier workers invoked the action of glaciers, for which there is no independent supporting evidence, a factor which caused Flint *et al.* (1980) to discard this theory, Frakes and Francis (1988) suggested that the transportation of the exotic clasts was by marine shore ice or river ice developed in a seasonally freezing climatic regime. In addition, the penetration structures in the laminae below the clasts indicated that they were dropstones, entering the sediment after falling vertically through the water column, an observation also made in this study; indeed, no evidence of lonestone emplacement by lateral flows has been found. The origin of the clasts from river beds or shorelines explains their typically well rounded nature. Independent evidence in support of this theory exists in the form of glendonite nodules which have been reported from Bulldog Shale material, and for which it is known that cold bottom water conditions are required for their formation (§7.3.2). Quartz sand grains with surface textures characteristic of glacial regimes are also associated with the exotic clasts, and poorly sorted diamictite-like layers, commonly associated with lonestones, probably represent finer grained fluvial and shore material also entrained within the winter ice. The distribution of the exotic clasts within the Bulldog Shale in an arc around the southern margin of the Eromanga Basin may also represent further evidence in favour of ice-rafting as the dominant mechanism (Krieg *et al.*, 1991).

Woolnough and David (1926) and Wopfner *et al.* (1970) observed that the clasts exist in Bulldog Shale which also bears fossilised tree material, and they thus considered the hypothesis that the boulders were rafted into the basin in the roots of fallen trees. This hypothesis was discarded however, as a viable mechanism for transportation and emplacement of the clasts, with Woolnough and David (1926) discarding the idea altogether in favour of the ice rafting mechanism, on the basis that even vast rafts of timber could not be responsible for such a large number of weighty clasts. Wopfner *et al.* (1970) were more guarded and accepted that tree rafting of clasts may be responsible for some, but by no means all of the material observed. Frakes and Francis (1988) also discarded tree rafting as the transporting mechanism for similar reasons to those outlined above. In addition, Francis (pers. comm. 1993) noted the global abundance of

wood-rich shales deposited at this time but, as described in Frakes and Francis (1988), the existence of shales containing exotic clasts is limited to those black shales deposited at high palaeolatitude, further evidence in favour of the ice-rafting mechanism.

The final two mechanisms involve the downslope movement of the boulders from shorelines located on basement highs over low angle slopes, under the action of gravity either by slow sediment creep (Wopfner *et al.*, 1970), or within episodic debris flows (Flint *et al.*, 1980). However, Frakes and Francis (1988) considered that these theories could be discarded owing to the lack of features characteristic of mass-movement processes, and to the nature of the deformed sediment around the clasts indicating vertical not lateral emplacement, features also noted in this study.

More recently, Frakes and Krassay (1992) have inferred ice-rafting for the emplacement of exotic clasts within mudstones of the Carpentaria Basin similar in age to the Bulldog Shale.

7.3.2 Glendonites

Glendonite nodules have been recovered from Bulldog Shale material in the present study, and by Sheard (1990) from Petermorra Creek site VII (§2.8). Glendonite nodules are stellate aggregations of certain crystal types, though as noted by Sheard (1990) the glendonites of the Bulldog Shale are pseudomorphs of calcite and gypsum after the original material, most commonly ikaite. Two distinct morphological types of Bulldog Shale glendonite are recovered from the Petermorra Creek site VII locality. The most common glendonites from the Bulldog Shale comprise small (individual crystals less than 15mm across in cross-section) tight stellate forms; less common, though still significant in number are larger forms with distinct bladed and curved faces and edges (§2.8; Fig.2.30). Ikaite is unstable above 5°C and reverts to white microcrystaline calcite and water rapidly above this temperature (Jansen *et al.*, 1987; Kemper, 1987; Sheard, 1990). Clearly the existence of glendonite nodules, particularly in rocks containing numerous apparently ice-rafted boulders, is a beguiling indicator that bottom waters of the Eromanga Sea, and regional palaeoclimates in the Eromanga Basin region at the time of Bulldog Shale deposition, underwent at least seasonal periods of cool and freezing conditions.

7.3.3 Other analyses

The climatic regime inferred from the presence of lonestones and glendonites from the Bulldog Shale is also indicated by palaeontological and isotopic studies, and by computer modelling.

Palaeontology

During the Cretaceous, diverse and lush forests existed within the northern and southern polar (and peripolar) regions (Francis and Frakes, 1993). The plants and animals of these forests must have been physiologically adapted to the long months of winter darkness experienced at these latitudes, though larger animals, including dinosaurs, may have migrated elsewhere for the winter.

In the Southern high latitude region, Dettmann (1986) and Drinnan and Chambers (1986), working on the palynoflora and flora respectively, of the Early Cretaceous (?Barremian - Albian) Koonwarra Fossil Bed of the Gippsland Basin in Victoria, inferred a cool climate with some seasonality. Waldman (1971) and Jell and Duncan (1986) working on fish and invertebrates from the Koonwarra Bed, linked apparent mass mortalities of organisms to anoxic water conditions developed beneath a winter cover of ice. Implicit in this conclusion is the existence of seasonality.

Of particular importance to the present study are Frakes and Francis' (1990) tree-ring analyses of permineralised wood from the Bulldog Shale and the underlying Cadna-owie Formation of the southwestern Eromanga Basin. This wood represents the remains of trunks and branches washed into the basin from bordering forests. Growth rings from the wood are clear and well defined, a feature of strongly seasonal growth; in addition, the rings vary little in thickness from year to year, indicating reasonably uniform climatic conditions. However, two separate populations of wood with different ring characteristics were defined, an indication that the two groups grew at different rates. The population with the narrower rings originated from environments relatively unfavourable for trees where slow growth only was attainable, a similar situation to that observed in living trees from cold temperate mountainous regions of South America. Here, the slow growth rates are due to a continuously cold and wet climate with a mean annual temperature of 6.0°C and an annual range of only 4.0°C. The second population with the larger rings, representative of a faster growth rate, probably originated from regions more favourable to tree growth, similar to modern southern hemisphere forests of temperate types in areas of warm summers and cool winters. These two separate

populations were taken to represent two forest sources growing in different climates, transported and mixed by rivers draining into the Eromanga Basin. Frakes and Francis (1990) proposed that the trees of the slower growing population grew in highland areas to the south of the Eromanga Basin, while the faster growing trees originated from forests growing at lower altitudes closer to the basin shoreline.

Oxygen isotopes

Analysis of oxygen isotope ratios preserved in the mineral skeletons of marine organisms provides important information regarding past temperatures of the oceans. Studies of oxygen isotope ratios from various sites have indicated that equatorial surface water temperatures during the Cretaceous were similar to today's, at approximately 28-30°C, however the equator to pole temperature difference was considerably less than at present (Francis and Frakes, 1993; Sellwood *et al.*, 1994). Furthermore, polar sea surface temperatures may have been as low as 0°C, and thus the formation of sea ice in the polar regions during the cold winter months would have been possible.

Of more local relevance to the Eromanga Basin are palaeotemperature data obtained from the Otway and Gippsland Basins of Victoria, and the Carnarvon Basin of Western Australia, which in the Early Cretaceous occupied slightly higher and lower palaeolatitudes than the Eromanga Basin, respectively. Studies of the oxygen isotopic composition of calcite from early-diagenetic carbonate concretions from the Valanginian to Albian continental fluvial deposits of the Otway and Gippsland Basins indicated that the mean annual temperature experienced in this region of the Early Cretaceous world was less than 5°C, and possibly below 0°C (Gregory *et al.*, 1989). These palaeotemperature estimates are sufficiently low to infer the existence of permanent ice within the southern polar circle if the land masses were sufficiently uplifted. Furthermore, palaeotemperature values obtained from oxygen isotope analyses of belemnite guards from the Albian Gearle Siltstone of the Carnarvon Basin has produced mean palaeotemperature values of approximately 10.1°C (Pirrie *et al.*, 1995) .

Elsewhere, a mean palaeotemperature for the Aptian and Albian Kotick Point Formation, from James Ross Island off the Antarctic Peninsula, of 10.1°C has also been calculated (Ditchfield *et al.*, 1994). During the Early Cretaceous this region occupied similar palaeolatitudes to the Eromanga Basin.

Computer modelling

Detailed computer models of Cretaceous climate support the seasonally freezing view of high palaeolatitudes. For varying combinations of equator to pole sea surface temperature gradients, polar warmth conditions, geography and topography, equable (i.e. ice-free) climates in continental interiors at middle and high latitudes were not produced by these models due to strong seasonality effects in these regions (Sloan and Barron,1990; Crowley and North, 1991). For example, Barron and Washington (1982) calculated Cretaceous Australian surface temperatures of +17°C for the Austral summer and -13°C for the Austral winter. Warm summers probably prevented the occurrence of permanent ice cover (Sloan and Barron, 1990).

These models also support the hypothesis that equator to pole temperature differences were less distinct in the Cretaceous. For example, Barron (1983) calculated Cretaceous equator to pole temperature differences of 17° to 26°C, as compared to the present day temperature difference of 41°C.

7.3.4 Seasonally freezing climates and the Bulldog Shale

It is evident, from the evidence presented in section 7.3, that during the Aptian and Albian, southern high latitude climates were cool, with at least seasonal freezing. Within this climatic regime the Bulldog Shale was deposited in the epeiric Eromanga Basin. Parts of the Bulldog Shale were laid down in strongly oxygen-deficient conditions resulting from deepening of the water column due to marine transgression, and associated seasonal density stratification. Variations in Bulldog Shale PFTs are therefore related to changes in water depth. There is no evidence to link PFT variations with climatic or temperature change, save for the affects these may have on sea level. Indeed, neither the occurrence of lonestones or glendonites can be linked to specific PFTs. The potential exists perhaps for a study which incorporates PFT and palaeotemperature (oxygen isotope) analyses throughout the Bulldog Shale succession. However, a correlation between the two is considered unlikely since the observed PFT variations are well explained through water depth variations and associated changes in bottom-water oxygenation levels and environmental energy levels.

7.4 Bulldog Shale palaeobathymetry

7.4.1 The roles of eustasy, sediment supply, epeirogeny and local tectonics

In his study of eustasy in the Cretaceous of Australia, Morgan (1980) concluded that the Great Australian Basin, of which the Eromanga Basin comprises a major part, was one in which the distribution of environments was affected principally by eustasy, and that variations in the vertical motion of the continent and in sediment supply comprised but minor factors. While Morgan's (1980) sea level curve (Fig.1.02) for the Cretaceous sediments of the Australian intracratonic basins has proved extremely useful, subsequent studies have indicated that both vertical motion of the Australian continent and variations in sediment supply play important roles in the development of the Eromanga Basin, and control the extent and duration of the marine incursions so evident in the sedimentary record.

For example, while the transgressive pulse which preceded Toolebuc Formation deposition broadly coincides with Albian transgressions reported elsewhere from passive margins and epeiric basins, the consistently high sea level evident during the middle and late Albian and the regression which terminated marine deposition in the Eromanga Basin, do not correlate with events on other continents or the general pattern of eustasy recorded on the curve of global sea level by Haq *et al.* (1988) (Haig and Lynch, 1993). Indeed, during the middle to late Albian, Australian sea levels may have been increasingly influenced by continental subsidence and uplift associated with the tectonic climax in the volcanic arc along the eastern margin of the continent, as advocated by Veevers (1984, 1991). The Aptian/Albian marine incursion over Australia 110-95 Ma, which facilitated Bulldog Shale deposition, was caused by subsidence of the Australian continent by approximately 150m, together with a sea level rise from -30m in the Late Jurassic to +75m (relative to the present-day sea level) in the Aptian and Albian; and the latest Albian to Cenomanian regression was the result of rapid uplift of the continent by about 280m, followed by relaxation and subsidence by approximately 180m during the Cenozoic (Veevers, 1984).

Furthermore, during the Cretaceous the observed inundation of Australia is out of phase with published global eustatic sea level curves; in particular the late Albian regression occurred approximately at a time when global sea level was considered to be near maximum height, as illustrated by Haq *et al.* (1988) (Russell and Gurnis, 1994). Indeed, sea level curves for basins of the Australian western margin closely resemble Haq *et*

al.'s (1988) global curve, a feature which supports the hypothesis that Australia experienced several episodes of potentially craton-wide vertical motion during the Cretaceous. However, models of simple continental subsidence and/or tilting have been unable to recreate the flooding experienced during the Aptian and Albian, and therefore much of this marine inundation may have resulted from rapid small-scale regional motions (Russell and Gurnis, 1994).

To add further complication, the formation of the Eromanga Basin was characterised by a gradual increase in the extent of sedimentation with localised subsidence from Late Triassic to Early Cretaceous, and a large extension of sedimentation with rapid subsidence during the Early and Middle Cretaceous, followed by local and gradual subsidence (Zhou, 1989; 1993). Indeed, apparent subsidence rates of the Eromanga Basin have been calculated to have increased by a factor of 5-10 during the Early Cretaceous, the rapid subsidence corresponding to a large influx of volcanogenic detritus from the convergent eastern Australian margin (Gallagher *et al.*, 1994).

Sea level rise and fall in the Eromanga Basin was controlled partly by eustacy, but the expression of this over the entire basin and in different areas of the basin has been modified by different rates of sedimentation and variation in continental uplift and depression (Haig and Lynch, 1993). These findings hold important implications when considering the global significance of marine events and occurrences of basin anoxia within the Australian epeiric basins. In particular Haig and Lynch (1993) argued against Arthur *et al.*'s (1990) invocation of a global anoxic event to explain the deposition of the Toolebuc Formation, for they suggested that deposition of this unit, confined to the central regions of the enclosed and silled Eromanga Sea, was the consequence of high-water lag after a transgressive pulse that lead to peak sea levels in many areas. This transgression could have been global in extent as its pattern of expression within the marginal and intracontinental Australian basins would suggest (greatest transgression was experienced in those basins closest to the open ocean), or it may have been associated with increased tectonism along the eastern continental margin and subsequent continental tilting, as reflected by an increase in volcanogenic sediment deposited in the Australian basins during the early Albian.

7.4.2 Comparison with other Australian basins

As described previously (§6.4.1), the palaeobathymetric curve presented in this study broadly correlates with that of Morgan (1980). Morgan (1980) compared his sea level curve for the Early and middle Cretaceous of the Eromanga Basin, with palaeobathymetric information obtained from sediments of the same age from other Australian epicontinental and marginal basins.

From the correlation of the Bulldog Shale palaeobathymetric curve with Morgan's (1980) descriptions, it is evident that a similar sequence of relative sea level changes can most clearly be identified/correlated in sediments from the other interlinked constituent basins of the Great Artesian Basin complex. Elsewhere in Australia, from marginal continental basins, while parts of the Eromanga Basin sea level curve can be identified, the sequence has been modified through tectonic activity, and in places, by periods of sustained erosion.

More detailed work on sedimentary cycles of the Jurassic and Cretaceous sediments of the Surat Basin, which forms part of the Great Artesian Basin complex and was linked to the Eromanga Basin at the time of Bulldog Shale deposition (Fig.1.01; 1.04), allowed the definition of two Cretaceous transgressive-regressive sedimentary successions (Exon and Burger, 1981) (Fig.7.02). These correspond with the following sub-units of the Eromanga Basin Bulldog Shale palaeobathymetric curve:

(i) sub-unit α transgression to sub-unit δ-ε boundary regression;

(ii) sub-unit ε-ζ boundary transgression to sub-unit η-κ regression.

These sedimentary cycles were related by Exon and Burger (1981) to the global sea level curve defined by Vail *et al.* (1977) (§7.4.3), though they did advocate the possibility of some local tectonic influence.

More recently, Burger (1986) defined three early Aptian - Middle Albian transgressive - regressive sedimentary cycles from the north east Eromanga Basin in Queensland, the south west Eromanga Basin in South Australia (Oodnadatta 1 section), and the Surat Basin. These sequences tie in with those of the Bulldog Shale palaeobathymetric curve presented here (Fig.7.02). Thus, it is evident that the Surat Basin did experience all

three relative increases and decreases in sea level defined for the Eromanga Basin at this time. These three cycles are represented by the following sub-units:

(i) sub-unit α transgression to sub-unit β-γ boundary regression;

(ii) sub-unit γ-δ transgression to sub-unit δ-ε regression;

(iii) sub-unit ε-ζ boundary transgression to sub-unit η-κ regression.

7.4.3 Palaeobathymetry of the Eromanga Basin and global considerations

Epeirogeny and local tectonics played an important part in the marine flooding history of the Eromanga Basin, indeed the role of epeirogeny may be considered to have been central to the story. As described previously (§7.4.1), epeirogenic subsidence, coupled with an approximately synchronous eustatic rise in sea level, was responsible for the initial flooding of the Eromanga Basin and associated members of the Great Artesian Basin during the earliest Aptian. Indeed, according to the figures provided by Veevers (1984) (§7.4.1), without epeirogenic subsidence the fortuitously contemporaneous eustatic marine transgression would not have flooded the Eromanga Basin at all.

Later, during the Albian Australia experienced epeirogenic uplift (§7.4.1), which resulted in the complete withdrawal of marine conditions from the Eromanga Basin at a time when global eustatic sea levels were reaching their maximum height (Haig and Lynch 1993; Russell and Gurnis 1994). Furthermore, Russell and Gurnis (1994) had to invoke local tectonic movements in order to recreate the Eromanga Basin Aptian and Albian flooding pattern (§7.4.1), and Zhou (1989; 1993) and Gallagher *et al.* (1994) reported large variations of subsidence and sedimentation rates within the Eromanga Basin during the Early Cretaceous.

Comparison with published sea level curves

From the above discussion an impression may be given that the identification of eustatic-driven global sea level variations from Bulldog Shale sediments is not possible. This is not the case, however, for comparisons of the Eromanga Basin palaeobathymetric curve with those of other contemporaneous deposits located on other continents indicate some measure of similarity.

Comparisons between the Bulldog Shale palaeobathymetric curve with those of other contemporaneous deposits located on other continents, and global curves for onlap or eustacy derived from many individual sections, are given in Fig.7.02.

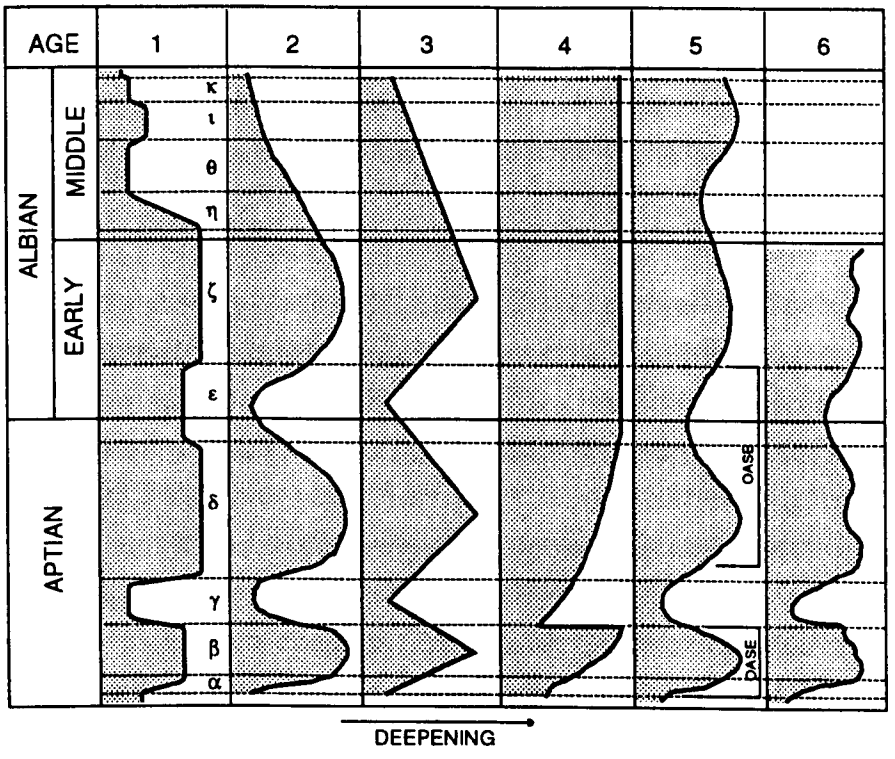

Fig.7.02 Comparison of the Bulldog Shale palaeobathymetric curve with other palaeodepth and eustatic curves for the Aptian - Middle Albian:
(1) Palaeobathymetric curve of the Bulldog Shale, from this study;
(2) Scott *et al.*'s (1988) palaeodepth curve for the Texas Gulf coast;
(3) Cooper's (1977) curve of global relative coastal onlap (originally defined as eustatic curve);
(4) Vail *et al.*'s (1977) curve of global relative coastal onlap (originally defined as eustatic curve);
(5) Haq *et al.*'s (1988) curve of global eustatic changes, and position of Arthur *et al.*'s (1990) Aptian and Albian OASEs;
(6) Ruffell and Wach's (1991) curve of relative sea level for the Lower Greensand of south east England.

From Fig.7.02 it is evident that the Bulldog Shale palaeobathymetric curve exhibits considerable similarity with the other palaeobathymetric and eustatic curves, and thus a eustatic component is evident within the Bulldog Shale succession.

In particular, the Bulldog Shale palaeobathymetric curve resembles Scott *et al.*'s (1988) palaeodepth curve for the Texas Gulf coast and Cooper's (1977) curve of global relative coastal onlap. Each of these curves exhibit the three transgressive and regressive Bulldog Shale cycles, the effects of which were evidently contemporaneous. Detail is sufficient to note that the final regression (sub-units η-κ) in both curves has a gradual nature as in the Bulldog Shale palaeobathymetric curve. Vail *et al.*'s (1977) curve of global coastal onlap lacks the detail of Cooper's (1977) curve and comprises only two relative deepening events separated by a shallowing event. However, Vail *et al.*'s (1977) curve does exhibit the sub-unit α transgression and the sub-unit β-γ boundary regression.

In comparison with the eustatic curve of Haq *et al.* (1988) the Bulldog Shale palaeobathymetric curve exhibits considerable differences. While all the relative deepening and shallowing events defined in the Bulldog Shale curve can be picked out in Haq *et al.*'s (1988) curve (Fig.7.02), the upper part of the two curves are very different. While the Bulldog Shale curve from sub-unit η to κ exhibits a generally regressive nature, related in part to the epeirogenic uplift of Australia, the global eustatic curve of Haq *et al.* (1988) exhibits a generally transgressive nature, related to the gradual increase in sea levels up to the Cenomanian maximum. Ruffell and Wach's (1991) curve of relative sea level for the Lower Greensand of south east England is unaffected by epeirogenic processes, and exhibits similar trends to that of Haq *et al.* (1988).

In conclusion, it is evident that while epeirogeny may have been the driving force behind the initial flooding of the Eromanga Basin during the latest Neocomian and earliest Aptian, and the withdrawal of marine conditions from the Eromanga Basin during the Upper Albian and Cenomanian, intervening eustatic sea level changes have left their imprint on the sediments of the Bulldog Shale. The palaeobathymetric curve produced for the Bulldog Shale is therefore a record of epeirogeny and eustacy, and the effects of each can be defined. In addition, the Bulldog Shale palaeobathymetric curve probably also incorporates the affects of local tectonics and variations in sedimentation and subsidence rates, these factors are, however, much more difficult to define.

7.5 Comparison of the Eromanga Basin to other high latitude Cretaceous basins

During the Aptian and Albian, at the time of Bulldog Shale deposition in the Eromanga Basin, deposition of similar sediments was also occurring in other basins of high palaeolatitude. Three examples of these basins and their Aptian and Albian sediments are briefly described here.

7.5.1 James Ross Basin

Early Cretaceous palaeolatitude: 60°S (Ditchfield *et al.*, 1994).

During the Mesozoic and Tertiary, the Antarctic Peninsula was a site of active arc magmatism, and major Mesozoic sedimentary basins were developed in both fore and back arc settings (Ditchfield *et al.*, 1994), a very different setting from that of the epicontinental Eromanga Basin, though a volcanic arc did exist to the east of the Eromanga Basin during the Cretaceous. Of importance here is the James Ross Basin, a sub-basin of the back-arc Larsen Basin (Fig.7.03).

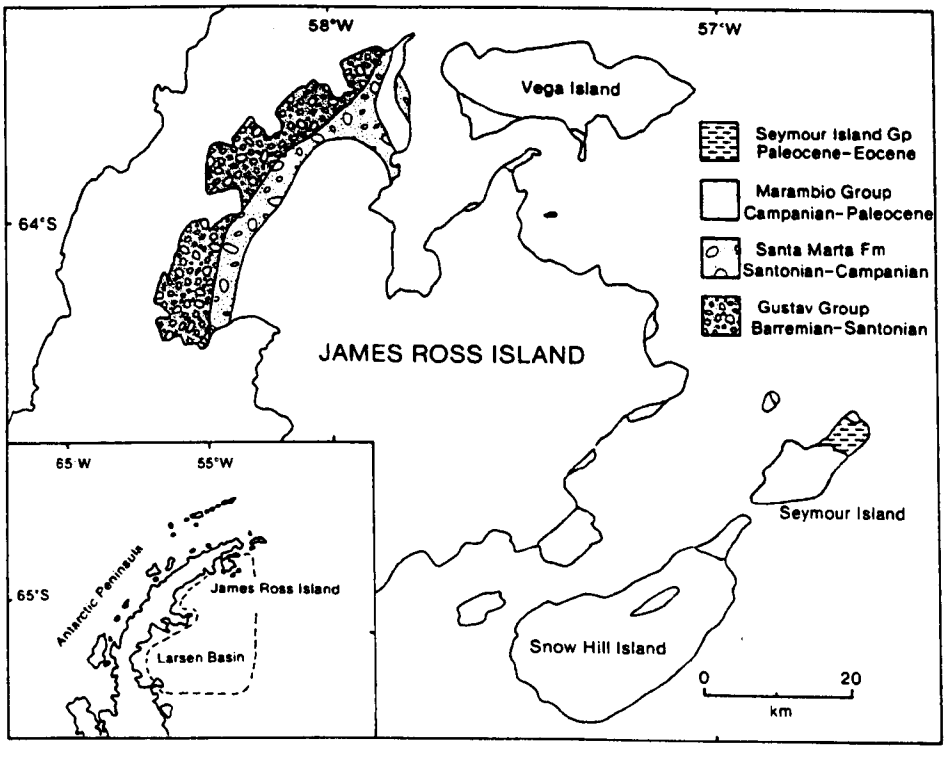

Fig.7.03 Locality map of James Ross Island and the Larsen Basin. From Pirrie and Marshall (1991).

During the Aptian and Albian sediments of the Kotick Point and Whisky Bay Formations of the Gustav Group (Fig.7.03) were deposited within the James Ross Basin, and are now exposed on James Ross Island. The Gustav Group comprises sediments proximal to the palaeoshoreline but from water depths between 300m and 1000m (Ditchfield *et al.*, 1994), representing two contrasting depositional systems: mud-rich deposits of slope apron systems in which sedimentation is controlled largely by intrabasinal tectonics; and conglomeratic sediments of submarine fan systems (Ineson, 1989). Of particular relevance to the present study is the Kotick Point Formation, which dates from the Aptian to middle Albian (Ineson, 1989), and is thus a temporal equivalent of the Bulldog Shale.

The Kotick Point Formation is largely mud dominated, representing deposition principally in a slope apron system setting, and reaches up to 700m thick. The unit comprises laterally persistent interbedded sandstone and mudstone units in which bioturbation is common. The sandstone beds bear planar lamination and cross lamination, and were defined by Ineson (1989) to represent deposition from low density turbidity currents. Muddy mass flow deposits and allochthonous blocks emplaced by sliding are also recorded. The presence of material deposited by turbidity currents and mass flow processes testifies to the steepness of the tectonically-controlled basin margin, very different from the gentle gradients of the Eromanga Basin margin. Erosional features are rare however, and sedimentary structures are indicative of deposition within a low energy, sub-wave base setting, similar to that considered for much of the Bulldog Shale. The middle of the Kotick Point Formation contains a prominent conglomeratic member, representative of deposition within a gravely submarine fan setting, and is similar to much of the overlying Whisky Bay Formation.

Trace fossils of the Kotick Point Formation include *Chondrites*, *Phycosiphon* (dissimilar to Bulldog Shale *Anconichnus* material), *Ophiomorpha*, *Planolites*, *Teichichnus* and *Zoophycos* (Ineson, 1987). *Planolites*, *Chondrites* and *Phycosiphon* are ubiquitous and independent of sedimentary facies, *Zoophycos* and to a lesser extent *Teichichnus* are restricted to muddy horizons, and *Ophiomorpha* are restricted to coarse-grained facies. These assemblages are similar to those from the Bulldog Shale, though the presence of *Zoophycos* is probably indicative of deposition in deeper water conditions. Ineson (1987) considered that the trace fossils from the Gustav Group sediments reflect only local environmental conditions of substrate type, energy level and oxygenation levels. However, detailed analysis utilising the PFT methodology may

provide for the definition of broader scale palaeoenvironmental (palaeobathymetric) variation.

7.5.2 Svalbard Basin

Early Cretaceous palaeolatitude: 65°N (Frakes and Francis, 1988).

Throughout much of the period from Devonian to Tertiary, Svalbard was covered by a broad basin (Fig.7.04), which experienced near-continuous deposition. Periods of active deposition or hiatus were governed, in part, by local and regional tectonics, and by global eustatic variations (Aga *et al.*, 1986).

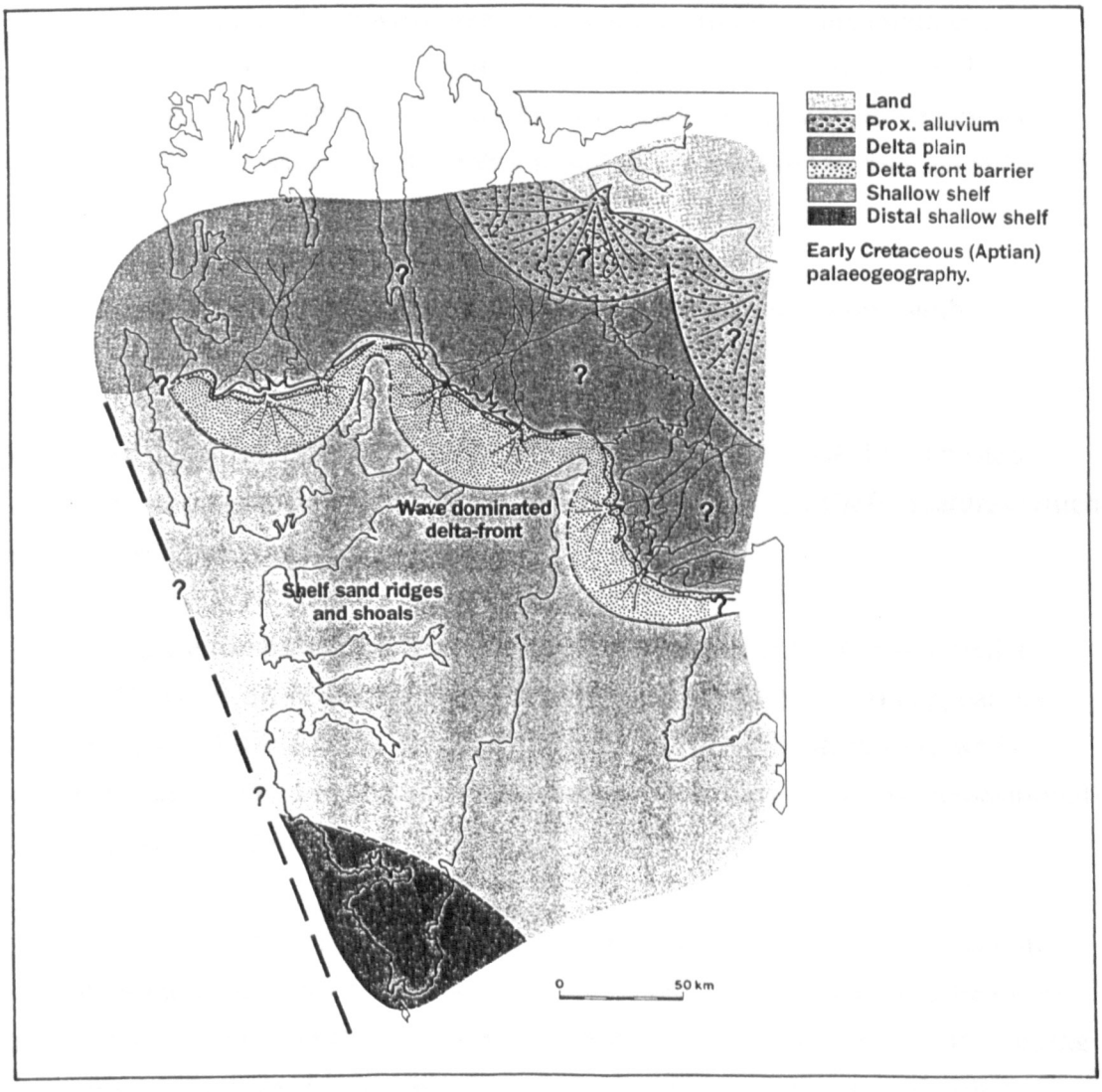

Fig.7.04 Locality map of the Svalbard Basin. From Aga *et al.* (1986).

Aptian and Albian deposition is represented by the Carolinefjellet Formation (Parker, 1967), which comprises highly bioturbated shallow water marine shales and sandstones deposited in a shallow marine shelf setting. The Carolinefjellet Formation is divided into three members which are, from the base, the Dalkjegla, Innkjegla and Langstakken members.

The Dalkjegla Member comprises sandstone-dominated, shallow water, possibly tidally influenced deposits, from which Nottvedt and Kriesa (1987) recorded high levels of hummocky cross-stratification. Deposition under the influence of waning storm conditions is therefore implied, and similarities are noted with PFT/F and G from the Bulldog Shale.

The Innkjegla Member comprises a thick shale and siltstone sequence with occasional thin sandy interbeds. Fossilised wood and cone-in-cone structures are common. Shallow, low energy conditions are implied for the deposition of this unit, and similarities are noted with PFT/A-E of the Bulldog Shale, though no information is given regarding trace fossils and ichnofabrics, and therefore considerable scope for further study exists.

The Langstakken Member marks a return to shallower water conditions, with interbedded sandstone and shale horizons.

Deposition of these bathymetrically different sediments can be related to repeated phases of deltaic progradation and lobe abandonment (Aga *et al.*, 1986), features which are not observed from the Bulldog Shale.

No details of trace fossils and ichnofabrics have been given for the Carolinefjellet Formation. However, from descriptions given by Parker (1967) it would appear that during deposition of this unit the bottom waters of the Svalbard Basin were well-oxygenated, and no apparent intervals representative of anoxic or dysoxic depositional conditions have been defined.

Conditions were not always like this in the Svalbard Basin however. In the Jurassic, deposition of the Janusfjellet Subgroup and its two constituent formations, the lower Agardhfjellet Formation and the upper Rurikfjellet Formation did occur under varying oxygenation levels. Indeed, one interval from the lower part of the Agardhfjellet Formation was deposited under probable anoxic conditions, preserved as an interval of

unbioturbated paper shales with organic carbon levels of up to 12% (Dypvik, 1985; Dypvik *et al.*, 1991). Of particular interest to the present study, Dypvik (1985) recorded broad scale variation in bioturbation levels within and between the Agardhfjellet and Rurikfjellet formations which he related to shoreline proximity. No details of individual trace fossils or ichnofabrics were given, and there is considerable potential for the application of the PFT methodology to these sediments.

Also of interest in the Svalbard Basin sequence, this time from the Lower Tertiary Sarkofagen Formation, is the presence of apparently ice-rafted exotic clasts in alternating sandstone and shale dominant units (Dalland, 1976).

7.5.3 Sverdrup Basin

Early Cretaceous palaeolatitude: 70°N (Frakes and Francis, 1988).

The Sverdrup Basin of the Canadian Arctic Archipelago (Fig.7.05) contains up to 13000m of Carboniferous to Lower Tertiary strata (Embry, 1993). During the Aptian and Albian, and therefore contemporaneous with the Bulldog Shale, deposition of the Christopher Formation occurred. The Christopher Formation comprises two members, the Barremian to Albian Invincible Point Member and the Middle Albian Macdougall Point Member (Embry, 1985). Within the Sverdrup Basin sedimentation was dominated by deltaic progradation and subsequent breakdown, features not observed within the Eromanga Basin. Indeed, the Christopher Formation represents open marine shelf depositional conditions, and occurs between the conformably underlying sandstone dominated delta front and delta plain deposits of the Isachsen Formation's Walker Island Member, and the sandstone dominated overlying Hassel Formation.

The invincible Point Member comprises medium to dark grey, silty shale and siltstone, with interbeds of silty sandstone which become less common towards the basin centre. The sandstone interbeds typically contain thin beds of shale and siltstone, and are dominated by hummocky cross-stratification, cross lamination, and undescribed trace fossils. Deposition below fair weather wave base is inferred, with the sands deposited from waning storm generated currents (Embry, 1985).

The conformably overlying Macdougall Point Member comprises dark grey to black shale and siltstone, with interbeds of sandstone in the increasingly silty upper part. The basal section consists of very dark grey to black clay-rich shale. This member is

inferred to have resulted from deposition in offshore open marine to prodelta setting (Embry, 1985).

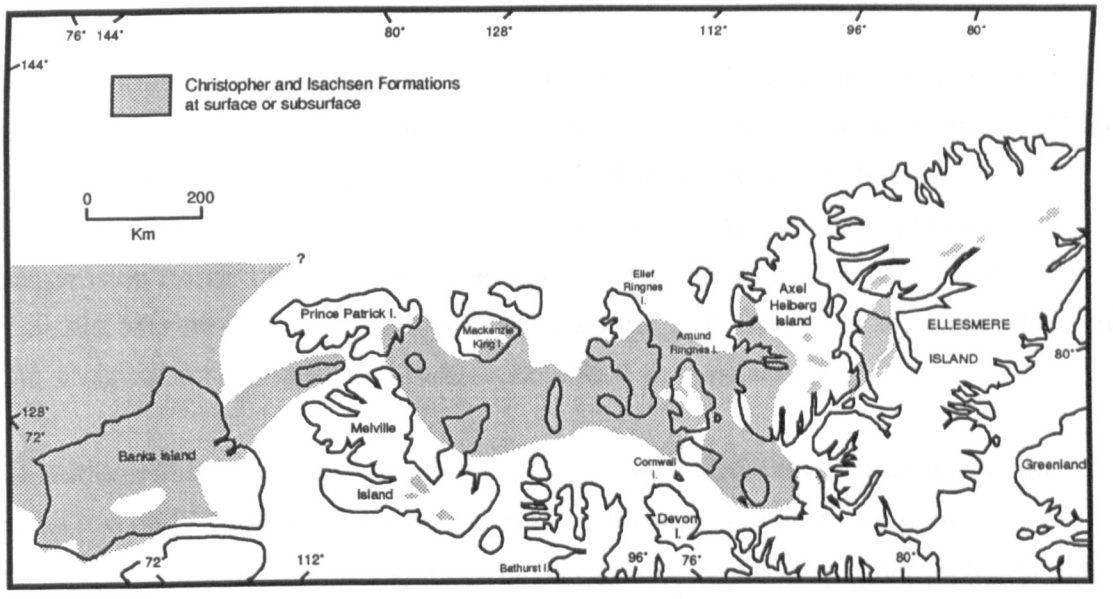

Fig.7.05 Locality map for the surface and subsurface distribution of the Christopher Formation and the underlying Isachsen Formation within the Sverdrup Basin. Redrawn from Embry (1985).

The control on sedimentation by deltaic progradation and degradation is clearly different from sedimentary patterns observed for the Bulldog Shale, though may have some similarities to the deposition of the upper Cadna-owie Formation and Parabarana Sandstone (Fig.1.05). However, the sedimentary features observed in both the Invincible Point Member and the Macdougall Point Member of the Christopher Formation, have much in common with those described form the Bulldog Shale. Unfortunately individual trace fossils and ichnofabrics have not been described, though the potential exists for useful future study of this, and associated formations, through the PFT methodology.

Chapter 8

Conclusion

The epicontinental Eromanga Basin extends over one million square kilometres of central Australia, and contains Mesozoic sediments of Toarcian to Turonian age. Much of the Jurassic sequence represents non-marine, fluvial deposition. Non-marine conditions prevailed until the latest Barremian / earliest Aptian when a marine transgression flooded the entire Eromanga Basin and introduced marine depositional processes. Marine conditions then predominated until the Cenomanian, when wholesale marine regression occurred, and fluvial deposition re-commenced.

The Bulldog Shale was deposited in the south-western Eromanga Basin during the Aptian and early Albian as a result of the initial basin-flooding transgression. Deposition of this clay and silt dominated unit was terminated by a marine regression which led to the deposition of the shallower water Coorikiana Sandstone. The Cretaceous marine incursion into the Eromanga Basin was partly the result of a 105m eustatic sea level rise. Equally important however, was synchronous epeirogenic subsidence of the Australian continent by approximately 150m. Furthermore, withdrawal of the sea from the Eromanga Basin in the latest Albian and Cenomanian had no eustatic component and was solely due to the rapid uplift of the continent by approximately 280m (Veevers, 1984).

During the Aptian to middle Albian the Eromanga Basin was connected to the open ocean via silled channels, and probably maintained a positive water balance. This, coupled with transgressive conditions which resulted in at least seasonally anoxic bottom waters, facilitated the deposition of organic-rich sediments. The key to both the transgressive black shales model (Wignall, 1991) and the seasonal anoxia model (Tyson and Pearson, 1991) is water depth. Indeed, water depth is considered to be the dominant control on the varied rock fabrics of the Bulldog Shale, as expressed through variations in trace fossil associations and lithology caused by changes in bottom water oxygenation levels and environmental energy levels. Such palaeoenvironmental trends can be identified and defined through the use of the Palaeoenvironmental Fabric Type methodology.

Seven palaeoenvironmental fabric types (denoted PFT/A-G) have been defined from Bulldog Shale material, based on:
percentage bioturbation;
trace fossil diversity and assemblage analysis;
dominant sedimentary grain size;
physical sedimentary structures;
body fossils.

Through the detailed analysis of both the biogenic and physical fabrics of the rock, each PFT characterises the specific palaeoenvironmental parameters in which the fabrics were imparted.

Important palaeoenvironmental factors were bottom water oxygenation levels and hydraulic energy levels. Both of these parameters were controlled by the primary factor of relative water depth. Three PFT 'end members' are most important:

PFT/A represents deposition in relatively deep basinal conditions characterised by low energy and strongly dysaerobic to anaerobic palaeoenvironments, the low bottom water oxygenation levels largely precluding the existence of trace-making organisms. Therefore, physical sedimentary structures dominate and biogenic structures are absent to very rare components of the rock fabric. Physical sedimentary structures largely comprise planar and slightly irregular lamination. Where present, trace fossils represent the fodinichnia of deposit feeders.

PFT/E represents deposition in shallower conditions at, or just below, storm wave base, where neither bottom-water oxygenation levels nor environmental energy levels were limiting factors on biological processes. Biogenic sedimentary structures dominate and generally obscure physical structures, and represent the fodinichnia and domichnia of deposit feeders, and more occasionally the domichnia of suspension feeders.

PFT/G represents deposition in very shallow conditions, where storm-derived sedimentation was dominant, and thus strongly limited or even precluded, biological processes. Therefore, physical sedimentary structures dominate the fabric, and biogenic structures are generally absent to very rare. Where present, traces represent the fodinichnia, and more occasionally the domichnia, of deposit feeders, and rarely the domichnia of suspension feeders.

Analyses of palynomorph assemblages by other workers (Haig and Lynch, 1993) have indicated water depths of no greater than 50m for deposition of the Bulldog Shale. Therefore, on the basis of PFT analyses, these maximum water depths are represented by PFT/A dominated successions. This conclusion is backed up by analyses of storm-derived sedimentation patterns, which have enabled the values of 20-15m water depth to be inferred for PFT/E, and less than 10m for PFT/G.

The identification of up-section associations of palaeoenvironmental fabric types, coupled with an understanding of palynostratigraphy, has enabled the division of the Bulldog Shale into ten sub-units (denoted α to κ). These sub-units exhibit considerable lateral persistence, though local hiatuses may be present, and their definition has enabled correlation between sections throughout a basin margin transect in excess of 550km. Variations between sections are minor, and are predominantly the result of distance from palaeoshoreline. Of particular importance, sub-unit determination provides a means for future identification of stratigraphic position in field sites.

The identification of specific PFT-characterised sub-units, deposited within definite palaeobathmetric limits, has enabled the construction of relative sea level curves, which may be related to basin-wide transgressions and regressions. Similar curves have been constructed for all analysed sections from the south western Eromanga Basin, and thus local tectonic effects on sea level variation in this region were minor to absent. Some diachroneity of palaeobathymetric change is observed between sections, a feature probably related to distance from the connection with the open ocean, and the migration of transgressive and regressive pulses through the basin.

The Bulldog Shale sea level curve comprises four relative deepening and shallowing cycles (sub-units α to γ; γ to ε; ε to θ; and θ to κ). The base of the unit represents a rapid transgression (sub-unit α), while the upper sub-units (η to κ) represent a gradual relative regression which ultimately resulted in deposition of the Coorikiana Sandstone.

The relative sea level curves presented here concur with previously published sea-level curves of this time interval for the Eromanga Basin, though those presented here are more detailed, and contain quantitative estimates of actual water depth. This relative sea level curve provides an illustration of temporal and spatial relative sea level, and associated palaeoenvironmental changes during deposition of the Bulldog Shale. In addition, comparison of the Bulldog Shale palaeobathymetric curve with those for sea level from other Australian basins and globally, enable the affects of global eustatic

changes and Australian continental epeirogeny on the palaeobathymetric curve to be defined. Initial flooding was the result of epeirogenic subsidence coupled with eustatic sea level rise, the gradual regression leading up to Coorikiana Sandstone deposition was the result of epeirogenic uplift, while the intervening sea level variations were the likely result of global eustatic changes.

Deposition of the Bulldog Shale is synchronous with an apparent Oceanic Anoxic Sub-Event (OASE), though this is not required as a mechanism for Bulldog Shale deposition. Indeed, Bulldog Shale sedimentation is explained well through the silled geometry of the Eromanga Basin, the probable existence of a positive water balance, and the consequent establishment of a density stratified water column during periods of basin deepening.

Contemporaneous with deposition of the Bulldog Shale, other organic- and/or clay-rich units were deposited in a variety of high palaeolatitude basinal settings. These have largely not undergone detailed trace fossil or ichnofabric studies, and so there is much potential for the application of the PFT methodology to these sediments.

During the Aptian and Albian the Eromanga Basin occupied palaeolatitudes in excess of 65°S. Regional climate is regarded as being cool and humid, with at least seasonal freezing. From the present study, seasonal freezing is indicated by the presence of lonestones, and at least near-freezing conditions by the presence of glendonites. It is unlikely that PFT variations register changes in palaeotemperature, since they are well explained by changes in water depth and associated factors.

8.1 Suggestions for further work

The PFT methodology provides a comprehensive, yet flexible and relatively quick, method of palaeoenvironmental determination for sedimentary deposits. As such, future work utilising this tool is constrained only by the sediments available, and may, in various modified forms, be applicable to any sedimentary sequence, ancient or modern.

Limitations to biogenic processes are varied, and thus the PFT methodology can be tailored to any situation in order to define and constrain those limiting factors prevailing. Indeed, the PFT methodology may even prove to be a valuable method for tracing anthropogenic pollution patterns in modern depositional settings.

Of particular interest would be the application of the PFT methodology in an expanded study, encompassing all the marine units of the Eromanga Basin in order to build up a more complete account of the central Australian inundation. Furthermore, the expansion of such a study across state boundaries would encompass a broader range of marginal and basinal environments, and would greatly expand knowledge regarding spatial palaeoenvironmental variation within the Eromanga Basin. In addition, such a study may help to determine true eustatic effects from more local epeirogenic, and in particular, tectonic influences.

Finally, as mentioned previously, sediments from other high latitude basins, of Cretaceous or other age, have largely escaped detailed ichnofabric study. The PFT methodology may well prove useful in the palaeoenvironmental analysis of these sediments, and the potential for future work is great.

Reference list

Aga, O.J., Dalland, A., Elverhøi, A., Thon, A., and Worsley, D. (1986). *The Geological History of Svalbard, Evolution of an Arctic Archipelago*. Stavanger, Norway, Den Norske Stats Oljeselskap a.s. 121pp.

Aigner, T. and Reineck, H.E. (1982). Proximality trends in modern storm sands from the Helgoland Bight (North Sea) and their implications for basin analysis. *Senckenbergiana maritima* **14**: 183-215.

Alley, N.F. (1985). Preliminary report on the palynostratigraphy of SADME Toodla No. 1 well, south-western Eromanga Basin. South Australian Department of Mines and Energy, Report Book No. 80/128.

Alley, N.F. (1988). Age and correlation of palynofloras from the type Cadna-owie Formation, southwestern Eromanga Basin. *Association of Australasian Palaeontologists Memoir* **5**: 187-194.

Alley, N.F. (1993). Palynology as an aid in mapping rock unit boundaries in Early Cretaceous strata, southern Eromanga Basin, Australia. *Program with abstracts. Joint annual meeting of the Geological Association of Canada / Canadian Geophysical Union* **18**: 1.

Allison, P.A., Wignall, P.B., and Brett, C.E. (1995). Palaeo-oxygenation: effects and recognition. In: D.W.J. Bosence and P.A. Allison (eds.), *Marine Palaeoenvironmental Analysis from Fossils*. Geological Society Special Publication No. 83. 97-112.

Alpert, S.P. (1974). Systematic review of the genus *Skolithos*. *Journal of Paleontology* **48**(4): 661-669.

Alpert, S.P. (1975). *Planolites* and *Skolithos* from the Upper Precambrian-Lower Cambrian, White-Inyo Mountains, California. *Journal of Paleontology* **49**(3): 508-521.

Ambrose, G.J. and Flint, R.B. (1981). *Explanatory notes for the Billa Kalina 1:250000 geological map, sheet SH/53-7*. Department of Mines and Energy, South Australia. 36pp.

Arthur, M.A., Brumsack, H.-J., Jenkyns, H.C., and Schlanger, S.O. (1990). Stratigraphy, geochemistry, and palaeoceanography of organic carbon-rich Cretaceous sequences. In: R.N. Ginsburg and B. Beaudoin (eds.), *Cretaceous Resources, Events and Rhythms*. Kluwer Academic Publishers. 75-119.

Arthur, M.A. and Sageman, B.B. (1994). Marine black shales: depositional mechanisms and environments of ancient deposits. *Annual Review of Earth and Planetary Sciences* **22**: 499-551.

Ausich, W.J. and Bottjer, D.J. (1982). Tiering in suspension-feeding communities on soft substrata throughout the Phanerozoic. *Science* **216**: 173-174.

Barron, E.J. (1983). A warm equable Cretaceous: the nature of the problem. *Earth Science Reviews* **19**: 305-338.

Barron, E.J. and Washington, W.M. (1982). Cretaceous climate: a comparison of atmospheric simulations with the geologic record. *Palaeogeography, Palaeoclimatology, Palaeoecology* **40**: 103-133.

Berner, R.A. (1981). A new geochemical classification of sedimentary environments. *Journal of Sedimentary Petrology* **51**(2): 359-365.

Bottjer, D.J. and Ausich, W.I. (1986). Phanerozoic development of tiering in soft substrata suspension-feeding communities. *Paleobiology* **12**(4): 400-420.

Bottjer, D.J. and Droser, M.L. (1991). Ichnofabric and Basin Analysis. *Palaios* **6**: 199-205.

Bottjer, D.J., Campbell, K.A., Schubert, J.K., and Droser, M.L. (1995). Palaeoecological models, non-uniformitarianism, and tracking the changing ecology of the past. In: D.W.J. Bosence and P.A. Allison (eds.), *Marine Palaeoenvironmental Analysis from Fossils*. Geological Society Special Publication No. 83. 7-26.

Bottrell, S.H., Bartle, K.D., Louie, P.K.K., Taylor, N., Kemp, W., Steedman, W., and Wallace, S. (1991). Determination of coal reactivity during coprocessing using stable isotope mass spectrometry. *Fuel* **70**: 442-446.

Boutton, T.W. (1991a). Stable carbon isotope ratios of natural materials: I. Sample preparation and mass spectrometric analysis. In: D.C. Coleman and B. Fry (eds.), *Carbon isotope techniques*. Academic Press Inc. 155-171.

Boutton, T.W. (1991b). Stable carbon isotope ratios of natural materials: II. Atmospheric, terrestrial, marine, and freshwater environments. In: D.C. Coleman and B. Fry (eds.), *Carbon isotope techniques*. Academic Press Inc. 173-185.

Bradley, J. (1981). *Radionereites*, *Chondrites*, and *Phycodes*, trace fossils of Anthoptiloid sea pens. *Pacific Geology* **15**: 1-16.

Bralower, T.J., Arthur, M.A., Leckie, R.M., Sliter, W.V., Allard, D.J., and Schlanger, S.O. (1994). Timing and Paleoceanography of Oceanic Dysoxia/Anoxia in the Late Barremian to Early Aptian (Early Cretaceous). *Palaios* **9**: 335-369.

Bromley, R.G. (1990). *Trace Fossils Biology and Taphonomy*. London, Unwin Hyman. 280pp.

Bromley, R.G. and Asgaard, U. (1972). A large radiating burrow-system in Jurassic micaceous sandstones of Jameson Land, east Greenland. *Grønlands Geoloiske Undersøgelse Rapport* **49**: 23-30.

Bromley, R.G. and Frey, R.W. (1974). Redescription of the trace fossil *Gyrolithes* and taxonomic evaluation of *Thalassinoides*, *Ophiomorpha* and *Spongeliomorpha*. *Bulletin of the Geological Society of Denmark* **23**: 311-335.

Bromley, R.G. and Ekdale, A.A. (1984). *Chondrites*: a trace fossil indicator of anoxia in sediments. *Science* **224**: 872-874.

Bromley, R.G. and Ekdale, A.A. (1986). Composite ichnofabrics and tiering of burrows. *Geological Magazine* **123**(1): 59-65.

Brown, H.Y.L. (1905). Report on geological explorations in the west and northwest of South Australia. *Parliamentary Papers of South Australia* **71**: 5-12.

Buckman, J.O. (1994). *Rhizocorallium* Zenker 1836 not *Teichichnus repandus* Chamberlain 1977. *Ichnos* **3**: 135-136.

Burger, D. (1986). Palynology, cyclic sedimentation, and palaeoenvironments in the Late Mesozoic of the Eromanga Basin. In: D.I. Gravestock, P.S. Moore and G.M. Pitt (eds.), *Contributions to the geology and hydrocarbon potential of the Eromanga Basin*. Geological Society of Australia, Special Publication No. 12. 53-70.

Byers, C.W. (1977). Biofacies patterns in euxinic basins: a general model. In: H.E. Cook and P. Enos (eds.), *Deep water carbonate environments*. Society of Economic Paleontologists and Mineralogists Special Publication No. 25. 5-17.

Byers, C.W. (1982). Geological significance of marine biogenic sedimentary structures. In: P.L. McCall and M.S.J. Tevesz (eds.), *Animal - Sediment Relations*. New York and London, Plenum Press. 221-256.

Callen, R.A., Sheard, M., and Hough, P. (1990). Skeleton 2 well completion report geological survey. Department of Mines and Energy South Australia, Report Book No. 90/77.

Chamberlain, C.K. (1978). Recognition of trace fossils in cores. In: P.B. Basan (ed.), *Trace Fossil Concepts*. Oklahoma City, Society of Economic Paleontologists and Mineralogists, Short Course No. 5. 133-183.

Cooper, M.R. (1977). Eustacy during the Cretaceous: its implications and importance. *Palaeogeography, Palaeoclimatology, Palaeoecology* **22**: 1-60.

Cowley, W.M. and Martin, A.R. (1991). *Explanatory notes for the Kingoonya 1:250000 geological map, sheet SH53-11*. Department of Mines and Energy South Australia. 64pp.

Crowley, T.J. and North, G.R. (1991). *Paleoclimatology*. Oxford Monographs on Geology and Geophysics No.18. New York, Oxford University Press. 339pp.

Curran, H.A. (1985). The trace fossil assemblage of a Cretaceous nearshore environment: Englishtown Formation of Delaware, U.S.A. In: H.A. Curran (ed.), *Biogenic structures: their use in interpreting depositional environments*. Tulsa, Oklahoma, Society of Economic Paleontologists and Mineralogists, Special Publication No. 35. 261-276.

Curran, H.A. and Frey, R.W. (1977). Pleistocene trace fossils from North Carolina (U.S.A), and their Holocene analogues. In: T.P. Crimes and J.C. Harper (eds.), *Trace Fossils 2*. Liverpool, Seel House Press. 139-162.

Dalland, A. (1976). Erratic clasts in the Lower Tertiary deposits of Svalbard - evidence of transport by winter ice. *Norsk Polar-institutt Arbok* **1976**: 151-165.

Deer, W.A., Howie, R.A., and Zussman, J. (1966). *An introduction to the rock forming minerals*. New York, Longman Scientific and Technical. 528pp.

Demaison, G.J. and Moore, G.T. (1980). Anoxic environments and oil source bed genesis. *The American Association of Petroleum Geologists Bulletin* **64**(8): 1179-1209.

Dettmann, M.A. (1986). Early Cretaceous palynoflora of subsurface strata correlative with the Koonwarra Fossil Bed, Victoria. In: P.A. Jell and J. Roberts (eds.), *Plants and invertebrates from the Lower Cretaceous Koonwarra Fossil Bed, South Gippsland, Victoria*. 79-108.

Ditchfield, P.W., Marshall, J.D., and Pirrie, D. (1994). High latitude palaeotemperature variation: New data from the Tithonian to Eocene of James Ross Island, Antarctica. *Palaeogeography, Palaeoclimatology, Palaeoecology* **107**: 79-101.

Drinnan, A.N. and Chambers, T.C. (1986). Flora of the Lower Cretaceous Koonwarra Fossil Bed (Korumburra Group), South Gippsland, Victoria. In: P.A. Jell and J. Roberts (eds.), *Plants and invertebrates from the Lower Cretaceous Koonwarra Fossil Bed, South Gippsland, Victoria*. 1-77.

Droser, M.L. (1991). Ichnofabric of the Paleozoic *Skolithos* Ichnofacies and the Nature and Distribution of *Skolithos* Piperock. *Palaios* **6**: 316-325.

Droser, M.L. and Bottjer, D.J. (1986). A semiquantitative field classification of ichnofabric. *Journal of Sedimentary Petrology* **56**: 558-559.

Droser, M.L. and Bottjer, D.J. (1989). Ichnofabric of Sandstones Deposited in High-Energy Nearshore Environments: Measurement and Utilization. *Palaios* **4**: 598-604.

Droser, M.L. and Bottjer, D.J. (1991). Trace fossils and ichnofabric in Leg 119 cores. In: J. Barron, J. Anderson, J.G. Baldouf and B. Larsen (eds.), *Proceedings of the Ocean Drilling Program, Scientific Results* **119**: 635-641.

Droser, M.L. and O'Connell, S. (1992). Trace Fossils and Ichnofabric in Triassic Sediments from Cores Recovered on Leg 122. In: U. von Rad and B.U. Haq (eds.), *Proceedings of the Ocean Drilling Program, Scientific Results* **122**: 475-485.

Droser, M.L. and Bottjer, D.J. (1993). Trends and Patterns of Phanerozoic Ichnofabrics. *Annual Review of Earth and Planetary Science* **21**: 205-225.

Droser, M.L. and Bottjer, D.J. (1994). New Approaches to Ichnofabric and Trace Fossil Analyses: Examples from Mesozoic and Cenozoic Outcrops of Coastal California. In: *1994 GSA Cordilleran Section Guidebook Trip 3*. 55-57.

Dypvik, H. (1985). Jurassic and Cretaceous black shales of the Janusfjellet Formation, Svalbard, Norway. *Sedimentary Geology* **41**: 235-248.

Dypvik, H., Nagy, J., Eikeland, T.A., Backer-Owe, K., and Johansen, H. (1991). Depositional conditions of the Bathonian to Hauterivian Janusfjellet Subgroup, Spitsbergen. *Sedimentary Geology* **72**: 55-78.

Edwards, B.D. (1985). Bioturbation in a dysaerobic bathyal basin: California borderland. In: H.A. Curran (ed.), *Biogenic structures: their use in interpreting depositional environments*. Society of Economic Palaeontologists and Mineralogists Special Publication No. 35. 309-331.

Ekdale, A.A. (1985). Paleoecology of the marine endobenthos. *Palaeogeography, Palaeoclimatology, Palaeoecology* **50**: 63-81.

Ekdale, A.A. and Bromley, R.G. (1983). Trace fossils and ichnofabric in the Kjølby Gaard Marl, uppermost Cretaceous, Denmark. *Bulletin of the Geological Society of Denmark* **31**: 107-119.

Ekdale, A.A., Bromley, R.G., and Pemberton, S.G. (1984). *Ichnology: trace fossils in sedimentology and stratigraphy*. Society of Economic Paleontologists and Mineralogists Short Course No. 15. 317pp.

Ekdale, A.A. and Mason, T.R. (1988). Characteristic trace-fossil associations in oxygen-poor sedimentary environments. *Geology* **16**: 720-723.

Ekdale, A.A. and Bromley, R.G. (1991). Analysis of composite ichnofabrics: an example in uppermost Cretaceous chalk of Denmark. *Palaios* **6**: 232-249.

Ekdale, A.A. and Lewis, D.W. (1991). Trace fossils and paleoenvironmental control of ichnofacies in a Late Quaternary gravel and loess fan delta complex, New Zealand. *Palaeogeography, Palaeoclimatology, Palaeoecology* **81**: 253-279.

Embry, A.F. (1985). Stratigraphic subdivision of the Isachsen and Christopher formations (Lower Cretaceous), Arctic Islands. *Geological Survey of Canada, Current Research Part B* **85-1B**: 239-246.

Embry, A.F. (1993). Transgressive - regressive (T-R) sequence analysis of the Jurassic succession of the Sverdrup Basin, Canadian Arctic Archipelago. *Canadian Journal of Earth Sciences* **30**: 301-320.

Exon, N.F. and Senior, B.R. (1976). The Cretaceous of the Eromanga and Surat Basins. *BMR Journal of Australian Geology and Geophysics* **1**: 33-50.

Exon, N.F. and Burger, D. (1981). Sedimentary cycles in the Surat Basin and global changes of sea level. *BMR Journal of Australian Geology and Geophysics* **6**: 153-159.

Fillion, D. (1989). Critical use of criteria in discriminating between *Palaeophycus*, *Planolites* and *Macaronichnus*, a synthesis. *Comptes Rendus des Séances de l'Académie des Sciences. Série II - Mécanique, Physique, Chimie, Sciences de l'Univers, Sciences de la Terre* **309**: 169-172.

Fillion, D. and Pickerill, R.K. (1990). Ichnology of the Upper Cambrian? to Lower Ordovician Bell Island and Wabana groups of eastern Newfoundland, Canada. *Palaeontographica Canadiana* **7**. Canadian Society of Petroleum Geologists, Geological Association of Canada. 119pp

Flint, R.B., Ambrose, G.J., and Campbell, K.S.W. (1980). Fossiliferous Lower Devonian boulders in Cretaceous sediments of the Great Australian Basin. *Transactions of the Royal Society of South Australia* **104**(3): 57-65.

Forbes, B.G. (1966). *The geology of the Marree 1:250000 map area*. Department of Mines, South Australia Geological Survey. Report of investigations No.28. 47pp.

Forbes, B.G. (1986). Margin of the Eromanga Basin, South Australia. In: D.I. Gravestock, P.S. Moore and G.M. Pitt (eds.), *Contributions to the geology and hydrocarbon potential of the Eromanga Basin*. Geological Society of Australia Special Publication No. 12. 85-95.

Frakes, L.A., Burger, D., Apthorpe, M., Wiseman, J., Dettman, M., Alley, N., Flint, R., Gravestock, D., Ludbrook, N., Backhouse, J., Skwarko, S., Schiebnerová, V., McMinn, A., Moore, P.S., Bolton, B.R., Douglas, J.G., Christ, R., Wade, M., Molnar, R.E., McGowran, B., Balme, B.E., and Day, R.A. (1987). Australian Cretaceous shorelines, stage by stage. *Palaeogeography, Palaeoclimatology, Palaeoecology* **59**: 3-29.

Frakes, L.A. and Francis. J.E. (1988). A guide to Phanerozoic cold polar climates from high-latitude ice rafting in the Cretaceous. *Nature* **333**: 547-549.

Frakes, L.A. and Francis, J.E. (1990). Cretaceous palaeoclimates. In: R.N. Ginsburg and B. Beaudoin (eds.) *Cretaceous Resources, Events and Rhythms*. Kluwer Academic Publishers. 273-287.

Frakes, L.A. and Krassay, A.A. (1992). Discovery of probable ice-rafting in the Late Mesozoic of the Northern Territory and Queensland. *Australian Journal of Earth Sciences* **39**: 115-119.

Frakes, L.A., Francis, J.E., and Syktus, J.I. (1992). *Climate modes of the Phanerozoic*. Cambridge, Cambridge University Press.274pp.

Francis, J.E. and Frakes, L.A. (1993). Cretaceous climates. In: V.P. Wright (ed.), *Sedimentology Review 1*. London, Blackwell Scientific Publications17-30.

Frey, R.W., Howard, J.D., and Pryor, W.A. (1978). *Ophiomorpha*: its morphologic, taxonomic, and environmental significance. *Palaeogeography, Palaeoclimatology, Palaeoecology* **23**: 199-229.

Frey, R.W. and Howard, J.D. (1981). *Conichnus* and *Schaubcylindrichnus*: redefined trace fossils from the Upper Cretaceous of the Western Interior. *Journal of Paleontology* **55**(4): 800 - 804.

Frey, R.W. and Bromley, R.G. (1985). Ichnology of American chalks: the Selma Group (Upper Cretaceous), western Alabama. *Canadian Journal of Earth Sciences* **22**: 801-828.

Frey, R.W. and Wheatcroft, R.A. (1989). Organism-substrate relations and their impact on sedimentary petrology. *Journal of Geological Education* **37**: 261-279.

Frey, R.W. and Pemberton, S.G. (1991). The ichnogenus *Schaubcylindrichnus*: morphological, temporal, and environmental significance. *Geological Magazine* **128**(6): 595-602.

Freytag, I.B. (1966). Proposed rock units for marine Lower Cretaceous sediments in the Oodnadatta region of the Great Artesian Basin. *South Australian Geological Survey Quarterly Geological Notes* **18**: 3-7.

Fürsich, F.T. (1973). A revision of the trace fossils *Spongeliomorpha*, *Ophiomorpha* and *Thalassinoides*. *Neues Jahrbuch für Geologie und Paläontologie Monatshefte* **12**: 719-735.

Fürsich, F.T. (1974). Ichnogenus *Rhizocorallium*. *Paläontologische Zeitschrift* **48**(1): 16-28.

Gallagher, K., Dumitru, T.A., and Gleadow, A.J.W. (1994). Constraints on the vertical motion of eastern Australia during the Mesozoic. *Basin Research* **6**: 77-94.

Goldring, R. (1993). Ichnofacies and facies interpretation. *Palaios* **8**: 403-405.

Goldring, R. (1995). Organisms and substrate: response and effect. In: D.W.J. Bosence and P.A. Allison (eds.), *Marine Palaeoenvironmental Analysis from Fossils*. Geological Society Special Publication No. 83. 151-180.

Goldring, R., Pollard, J.E., and Taylor, A.M. (1991). *Anconichnus horizontalis*: a pervasive ichnofabric-forming trace fossil in post-Palaeozoic offshore siliciclastic facies. *Palaios* **6**: 250-263.

Gregory, R.T., Douthitt, C.B., Duddy, I.R., Rich, P.V., and Rich, T.H. (1989). Oxygen isotopic composition of carbonate concretions from the Lower Cretaceous of Victoria, Australia: implications for the evolution of meteoric waters on the Australian continent in a paleopolar environment. *Earth and planetary science letters* **92**: 27-42.

Griffiths, M. (1980). Toodla No. 1 well completion report. Department of Mines and Energy South Australia, Report Book No. 80/128.

Haig, D.W. and Lynch, D.A. (1993). A late early Albian marine transgressive pulse over northeastern Australia, precursor to epeiric basin anoxia: foraminiferal evidence. *Marine micropaleontology* **22**: 311-362.

Hallam, A. (1970). *Gyrochorte* and other trace fossils in the Forest Marble (Bathonian) of Dorset, England. In: T.P. Crimes and J.C. Harper (eds.), *Trace fossils.* Liverpool, Seel House Press. 189-200.

Häntzschel, W. (1975). *Trace fossils and problematica*. Boulder, Colorado and Lawrence, Kansas, The Geological Society of America. 269pp.

Haq, B.U., Hardenbol, J, and Vail, P.R. (1988). Mesozoic and Cenozoic chronostratigraphy and cycles of sea-level change. In: C.K. Wilgus, B.S. Hastings, C.G.St.C. Kendall, H.W. Posamentier, C.A. Ross and J.C. Van Wagoner (eds.), *Sea-level Change: An Integrated Approach*. Society of Economic Palaeontologists and Mineralogists Special Publication No. 42. 71-108.

Harris, W. K. (1982). Palynology and age determination of cores from Santos CBH2 bore hole, Eromanga Basin. Report for Santos Ltd.

Heinberg, C. (1973). The internal structure of the trace fossils *Gyrochorte* and *Curvolithus*. *Lethaia* **6**: 227-238.

Helby, R., Morgan, R., and Partridge, A.D. (1987). A palynological zonation of the Australian Mesozoic. *Association of Australasian Palaeontologists, Memoir* **4**: 1-94.

Hester, N.C. and Pryor, W.A. (1972). Blade-shaped crustacean burrows of Eocene age: a composite form of *Ophiomorpha*. *Geological Society of America Bulletin* **83**: 677-688.

Ineson, J.R. (1987). Trace fossils from a submarine fan - slope apron complex in the Cretaceous of James Ross Island, Antarctica. *British Antarctic Survey Bulletin* **74**: 1-16.

Ineson, J.R. (1989). Coarse-grained submarine fan and slope apron deposits in a Cretaceous back-arc basin, Antarctica. *Sedimentology* **36**: 793-819.

Jack, R.L. (1915). The geology and prospects of the region to the south of the Musgrave Ranges, and the geology of the western portion of the Great Australian Artesian Basin. *Bulletin of the Geological Survey, South Australia* **5**.

Jansen, J.H.F., Woensdregt, C.F., Kooistra, M.J., and van der Gaast, S.J. (1987). Ikaite pseudomorphs in the Zaire deep-sea fan: an intermediate between calcite and porous calcite. *Geology* **15**: 245-248

Jell, P.A. and Duncan, P.M. (1986). Invertebrates, mainly insects, from the freshwater Lower Cretaceous Koonwarra Fossil Bed (Korumburra Group), South Gippsland, Victoria. In: P.A. Jell and J. Roberts (eds.) *Plants and invertebrates from the Lower Cretaceous Koonwarra Fossil Bed, South Gippsland, Victoria*. 111-205.

Kemper, E. (1987). Das Klima der Kreide Zeit (The climate of the Cretaceous Period). *Geologisches Jahrbuch* **96A**: 5-185.

Kennedy, W.J. (1967). Burrows and surface traces from the Lower Chalk of Southern England. *Bulletin of the British Museum (Natural History) Geology* **15**(3): 125-167.

Kennedy, W.J. and MacDougal, J.D.S. (1969). Crustacean burrows in the Weald Clay (Lower Cretaceous) of south-eastern England and their environmental significance. *Palaeontology* **12**(3): 459-471.

Kern, J.P. (1978). Paleoenvironment of new trace fossils from the Eocene Mission Valley Formation, California. *Journal of Paleontology* **52**: 186-194.

Kern, J.P. and Warme, J.E. (1974). Trace fossils and bathymetry of the Upper Cretaceous Point Loma Formation, San Diego, California. *Geological Society of America Bulletin* **85**: 893-900.

Krieg, G.W. (1982). Stratigraphy and tectonics of the Dalhousie Anticline, southwest Eromanga Basin. In: P.S. Moore and J.J. Mount (eds.), *Eromanga Basin Symposium summary papers*. Adelaide, Geological Society of Australia and Petroleum Exploration Society of Australia.

Krieg, G.W. (1986). Stratigraphy and tectonics of the Dalhousie Anticline, southwest Eromanga Basin. *Geological Society of Australia Special Publication* **12**: 175-182.

Krieg, G.W., Rogers, P.A., Cullen, R.A., Freeman, P.J., Alley, N.F., Forbes, B.G. (1991). *Curdimurka South Australia Explanatory Notes, 1:250000 Geological Map Series, sheet SH53-8*. Department of Mines and Energy South Australia. 60pp.

Krieg, G.W., Alexander, E.M., and Rogers, P.A. (1995). Jurassic - Cretaceous epicratonic basins - Eromanga Basin. In: J.F. Drexel and W.V. Preiss (eds.),*The Geology of South Australia Volume 2, The Phanerozoic*. South Australian Geological Society. Bulletin **54**.

Kuang, K.S. (1985). History and style of Cooper-Eromanga Basin structures. *Australian Society of Exploration Geophysics* **16**(2): 245-248.

Lemon, N.M. (1988). Tidal influences in the marginal Eromanga Basin. *Geological Survey of South Australia, Quarterly Geological Notes* **105**: 7-11.

Lessertisseur, J. (1955). Traces fossiles d'activité animale et leur signification paléobiologique. *Memoires Societé Geologié France* **74**: 7-150.

Ludbrook, N.H. (1966). *Cretaceous biostratigraphy of the Great Artesian Basin in South Australia.* Department of Mines South Australia, Geological Survey of South Australia Bulletin No. 40. 217pp.

McKirdy, D.M., Emmett, J.F., Mooney, B.A., Cox, R.E., and Watson, B.L. (1986). Organic geochemical facies of the Cretaceous Bulldog Shale, western Eromanga Basin, South Australia. In: D.I. Gravestock, P.S. Moore and G.M. Pitt (eds.), *Contributions to the geology and hydrocarbon potential of the Eromanga Basin.* Geological Society of Australia Special Publication No. 12. 287-304.

Moore, D.M. and Reynolds Jr., R.C. (1989). *X-Ray Diffraction and the Identification and Analysis of Clay Minerals.* Oxford, Oxford University Press. 332pp.

Moore, P.S. (1986a). An exploration overview of the Eromanga Basin. In: D.I. Gravestock, P.S. Moore and G.M. Pitt (eds.), *Contributions to the geology and hydrocarbon potential of the Eromanga Basin.* Geological Society of Australia Special Publication No. 12. 1-8.

Moore, P.S. (1986b). Jurassic and Triassic stratigraphy and hydrocarbon potential of the Poolowanna Trough (Simpson Desert region) northern South Australia. In: D.I. Gravestock, P.S. Moore and G.M. Pitt (eds.), *Contributions to the geology and hydrocarbon potential of the Eromanga Basin.* Geological Society of Australia Special Publication No. 12. 39-51.

Moore, P.S. and Pitt, G.M. (1984). Cretaceous of the Eromanga Basin - implications for hydrocarbon exploration. *The APEA Journal* **24**: 358-376.

Moore, P.S. and Pitt, G.M. (1985). Cretaceous subsurface stratigraphy of the southwestern Eromanga Basin: a review. In: J.M. Lindsay (ed.), *Stratigraphy, paleontology, malacology. Papers in honour of Dr. Nell Ludbrook.* South Australian Department of Mines and Energy Special Publication No. 5. 269-286.

Moore, P.S., Pitt, G.M., and Dettman, M.E. (1986). The Early Cretaceous Coorikiana Sandstone and Toolebuc Formation: their recognition and stratigraphic relationship in the southwest Eromanga Basin. In: D.I. Gravestock, P.S. Moore and G.M. Pitt (eds.), *Contributions to the geology and hydrocarbon potential of the Eromanga Basin*. Geological Society of Australia Special Publication No. 12. 97-114.

Morgan, R. (1980). *Eustasy in the Australian Early and Middle Cretaceous*. Geological Survey of New South Wales, Bulletin No. 27. 99pp.

Myrow, P.M. (1995). *Thalassinoides* and the enigma of early Paleozoic open-framework burrow systems. *Palaios* **10**(1): 58-74.

Nottvedt, A. and Kreisa, R.D. (1987). Model for the combined flow origin of hummocky cross-stratification. *Geology* **15**: 357-361.

Oschmann, W. (1991). Anaerobic-poikiloaerobic-aerobic: a new facies zonation for modern and ancient neritic redox facies. In: G. Einsele (ed.), *Cycles and Events in Stratigraphy*. Berlin, Springer-Verlag. 565-571.

Osgood, R.G. (1970). Trace fossils of the Cincinnati area. *Palaeontographica Americana* **6** (Issue No. 41): 281-444.

Ozimic, S. (1986). The geology and petrophysics of the Toolebuc Formation and its time equivalents, Eromanga and Carpentaria Basins. In: D.I. Gravestock, P.S. Moore and G.M. Pitt (eds.), *Contributions to the geology and hydrocarbon potential of the Eromanga Basin*. Geological Society of Australia Special Publication No. 12. 119-137.

Ozimic, S. (1988). *Palaeoenvironmental and geological controls on the quality of the Toolebuc Formation oil shale, Queensland.* In: Extended Abstracts - Palaeogeography, Sea Level and Climate, Implications for Resource Exploration, Canberra, BMR.

Parker, J.R. (1967). The Jurassic and Cretaceous sequence in Spitsbergen. *Geological Magazine* **104**: 487-505.

Pedersen, T.F. and Calvert, S.E. (1990). Anoxia vs. productivity: what controls the formation of organic-carbon-rich sediments and sedimentary rocks. *American Association of Petroleum Geologists Bulletin* **74**(4): 454-466.

Pemberton, S.G. and Frey, R.W. (1982). Trace fossil nomenclature and the *Planolites-Palaeophycus* dilemma. *Journal of Paleontology* **56**(4): 843-881.

Pemberton, S.G. and Frey, R.W. (1984). Quantitative methods in ichnology: spatial distribution among populations. *Lethaia* **17**: 33-49.

Pemberton, S.G. and Wightman, D.M. (1992). Ichnological characteristics of brackish water deposits. In: S.G. Pemberton (ed.), *Applications of ichnology to petroleum exploration: a core workshop*. Society of Economic Paleontologists and Mineralogists Core Workshop No. 17. 141-167.

Pirrie, D. and Marshall, J.D. (1991). Field relationships and stable isotope geochemistry of concretions from James Ross Island, Antarctica. *Sedimentary Geology* **71**: 137-150.

Pirrie, D., Doyle, P., Marshall, J.D., and Ellis, G. (1995). Cool Cretaceous climates: new data from the Albian of Western Australia. *Journal of the Geological Society, London* **152**: 739-742.

Pollard, J.E., Goldring, R, and Buck, S.G. (1993). Ichnofabrics containing *Ophiomorpha*: significance in shallow-water facies interpretation. *Journal of the Geological Society, London* **150**: 149-164.

Preiss, W.V. and Harris, W.K. (1982). Mesozoic and ?Cambrian stratigraphy of Santos borehole CBH-2, near Blanchewater Hill, E.L.691. Department of Mines and Energy South Australia, Report Book No. 82/38.

Reineck, H.E. (1963). Sedimentgefüge im Bereich der südlichen Nordsee. *Abhandlungen der senckenbergische naturforschende Gesellschaft* **505**: 1-138.

Rhoads, D.C. and Morse, J.W. (1971). Evolutionary and ecologic significance of oxygen-deficient marine basins. *Lethaia* **4**: 413-428.

Richter, R. (1927). Die fossilen Fährten und Bauten der Würmer, ein Überblick über ihre biologischen Grundformen und deren geologische Bedeutung. *Paläontologische Zeitschrift* **9**: 193-240.

Richter, R. (1952). Fluidal-textur in sediment-gesteinen und über sedifluktion überaupt. *Notizblatt des Hessichen Landesamtes für Bodenforschung zu Wiesbadan* **3**: 67-81.

Rogers, P.A., Krieg, G.W., Forbes, B.G., and Alley, N.F. (1989). *Well completion report: Finniss 2, Alford 1, Crowsnest 2*. Department of Mines and Energy South Australia, Report Book No.89/33.

Rogers, P.A. and Freeman, P.J. (in prep). *Explanatory notes for the Warrina 1:25000 geological map*. Department of Mines and Energy South Australia.

Ruffell, A.H. and Wach, G.D. (1991). Sequence stratigraphic analysis of the Aptian - Albian Lower Greensand in southern England. *Marine and Petroleum Geology* **8**: 341-353.

Russell, M. and Gurnis, M. (1994). The planform of epeirogeny: vertical motions of Australia during the Cretaceous. *Basin Research* **6**: 63-76.

Savrda, C.E., Bottjer, D.J., and Gorsline, D.S. (1984). Development of a comprehensive oxygen-deficient marine biofacies model: evidence from Santa Monica, San Pedro, and Santa Barbara Basins, California continental borderland. *American Association of Petroleum Geologists Bulletin* **68**: 1179-1192.

Savrda, C.E. and Bottjer, D.J. (1986). Trace-fossil model for reconstruction of paleo-oxygenation in bottom waters. *Geology* **14**: 3-6.

Savrda, C.E. and Bottjer, D.J. (1987a). The exaerobic zone, a new oxygen-deficient marine biofacies. *Nature* **327**: 54-56.

Savrda, C.E. and Bottjer, D.J. (1987b). Trace fossils as indicators of bottom-water redox conditions in ancient marine environments. In: D.J. Bottjer (ed.), *New concepts in the use of biogenic sedimentary structures for palaeoenvironmental interpretation*. Society of Economic Paleontologists and Mineralogists Pacific Section Guidebook **52**: 3-26.

Savrda, C.E. and Bottjer, D.J. (1989). Trace-fossil model for reconstructing oxygenation histories of ancient bottom waters: application to Upper Cretaceous Niobara Formation, Colorado. *Palaeogeography, Palaeoclimatology, Palaeoecology* **74**: 49-74.

Savrda, C.E. and Bottjer, D.J. (1991). Oxygen-related biofacies in marine strata: an overview and update. In: R.V. Tyson and T.H. Pearson (eds.), *Modern and ancient continental shelf anoxia*. London, Geological Society Special Publication No. 58. 201-219.

Schlanger, S.O. and Jenkyns, H.C. (1976). Cretaceous oceanic anoxic events: causes and consequences. *Geologie En Mijnbouw* **55**: 179-184.

Scott, R.W., Frost, S.H., and Schaffer, B.L. (1988). Early Cretaceous sea-level curves, Gulf coast and southeastern Arabia. In: C.K. Wilgus, B.S. Hastings, C.G.St.C. Kendall, H.W. Posamentier, C.A. Ross and J.C. Van Wagoner (eds.), *Sea-level changes: an integrated approach*. Society of Economic Paleontologists and Mineralogists, Special Publication No. 42. 275-284.

Seilacher, A. (1953). Studien zur palichnologie I. Über die methoden der palichnologie. *Neues Jahrbuch für Geologie und Paläontologie* **96**(3): 421-452.

Seilacher, A. (1955). Spuren und fazies im Unterkambrium. In: O.H. Schindewolf and A. Seilacher (eds.), *Beiträge zur Kenntnis des Kambriums in der Salt Range (Pakistan), Akademie der Wissenschaften und der Literatur zu Mainz, Mathematisch-Naturwissen-Schaftliche Klasse, Abhandlingen*, **10**: 117-143.

Seilacher, A. (1964). Biogenic sedimentary structures. In: J. Imbrie and N. Newall (eds.), *Approaches to paleoecology*. New York, John Wiley and sons inc. 296-316.

Seilacher, A. (1967). Bathymetry of trace fossils. *Marine Geology* **5**: 413-428.

Sellwood, B.W. (1970). The relation of trace fossils to small scale sedimentary cycles in the British Lias. In: T.P. Crimes and J.C. Harper (eds.), *Trace Fossils*. Liverpool, Seel House Press. 489-504.

Sellwood, B.W., Price, G.D., and Valdes, P.J. (1994). Cooler estimates of Cretaceous temperatures. *Nature* **370**: 453-455.

Sheard, M.J. (1990). Glendonites from the southern Eromanga Basin in South Australia: palaeoclimatic indicators for Cretaceous ice. *Quarterly Geological Notes of the Geological Survey of South Australia* **114**: 17-23.

Sheard, M.J. and Cockshell, C.D. (1992). *Seismic interpretation of Mt. Hopeless Line 1*. Department of Mines and Energy South Australia, Report Book No.92/17.

Sheard, M.J. and Flint, R.B. (1992). Cretaceous wave-polished granite surfaces, northern Mount Babbage Inlier, South Australia. *Quarterly Geological Notes of the Geological Survey of South Australia* **122**: 19-23.

Simpson, S. (1956). On the trace fossil *Chondrites*. *Quarterly Journal of the Geological Society, London* **112**: 475-499.

Sloan, L.C. and Barron, E.J. (1990). "Equable" climates during Earth history? *Geology* **18**: 489-492.

Tauber, A.F. (1949). Paläobiologische analyse von *Chondrites furcatus* Sternberg. *Geol. Bundesant., Jahrb., Bd.* **93**: 141-154.

Taylor, A. M. (1987). (Unpublished) *Key to identification of marine animal traces as seen in split core*. Dept. of Geology, University of Manchester.

Taylor, A.M. and Goldring, R. (1993). Description and analysis of bioturbation and ichnofabric. *Journal of the Geological Society, London* **150**: 141-148.

Thompson, J. B., Mullins, H.T., Newton, C.R., and Vercoutere, T.L. (1985). Alternative biofacies model for dysaerobic communities. *Lethaia* **18**: 167-179.

Tyson, R.V. (1987). The genesis and palynofacies characteristics of marine petroleum source rocks. In: J. Brooks and A.J. Fleet (eds.), *Marine Petroleum Source Rocks*. London, Blackwell Scientific Publications, Geological Society Special Publication No. 26. 47-67.

Tyson, R.V. and Pearson, T.H. (1991). Modern and ancient continental shelf anoxia: an overview. In: R.V. Tyson and T.H. Pearson (eds.), *Modern and ancient continental shelf anoxia*. London, Geological Society Special Publication No. 58. 1-24.

Ulrich, E.O. (1910). Fossils and age of the Yakutat formation. Descriptions of collections made chiefly near Kodiak, Alaska. In: B.K. Emerson (ed.), *Harriman Alaska Series, Geology and Paleontology* **4**: 125-146.

Vail, P.R., Mitchum, J.R.M., and Thompson III, S. (1977). Seismic stratigraphy and global changes of sea level, Part 4: global cycles of relative changes of sea level. In: C.E. Payton (ed.) *Seismic stratigraphy - applications to hydrocarbon exploration*. American Association of Petroleum Geologists Memoir **26**: 83-97.

Veevers, J.J. (1962). *Rhizocorallium* in the Lower Cretaceous rocks of Australia. *Bulletin of the Australian Bureau of Mineral Resources, Geology and Geophysics* **62**: 1-21.

Veevers, J.J. (1984). *Phanerozoic Earth History of Australia*. Oxford Monographs on Geology and Geophysics No. 2. Oxford, Clarendon Press. 418pp.

Veevers, J.J. (1991). Mid-Cretaceous tectonic climax, Late Cretaceous recovery, and Cainozoic relaxation in the Australian region. *Geological Society of Australia Special Publication* **18**: 1-14.

Vossler, S.M. and Pemberton, S.G. (1988a). Superabundant *Chondrites*: a response to storm buried organic material? *Lethaia* **21**: 94.

Vossler, S.M. and Pemberton, S.G. (1988b). *Skolithos* in the Upper Cretaceous Cardium Formation: an ichnofossil example of opportunistic ecology. *Lethaia* **21**: 351-362.

Waldman, M. (1971). Fish from the freshwater Lower Cretaceous of Victoria, Australia with comments on the palaeo-environment. *Special papers in Palaeontology* **9**: 1-124.

Weimer, R.J. and Hoyt, J.H. (1964). Burrows of *Callianassa major* Say, geologic indicators of littoral and shallow neritic environments. *Journal of Paleontology* **38**(4): 761-767.

Wetzel, A. (1991). Ecologic interpretation of deep-sea trace fossil communities. *Palaeogeography, Palaeoclimatology, Palaeoecology* **85**: 47-69.

Wetzel, A. and Bromley, R.G. (1994). *Phycosiphon incertum* revisited: *Anconichnus horizontalis* is its junior synonym. *Journal of Paleontology* **68**(6): 1396-1402.

Wheatcroft, R. A. and R. W. Frey (1990). Special autocorrelation of bioturbate texture: a new quantitative measure of mixing intensity. *Poster Abstract 13th International Sedimentological Congress, Nottingham, England*: 230.

Wignall, P.B. (1991). Model for transgressive black shales. *Geology* **19**: 167-170.

Wignall, P.B. (1994). *Black shales*. Oxford Monographs on Geology and Geophysics No. 30. Oxford, Clarendon Press. 127pp.

Wignall, P.B. and Myers, K.J. (1988). Interpreting benthic oxygen levels in mudrocks: a new approach. *Geology* **16**: 452-455.

Woolnough, W.G. and David, T.W.E. (1926). Cretaceous glaciation in central Australia. *Quarterly Journal of the Geological Society, London* **82**: 332-351.

Wopfner, H., Freytag, I.B., and Heath, G.R. (1970). Basal Jurassic-Cretaceous rocks of western Great Artesian Basin, South Australia: stratigraphy and environment. *American Association of Petroleum Geologists Bulletin* **54**: 383-416.

Zhou, S. (1989). *Subsidence history of the Eromanga Basin, Australia.* In: B.J. O'Neil (ed.), The Cooper and Eromanga Basins Australia, Adelaide, Proceedings of Petroleum Exploration Society of Australia, Society of Petroleum Engineers, Australian Society of Exploration Geophysicists (SA Branches). 329-335.

Zhou, S. (1993). A 3-D backstripping method and its application to the Eromanga Basin in central and eastern Australia. *Geophysical Journal International* **112**: 225-243.

Appendix 1

Structure of the south-west Eromanga Basin Mesozoic fill

As noted by Haig and Lynch (1993), despite the apparent epeirogenic events affecting Australia since the deposition of the Eromanga Basin sediments, these strata remain relatively undeformed and flat-lying. However, structure is still evident and has important implications for economic hydrocarbon reserves and the exploitation of the Great Artesian Basin's aquifers.

Structurally, as summarised by Krieg *et al.* (1995), the Eromanga Basin in South Australia can be divided into two regions, north-eastern and south-western, by a north-west trending hinge zone. North-east of this hinge zone the thickness of the sediment increases rapidly and attains in excess of 3000m in the far north-east of South Australia (Krieg *et al.*, 1995). West and south-west of the hinge zone around the margin of the basin, the still contiguous basin fill is much thinner due to depositional thinning and erosional stripping of the uppermost stratigraphic units (Krieg *et al.*, 1995); this is the region which concerns us here.

Moore and Pitt (1984) reported at least two phases of structuring of the south-western Eromanga Basin sediments. The first phase comprised syn-sedimentary structuring, largely folding by drape and compaction, while the second more significant phase, which imparted most of the structure, was post-depositional and comprised Early Tertiary folding which enhanced pre-existing structures and produced some very large anticlines, and was probably caused by the effects of continental breakup and collision. Krieg *et al.* (1991) noted that the predominant features in the Mesozoic Eromanga Basin structures reflect the major north-westerly fault trends in the underlying Adelaidean; these faults extend up into the Bulldog Shale and then apparently pass into low amplitude folds in the stratigraphically higher units. In a study of more basinal Eromanga Basin structures, Kuang (1985) noticed that many faults are concentrated in the Cadna-owie Formation, and sole out into the basal Bulldog Shale; thus much of the Bulldog Shale is frequently unfaulted. Fault style is predominantly high-angle normal, with a smaller component high angle reverse displacement producing a shallow horst and graben profile in the Adelaidean and overlying lower Eromanga Basin units, structure which Krieg *et al.* (1991) related to Cenozoic uplift and downwarp.

Characteristic of the structure of the south-western Eromanga Basin are large broad anticlines, long axes oriented approximately north - south, such as Dalhousie Anticline described by Krieg (1982; 1986), and which is over 50km across. Krieg (1986) inferred that growth of the Dalhousie Anticline had formed along faults or monoclines and had produced an essentially polygonal structural pattern. While Krieg (1982; 1986) considered that the formation of the Dalhousie Anticline occurred during the Quaternary and may be continuing today, Moore and Pitt (1984) disagreed and related the growth of all the south-western Eromanga Basin anticlines to Early Tertiary tectonics. In summary, Moore and Pitt (1984) described a single, prolonged phase of post-Cretaceous folding which commenced prior to Tertiary deposition in the Late Eocene and probably continued until late Oligocene at the earliest. Sheard and Cockshell (1992) noted that this Tertiary deformation was probably related to uplift of the adjacent Flinders Ranges.

Appendix 2

Palaeoenvironmental Fabric Types of field localities

Field locality	Unit	PFT	Trace fossil taxa
Bulldog Creek (Fig.2.02)	Bulldog Shale	A-C	*Anconichnus*
Lambing Creek (Fig.2.02)	Bulldog Shale	A-B	*Anconichnus*
Levi Creek (Fig.2.02)	Bulldog Shale	A-D	*Anconichnus, Planolites, Skolithos, Rhizocorallium*
Davenport Springs (Fig.2.05)	Bulldog Shale	A-B	*Anconichnus, Planolites*
Petermorra Creek (Fig.2.05) Site I	Cadna-owie Formation and Parabarana Sandstone	Variable	*Thalassinoides*
Petermorra Creek (Fig.2.05) Site II	Parabarana Sst and Bulldog Shale	F-G B	*Anconichnus* *Anconichnus, Planolites, Chondrites*
Petermorra Creek (Fig.2.05) Site III	Parabarana Sandstone	Variable	Indistinct
Petermorra Creek (Fig.2.05) Site IV	Bulldog Shale	A-D	*Anconichnus, Planolites*
Petermorra Creek (Fig.2.05) Site V	Bulldog Shale	A-D	Indistinct
Petermorra Creek (Fig.2.05) Site VI	Bulldog Shale	C-D	*Anconichnus, Planolites*
Petermorra Creek (Fig.2.05) Site VII	Bulldog Shale	A-C	*Anconichnus, Planolites, Palaeophycus tubularis, Ophiomorpha nodosa*
Petermorra Creek (Fig.2.05) Site VIII	Bulldog Shale	A-C	*Anconichnus, Planolites*
Petermorra Creek (Fig.2.05) Site IX	Bulldog Shale	A-C	*Anconichnus, Planolites*
Petermorra Creek (Fig.2.05) Site X	Bulldog Shale	A-C	*Anconichnus, Planolites*

Field locality	Unit	PFT	Trace fossil taxa
Yerila Creek (Fig.2.06) Site I	Bulldog Shale	B-D	*Anconichnus*, *Planolites*, *Ophiomorpha irregulaire*, *Palaeophycus tubularis*, *P. heberti*, *Chondrites*, *Rhizocorallium*, *Thalassinoides*
Yerila Creek (Fig.2.06) Site II	Bulldog Shale	B-D	*Anconichnus*, *Planolites*, *Palaeophycus tubularis*, *Chondrites*, *Thalassinoides*
Gunpowder Bore (Fig.2.06)	Parabarana Sst. Bulldog Shale	F A-D	*Skolithos*, *Planolites* Indistinct
Boulder Bed (Fig.2.06)	Bulldog Shale	A-D	*Anconichnus*, *Planolites*, *Palaeophycus tubularis*, *Chondrites*
Parabarana Hill (Fig.2.07)	Bulldog Shale	A-C	*Anconichnus*, *Planolites*, *Palaeophycus heberti*, *Gyrochorte*

Appendix 3

X-ray diffraction for clay mineral analysis: sample preparation methodology

In total, 24 samples were prepared and analysed from cored Bulldog Shale material. These samples comprise material from each of the four cores under study, and represent each of the seven palaeoenvironmental fabric types throughout the unit from close to the boundary with the Cadna-owie Formation at the base, to close to the boundary with the Coorikiana Sandstone Member at the top of the unit. Thus, Bulldog Shale clay mineral analyses have been performed extensively over lateral and vertical sections, and from the complete range of non-carbonate lithologies.

Sample preparation comprised several steps, performed in order and for each sample:
1) Initial grinding. 1g of sample gently ground in pestle and mortar until in granule-grade pieces.
2) Disaggregation. Ground sample into small bottle, half filled with distilled water and into mixer mill for three minutes, or until disaggregated.
3) Initial particle size separation. Disaggregated sample and water into beaker. Initially, further distilled water was added to the sample to approximately 100ml for sample dispersal, however a problem with flocculation was encountered, and thus the anti-flocculating agent sodium hexametaphosphate was used, after testing that its diffraction lines would not interfere with those of the Bulldog Shale clay minerals. Therefore, sodium hexametaphosphate solution (180mg dissolved in 500ml distilled water) was used to bring the sample up to 100ml, whereupon it was stirred and dispersed.
4) Further particle size separation. Samples centrifuged at 1000r.p.m. for two minutes. This separates out all particles over 2μm.
5) Final particle size separation. 40ml of sample carefully pipetted into centrifuge tube (two samples per centrifugation - carefully balanced) and centrifuged at 6000r.p.m. for 6 minutes to separate out 2μm and less fraction.
6) The glass slide method of sample preparation was employed here, as described by Moore and Reynolds (1989). Overlying fluid was carefully poured off from the thixotropic sediment. Residual sediment thoroughly mixed with a PTFE rod, and the sample sucked into a disposable pipette and painted onto half of one side of a clean labelled (by engraving) slide. Slide and sample dried in an oven at approximately 100°C.
7) Samples analysed.

Appendix 4

Organic carbon geochemistry: sample preparation and analysis

Whole rock samples were fragmented to granular-grade material, and then crushed within a shaker mill until disaggregated. 5-10g of each sample was added to individual pre-weighed beakers and placed in an oven at 100°C to dry overnight. After cooling the beakers and samples were reweighed to obtain the dry mass of the sample. In order to remove any carbonate carbon from the Bulldog Shale samples, approximately 100ml of 10% dilute HCl was added to each sample, stirred, and allowed to settle overnight. Visible effervescence was rare, occurring in only one in thirty-four samples, confirming the minor nature of carbonate carbon within the Bulldog Shale away from the concretions. The HCl also acted to dissolve certain iron containing materials, which imparted a green colouration to the HCl solution; important to note here is that mass loss due to treatment with HCl is not due to carbonate carbon alone, and thus carbonate carbon values cannot be determined through this method. After acid washing each sample was decanted, and then twice washed with 200ml distilled water. Upon allowing to settle, samples were again decanted and subsequently dried in an oven at 100°C. After cooling, samples and beakers were reweighed, and re-homogenised with a pestle and mortar prior to sealing for analysis.

15-20cm long combustion tubes were produced from 9mm diameter quartz tubing, as described by Boutton (1991a). Each combustion tube was marked with an identification number using a ceramic glaze pen, and subsequently heated within a muffle furnace at 850°C for three hours to remove any adsorbed organic material. Using a top pan balance, between 20-30mg of sample was placed in a tared pestle and mortar, and the accurate mass of the sample noted. An approximately equal amount of copper(II)oxide was added and thoroughly mixed with the sample; the mixed sample and copper(II) oxide were loaded in a combustion tube using a long-necked funnel. The copper(II) oxide had also been heated to 850°C with the sample tubes to remove adsorbed organic material and other gases. All sample-handling apparatus was thoroughly cleaned between sample loadings. Also added to each sample was approximately 5cm of folded silver and copper wires. During combustion the copper(II) oxide undergoes pyrolytic decomposition, providing O_2 for the oxidation of organic carbon to CO_2. The silver wire removes any sulphur by reacting to form silver

sulphides, and the copper wire removes oxides of nitrogen by reducing them to nitrogen.

Each tube was then evacuated and sealed prior to combustion, this enables the oxidation of organic carbon to CO_2 (Boutton, 1991a). For combustion, sealed tubes were heated within a furnace to 870°C and this temperature was maintained for 12 hours; the tubes were subsequently allowed to cool slowly. Prior to combustion each tube was placed within a shielding stainless steel cylinder to protect it, other tubes, and the interior of the furnace, should a tube explode.

The resultant CO_2 is then extracted by cryogenic distillation in a vacuum line, see Boutton (1991a) and Bottrell, et al. (1991) for details. After isolation, the pressure (P) exerted by the CO_2 within a known measuring volume was noted, enabling future calculation of CO_2 volume and thus TOC for the sample. Each CO_2 sample was then mass spectrometrically analysed, see Bottrell, et al. (1991) for details of instrumentation, and Boutton (1991a) for general methodology, and $\partial^{13}C$ determined.